The Influence of Atmospheric Moisture on the Corrosion of Chloride-Contaminated Wrought Iron

Mark R.T. Lewis

Thesis submitted to
Cardiff University
in candidature for the degree of
PhD

September 2009

ProQuest LLC
789 East Eisenhower Parkway
P.O. Box 1346
Ann Arbor, MI 48106-1346

STUDENT ID NUMBER: 016130151

SUMMARY OF THESIS

Wrought iron with a remaining metallic core recovered from marine and terrestrial archaeological contexts is unstable and has the potential for further corrosion after recovery or excavation. Where metallic iron remains within the object, it deteriorates as crystals of new, chloride-bearing, corrosion products form at the metal/corrosion interface, resulting in the loss of overlying corrosion. This is undesirable, for the information on the form of the original, uncorroded, artefact is commonly found within the overlying corrosion which is detached.

A mechanism for this type of deterioration, based upon the retention of chloride counter-ions as part of the electrochemical corrosion process, was identified by Turgoose (1982) for archaeological iron and his research has informed the storage of chloride-contaminated wrought iron in museum collections ever since: Iron corrodes in the presence of ferrous chloride tetrahydrate but not its dihydrate. Precise data for the relative humidities at which these respective hydrates are stable, and at which iron in association with ferrous chloride corrodes, has been produced by the research presented in this thesis.

The role of a commonly encountered chloride-bearing oxidation product of ferrous chloride tetrahydrate, βFeOOH (akaganéite), in the deterioration of wrought iron, and its relationship with atmospheric moisture, were also investigated.

Corrosion of iron was observed at relative humidities as low as 22%RH in the presence of ferrous chloride and as low as 15%RH in the presence of unwashed βFeOOH. The effect of temperature on transitional RH values was demonstrated.

The results of this research enable informed management decisions about environmental parameters for the storage of chloride-contaminated wrought iron recovered from maritime contexts and terrestrial archaeological contexts stored in museum collections.

Keywords

Corrosion, conservation, wrought iron, chloride, ferrous chloride, akaganéite, βFeOOH, desiccated storage, dehumidification, threshold relative humidity, atmospheric moisture.

Declaration

This work has not previously been accepted in substance for any degree, and is not concurrently submitted in candidature for any degree.

Signed.....(candidate) Date...02/09/09...

STATEMENT 1

This thesis is being submitted in partial fulfilment of the requirements for the degree of PhD.

Signed.....(candidate) Date...02/09/09.....

STATEMENT 2

This work is the result of my own independent work/investigation, except where otherwise stated. Other sources are acknowledged by explicit references.

Signed.....(candidate) Date...02/09/09.....

STATEMENT 3

I hereby give consent for my thesis, if accepted, to be openly available for inter-library loan and for photocopying, and the title and summary to be made available to outside organisations.

Signed.....(candidate) Date...02/09/09.....

STATEMENT 4: ANY PREVIOUSLY APPROVED BAR ON ACCESS

I hereby give my consent for my thesis, if accepted, to be available for photocopying and for interlibrary loans after the expiry of a bar on access if previously approved by the Graduate Development Committee.

Signed.....(candidate) Date...02/09/09.....

Mark R.T. Lewis M.Sc.

"Now, what I want is, Facts.
Teach these boys and girls nothing but Facts.
Facts alone are wanted in life.
Plant nothing else, root out everything else.
You can only form the minds of reasoning animals on Facts:
nothing else will ever be of any service to them.
This is the principle on which I bring up these children.
Stick to Facts, Sir!"

Charles Dickens, Hard Times, London, 1854.

Acknowledgements

The author is indebted to David Watkinson, supervisor and Reader in Conservation, Cardiff University, for the opportunity to be involved with this avenue of research and for his support, encouragement and enthusiastic criticism.

I am grateful to Dr Anthony Oldroyd of the Department of Earth Sciences, Cardiff University, for his interest in my work and for independently conducting the x-ray diffraction (XRD) analyses herein reported.

I would like to thank Phil Parkes of Cardiff Conservation Services for the use of a Rotronic™ Datalogger during part of this study.

I acknowledge, with thanks, the financial support of the South West Museums Council, the Heritage Lottery Fund, the ss Great Britain Project, Bristol, and its Director and Curator, Matthew Tanner, for his support, criticism and enthusiasm, for initiating this research and providing samples of chloride-contaminated wrought iron of marine origin (from the ship itself) for use in this study for comparative purposes.

I acknowledge, with thanks, the financial support of Amgueddfa Cymru - National Museum Wales.

I am grateful to the Postgraduate Research Committee of the School of History and Archaeology, Cardiff University, The Roman Legionary Museum-National Museums and Galleries of Wales, The Fox Travel Fund and to the ss Great Britain Project for financial support enabling me to co-present some of the research outcomes of this study at Metal '04, Canberra, Australia in October 2004.

I would like to thank my family, friends and colleagues for their understanding and patience during the course of this (part time) work.

TABLE OF CONTENTS

TABLE OF FIGURES

TABLES

The influence of atmospheric moisture on the corrosion of chloride-contaminated wrought iron

1 Introduction: The rationale for this research

1.1 A practical research problem: preserving chloride-contaminated wrought iron, a large and significant curatorial challenge

Wrought iron structures and artefacts comprise diverse, highly significant and numerous elements of the historic environment and archaeological resource. Prior to the development and widespread use of cast iron, where suitable, wrought iron was historically used for its strength, durability, ductility, malleability and as a base material for carburizing to form steel (Tylecote, 1976 & 1986). The cultural importance of wrought iron in the past, and its importance as a resource for studying the technology, engineering and design of the past 2,700 years, is immense. Wrought iron forms a highly significant proportion of iron age, Roman, medieval and post-medieval archaeological museum collections as well as social history, industrial and maritime collections (Megaw and Simpson, 1979; Manning, 1972 & 1985; Chapman, 2005; Keene, 1994; Thickett, 2008; Pearson, 1987; Mathias *et al.*, 2004; Rowland, 1971; Corlett, 1990; Cox & Tanner, 1999; Turner *et al.*, 1999). Wrought iron has been extensively used historically by engineers because of its excellent performance under tension as well as compression so it is also a major component of many massive open-air structures forming part of the historic environment, e.g. the first modern suspension bridge - Telford's 1826 Menai bridge, and his 1805 Pontcysyllte aqueduct, designated a World Heritage Site by UNESCO in 2009. Brunel revolutionised ship design and construction by combining the use of screw propulsion with the use of wrought iron for the hull of the ss Great Britain which is now preserved and displayed to the public within the dry dock in which she was constructed in 1843 (Corlett, 1990; Rowland, 1971).

The heritage sector aims to preserve the vast wrought iron heritage resource to enable its enjoyment and study by current and future generations (UKIC, 1983; Corfield, 1988; English Heritage, 2008). Unfortunately, metallic wrought iron has a heterogeneous

composition and is thermodynamically unstable with respect to its ores (Scully, 1966). It requires optimised conditions to enhance its preservation. Where wrought iron has never been contaminated by corrosive contaminants, coatings and/or dry environments have commonly proved effective for preserving large internal and external structures (Vernon, 1927; Evans, 1972; Donovan, 1986). Unfortunately, much of the wrought iron of the historic and archaeological resource has been contaminated by corrosive contaminants through having been buried in the ground, immersed in seawater or used or stored in maritime or polluted urban environments (Evans, 1972; Duncan & Ganiaris, 1987; Turgoose, 1982a; North, 1987; Duncan and Balance, 1988; Tidblad *et al.*, 2000; Neff *et al.*, 2004, 2005 & 2007; Tetrault, 2005). The conservation profession recognises the most significant corrosive and destructive contaminant for wrought iron as being chloride ions (Foley, 1970: 62; Knight, 1982 & 1990; Turgoose, 1982a & b, 1985a; North, 1987; North & McCleod, 1987; Selwyn *et al.*, 2001).

The conservation profession lacks a single, standardised, successful and agreed methodology for the treatment and preservation of chloride-contaminated wrought iron. Attempts to remove the corrosive chloride ions from contaminated wrought iron by various aqueous washing techniques are reported to be ineffective in preventing further corrosion and unpredictable (North, 1982; Watkinson, 1983 & 1996; Watkinson & Al-Zahrani, 2008; Keene & Orton, 1984; Keene, 1994). Attempts to prevent electrochemical corrosion of chloride-contaminated wrought iron through the removal of liquid water and water vapour are also reported to be ineffective (Keene, *ibid.*). Anoxic (oxygen-free) storage (Mathias *et al.*, 2004) is not always feasible or economically desirable, especially for large artefact assemblages or large/working objects and structures. Similarly, hydrogen reduction is not always feasible, especially for large or composite artefacts or structures, and is not always successful in removing all of the chloride content from the object (Daniels *et al.*, 1979; Barker *et al.*, 1982; Patscheider & Veprek, 1986; Archer & Barker, 1987; Sjøgren & Buchwald, 1991). The plasma method commonly only volatilises chloride in the outermost layers, with removal of chloride from deeper layers reportedly less successful (Oswald, 1997: 135).

This study focuses on identifying the mechanisms by which chloride-contaminated wrought iron corrodes and how atmospheric moisture levels (conventionally cited as relative humidity) affects them, especially at low relative humidities (RH). The most significant chloride-bearing corrosion products are identified and their corrosive effect when in contact with metallic iron is studied at different atmospheric moisture levels (RH).

1.2 Why preserve iron? Conservation ethics and the preservation of information obtainable from wrought iron objects, large and small

Wrought iron objects or structures with heritage or cultural significance are recognised as being an important potential resource for information on factors such as their technology, function and design. Their conservation aims to identify and preserve the information that may be gained from their study.

Historically it had been common practice to replace severely decayed elements of large wrought iron structures such as bridges, steam engines or ships with the aim of "restoring" the overall appearance and structural integrity of the structure but with the loss of original material which is an inevitable result of this approach. "Restoration" i.e. replacement of decayed component parts with replicated substitutes was commonly dictated by the scale of the structure in terms of the sheer quantity of artefact to preserve and the commensurate cost. The conservation profession today distinguishes this "restoration" approach to preservation from true "conservation"; the recovery, stabilization and retention of the original wherever practical.

The United Kingdom Institute for Conservation "Guidance for Conservation Practice" (1983) stated that *"conservation is the means by which the true nature of the object is preserved"* for present and future generations (Corfield, 1988). All other ethical considerations in conservation stem from this. The curator and conservator must firstly identify which features of a cultural artefact (object or cultural property) are of great

significance and investigate all aspects of the information which it may impart. Where the condition of the object is such that it necessitates some form of intervention to ensure its long-term survival, priority should be given to the most significant aspects of the object. It then falls to the conservator to reveal and record the true nature of the object so that none of the information contained within it is lost, but is preserved and made accessible.

The conservator must balance preservation needs against the need to use (access/handle), understand and appreciate the object. Replacement of missing parts may be necessitated by aesthetic or structural considerations. This could be to aid interpretation or ensure the stability of the object e.g. to enable handling. It should be possible to tell replacement parts or additional material from the original material and they should be removable (reversible) if, at some stage in the future, they are deemed unsatisfactory or to hide original material worthy of study and/or presentation (UKIC, 1981 and 1983).

The concept of artefact form and fabric as an information resource is established in archaeological conservation where the *"original surface"* is commonly found to exist near the magnetite/goethite interface of mineralized or part mineralized wrought iron archaeological artefacts (Cronyn, 1990: 182; Neff *et al.,* 2004: 740). More recently, Bertholon (2007: 35) has offered a standardized definition of the "original surface" as *"the original surface of the artefact at the time of its abandonment"* but goes further to establish a *"limitos" – "the limit between the materials of the artefact and the surrounding environment at the time of the abandonment".* This *"limitos"* concept is a useful abstract concept for social history artefacts or larger wrought iron structures such as bridges, steam engines or historic ships: the 'time of abandonment' could be redefined as the point at which the artefact was acquired or collected by the heritage institution and became an object for conservation rather than restoration, or the time that the uppermost, i.e. latest, surviving historically important coating or paint scheme was applied to the object.

Dillmann *et al.* (2002), Neff *et al.* (2003 and 2005) and Chitty *et al.* (2005) identified greater complexity in the composition of archaeological iron corrosion products than layers of magnetite/goethite alone and defined a general corrosion system for archaeological wrought iron that allowed for this complexity. Using their nomenclature the *"limitos"* for archaeological material may be identified as the interface between the dense product layer (DPL) lying adjacent to the core of the artefact (and looking denser than the outer parts of the corrosion products) and the transformed medium (TM), defined as the less dense transition zone between the DPL and the soil (figure 1). It is clearly desirable to retain and preserve the DPL which preserves the information on the original form of the archaeological artefact at its interface with the TM.

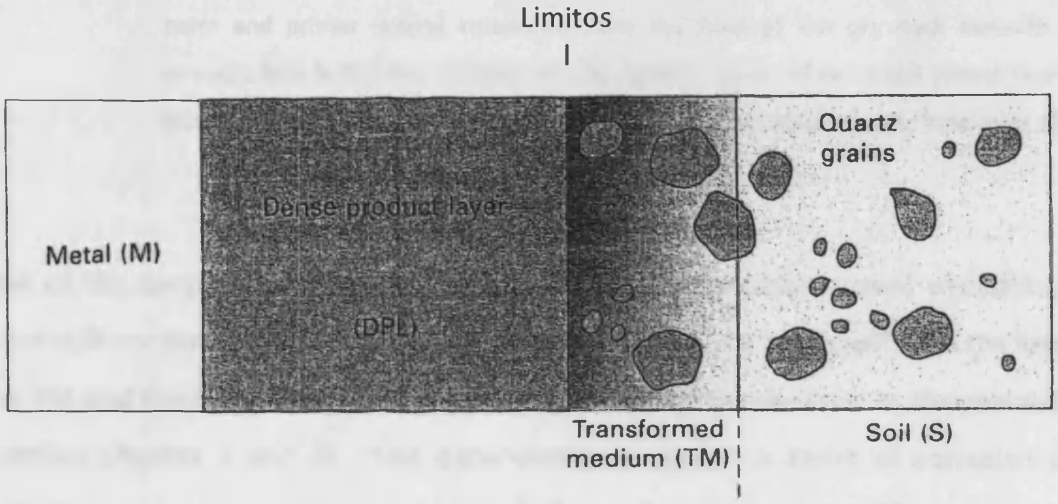

Figure 1 **A schematic representation of the corrosion system and limitos concept for archaeological wrought iron artefacts buried in soil (after Neff et al., 2007: 45, *figure 4.1*).**

For historic structural wrought iron structures the *"limitos"* may be the remaining surface of historically significant paint with a DPL beneath, and wrought iron core beneath that where it remains (figure 2). It is again desirable to retain the corrosion products for these underlie the paint that comprises the "original surface" as defined. Where older or original paint has been over-painted in recent times, the *"limitos"* could be argued to be the last paint surface which has historic significance for the structure

e.g. applied during its working life or, perhaps, an historically significant early preservation attempt.

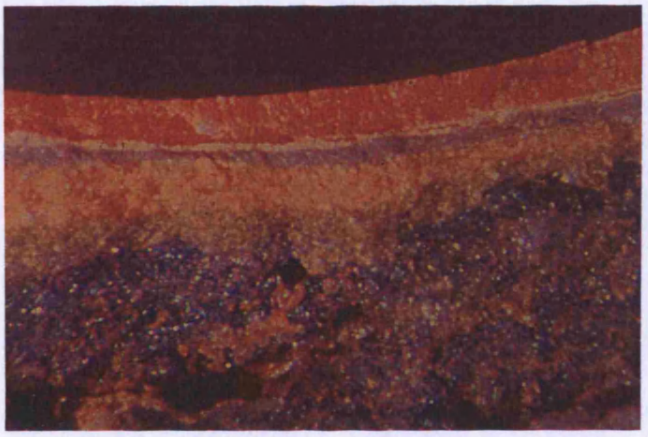

Figure 2. **A photomicrograph of a cross-section of a sample of spalled corrosion (with overlying paint and primer layers) recovered from the floor of the dry dock beneath the wrought iron hull of the ss Great Britain, Bristol. Layers of paint and primer overly a thick dense product layer (DPL) identified by XRD as mainly magnetite (appendix 4).**

One of the specific problems encountered with chloride-contaminated wrought iron which still contains a metallic core is its capacity to *"break up"* or *"spall"* with the loss of the TM *and* the information-rich DPL, which separate from the core at the metal/DPL interface (figures 2 and 3). This deterioration occurs as a result of corrosion and oxidation processes requiring moisture which result in disruptive solid crystal growth which will be considered in section 2.8.4. (Knight, 1982). For buried archaeological wrought iron and submerged marine wrought iron this destructive phenomenon is only observed to occur after recovery from the soil or the sea and following exposure to the air which has much higher oxygen levels than the soil or the sea (Mathias, 1999 & 2004; Turgoose, 1985a). Wrought iron has commonly been reported to break up whilst stored in museums or displayed in the open air (Knight, *ibid.*).

Figure 3. **A Roman wrought iron carpentry gouge from Usk, Monmouthshire, showing signs of post-excavation corrosion resulting in the loss of its surface during museum storage.**

Historically, electrolytic or chemical stripping of chloride-contaminated wrought iron artefacts effectively achieved the complete removal of the harmful chloride ions and chloride-bearing corrosion products from the metallic core that was left after the treatment (Plenderleith & Werner, 1971). Whilst stripping usually rendered the remaining metallic core of the artefact stable, the technique is unable to discriminate between the DPL (which should be retained) and the TM which is to be removed for there is not sufficient chemical distinction between them. Stripping results in the inevitable loss of all corrosion products (including the DPL) and renders the artefacts of limited value where information is lost with the loss of the *limitos.* The appearance of the artefact is also significantly altered. Stripping, which is clearly an irreversible treatment, is now rarely considered to be an ethical conservation treatment for heavily corroded chloride-contaminated wrought iron artefacts for these reasons but it is still used successfully where a solid metallic core retaining the form of the artefact remains with only a superficial layer(s) of overlying corrosion (Cronyn, 1990). Complete chloride removal and artefact stabilisation without the loss of the DPL using aqueous washing methods has not been mastered and is unpredictable (see section 1.1).

'Preservation by record' is a concept widely employed in archaeology to capture information from the archaeological resource where archaeological remains can not be preserved (Barker, 1982: 11-12). It entails the complete systematic study, and

sequential removal, of the remains. It is possible to argue for a 'preservation by record' approach for unstable, chloride-contaminated wrought iron, where objects may be studied (through x-radiography, metallurgy and/or investigative cleaning) and discarded if they deteriorate irreparably after a "full" record of them has been made. But there will inevitably be occasions where the importance of the original artefact will dictate that special measures to attempt to preserve it, or a significant aspect of it, must be applied. The "fullness" of original analyses and recording may also alter over time. As new methods and techniques are developed and become accepted as the minimum standard (e.g. digital data) the original record may become insufficient. Preservation of the original artefact is preferable where feasible.

1.3 Prioritising a conservation treatment for chloride-contaminated wrought iron

It is not the focus of this study to conduct a detailed review all of the methods which are or have been employed in the treatment of chloride-contaminated wrought iron artefacts, e.g. thioglycolic acid (Stambolov and van Rheeden, 1968), ethylenediamine at 70°C (Argo & Turgoose, 1985; Mc.Cawley, 1984; Argyropoulos *et al.*, 1997; Selwyn and Argyropoulos, 2005), hydrogen plasma reduction (Daniels *et al.*, 1979; Barker *et al.*, 1982; Patscheider & Veprek, 1986; Archer & Barker, 1987; Sjøgren & Buchwald, 1991) or ethylene oxide treatments (Duncan, 1986). A summary of their limitations has been published elsewhere (Watkinson and Lewis, 2004: 90, table 2). Large scale methods employing traditional industrial practices, including indiscriminate abrasive cleaning, stripping and traditional surface treatments such as needle gun corrosion removal, damage the badly corroded chloride-contaminated wrought iron and remove its DPL. When employed in the past these have not been successful in halting ongoing corrosion and repeated application results in further significant loss of original fabric or surface, especially where it now exists as corrosion product (DPL).

It has been proposed that the (non-interventive) removal of moisture by desiccation or dehumidification would prevent the break up of chloride-contaminated wrought iron, preserving the original form of the artefact at the surface of the dense product layer

(Knight, 1982; Turgoose, 1982b). The ethics that underpin conservation, namely *maximum preservation using minimal intervention and reversible treatments*, guide the identification of the aims and objectives of this study. The conservation aims for chloride-contaminated wrought iron are identified as (i) to prevent the further corrosion and break up of chloride-contaminated wrought iron or (ii) to significantly reduce its corrosion rate, whilst retaining overlying iron corrosion products *and* remaining accessible for study and/or enjoyment. The least interventive treatment option to offer maximum preservation with complete reversibility, retaining overlying corrosion products and allowing continuous access for study and enjoyment, is identified as the removal of water from the corrosion process through climatic, i.e. environmental, control (Knight, 1982; Watkinson & Neal, 1998; Turner, Tanner and Casey, 1999: 61-64). The abilities to retain the DPL, and control, monitor and halt desiccation, without reversibility problems conform with conservation ethics. The case for the standardised use of low humidity storage of chloride-contaminated wrought iron in conservation is ethically strong if its effectiveness can be demonstrated and its mechanisms understood.

The study of the mechanisms by which chloride-contaminated wrought iron corrodes, and the relationship between these and the prevailing environmental moisture levels, especially at low relative humidities (RH), coupled with the study of the corrosive effect of chloride bearing corrosion products in contact with metallic iron, may be used to inform decisions on whether, and/or how, to employ non-interventive environmental control as a standard conservation treatment for chloride-contaminated wrought iron. The relationships between levels of atmospheric moisture and the corrosion of chloride-contaminated wrought iron, and iron in the presence of chloride bearing corrosion products, have been identified as research priorities and the basis for this study. The question posed by the use of desiccation or dehumidification as a means of preserving chloride-contaminated wrought iron is:

"At what relative humidity would the corrosion of chloride-contaminated wrought iron cease?"

1.4 Aims and objectives identified for this study

The aims are to:

- determine how dry an environment would need to be to prevent the corrosion of iron in contact with the most relevant, i.e. chloride bearing, solid corrosion products;
- examine the corrosion rate of iron where metallic iron is in contact with relevant solid chloride bearing corrosion products in environments with different moisture contents (relative humidity);
- identify further areas of study whose results will support the long-term preservation of chloride-contaminated wrought iron.

By extrapolating the results of the experimental work undertaken as part of this study, this research can be used to support the objectives of the conservation profession by:

- providing a corrosion threshold relative humidity (below which iron does not corrode within the parameters of the corrosion model proposed) which can be used by conservators, engineers and architects in their specification, design and running parameters of environmental control methods and air conditioning plant;
- reporting iron corrosion rates as a function of increasing relative humidity to show how low environmental humidity *enhances* the stability of iron, even if it is not low enough to stop corrosion. This facilitates better interpretation of the operating parameters for the proposed method(s) of environmental control.

The overall objective of this research was to examine mechanisms for the corrosion of chloride-contaminated iron under a range of environmental conditions. The conclusions may be extrapolated to produce a preservation model for chloride-contaminated wrought iron artefacts and structures of all sizes from both terrestrial and marine contexts.

The identified objectives comprise:

- A literature search to identify existing corrosion models for chloride-contaminated iron.
- Experimental work to examine the influence of relative humidity (atmospheric moisture) on:
  - selected chloride bearing corrosion products identified as the most significant in the corrosion models;
  - mixtures of these corrosion products;
  - the behaviour of iron in contact with these corrosion products.

2 The Problem: A review of published scientific models for the corrosion of wrought iron

"If you know the answer, you probably don't understand the question"

Anon.

2.1 The agencies of deterioration

Moisture is present in nearly all natural environments either as liquid water or water vapour. Where water is present the corrosion of wrought iron is electrochemical in nature (West, 1970; Jones, 1992). Electrochemical corrosion of iron and any other reactive metal requires moisture (water), dissolved salts (which, because they are in solution during active corrosion, comprise electrolyte) and oxygen. In general, at a fixed temperature, the levels of availability of these three agencies of deterioration (i.e. dissolved salts, water and oxygen), determine how aggressive (extensive and fast) the wrought iron corrosion will be. Conversely, remove or reduce the levels of one of these three agencies of deterioration and corrosion stops or reduces in rate (Mathias *et al.*, 2004). In theory, the *"answer"* to the problem is as simple as that. All conservation treatments for chloride-contaminated wrought iron aim to remove, or reduce the level of, one or more of these three agencies of deterioration.

Each of the three agencies of deterioration is abundantly present under ambient atmospheric conditions once freshly excavated archaeological wrought iron or freshly recovered marine wrought iron is exposed to the air. A wide range of factors can influence the occurrence and extent of corrosion, as well as the nature of resulting corrosion products. The amounts of moisture, oxygen and salt(s) contribute to corrosion rate, while the range of salts and pollutants influence the types of corrosion products formed, as well as corrosion rate and corrosion mechanisms (ISO 9223; Turgoose, 1982a; Knight, 1990; Thickett, 2007 and Thickett, forthcoming; Tidblad *et al.*, 2000; Duncan & Ballance, 1988).

2.2 Sources of chloride contamination

2.2.1 The sea - an electrolyte and contaminant

Sea water, being saline – an ionic solution, acts as an electrolyte for the corrosion of wrought iron when they are in contact. Aerated marine (saline aqueous) and maritime environments have long been acknowledged to be more highly corrosive to both wrought and cast iron than most other (unpolluted) natural environments (Hudson and Stanners, 1953; Duncan & Ballance, 1988; Tidblad *et al.*, 2000: 24; also see Robinson, 1982 with its literature overview from 1948 to 1982). This is due to the accelerating effects of the abundant dissolved or atmospheric oxygen and the dissolved salts which aerated sea water or sea water aerosols contain (Evans, 1972; Rees-Jones, 1972; Barkman, 1975; Pearson, 1987).

Hudson and Stanners (1953) reported that rates of atmospheric corrosion on surf beaches in the tropics are about five times greater than in the most corrosive atmospheres in [industrial] Britain. They found that the most corrosive (maritime) environment tested overseas was two hundred times more corrosive than the least corrosive overseas location. They found that corrosion was associated with salt spray from the sea and that the rate of corrosion falls off rapidly with increasing distance from the surf line. Steel pillars 25m distant from the sea coast will corrode 12 times faster than the same steel pillars 250m further inland (Garverick, 1994: 3). Hudson and Stanners (1953: 96) reported that corrosion at a site half a mile from the surf line was less than one tenth of that at a site 220 yards from it. Carriage of airborne sea-salt from 20km to 50km inland from ocean coasts was demonstrated by Duncan and Ballance (1988) to be a significant factor in corrosion there, and of greater significance to corrosion rates on oceanic islands such as New Zealand [and Great Britain] than had hitherto been demonstrated for continental land masses (Winkler & Junge, 1972; Winkler, 1973).

Salt water contains significant quantities of dissolved sodium chloride (NaCl) and magnesium chloride ($MgCl_2$) (Florian, 1987; Memet, 2007: 154 and table 1). When

dissolved in water, ionic substances such as sodium chloride completely dissociate into their constituent positive and negative ions, i.e. sodium (Na^+) and chlorine [or chloride if referring specifically to the ion] (Cl^-) respectively (see glossary appended). The presence of the chloride ion is known to promote aggressive electrochemical corrosion of wrought iron in the presence of air or, more specifically, oxygen and water (which may be supplied as atmospheric moisture) (Foley, 1970; Traubenberg and Foley, 1971; Gilberg and Seeley, 1981; North, 1982; Duncan and Balance, 1988; Graedel and Frankenthal, 1990). Chlorides also have hygroscopic properties which, in the open air, contribute to the creation of an electrolyte layer and prolong the time of wetting (section 2.7). In recognition of this, the International Organisation for Standardisation (ISO) has developed an international classification system of atmospheric corrosivity; **"Corrosion of metals and alloys – Corrosivity of atmosphere – Classification" (ISO 9223)** which is based on three parameters: time of wetness, sulphur dioxide concentration (see section 2.9) and deposition of sea salt aerosols (Tidblad *et al.*, 2000). Concentrations of the most abundant ions in seawater are given by Roberge (2000: 1140).

Cations	(g/l)	Anions	(g/l)
Na^+	11.04	Cl^-	19.88
Mg^{2+}	1.30	SO_4^{2-}	2.74
Ca^{2+}	0.42	HCO_3^-	0.18
K^+	0.39	Br^-	0.07
Sr^+	0.008	F^-	0.015

Table 1. **Concentrations of the most abundant ions in seawater after Roberge (2000) which accords with data presented by Rogers (1968) also.**

Sea water contains almost ten times as much chloride ion as sulphate ion and almost ten times as much sodium ion as the next most abundant cationic competitor, magnesium (Greathouse & Wessel, 1954: 112; Kaye & Laby, 1966). Although the total mass of dissolved salts in seawater (salinity) can vary between different oceans, the concentration ratio of the listed elements is stable (Memet, *op. cit.*). It can be seen that the dominance of chloride makes it the most significant anionic factor in marine and

maritime artefact corrosion. Sulphate anions are the next most abundant. The high concentration of dissolved salts makes seawater a highly effective electrolyte with high conductivity.

In seawater, salinity increases with the decrease in dissolved oxygen concentration. This means that salt concentration increases between the immersed zone and the mud zone potentially affecting the chloride content of some corrosion products formed on buried and partially buried artefacts (Memet, 2007: 155). Foley (1970: 59) reports that Vernon (1945) found a linear relationship between iron corrosion and oxygen pressure from 0 to 25 atm. Sub marine corrosion was shown to be inversely proportional to chloride concentration due to increased oxygen solubility at lower chloride concentrations. A build up of contaminants (e.g. calcium carbonate and other marine concretions), corrosion products, their surface morphology and the alloying and purity of the corroding iron will also influence the corrosion mechanisms, and their rates, in sea water, and post-recovery from the sea (North, 1982 & 1987; MacLeod, 1980, 1987 & 1989; Macleod *et al.*, 2004). Inter-relationship between individual corrosion parameters means that corrosion mechanisms are complex and varied. Distinction between maritime environments, aerated marine environments and sub-sea marine environments ceases to be of primary significance if the object is removed from these contexts, e.g. to a museum.

All wrought iron recovered from marine contexts will be significantly chloride-contaminated and potentially unstable post-recovery regardless of the depth etc. from which it came. Proximity to the sea in maritime areas is a significant factor in assessing the potential for chloride contamination of wrought iron from these contexts.

2.2.2. The burial environment as a source of chloride

Chloride ions are virtually ubiquitous. Chloride ions are present in terrestrial soils as well as in seawater, although in much lower concentrations, and are responsible for regulating the osmotic pressure and cation balance in plants (Zucchi *et al.,* 1977; Bunting, 1967: 134-8; FitzPatrick, 1974: 69-71 and 84). Other halide ions also promote corrosion but are far less common than chloride ions in nature (Foley, 1970). Turgoose (1982a, b and 1985) specifically addressed the problem of a mechanism for the post-excavation deterioration of archaeological chloride-contaminated wrought iron from terrestrial contexts but he also demonstrated that the corrosion of chloride-contaminated wrought iron from both terrestrial and marine contexts conforms to the same model once removed from the ground or the sea respectively. His model, which will be reported and analysed in section 2.6, explains the mechanism for the concentration of chloride ions within wrought iron artefacts which results in levels of chloride at the metal surface which greatly exceed the levels of chloride expected in most terrestrial (or marine) contexts.

2.3 *Electrochemical corrosion*

Electrochemical corrosion of wrought iron requires moisture, i.e. $H_2O_{(liquid\ state)}$ and is outlined by reaction [1].

	oxidation				
M	→	**M^{n+}**	+	**ne^-**	[1]
metal atom		metal cation		electrons	

oxidation process / anodic reaction

Metal ions are produced at anode sites and result in the loss of metal into the surrounding aqueous electrolyte solution. The electrons which are produced must be consumed by an electron acceptor at a cathodic site; usually the rate determining step in oxygen-rich environments. The ability of electrons to flow as a current through solid, conductive, iron corrosion products (such as magnetite or akaganéite) means that the cathodic site may be remote from the anode; often at the surface of a conducting corrosion product where the oxygen supply is greater (Donovan, 1986: 36, *fig. 3.4*). Where both moisture and oxygen are plentiful they combine and accept electrons to form hydroxyl ions which either diffuse into the (aqueous) environment or react with the cations to form insoluble corrosion products including oxides and hydroxides.

O_2	+	**$2H_2O$**	+	**$4e^-$**	→	**$4(OH)^-$**	[2]
Oxygen		water		electrons		hydroxyl ions	

reduction process / cathodic reaction

The cations either diffuse into the environment and disperse or combine with anions to form dissolved soluble products or insoluble neutral products. As the cations diffuse away from the anode they attract negative anions from the electrolyte solution which balance their charge. Chloride and sulphate anions are plentiful in the groundwater of many burial contexts and seawater (sections 2.2.1. and 2.2.2.) and high concentrations

of anions can accumulate at anodic sites on the surface of the iron (Suzuki *et al.*, 1973; Knight, 1990 and see section 2.6 of this thesis).

2.4 Atmospheric moisture and the corrosion of wrought iron

Corrosion of wrought iron may be influenced by the presence of chloride or other ions, hygroscopic or deliquescent salts, or chloride-bearing, or other, corrosion products which can attract water to form an electrolyte according to atmospheric moisture levels according to various mechanisms. Environmental moisture levels can influence both whether corrosion of wrought iron takes place for a given corrosion mechanism, and the rate at which it occurs (Turgoose, 1982a, b & 1985; Watkinson & Neal, 1998). Different moisture-dependent corrosion mechanisms require different levels of environmental moisture to occur. Low humidity and desiccated environments will draw water from electrolytes, hydrated corrosion products and corrosion products with surface-adsorbed water minimising its availability to promote further corrosion. The following sections identify and examine different corrosion mechanisms which require different levels of atmospheric moisture for them to occur. Where a humidity level below which corrosion does not occur, and/or above which corrosion does occur, is identified for a corrosion mechanism, this is termed the critical humidity or threshold humidity for corrosion occurring as a result of that mechanism.

Surface morphology is of great significance in determining rates of corrosion in reality. Microporous corrosion products can significantly increase times of wetness. Capillary condensation can cause the condensation of moisture far below the critical humidity value because of the differences in vapour pressure across a curved surface compared with a flat surface. A 1.5nm capillary will condense moisture at 50%RH whereas a 36nm capillary will condense moisture at 98%RH (Garverick, *op. cit.*). Micro-capillary pore size determines moisture adsorbing properties and this is utilised commercially, e.g. silica gel, whose micro-capillaries (so small that 1 teaspoon of silica gel has the surface area of a football pitch) adsorb or desorb water molecules until vapour pressure equilibrium is achieved with the relative humidity of the surrounding air (Weintraub, 2002). The lower the value of the environmental relative humidity, the lower the amount of

capillary condensation possible (with resultant corrosion). Electrolyte can form in micro cracks *and* in contact angles between dust particles or other overlying materials. Atmospheric corrosion of wrought iron can progress along internal planes formed during rolling, especially if exposed across its grain boundaries. Any soluble salts or their ions can further lower the saturated vapour pressure above them by forming a saturated solution, itself an electrolyte for electrochemical corrosion.

2.5 Corrosion of uncontaminated polished metal: Critical Humidity - the first corrosion threshold relative humidity

Water begins to adhere to an uncontaminated, polished, metal surface at an estimated 55%RH, forming a thin film which will increase in thickness as relative humidity increases (Garverick, 1994: 5). These, thin, water layers are able to support electrochemical corrosion but polarisation of the anode and cathode sites usually slows the process as film thickness decreases. As a result, corrosion all but ceases at about 60%RH – termed the "critical humidity" value (see the appended Glossary for a precise definition of this term). This value constitutes the most basic and fundamental criterion for ongoing iron corrosion under these conditions and the critical humidity could be considered to be the "first corrosion threshold". Above the critical humidity value corrosion can occur. Below the critical humidity value there is no water for electrolyte and electrochemical corrosion does not occur (Vernon, 1927 & 1935). Hudson and Stanners (1953: 91) collected meteorological data for Delhi, India, and found that the relative humidity at that location was below 70%RH (Vernon's critical humidity, *ibid.*) for most of the year. They concluded that the lack of corrosion of the iron Delhi pillar is primarily due to this factor rather than the composition of the iron of the pillar.

The corrosion rate reaches a maximum when the water film thickness exceeds 150µm (Garverick, 1994). In reality, few, if any, wrought iron surfaces in the historic environment are polished and no archaeological examples are! Contaminants or corrosion products alter the metal surface but, with the notable exception of chloride contamination, the critical humidity (or threshold humidity) for corroded iron otherwise

lies within the range of 60-70%RH (Donovan, 1986: 192). Garverick (*ibid.*) cites the critical humidity for iron as "about 60%RH" but notes a sharp increase in corrosion expected between 75%-80%RH due to capillary condensation of water within the corrosion product layer(s). A second increase in corrosion rate is cited at 90%RH, corresponding with the vapour pressure of ferrous sulphate where present (Garverick, *ibid.*).

2.6 The role of cations in the corrosion process: The counter-ion model for the accumulation of chloride ions during burial in the ground or contact with seawater

"The history of science convincingly shows that any theory is better than no theory. In the long run, any mistakes that are made reinforce their own correction by their incompatibility with experience. But if no attempt is made to understand nature, there can be no progress."

Forbes & Dijksterhuis (1963)

The unyielding retention of chloride ions by metallic wrought iron artefacts, despite scores of years of research dedicated to developing chemical washing methods aimed at optimising their removal (Watkinson and Lewis, 2004: *table 2*; Watkinson, 1982; Watkinson and Al-Zahrani, 2008; Selwyn & Logan, 1993; Scott & Seeley, 1986; Selwyn *et al.*, 2001), has made chloride-contaminated wrought iron one of the most unstable materials in museum collections and the historic environment.

Problems accessing and removing chloride ions due to surface morphology (with overlying corrosion products, micro-capillaries, etc.) have been cited as one of the obstacles to the total removal of chloride and, therefore, the total stabilisation of the artefacts through aqueous washing techniques (Selwyn *et al.*, 1999). Attempts to identify a "safe" or "threshold" relative humidity for the storage of chloride-contaminated wrought iron have been criticised because of the complexity of

contributions (many synergistic) of multiple variables given that it is only possible to initially study and quantify the behaviour of one unknown in any equation (or process) at a time. However, if no attempt is made to understand each of the identified factors it will not be subsequently possible to identify their relative contributions to corrosion when measuring the overall corrosion rate (e.g. by measuring corrosion current or weight gain etc.).

To understand the role of chloride ions (Cl^-) in iron corrosion and their unyielding retention by wrought iron objects it is necessary to consider the corrosion models proposed for archaeological wrought iron from terrestrial contexts (Turgoose, 1982a and b, 1985a; Knight, 1982; Selwyn *et al.*, 2001) and wrought iron from marine contexts (additionally North, 1987; North & McCleod, 1987). These corrosion models offer an explanation for the very strong attraction between chloride ions and the surface of the remaining metal which prevents their effective removal through aqueous washing.

Wrought iron corrodes electrolytically: metallic iron oxidises to positive ferrous cations (iron as Fe^{2+} / Fe(II) but actually dissolved in and hydrated by water $[Fe(H_2O)_6]^{2+}$) or ferric (Fe^{3+} / Fe(III)) cations at anodic sites on the metal surface. These ferrous/ferric ions create an overall positive charge that is counterbalanced by negative ions attracted towards them from the surrounding environment. Chloride ions, being negatively charged, of very small radius, and highly mobile, move towards the positive ferrous ions at the anodic sites on the metal surface of corroding wrought iron (Foley, 1970). Weil and Menzel (1959 and 1960) demonstrated the diffusion of radioactive bromide ions through overlying corrosion products (by way of dislocations) to accumulate at the pitting site on the metal surface, accelerating the movement of Fe^{2+} ions outwards. At or very near the metal surface the ferrous ions and chloride ions form a highly conducting solution (Turgoose, 1982a). This concentration of chloride ions persists as long as anodic solid metallic iron is present to produce ferrous ions and water is present to transport and hydrate the ions.

Turgoose (1985a and 1993) argues for oxygen reduction rather than hydrogen evolution (Selwyn *et al.,* 1999: 218) giving

$$Fe + ½O_2 + H_2O \leftrightarrows Fe^{2+} + 2OH^- \qquad [3]$$

$$Fe + ½O_2 + 2H^+ \leftrightarrows Fe^{2+} + H_2O \qquad [4]$$

Within the corroding ironwork the accumulated chloride ions are retained as counter ions to the positive Fe^{2+} ions (Turgoose, 1985b; Knight, 1990). Chloride concentrations of up to 6M are reported to have been observed experimentally within anodic pits on stainless steel (Suzuki *et al.* 1973 and *c.f.* figures 8 and 9 of this thesis). Citing Turgoose's (1982b) observation that North's (1976) measurements of pH 4.7-4.8 on objects from under the sea implied a chloride [ion] concentration of 3-4M, Knight (1990: 37) notes an increase in concentration by a factor of approximately ten over the normal value of sea water and an increase by a factor of several thousand over the concentration of chloride in soils. A saturated solution of $FeCl_2$ is about 4.25M and has a pH of about pH4 (Selwyn *et al.*, 1999: 219). McCleod (1989: 227 and *fig. 1*) reported $FeCl_2$ concentrations up to 0.6M and typical pH values of 4.8 for marine iron, though pH is sometimes as low as 4.2 as a result of hydrolysis reactions such as [9] and [11] (section 2.8.1.). Degrigny and Spiteri (2004) confirm McCleod's pH of 4.8 at the metal surface, specifically anodic corrosion pits, for marine wrought iron and also at the metal/graphitised zone interface for marine cast iron artefacts. This compares with a pH of 8.2 ±0.2 for seawater.

Metallic iron must be present to form the anode to provide the source of ferrous (Fe^{2+}) ions which electrically attract the chloride (Cl^-) counter-ions beneath the overlying corrosion products (Watkinson, 1983). If the artefact becomes completely mineralised no more iron enters into solution (no anode) and the role of the counter ion is redundant. The soluble and highly mobile chloride ions diffuse away or react to form corrosion products.

Analyses of polished cross sections of archaeological iron confirm that chlorides concentrate at the metal surface, usually deep within anodic pits and crevices, and this helps explain why complete removal of chlorides is never achieved (Watkinson 1983 and 1996; Mathias, 1996: 124; Neff *et al.,* 2004 and 2005; Réguer *et al.,* 2007; Thickett and Odlyha, 2007; Watkinson & Al-Zahrani, 2008: 78, *fig. 1*). Some ferrous ions combine with oxygen and are oxidised to form a layer of insoluble iron corrosion products over the dissolved chloride and ferrous ions that are concentrated at the metal surface. The strong attraction between ferrous ions and chloride ions means that chloride ions are very difficult to remove from their location at the metal surface. Where chloride ions are concentrated in pits and fissures within the metal and beneath the corrosion layers, surface morphology provides additional obstacles to effective removal. In theory, removal of chloride ions could be achieved by stopping corrosion of the iron (e.g. stopping anodic production of Fe^{2+} ions or stifling the cathode reaction by removing oxygen) and providing an aqueous system for solvation and diffusion of the chloride ions (Pearson, 1972; North and Pearson 1975 and 1978; Rees-Jones, 1972; Gilberg & Seeley, 1981; Rinuy & Schweizer, 1981 and 1982; Keene, 1994; Watkinson and Al-Zahrani, 2008). Attempts (by many workers) to remove all chloride ions from chloride-contaminated wrought iron (using many different aqueous washing methods) have so far proved unsuccessful (Knight, 1997).

Chloride ions are also known to accelerate the corrosion of iron by interfering with the establishment and maintenance of passive films on iron (Vernon, 1927) because of their high charge density, capacity to form soluble species and their high degree of mobility due to their small size; which explains their ability to enter an oxide film (Foley, 1970; Selwyn *et al.*, 1999: 220; Scully, 1990: 111).

2.7 Corrosion post-recovery from ground or the sea: Salt deliquescence as a source of electrolyte - the second corrosion threshold relative humidity

The contamination of wrought iron by dissolved salts in the ground or in the sea can result in the presence of solid crystalline salts upon drying after recovery. Salts commonly have the potential to attract water to themselves and deliquesce (dissolve to become a solution of ions in the water they have attracted) to provide a highly corrosive electrolyte solution where one otherwise might not exist (and electrochemical corrosion would otherwise not proceed) (Charlson *et al.* 1978: 45 and see table 2 of this thesis). A saturated salt solution (e.g. $FeCl_2$) will continue to absorb atmospheric moisture from an environment maintained at a relative humidity much higher than the deliquescence point of that salt (Amorosso & Fassina, 1983: 115-117; Wallert, 1996). The saturated salt solution will become more and more diluted as RH rises and more and more atmospheric water is absorbed (figure 4).

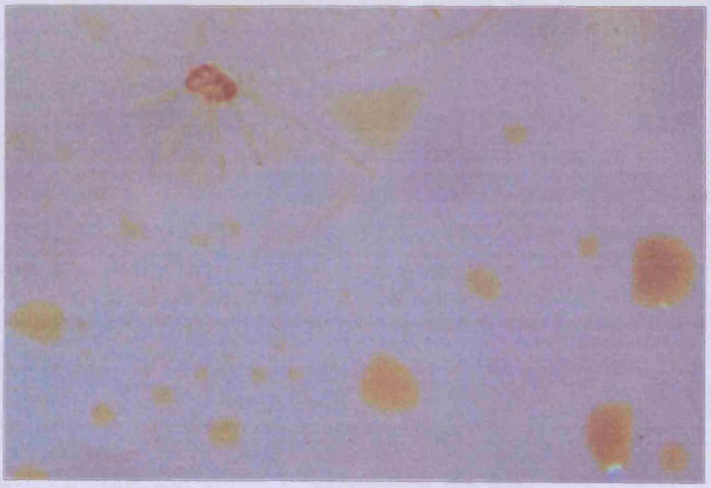

Figure 4. **Photomicrograph of saturated ferrous chloride solution ($FeCl_{2(aq)}$) droplets created by exposing individual $FeCl_2.4H_2O$ crystals to a relative humidity of 60%RH for one day (See also appendix 4, sample 7).**

Compound	R.H.%
$MgCl_2$	33
NH_4HSO_4	30-40
$NaNO_3$	64
$(NH_4)_3H(SO_4)_2$	81
NaCl	75
$(NH_4)_2SO_4$	85-93
$MgSO_4$	91
$ZnSO_4.7H_2O$	87

Table 2. **Salt bulk deliquescence points after Charlson *et al.* (1978: *table 2*). Temperatures not cited but comparison with other data supports temperatures of 20°C (*c.f.* Marsh, 1987: 160, *table 7.3.1.*).**

Water is adsorbed on surfaces at temperatures above the dew point (the point at which surface condensation occurs – see glossary) because of the affinity of salts for water. This hydrophilic property of salts is termed hygroscopicity and substances that attract water are termed hygroscopic. Johnson (1998) states that a saturated solution of sodium chloride will be hygroscopic and will adsorb moisture up to 6°C above the dew point; the vapour pressure of a saturated sodium chloride solution at 33°C is the same as water at 27°C. Thus, when the wet bulb temperature is 27°C, a surface covered with sodium chloride must be 6°C warmer (i.e. 33°C) to avoid condensation (*ibid.*, 622/2 and see Wallert, 1996: 200, *fig. 4*). Maintaining temperatures above this figure would be an effective way to prevent corrosion of halite-contaminated wrought iron that would form an electrolyte due to the deliquescence of solid sodium chloride at lower temperatures.

Wet bulb temperature is determined by the rate of evaporation of pure water from an uncontaminated cotton sock surrounding the bulb of a conventional mercury thermometer and is the primary standard for the measurement of relative humidity (RH). The rate of evaporation (and the resulting cooling, or depression, of the wet bulb thermometer) is determined by the moisture content of the environment compared with the total amount of moisture that can exist as vapour at a given ambient

temperature (measured by an ordinary, unmodified, dry bulb, thermometer). The 6°C or more difference between the wet bulb temperature and the dry bulb (ambient temperature) necessary to prevent condensation at 27°C places this condition on the 60%RH curve of the psychrometric chart (see figure 74). Plotting changes in wet bulb temperature, but maintaining a 6°C difference between this and the dry bulb temperature, produces a curve which reasonably closely approximates that of the 60%RH percentage saturation curve between ~20°C and ~40°C, but deviates from it increasingly at lower wet bulb temperatures. The formation of electrolyte due to hygroscopic salts is therefore closely related to the atmospheric relative humidity between about 20°C and about 40°C but with increasing deviation at lower wet bulb temperatures. This study will establish whether chloride-bearing corrosion products, especially hydrated ferrous chloride, contribute water to form electrolyte for the corrosion of chloride-contaminated wrought iron in a similar way.

Usefully, Charlson *et al.* (1978) provide a figure (copied here) that shows the two types of hygroscopic properties characteristic of salts and their effect on mole fraction, in this case, of sulphates (figure 5). H_2SO_4 exhibits a monotonic curve characteristic of simple hygroscopic behaviour where absorption and desorption are in continuous equilibrium through the full range of relative humidities. However, NH_4HSO_4 and $(NH_4)_2SO_4$ exhibit step-changes at 39% and 81% relative humidity respectively with monotonic curves at higher relative humidities only. This sudden uptake of water when the relative humidity exceeds a certain level is termed deliquescence and this phenomenon is demonstrated by many inorganic compounds, mainly salts, and some organic compounds. The deliquescence point - the relative humidity at which a compound deliquesces – is defined as the ratio of water vapour pressure above a plane surface of a saturated solution of the compound to the vapour pressure over a plane surface of pure water. The reverse process, a sudden release of water, with decreasing relative humidity is termed efflorescence, being the crystallisation of the solid.

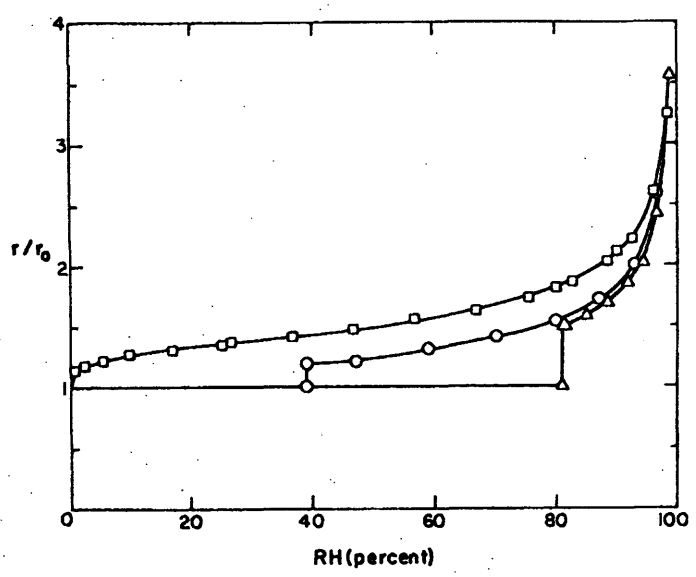

Figure 5. **Theoretical growth curves based on vapour pressure data for three sulphate aerosols exposed to increasing humidity**

□ H_2SO_4 ○NH_4HSO_4 △$(NH_4)_2SO_4$

after Charlson *et al.* (1978: 45, *Fig. 3*)

Hygroscopic/deliquescent compounds equilibrate rapidly with their environment and exhibit changes in size (and other properties) in response to relative humidity changes (Charlson *et al., op. cit.*: 45). Strictly hygroscopic substances (in their case studied as aerosols) exhibit monotonic growth curves whilst deliquescent substances (again, studied as aerosols) remain dry below the deliquescence point but grow suddenly, forming hygroscopic solution droplets, above that point. They published theoretical growth with increasing relative humidity curves for some sulphate compound aerosols and these are included here for comparative purposes for it is anticipated that the behaviour of deliquescent salts studied for this research will conform to one or more of these types of behaviour (figure 6).

Corrosion will be rapid in the presence of the hygroscopic, ionic, solutions present above the deliquescence point. Conversely, it would be reasonable to expect no promotion of wrought iron corrosion by solid salts at relative humidities below their respective deliquescence points, but this is not always the case. Furthermore, whilst deliquescence points are well defined when subjected to increasing relative humidity

from a dry, crystalline state, efflorescence and efflorescence points are not. Most compounds remain in solutions at concentrations higher than that of their saturation point and therefore at relative humidities well below the deliquescence point. This phenomenon of hysteresis is described by Orr *et al.* (1958), Junge (1963) and Winkler and Junge (1972).

Early research (Chandler, 1966; Chandler and Stanners, 1966 and Evans and Taylor, 1974) investigated the effect of solid and deliquesced salts (especially chloride-containing salts) on iron and reported that corrosion was much more aggressive above a salt's deliquescence point but that corrosion was **not** prevented beneath it. Sodium chloride deliquesces at 75%RH (Charlson *et al.*, 1978)[1] at ambient temperatures forming a powerful electrolyte for electrolytic corrosion cells where in contact with metallic iron. In the open air in the British Isles, or in damp, unheated, buildings, wrought iron will exist in environments at, or above, the deliquescence point of NaCl for much of the year (Vernon, 1927: 117).

[1] Or 76%RH (Michalski, 1993). Small differences of this magnitude are due to differences in temperature which are commonly not cited with the RH data.

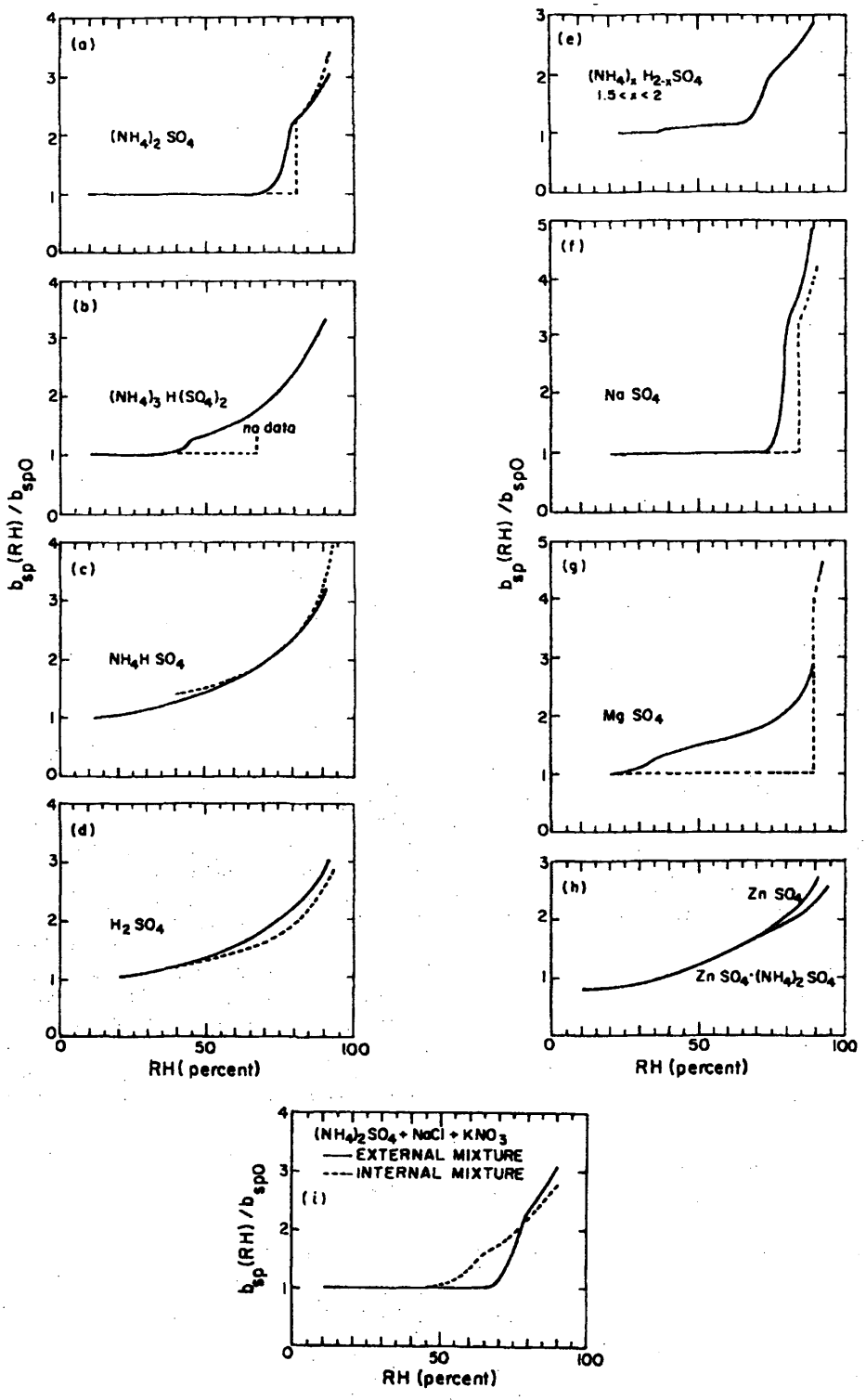

Humidograph data for pure, laboratory generated sulfate compounds. (a) $(NH_4)_2SO_4$. (b) $(NH_4)_3H(SO_4)_4$. (c) NH_4HSO_4. (d) H_2SO_4. (e) $(NH_4)_xH_{2-x}SO_4$ $1.5 < x < 2$. (f) $NaSO_4$. (g) $MgSO_4$. (h) $ZnSO_4$ and $ZnSO_4 \cdot (NH_4)_2SO_4$. (i) $(NH_4)_2SO_4 + NaCl + KNO_3$ internal vs external mixture. Except in (i) dashed curve is calculated.

Figure 6. **Humidograph data for pure, laboratory-generated, sulphate compounds showing hygroscopic/deliquescent behaviour (where $b_{sp}(RH)/b_{sp0}$ is a measure of hygroscopic growth [the increase in volume of the aqueous salt solution] based upon the light scattering coefficient of the particle matter, b_{sp}) after Charlson *et al.* (1978: 47, *Fig. 4*).**

Whilst some authors (Chandler, 1966, Evans and Taylor, 1974, Thickett, 2008a and b) suggest that corrosion of sodium chloride or chloride-contaminated iron is *"inappreciable"* or *"almost stopped"* beneath figures as high as 30%RH or 40-42% RH, this term is relative and does not indicate that corrosion/deterioration has ceased. The conservation goal of 'no active corrosion' (section 1.2) is not indicated by these terms. Further research has questioned the concept of *"inappreciable"* corrosion and has described corrosion processes in more detail (Evans and Taylor, 1974 and Turgoose, 1982b). Additionally, the effect of combining mixtures of deliquescent salts may produce a synergistic (combined) effect that lowers the deliquescence point below that of the lowest member of the mixture (Price and Brimblecombe, 1994; Padfield *et al.*, 1982).

Bukowiecki (1957 & 1966 with Joshi) confirmed Vernon's (1927 & 1935) findings that humidity levels must exceed a critical value for a given salt or salt mixture for aggressive, electrochemical corrosion to proceed. In most cases, Bukowiecki (*ibid.*) found that the critical relative humidity value is close to the saturated vapour pressure of a saturated solution of the salt in question. Where differences between observed saturated vapour pressures and those cited in literature were observed, this was due to the cited saturated vapour pressure referring to a flat surface of liquid rather than the high surface tension effect in capillaries and micro-capillaries as found in reality in corrosion products. Salt impurities also depress the effective value of the critical humidity of the most abundant salt (e.g. small amounts of magnesium chloride ($MgCl_2$) i.e. Mg^{2+} ions in solution, greatly lower the critical humidity of a mixture with larger concentrations of sodium chloride NaCl from that critical humidity expected for a saturated solution of sodium chloride alone, see Evans and Taylor, 1974). These and other complex relationships, synergistic effects and morphological factors have been cited as being obstacles to developing a model for a corrosion "threshold relative humidity" for the "safe" storage of chloride-contaminated wrought iron via desiccation.

Exposure to rainwater or programmed washing could help to stabilise chloride-contaminated iron by carrying away accessible harmful soluble contaminants. In theory, archaeological iron artefacts could be washed predictably to free soluble salts

under controlled, monitored and reproducible laboratory conditions. This is true for loosely associated deliquescent salts or adsorbed contaminants but this is not the case for chloride ions bound firmly as counter ions (see section 2.6) as demonstrated by experience and analysis (Watkinson, 1996; Watkinson & Al-Zahrani, 2008; Keene, 1994; Knight, 1997; Watkinson and Lewis, 2004).

2.8 Post-marine and post-excavation deterioration due to the continued corrosion of chloride-contaminated wrought iron

2.8.1. Ferrous chloride

Because the chloride counter-ion model is applicable to iron and steel of marine, terrestrial archaeological and (meteoric) geological origin (Turgoose, 1982a and b; Selwyn *et al.* 1999; North, 1987; Buchwald and Clarke, 1989; Howie, 1992), research in each of these, usually independent, fields of conservation and corrosion science may inform the others, so they were all studied and informed this research.

Relative concentrations of chloride counter ions and anodically produced ferrous ions increase upon drying, as water content falls. This causes a pH drop (acidity) at anodic areas due to hydrolysis reactions [5] and precipitation of hydroxides [6] with the effect of increasing the rate of dissolution (corrosion) at the metal surface (Turgoose, 1985a).

$$Fe_2^+ + H_2O \leftrightarrows Fe(OH)^+ + H^+ \qquad [5]$$

$$Fe(OH)^+ + H_2O \leftrightarrows Fe(OH)_2 + H^+ \qquad [6]$$

The concentration of chloride ions coupled with low pH makes the formation of solid ferrous chloride thermodynamically possible if sufficiently low relative humidity values prevail (figure 10, *c.f.* figure 7 and see Turgoose, 1982b). Pourbaix (1966) interpreted corrosion in terms of the potential-pH diagrams used in geochemistry and the Pourbaix diagrams included here indicate the theoretical thermodynamic environmental criteria for corrosion or preservation, and for the occurrence of different corrosion compounds, for the iron in sea-water system (figures 7 and 10). The Pourbaix or potential-pH diagrams for the iron-water-chloride system predict that ferrous chloride is only a stable solid below pH2. But this is more acidic than has been measured, or would be expected, in objects prior to their recovery from the sea or the ground (Turgoose, 1982b: 4).

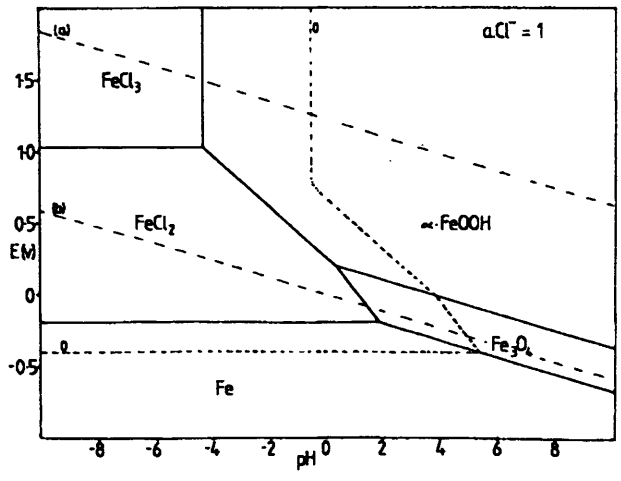

Figure 7. **Potential-pH diagram for the iron-water-chloride system at a chloride ion activity of 1 (1M) where the solid lines represent the boundaries between the stability fields for the solids and the contour line for Fe^{2+} = 1 is shown (a). After Turgoose (1982a, *fig. 4*).**

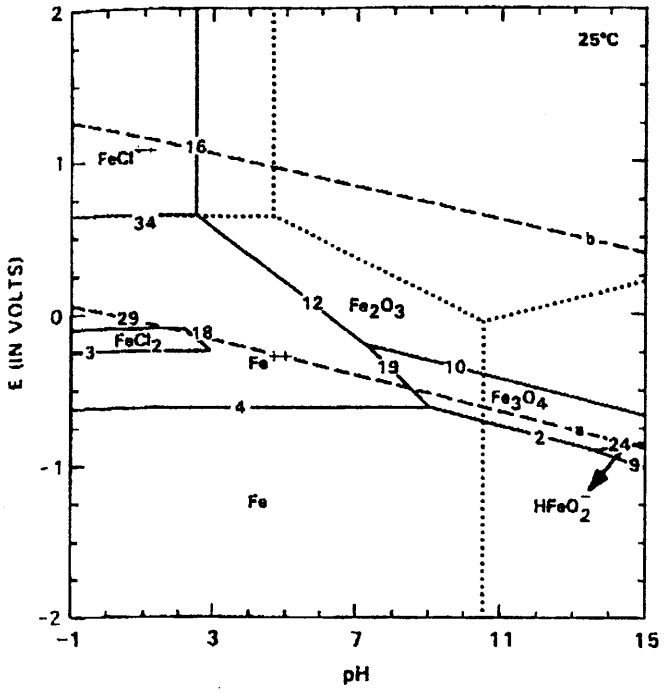

Figure 8. **"Pourbaix" or Potential-pH diagram for the Fe-Cl^- - H_2O system at 25°C for a saturated NaCl solution in which the Cl^- concentration is 5.6M. After Kesavan *et al.* (1989 and 1990).**

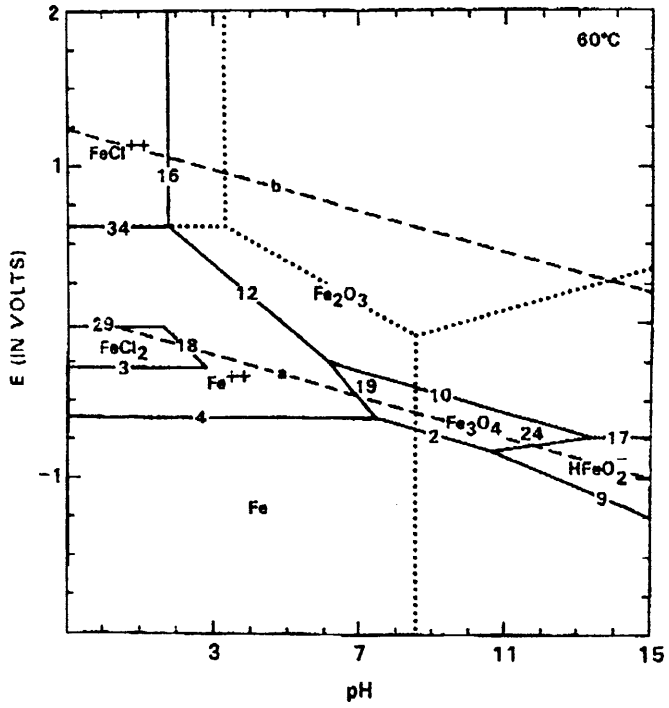

Figure 9. **"Pourbaix" or Potential-pH diagram for the Fe-Cl^- - H_2O system at 60°C for a saturated NaCl solution in which the Cl^- concentration is 5.72M. After Kesavan *et al.* (1989 and 1990).**

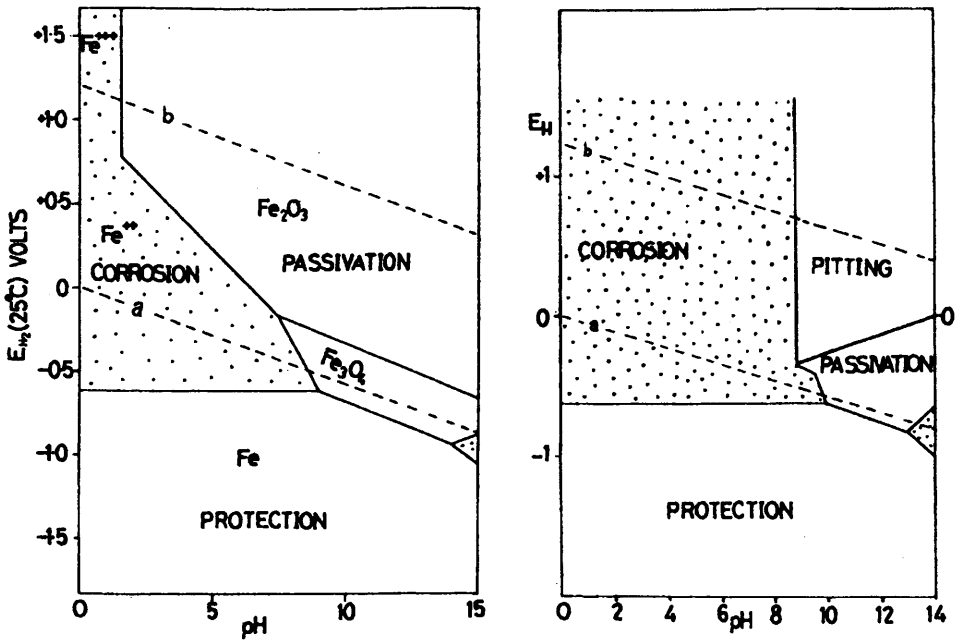

Figure a. Equilibrium potential – pH, or Pourbaix diagram, for iron – pure water system at 25°C.

Figure b. Pourbaix diagram for iron – 1M NaCl system at 25°C.

Figure 10. **"Pourbaix" or Potential-pH diagrams for the iron – pure water system (a) and the iron 1M sodium chloride system (b) at 25°C. After North & Pearson (1975a: 181, *fig. 5*).**

Whilst "passivity" predicts that insoluble corrosion products may be formed this does not guarantee that corrosion has ceased, merely that passivation is theoretically possible. Many insoluble corrosion products are not protective and do not prevent further corrosion; e.g. being conductive, acting as electron conveyors, or forming non-cohesive masses (enabling continued environmental access to the cathode, as opposed to compact, coherent, layers that could be potentially protective).

The Pourbaix diagrams presented here make the following general predictions possible. Under near ambient temperatures in seawater corroding iron is predicted to exist as ferrous (Fe^{2+}) ions for a significant range of potentials at pHs lower than pH 7. It is common for pH to fall markedly below pH 7 within corrosion pits at the metal's surface (section 2.6). Many of the insoluble corrosion products of iron are highly soluble in hydrochloric acid (HCl) and are unable to precipitate where acidic solutions (often pH<1) containing very high Cl^- concentrations are present (Turgoose, 1982b: 98).

Low potential alkaline environments, as would be expected where oxygen levels are low, will favour ferrous, i.e. iron (II), corrosion products and magnetite (Fe_3O_4). Where oxygen is plentiful the redox potential (E_H) is higher and iron is predicted to be present in the more oxidised ferric, i.e. iron (III), form e.g. αFe_2O_3 (haematite) and iron (III) oxyhydroxides (e.g. αFeOOH – goethite, βFeOOH –akaganéite or γFeOOH-lepidocrocite).

The thermodynamic effect of differences in temperature accounts for the differences between figures 8 and 9 but potential-pH diagrams do not predict rates of reaction.

Thickett and Odlyha (2007) excavated corrosion pits in freshly excavated wrought iron artefacts and observed pale yellow crystals (using optical microscopy) at the bases of the pits on the magnetite layer. Analysis with confocal Raman spectroscopy (Renishaw Raman System 1000 using a 514.5 Spectra-Physics argon ion laser) confirmed these to be ferrous chloride. Knight (1982: 51) cites Wyles and Biek (in press in 1982) as having identified crystalline $FeCl_2.4H_2O$ on an iron object. If sufficiently dry conditions are not achieved, then highly concentrated chloride bearing electrolytes can exist at the metal surface. Turgoose's model for post excavation corrosion of archaeological wrought iron

(1982a, b & 1985a) proposed that the ferrous chloride solution concentrates on drying, pH falls and, if water is removed, between 12°C and 72°C the solid that crystallises will be ferrous chloride tetrahydrate ($FeCl_2.4H_2O$). Similar localised chloride concentration is noted for the graphitised region of cast iron also (North, 1982; Degrigny & Spiteri, 2004; Weizhen & Chunchun, 2005).

If exposed to moist air, with oxygen readily available, ferrous ions oxidise in solution: a brown solid and a yellow solution are formed (figure 11):

$$4Fe^{2+} + O_2 + 6H_2O \leftrightarrows 4FeOOH + 8H^+ \qquad [7]$$

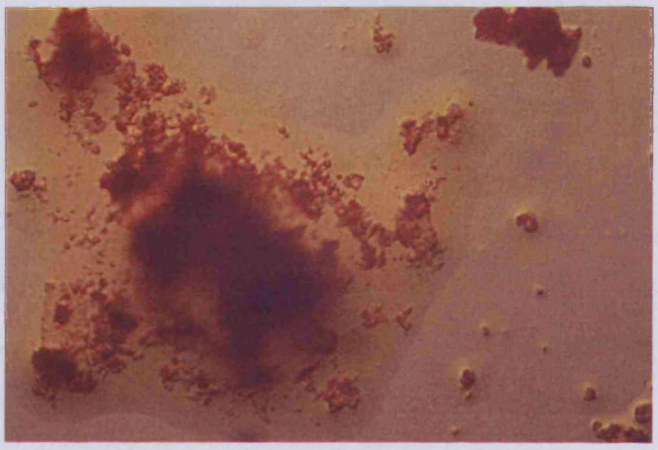

Figure 11 **Ferrous chloride$_{(aq)}$ with βFeOOH produced via aerial oxidation by the author at Cardiff University.**

Solid iron oxide hydroxides precipitate and the solution becomes more acidic causing further, cyclic, corrosion. Gilberg and Seeley (1981) report that where HCl is of greater concentration than 1N and exposed to high humidity crystals of $FeCl_2.4H_2O$ form first. After some time a solid membrane covers the ferrous chloride. The solid is βFeOOH (akaganéite) and the solution contains ferrous, ferric and chloride ions with a pH of 0.4-0.9, i.e. less than pH1 (Turgoose, 1982b: 98). Gilberg and Seeley (*ibid.*) reported that at NaCl concentrations greater than 1N βFeOOH (akaganéite) is the only iron corrosion

product formed, whereas below 1N αFeOOH and γFeOOH are also formed. Refait and Genin (1997) estimated that Cl^- levels of 2 to 3.6M are necessary for βFeOOH formation. In Turgoose's model chloride ions increase the conductivity of the electrolyte and the ferrous chloride solution attracts more water because it is hygroscopic, but the chloride ions are not cyclically consumed. The chloride ions balance the charges of the ferrous ions in solution.

$$2Fe_{(s)} + 4H^+_{(aq)} + 4Cl^-_{(aq)} + O_{2(g)} \leftrightarrows 2Fe^{2+}_{(aq)} + 4Cl^-_{(aq)} + 2H_2O \quad [8]$$

$$2Fe^{2+}_{(aq)} + 4Cl^-_{(aq)} + 3H_2O + \tfrac{1}{2}O_{2(g)} \leftrightarrows 2FeOOH + 4H^+_{(aq)} + 4Cl^-_{(aq)} \quad [9]$$

Askey *et al.* (1993) also suggest a prominent role for the chloride ions in solution. Their model was for iron contaminated with hydrochloric acid (HCl) and was summarised as

$$2Fe_{(s)} + 4HCl_{(aq)} + O_{2(g)} \leftrightarrows 2FeCl_{2(aq)} + 2H_2O \quad [10]$$

$$2FeCl_{2(aq)} + 3H_2O + \tfrac{1}{2}O_{2(g)} \leftrightarrows 2FeOOH_{(s)} + 4HCl_{(aq)} \quad [11]$$

Selwyn *et al.* (1999) and Selwyn (2004: 296) claim that this model gives chloride ions a more direct role in the corrosion process, producing HCl. Askey *et al.* (1993) called this model the "*acid regeneration cycle*" because the acid used up in the initial solution is regenerated upon the oxidation of the ferrous chloride to form oxide hydroxides (oxyhydroxides). Askey *et al.* (*ibid.*: 246) reported that mild steel reacts directly with gaseous atmospheric HCl, even at relatively low concentrations, giving ferrous $chloride_{(aq)}$ ($FeCl_2$) which then oxidises to give iron (ferric) oxyhydroxide (FeO(OH) or FeOOH), magnetite (Fe_3O_4) or haematite (Fe_2O_3), liberating its chloride as HCl, depending on humidity and oxygen access which is itself dependent on scale thickness. $FeCl_2$ in the presence of lepidocrocite (γ-FeO(OH)) were identified as the corrosion products by X-ray diffraction. βFeOOH was not identified.

Turgoose (1982b: 98) stated that one of the specific effects of chloride as opposed to other ions is that *"they will aid the dissolution of iron oxides which occurs faster in HCl*

than in say H_2SO_4" noting that *"even if no solution is visible, a pH<1 can be measured at the points of formation of the reddish brown powder* [βFeOOH] *with sufficient water to moisten the surface if necessary" (ibid.*: 97). Turgoose (1985b) implies residual hydrochloric acid (HCl) where ferrous ions and chloride ions (and water) comprise the electrolyte.

Regardless of the emphasis placed upon the chloride ions in the above models, chloride ions produce soluble ferrous chloride which allows both models to proceed cyclically. Ferrous $chloride_{(s)}$ and ferrous $chloride_{(aq)}$ may oxidise to form akaganéite (βFeOOH). Selwyn *et al.* (1999) note that if the chloride bearing salt was insoluble, it would form as a precipitate and the cycle would be broken. The ferrous chloride solution and its potential oxidation products are therefore central to any model for the corrosion processes observed for wrought iron following excavation or recovery from the sea. Understanding their possible roles in corrosion and identifying their properties relative to ambient environments are critical to the model for any storage system based on environmental control.

2.8.2. βFeOOH [Akaganéite]

Aerial oxidation of the ferrous and chloride ion solution (or hydrated solid ferrous chloride tetrahydrate) forms the voluminous chloride bearing corrosion product akaganéite (βFeOOH) and other FeOOH polymorphs, including αFeOOH (goethite) and γFeOOH (lepidocrocite), depending on pH and chloride concentration (Argo, 1981a; Refait and Genin, 1997 and with Olowe, 1993). The corrosion product βFeOOH (akaganéite) *is* expected to be present on chloride-contaminated wrought iron corroding in the atmosphere because βFeOOH is formed when damp $FeCl_2.4H_2O$, or concentrated ferrous chloride solutions and ferric chloride solutions (characterised by "weeping") slowly oxidise in air (Mackay, 1960; Keller, 1969; Argo, 1981; North, 1982; Selwyn *et al.,* 1999; Selwyn, 2004).

Wang (2007b) reported the formation of akaganéite bubbles, oxidised from deliquesced ferrous chloride tetrahydrate, on iron foil at 75%RH but the formation of elongated akaganéite crystals (like those shown in figures 18 and 19) on iron foil in the presence of solid ferrous chloride tetrahydrate at 54%RH. Maeda *et al.* (1992) confirmed the expected presence of βFeOOH on nails collected at the 'sea coast' and Refait *et al.* (1992) demonstrated its presence on "refurbished", i.e. cleaned, museum objects from Mauritania. Whilst other iron oxyhydroxides will be abundantly present on corroded wrought iron and are acknowledged to play a role in the corrosion or passivation of metallic iron (Misawa *et al.*, 1974), βFeOOH (akaganéite) has been expected to contribute to the corrosion processes far more significantly than the others. This is because of its association with chloride (and other halide) ions which are integral to the structure of βFeOOH such that it can not form or exist without their stabilising its hollandite, tunnel-like, crystal lattice (Mackay, 1960; Gallagher, 1970; Zucchi *et al.*, 1977; Childs *et al.*, 1980; Stahl *et al.*, 2003). Kaneko *et al.* (1975), Ishikawa *et al.* (1986 and 1988), Naono *et al.* (1993) and others reported that water molecules also occupied the tunnels but this is no longer accepted (Stahl *et al.*, 2003). Childs *et al.* (1980) predicted that the cavities which form the tunnels of βFeOOH could theoretically contain spheres of a diameter of up to 3.5Å. They noted that the diameter of the chloride ion is very close to the calculated diameter of the cavities in βFeOOH at 3.6 Å. The chloride sits within the tunnel-like cavities in every second cavity down the tunnel but with only two thirds occupancy of the potential Cl^- sites where the remaining one third are vacant (Childs *et al., ibid.* & Stahl *et al.*, 2003). The cavity necks are only 2.7 Å in diameter so chloride ions are held in the tunnels, unable to be released without breaking down the βFeOOH.

2.8.3. Fe (II) compounds similar or related to βFeOOH

Iron sulphate and nitrate compounds having the akaganéite structure were reported in the 1990's (Schwertmann & Cornell, 2000). The sulphate form (schwertmannite) occurs naturally as an oxidation product of pyrite and has sulphur in place of chlorine in its tunnels. Yabuki and Makoto (1979: 77) reported βFeOOH containing 3.5wt% Cl and

0.3wt% sulphur on archaeological artefacts from tombs in central Japan that had been in museum storage for 50 years. Mechanisms involving akaganéite, and its potential metastability, may be applicable to this mineral or *visa versa*. Pyrites can be encountered where archaeological iron has been retrieved from terrestrial or marine anaerobic deposits characterised by sulphate reducing bacteria that produce hydrogen sulphide (Ottar & Haagenrud, 1975; Duncan & Ganiaris, 1987, Goodburn-Brown, 1996). Metal sulphides are generally less stable than the corresponding oxides at ambient temperatures. Decomposition may produce hydrated iron oxide, oxides of sulphur sulphates and sulphuric acid. Howie (1977 & 1978) showed that pyrite stability is related to its structure and relative humidity. Fell and Williams (2004) identified sulphur-bearing corrosion products as the dominant components of the DPL on artefacts excavated at Fiskerton in 2001 and analysed by XRD in 2004. These included greigite (Fe_3S_4), mackinawite ($Fe_{1+x}S$) and pyrite (FeS_2) with the carbonate siderite ($FeCO_3$) but the SEM micrographs they presented did not show concentration of the sulphur-bearing compounds at the metal/DPL interface. They reported that the presence of iron sulphides *"...was concluded to be one factor in the **unusual** preservation of some of the ferrous artefacts..."*. Walker (2001) described the instability of iron sulphides on recently excavated artefacts but the presence of sulphides is only favoured by some, mostly anaerobic, burial environments (Duncan and Ganiaris, 1987).

In the absence of reports of post-excavation or post-recovery deterioration wrought iron being dominantly due to sulphate bearing corrosion products, including schwertmannite, from other, mostly aerobic, environments, sulphur-bearing corrosion products will not be further discussed or studied here (Argo, 1982; Buchwald & Clarke, 1987; Dillmann *et al.*, 2004; Selwyn *et al.*, 1999; Cronyn, 1990: 194-5). Samples of corrosion removed from the chloride-contaminated wrought iron hull of the ss Great Britain at the metal/DPL interface where the DPL had been lost due to spalling were analysed and confirmed as the chloride-bearing βFeOOH (Watkinson and Lewis, 2004 and figure 32). The prominent role of βFeOOH in the post-recovery physical deterioration of marine and archaeological chloride-contaminated wrought iron makes ferrous chloride and this corrosion product the focus for this study.

Réguer *et al.* (2007) have, only recently, demonstrated that unstable Fe (II) compounds such as $Fe(OH)_2$ and β-$Fe_2(OH)_3Cl$ (ferrous hydroxychloride) can precipitate where low oxygen levels prevail (Refait & Genin, 1997) at or near to the metal surface. Using the high resolution synchrotron technique μXANES (micro-X-ray absorption near edge structure experiments) Réguer *et al.* (*ibid.*) demonstrated the simultaneous presence of both β-$Fe_2(OH)_3Cl$ (containing 20 mass % Cl) and β-FeOOH (containing 8 mass % Cl) within the DPL at the metal/DPL interface or very near to the metallic core of the artefacts. β-$Fe_2(OH)_3Cl$ (ferrous hydroxychloride) was only found to be present in recently excavated samples and Réguer *et al.* (*ibid.*) argued that increased oxygen levels on exposure to the atmosphere provokes the disappearance of Fe(II) phases and the formation of akaganéite (βFeOOH). Misawa *et al.* (1974) demonstrated that in aqueous solution β-$Fe_2(OH)_3Cl$ (ferrous hydroxychloride) oxidises to the unstable intermediate chloride-rich Green Rust 1 ($GR(Cl^-)$) before oxidising to akaganéite (βFeOOH) as the localised chloride concentration at the metal/DPL interface increases to at least 2 or 3 $moll^{-1}$ (Refait and Genin, 1997). Thickett (2005) reported that corrosion of iron discs buried in cristobalite sand with NaCl and HCl solutions at 30°C, 50°C, 70°C and 90°C produced iron (II) chloride which oxidised to iron (III) chloride at its surface and subsequently oxidised to βFeOOH. Akaganéite (βFeOOH) is again identified as a significant factor which must be studied in order to establish the nature of its ongoing contribution to the corrosion of chloride-contaminated wrought iron.

The volumes occupied by iron oxyhydroxide corrosion products (given by Selwyn *et al.*, 1999) are approximately three times that of the metallic iron. The increased-volume corrosion products form in situ, on the surface of the remaining metal core, at the metal/corrosion product (metal DPL) interface. Their growth, coupled with metallic corrosion and the production of acidic environments, results in the lifting of outer corrosion layers at the metal/corrosion layer (metal/DPL) interface (Mathias *et al.*, 2004). This scaling, often termed 'spalling', is symptomatic of active corrosion (Turgoose, 1982a; Knight, 1982; Watkinson, 1983; Selwyn *et al.*, 1999). It is this process that is most damaging to the original surface or *limitos* of the artefact and the information it contains about its form and function (figures 2 and 12-15).

2.8.4. The primary significance of βFeOOH

The primary significance of akaganéite (βFeOOH) is the physical disruption and loss of the overlying DPL (magnetite and other corrosion products) and *limitos* as it is formed between them and the remaining metal core (Figures 2, 3, 12-15 and Mathias *et al.*, 2004). The presence of solid βFeOOH is highly informative because it cannot form unless the ferrous chloride solutions have a high chloride concentration and a very low pH (section 2.8.1. and figures 7-10). As drying proceeds, ambient atmospheric moisture levels influence the water content in the iron so that the ferrous, ferric and chloride ions become sufficiently concentrated and pH falls to the levels necessary to enable βFeOOH formation. These conditions will prevail as desiccation of chloride-contaminated wrought iron is approached. Water will be lost from solution as relative humidity falls. The pH will drop as the solution becomes more concentrated. Oxidation of the ferrous chloride solution ($Fe^{2+}_{(aq)}$ and $Cl^{-}_{(aq)}$), solid ferrous hydroxychloride (β-$Fe_2(OH)_3Cl$) or any solid ferrous tetrahydrate ($FeCl_2.4H_2O$) formed will form akaganéite (βFeOOH).

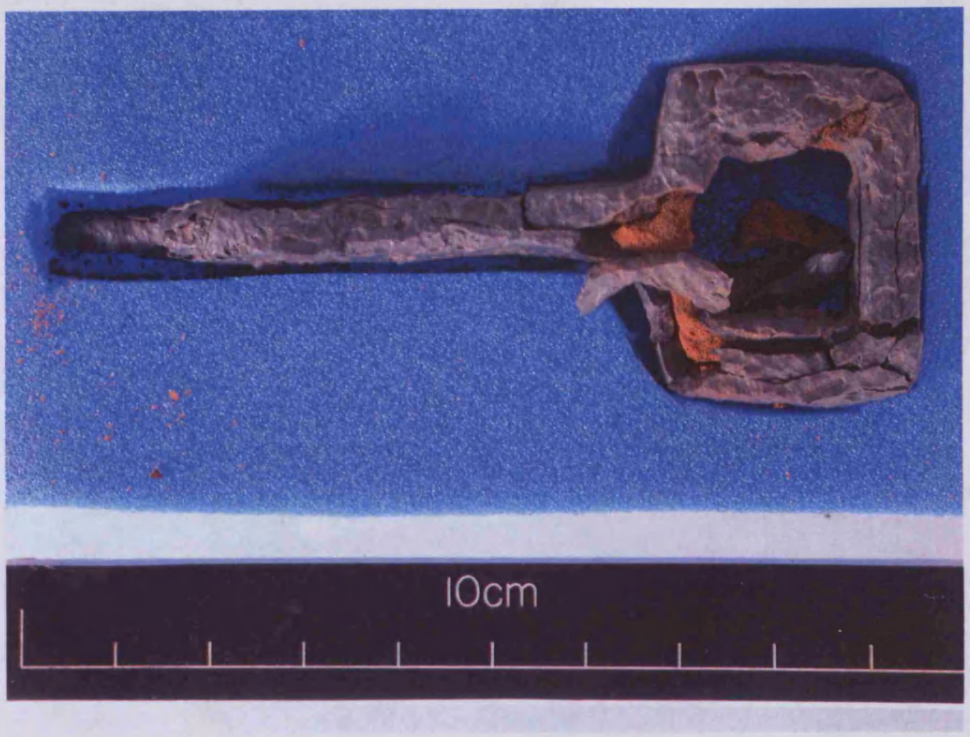

Figure 12. A Roman wrought iron artefact from Usk, Monmouthshire, showing signs of post-excavation corrosion during museum storage and the loss of its surface due to the formation of akaganéite (βFeOOH).

Figure 13. A photomicrograph of a wrought iron Roman punch from Usk, Monmouthshire, showing orange-brown (post-excavation) akaganéite (βFeOOH) growth at the metal/DPL interface. This crystal growth is clearly forcing the corrosion products (containing the artefact's original surface) off the metal core. The punch was excavated in 1974 and cleaned by air abrasion shortly afterwards. It was stored in a Stewart™ box with silica gel between 1974 and its re-conservation to address the apparent spalling in 2008.

Figure 14. A photomicrograph of the same artefact and orientation as in figure 13 but magnified to show the tower-like orange-brown akaganéite (βFeOOH) growing between the overlying, black, magnetite DPL (top) and metallic wrought iron core (bottom).

Figure 15. A photomicrograph of a cross-section of a sample of spalled corrosion (with overlying paint and primer layers) recovered from the floor of the dry dock beneath the wrought iron hull of the ss Great Britain. Layers of paint and primer overly a thick dense product layer (DPL) identified by XRD as mainly magnetite (appendix 4). Adhesive failure of the uppermost (red) paint layer is evident on this sample. Growths of βFeOOH (identified by XRD – see appendix 4) are apparent on the lower surface of the magnetite DPL.

Oxidation of more dilute ferrous chloride solutions can produce predominantly goethite (αFeOOH) and/or lepidocrocite (γFeOOH) as demonstrated by Selwyn *et al.* (1999) but, as they noted, this suggested high humidity (~100%RH i.e. near the dew point) diluting the ferrous chloride solution or formation of βFeOOH followed by conversion of this metastable product at high RH after initial formation. Wang (2007a: 127) reported the presence of "cotton wool shaped" goethite with βFeOOH within cracking ironwork and contributing to forcing it apart. All of the iron where goethite was present in this way had been treated in alkaline sulphite solution. Goethite is not expected to occur unless the artefact has undergone an aqueous conservation treatment of this type. Goethite has not been identified at the metal/DPL interface on the chloride-contaminated samples of marine wrought iron supplied from the ss Great Britain, nor reported before aqueous treatment elsewhere (ignoring the transformed medium of archaeological artefacts which is formed by independent oxidation mechanisms for outwardly diffusing iron ions). The presence of goethite was explained as possibly due to low chloride ion concentration where $[Cl^-]/[OH]^-$ <6 or equal to 6, and the presence of βFeOOH to higher chloride concentrations where $[Cl^-]/[OH]^-$ >8 or equal to 8 (Refait and Genin, 1997). Thickett (2005) reported the identification of a transformation layer associated with βFeOOH as lepidocrocite but this artefact had also been treated with alkaline sulphite. Al-Zahrani (1999) also reported goethite formation and/or magnetite formation when βFeOOH was subjected to hot aqueous washing, aqueous sodium hydroxide washing or aqueous alkaline sodium sulphite washing.

Whilst βFeOOH is thermodynamically less stable than the αFeOOH (goethite) and γFeOOH (lepidocrocite) polymorphs, the degree to which this influences its presence in reality, under the conditions (pH and Cl^- concentrations) at the surface of the metal core, must be questioned for it is found to be the most abundant corrosion product on untreated chloride-contaminated wrought iron object cores. For now, it will suffice to note that βFeOOH is still the end product initially formed post-recovery from the ground or the sea and therefore of significant interest to this study. Dilution of the ferrous chloride solutions would occur at high relative humidities, not at low relative humidities. This study is interested in low relative humidity environments not very high

relative humidity environments, where the formation of βFeOOH is, perhaps, less favoured. In all cases the starting point is the ferrous chloride solution for this has the potential to form the disruptive polymorph βFeOOH either directly or indirectly through oxidation of ferrous chloride.

βFeOOH and iron hydroxychlorides are suspected of playing active roles in cyclical corrosion processes. The presence of these corrosion products has been reported to promote corrosion of iron at low ambient relative humidity values. The experimental part of this study examines these low humidity corrosion processes.

2.8.5. The secondary significance of βFeOOH: Reported metastability of βFeOOH

βFeOOH is metastable with respect to αFeOOH, γFeOOH and αFe_2O_3. It is reported that ferric oxide hydroxides (FeOOH) become susceptible to form changes when two surface hydroxyl (-OH) groups chemisorb a water molecule (Kaneko & Inouye, 1974; Kaneko *et al.* 1975). The removal of adsorbed chlorides covering the predominant crystal face hastens the decomposition of βFeOOH (Atkinson *et al.*, 1977; Gilberg & Seeley, 1981; Knight, 1982 and 1990). Watson and Cardell (1962) reported that dehydration of βFeOOH in alcohol removed some water and chloride, decomposing it to γFe_2O_3. Very low pH (pH 1-2, with HCl), very high pH (pH 12-12.5, with NaOH) and seeding with hematite or goethite crystals at 65°C enhanced the transformation of βFeOOH in aqueous laboratory experiments (Atkinson *et al.,* 1977). On heating, βFeOOH is transformed to αFe_2O_3 at about 280 °C (Deszi *et al.,* 1967, give 295 °C) showing a rapid loss of 13% water at 230 °C (Bernal *et al.,* 1959). Childs *et al.* (1980) reported probable removal of surface-adsorbed water and irreversible dehydroxylation at temperatures as low as 105 °C. Boiling with water for six days converts βFeOOH to haematite (αFe_2O_3)(Bernal, *ibid.*). At room temperature βFeOOH immersed in aqueous solution (including those <pH7) slowly transforms to goethite via dissolution and precipitation (Cornell and Schwertmann, 1996). All of the above-cited references to βFeOOH

instability will have studied synthetic βFeOOH which was washed and filtered after synthesis to render it free of excess chloride from the production process.

Claims that βFeOOH could play a direct role in the post-excavation corrosion of archaeological iron because of its ability to release its lattice-bound chloride ions upon transformation to other iron corrosion products were made as early as 1977 (Zucchi *et al.*, 1977). Transformations to goethite, maghemite (Gilberg and Seeley, 1981; Buchwald and Clarke, 1989) and magnetite (Cornell and Schwertmann, 1996; Ishikawa *et al.*, 1988; Selwyn, 2004) are cited. Buchwald and Clarke (*ibid.*) stated that βFeOOH undergoes an "ageing" process over time that converts it to, mainly, goethite. They attributed the freeing and loss of chloride from βFeOOH to slow hydroxyl (OH^-) exchange under ambient and cold conditions. Gilberg and Seeley (1981) reported that the "lifetime" of βFeOOH sols (i.e. colloidal βFeOOH in solution) varied from a few months to 25 years, converting to goethite and releasing bound chloride as its hollandite tunnel structure breaks up.

Al-Zahrani (1999: *table 29*) reported that washing a sample of βFeOOH/Fe_3O_4 in a 0.5M sodium hydroxide solution in a "closed container" produced a 20.9%w/w increase in the amount of magnetite after one week with a 37.5%w/w conversion to magnetite after washing for one year. After one year 62.5%w/w βFeOOH remained compared with 79.1%w/w after one week. Al-Zahrani (1999: *table 28*) reported that washing a sample of βFeOOH/Fe_3O_4 in a 0.5M sodium hydroxide solution in an "aerated (open) container" produced an 11.1%w/w increase in the amount of magnetite after one week with a 34.0%w/w conversion to magnetite after washing for one year. After one year 66.0%w/w βFeOOH remained compared with 88.9%w/w after one week. Washing with deionised water in a closed container (Al-Zahrani, 1999: *table 31*) produced an 85.3%w/w increase in the amount of magnetite after one week with a 91.7%w/w increase in the amount of magnetite after washing for one year. After one year 8.3%w/w βFeOOH remained compared with 14.7%w/w after one week. Washing with deionised water in an open container (Al-Zahrani, 1999: *table 30*) produced a 4.1%w/w increase in the amount of magnetite after one week with a 84.3%w/w increase in the

amount of magnetite after washing for one year. After one year 15.7%w/w βFeOOH remained compared with 95.9%w/w after one week.

It is not possible to extrapolate the thermodynamic metastability of βFeOOH with respect to other oxide hydroxide polymorphs *in solution* to βFeOOH at ambient temperatures *and at low relative humidities*. Only small amounts of free water will be available in pits and micro capillaries in excavated archaeological iron and marine iron in dehumidified environments. The kinetics of any changes to βFeOOH merit further, experimental, study.

Lepidocrocite is metastable with respect to goethite but it exists on a time scale of ~10,000 years because its formation may be kinetically favoured and its transformation to goethite is extremely slow (Schwertmann & Cornell, 2000). Stahl *et al.* (2003) concluded that akaganéite will not transform or release chloride under normal conditions, i.e. temperatures below about 200°C. They concluded that akaganéite will **not** therefore pose *"...a threat to iron artefacts, but is rather a symptom of the presence of high concentrations of chloride in an acidic environment"*.

The key to these seemingly opposing viewpoints is likely to be the availability of water as either a vapour or a liquid, but varying methods of synthesis may be relevant also.

North (1982: 81) reported that *"... the question of the lability of chloride ions in βFeO(OH) needs further study. Structurally there appears to be only one type of chloride ion but chemically there would appear to be labile and non-labile fractions"*. Importantly, North (*ibid.*) demonstrated the rapid release of (labile) chloride ions in solutions of pH>7 until a (non-labile) chloride content of 2-3% in the solid βFeOOH is reached. Reductions below this level were very slow and were linked with slow phase transformation, as observed by other studies. The reduction of chloride content via washing was/is ascribed mostly to the removal of loosely bound, "labile" surface-adsorbed chloride (*c.f.* figures 89 and 90).

The reported instability of βFeOOH in solution and North's own (1982) observation that slow chloride removal below 2-3% was associated with phase transformation raises doubt over North's (1982) model predicting no release of lattice-bound chloride *"...even in the presence of water."* The chemistry literature is clear: Washing at elevated temperatures, or boiling, chloride-contaminated iron breaks down and releases its bound chloride. Soxhlet washing (especially in an oxygen free environment i.e. nitrogen) should be an ideal, economical, method for small artefacts (Scott and Seeley, 1987; Al-Zahrani, 1999; Watkinson & Al-Zahrani, 2008). Yet boiling and washing has been repeatedly demonstrated to fail to remove all of the chloride from chloride-contaminated iron (Watkinson, 1996).

Whilst North (1982) concluded that the residual, tunnel-bound, chloride ions *"...firmly locked in the crystal lattice..."* would not promote corrosion in the way that free chloride ions would, *"...even in the presence of water", his* claim for the presence of water requires further experimental research, especially with respect to atmospheric moisture. Otherwise this theory is central to the model for the low-humidity storage of chloride-contaminated wrought iron proposed by this study, i.e. that chloride ions *"...firmly locked in the crystal lattice..."* would not promote corrosion in the way that free chloride ions would. The stability of βFeOOH (and its crystal lattice chloride) under ambient conditions *was* subsequently supported by the detailed study conducted by Stahl *et al.* (2003).

2.8.6. Hygroscopicity - a third potential risk from βFeOOH

βFeOOH is hygroscopic. Turgoose (1982b) suggested that the presence of βFeOOH influences the corrosion threshold relative humidity for iron due to its hygroscopic nature. All fine-grained materials contain up to several percent of physically and chemically adsorbed water (Schwertmann & Cornell, 2000). Kaneko *et al.* (1979), Ishikawa *et al.* (1986 and 1988) and Murad & Bishop (2000) concluded that water molecules are adsorbed on the surface and in the tunnels of βFeOOH (see also Taylor, 1987).

Micale *et al.* (1985) characterised the surface properties of γFeOOH, αFeOOH and αFe_2O_3. After initial dehydration at 400°C all of the iron oxide samples they investigated had a high concentration of surface hydroxyl groups and were shown to be hydrophilic at 25°C. Studies of the water content of βFeOOH have been conducted in extreme environments (elevated temperatures e.g. thermogravimetric analysis (TG) or in the electron beam of a scanning electron microscope). The water loss of 5% by weight when washed βFeOOH was heated to 230°C during thermogravimetric analysis was entirely due to adsorbed water (Stahl *et al.*, 2003: 2573). Buchwald and Clarke (1989) observed that akaganéite appeared to exhibit shrinkage cracks like dried mud when observed in the scanning electron microscope (SEM). They noted a 5-10% weight loss during 2-10 minutes in the electron beam of the SEM with an increase in Fe counts and suggested that βFeOOH may contain significant quantities of adsorbed water.

The influence of the βFeOOH surface adsorbed water on the corrosion of iron under ambient conditions has received little attention. This is remarkable given the fact that βFeOOH is found to be present at the interface between the metallic core and magnetite layer of spalling chloride-contaminated wrought iron of marine or terrestrial origin more often than any other corrosion product (Selwyn *et al.*, 1999: 221; Thickett, 2005). Experimental work undertaken for this thesis will increase knowledge of βFeOOH properties at low relative humidity values (Selwyn, 2004).

2.8.7. Labile surface chloride: A fourth potential contribution to ongoing corrosion from βFeOOH

The nature and influence of the chloride within and on βFeOOH is of great interest. The failure to remove ***all*** chloride through washing and other chemical avenues is widely reported as is the ability to remove significant quantities of chloride through various aqueous washing techniques. These investigations aim to illuminate our understanding of the differently located chlorides and their *"...cause and effect"* (North, 1982).

Most reported laboratory syntheses (which usually involve the aerial hydrolysis of aqueous solutions of ferric chloride ($FeCl_3$) at elevated temperatures (~70°C)) also wash the brown precipitated βFeOOH *"... with water until the filtrate was chloride-free"* (Stahl *et al.,* 2003). Also see Schwertmann & Cornell, (2000: 19). Laboratory washing is likely to be efficient compared with chloride removal through rain washing or percolating groundwater. Archaeological wrought iron artefacts are not universally routinely washed after excavation. A goal of this study is to parallel the synthesis of experimental washed βFeOOH as closely as possible with its mechanism of post-recovery production on marine iron and archaeological iron objects.

Ishikawa and Inouye (1975) reported that the surface of βFeOOH is covered by a monolayer of chloride (Cl^-) ions. Ardizzone *et al.* (1983) demonstrated that, unlike αFe_2O_3, αFeOOH and γFeOOH, magnetite shows significant (but slow, pH dependent) adsorption of chloride anions. Kaneko and Inouye (1974) reported that iron oxyhydroxides (FeOOH) are susceptible to changes between their various forms when chemisorption between two of their surface hydroxyl (–OH) groups and a water molecule occurs. Surface adsorbed chloride and adsorbed or chemisorbed water could form hydrochloric acid (HCl) which would accelerate the dissolution of the iron oxyhydroxide and/or its transformation to a more stable polymorph. The tendency to change polymorph in the presence of water (and surface-adsorbed chloride) may account for the reported "metastability" of βFeOOH and its undesirable potential as a source of further chloride ions which could be freed upon transformation to another polymorph (section 2.8.5.). The surface coverage by chloride ions also reflects the variable chloride content of the βFeOOH as a result of different production and washing methods.

Atkinson (1977) and Ishikawa & Inouye (1975) claim that surface-adsorbed chloride protects βFeOOH from attack by sulphur dioxide, inhibits adsorption of water and inhibits the breakdown and transformation of βFeOOH to αFe_2O_3 at high temperatures. This would appear to contradict claims that the mobile (labile) chloride adsorbed on its surface (that is hygroscopic and will be released in water) will form an electrolyte for

the continued electrochemical corrosion or remaining metallic iron (North, 1982; Ishikawa *et al.* 1988; Watkinson and Lewis, forthcoming).

North (1982) proposed that models giving βFeOOH a direct role in the corrosion process "*... may be mistaking cause and effect*", citing Zucchi *et al.* (1977: 104) who noted that it was only found in the active zone of corroding artefacts and claimed that it could accelerate the corrosion process because of the release of Cl^- ions. North (1982) suggested that chloride bound within the tunnels of βFeOOH can not promote electrochemical corrosion as free chloride ions. He attributed corrosion in the presence of βFeOOH to its surface-adsorbed, labile, chloride ions. North produced his βFeOOH via precipitation from ferric chloride solution but does not mention washing the product or otherwise. North's tests, conducted with steel coupons at 50%RH ±5%, resulted in minimal increase in weight in the presence of βFeOOH as compared with deliquesced iron chloride salts and HCl under the same conditions. North concluded that the presence of liquid water was necessary for the free chloride ions adsorbed on βFeOOH to effect corrosion. This did not occur in the RH range tested. The properties of βFeOOH in relation to iron at low relative humidities require further elucidation because it is the most commonly cited and encountered destructive chloride-bearing corrosion product on deteriorating archaeological and marine wrought iron (for archaeological iron see figures 12-14, for marine iron see figures 2 and 15). X-ray diffraction analysis (XRD) as part of this study has identified βFeOOH as the corrosion product responsible for the loss of the DPL and *limitos* over significant areas of the wrought iron hull of the ss Great Britain (see figure 32 and appendix 4). The presence of βFeOOH is evidence that wrought iron is heavily contaminated with chloride ions ***and*** that βFeOOH is not sufficiently metastable under the environmental conditions that prevailed post-excavation or post-recovery from the sea to transform it into other oxide hydroxide polymorphs, such that it could not be identified (Stahl *et al.*, 2003).

Comparison of results for the exposure of iron powder to various humidities in the presence of both unwashed and washed βFeOOH will inform the debate surrounding the role of adsorbed chloride. Exposure of unwashed βFeOOH and wash solution after

washing labile chloride from it to other metals will help to explain the nature of the harmful surface adsorbed chloride on unwashed βFeOOH.

2.8.8. Conductivity of βFeOOH

βFeOOH is electrically conductive and can transfer electrons from anode sites to remote cathode sites (Kaneko, 1989). This facilitates remote cathodic reduction of oxygen allowing corrosion to continue where it might otherwise have been stifled by electrical discontinuity or passivation.

2.9 Atmospheric corrosion in the presence of pollutant gases or particulates in urban areas

Museums literature contains a growing corpus of work dedicated to the study of atmospheric pollutants (Tetrault, 2005). Most museums with major archaeological collections are situated in town and city centres where pollutant particulates and gases are commonly more abundant than non-urban locations (Brimblecombe, 1989a & b and 1990; Green and Bradley, 1997: 307). Indoor furnishings can contribute their own pollutants to the building environment (Thomson, 1987). Airborne pollutants from combustion, e.g. traffic and former heavy industry, can be expected to have contributed, and contribute, to the corrosion of wrought iron stored or displayed in these environments and this potential 'external' atmospheric threat must also be considered and weighed against the 'inherent' corrosion-promoting contaminants of the wrought iron (Askey *et al.*, 1993). Whilst the atmospheric corrosion of wrought iron due to pollutant gases or particulates is not the focus of this study, it is briefly reviewed here to inform observations on chloride-related mechanisms where similarities are identified (e.g. the acid regeneration cycle), and to demonstrate that pollutant gases and particulates present a very low level threat to wrought iron as compared with chloride contamination. Carbon dioxide (CO_2) does not play a significant role in the atmospheric corrosion of iron; high carbon dioxide levels within pore spaces within soil help to slow corrosion of archaeological iron.

Vernon (1927: 159-165, 182; and 1935) showed that spots of rust that appeared on polished, metallic, iron in dry (heated) and humid (unheated) room conditions (43%RH and 68%RH respectively) were connected with dust particles that caused pitting through differential aeration and pollutant salts or gases they absorbed in hygroscopically adsorbed water. Filtered air at the same relative humidities (up to ~70%RH) prevented corrosion. Surfaces of metals and particulate dirt show the classic sigmoidal water adsorption curve that bends sharply upwards at around 75%RH. This behaviour is attributed to the transition from two or three layers of adsorbed water molecules to a liquid film (Michalski, 1993). This magnitude of relative humidity (50-75%RH) therefore represents a significant rate determining factor in the rate of corrosion if iron, especially

where no dissolved salts are present. Vernon (1927) concluded that below this (high) "critical" humidity corrosion *"was inhibited"* in an unpolluted atmosphere (although a very small but constant weight gain was observed).

The models for a number of pollutant processes are linked to iron exposed to air containing sulphur as sulphur dioxide, hydrogen sulphide and/or other sulphur-bearing contaminants (Junge, 1954; Charlson *et al.*, 1978). Hudson and Stanners (1953: 95) reported that *"In Great Britain the determining factor for the rate of corrosion is the sulphur pollution of the atmosphere"* but also found that the corrosion of copper-steel (0.3% Cu) falls off as the exposure period is prolonged for *"...the rust layer, once formed, inhibits further attack"*. Soot particles only stimulate corrosion if sulphur compounds are adsorbed on them (Evans, 1948: 85; see also Charlson *et al.*, 1978: 44). Vernon (1932) found that sulphurous acid (H_2SO_3; formed when $SO_{2(g)}$ dissolves in water) adsorbed on the surface of nickel was catalytically oxidised above a critical humidity of 70%RH to form hygroscopic sulphuric acid (H_2SO_4). SO_2 is selectively absorbed on metal surfaces under humid conditions and metal oxide surfaces catalyse the SO_2 to sulphur trioxide (SO_3) and promote the formation of sulphuric acid (H_2SO_4). Askey *et al.* (1993: 233) reported that concentrations of atmospheric HCl are *"markedly"* lower than concentrations of atmospheric SO_2 (see Green and Bradley, 1997: 307, *table 1*).

$$SO_3 + H_2O \rightarrow H_2SO_4 \qquad [12]$$

Ahmad (2006) gives different ways in which sulphur dioxide may be oxidised:

$$SO_2 + xH_2O \rightarrow SO_2.xH_2O \qquad [13]$$

$$SO_2.xH_2O \rightarrow HSO_3^- + H_3O^+ + (x-2)H_2O + H_2O_2 \qquad [14]$$

$$HSO_3^- \rightarrow SO_4^{2-} \qquad [15]$$

The adsorption of sulphur dioxide in an aqueous layer leads to its acidification due to the formation of the sulphate ion as shown in [16]:

$$SO_2 + H_2O + \tfrac{1}{2} O_2 \rightarrow H_2SO_4 \quad [16]$$

The low pH formed by the sulphuric acid where sulphur dioxide is oxidised prevents the precipitation of protective hydroxide and corrosion proceeds in pits (often called sulphate nests) beneath a hydroxide layer at the anodic sites. As Fe^{2+} ions diffuse into the acidic electrolyte, the pits (nests) grow. The following reactions occur in the sulphate and Fe^{2+}-containing solution:

$$Fe + H_2O \rightarrow Fe(OH)_{ads} + H^+ + e^- \quad [17]$$

$$Fe(OH)_{ads} + H_2O \rightarrow Fe(OH)_{2ads} + H^+ + e^- \quad [18]$$

$$Fe(OH)_{2ads} + SO_4^{2+} \rightarrow FeSO_4 + 2OH^- \quad [19]$$

$$FeSO_4 \rightarrow Fe^{2+} + SO_4^{2-} \quad [20]$$

Iron's sulphate corrosion products were also found to play a direct role in the corrosion process (Sydberger and Vannerberg , 1972). Vernon (1935) exposed steel plates to sulphur dioxide and reported that corrosion was found to be rapid above 70%RH but that there was little attack beneath 70%RH. This was confirmed by Evans and Taylor (1974). Exposure to sulphur dioxide produced ferrous sulphate ($FeSO_4$). If relative humidity was maintained above 70%RH an aqueous solution of ferrous sulphate remained and electrochemical corrosion was supported by this electrolyte. Two cyclical processes were identified: an electrochemical cycle and an acid regeneration cycle. The electrochemical cycle formed magnetite that oxidised quickly to form a large volume of iron oxide hydroxides with a continual uptake of water.

Under wet conditions

$$8FeOOH + Fe^{2+}_{(aq)} + 2e^- \rightarrow 3Fe_3O_4 + 4H_2O \quad [21]$$

$$3Fe_3O_4 + 0.75O_2 + 4.5H_2O \rightarrow 9FeOOH \quad [22]$$

The acid regeneration cycle is based on the oxidation of ferrous sulphate to ferric sulphate, with hydrolysis to ferric hydroxide and/or basic sulphate, releasing sulphuric acid (Marcus, 2002). The sulphuric acid attacks more iron, producing more ferrous sulphate cyclically. Evans and Taylor (1974) reported that the acid regeneration cycle proceeded far more slowly, contributing far less to the overall corrosion process, than the electrochemical cycle.

$$4H_2SO_4 + 4Fe + 2O_2 \rightarrow 4FeSO_4 + 4H_2O \qquad [23]$$

The sulphuric acid is reformed by oxidative hydrolysis

$$2FeSO_4 + \tfrac{1}{2} O_2 + 3H_2O \rightarrow 2FeOOH + 2H_2SO_4 \qquad [24]$$

The production of $FeSO_4$ provides the electrolyte necessary to carry the electrical current and leads to the dissolution of the protective Fe_2O_3 or Fe_3O_4 film on iron and steel surfaces. Ahmad (*op. cit.*) reports that one sulphate ion can result in the dissolution of 100 atoms of iron but also agrees that the cycle repeats itself, although it is very slow compared with the electrochemical cycle. The acid regeneration cycle occurs over a period of days whereas the electrochemical process may repeat several times in one hour. The acid regeneration cycle continues until basic iron (III) sulphate is formed as an end product.

Oesch (1996) found that the effect of SO_2 on the corrosion of iron (in the form of unalloyed steel and weathering steel) exceeds that of NO_2, NO, O_3 and laboratory air by far. But since ambient SO_2 levels are considerably lower than those of NO_2 and O_3, their effects in atmospheric degradation must also be taken into account. Furthermore, at "low" relative humidity (50%) nitrogen dioxide was found to produce greater weight gain; higher than that for sulphur dioxide on unalloyed carbon steel. Strong synergistic effects were observed between SO_2 and NO_2 at low relative humidities and were attributed to the formation of an electrolyte containing nitrate on the surface, which enhances the uptake of sulphur dioxide.

Oesch (1996: 1364) demonstrated that the corrosion products of the samples exposed to 10ppm SO_2, at 25°C and 90% relative humidity, consisted of high amounts of rozenite ($FeSO_4.4H_2O$) and small amounts of ferric oxyhydroxides (αFeOOH). Experiments with NO_2 *and* O_3 yielded the corrosion products lepidocrocite (γFeOOH) and goethite (αFeOOH). The large amounts of sulphate compared with small amounts of nitrate were explained by the fast adsorption of sulphur dioxide on surface water films, its high water solubility (1.24mol (1 atm)$^{-1}$) and its fast oxidation to sulphate due to the catalytic effect of ferric oxyhydroxides as well as Fe^{3+}. In contrast, the water solubilities for the nitrogen oxides are small and their oxidation in clean surface water films comparatively slow (*ibid.*: 1363). Experiments with nitrous oxide (NO) only produced magnetite as the corrosion product (*ibid.*: 1365).

A corrosion "threshold" exists where iron sulphate changes from $FeSO_4.4H_2O$ to $FeSO_4.7H_2O$. Above this threshold corrosion occurs rapidly, aggressively promoted by the presence of the higher hydrate. Below this threshold, corrosion is not aggressively promoted by the lesser hydrate.

$$FeSO_4.4H_2O + 3H_2O_{(g)} \leftrightarrows FeSO_4.7H_2O \qquad [25]$$

melanterite rozenite

Various authors cite this threshold as a "critical humidity" in the region of 60% relative humidity (Evans, 1948; Jones, 1992). At 25°C others cite ~15% to 95% with a distinct clustering around 60-80%. Recent work agrees and supports a figure of approximately 63% relative humidity at 25°C (Hemingway *et al.*, 2002: 2). Importantly, Hemingway *et al.* (2002) provide a graphic comparison of the rozenite-melanterite equilibria they had encountered in literature (figure 16). This graphic clearly indicates that all research into this phenomenon shows that the relative humidity at which this "equilibrium", "transition" or "threshold" occurs is temperature dependent, varying with it.

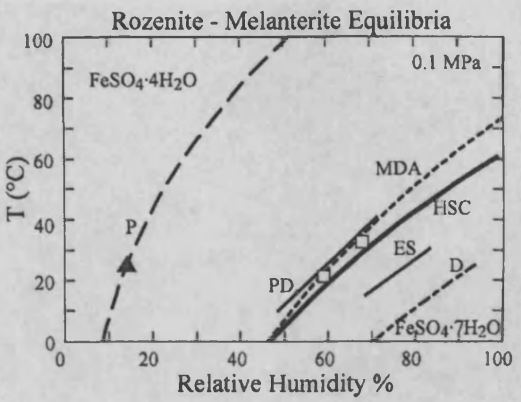

Figure 1. Comparison of estimates for the reaction of rozenite + H_2O to melanterite as a function of temperature and relative humidity. Open squares are results of Malinin and others (1979); filled triangle is result of Pribylov (1969). Sources of curves are: P, Pribylov (1969); PD, Parkinson and Day (1981); MDA, Malinin and others (1979); HSC, this study; ES, Ehlers and Stiles (1965); D, DeKock (1982).

Figure 16. Rozenite – Melanterite Equilibria after Hemingway *et al.* (2002).

The corrosion of iron is rapid in environments that support $FeSO_4.7H_2O$ as the stable hydrate and insignificant where $FeSO_4.4H_2O$ is stable. Theoretically, iron corrosion may be controlled by limiting the amount of moisture in the environment surrounding sulphate-contaminated iron. The "critical" region of relative humidity cited is relatively high (at around 60%RH or higher) but it is feasible to achieve and maintain humidity levels below this figure in most practical situations without great expense or difficulty in buildings or containers otherwise in the British climate.

Although openly stored or displayed wrought iron will be subject to SO_2 and its derivatives from the atmosphere of urban environments, their influence on the corrosion process will be insignificant compared with the electrochemical contribution of chloride bearing salts and deep-seated chloride ions present in chloride-contaminated wrought iron, especially if it were to be maintained within an environment kept at below 50% relative humidity (figure 16). The nature of the iron/sulphate corrosion mechanism suggests that low relative humidity will prevent this type of corrosion occurring.

Corrosion of chloride-contaminated wrought iron is known to proceed rapidly well below the critical relative humidities cited in figure 16 for the sulphate-related process.

The sulphate process is not therefore the most significant factor in the corrosion of chloride-contaminated wrought iron at low relative humidities. Tidblad *et al.* (2000) demonstrate that corrosion in marine SO_2 polluted atmospheres due to dry deposition is simply the sum of the individual contributions for dry deposition of SO_2 and chloride. Hudson and Stanners (1953) found that corrosion due to atmospheric sulphur dioxide falls off if its surface is covered with corrosion products which inhibit access. Historic or archaeological metallic wrought iron is usually covered, and protected from sulphur dioxide attack, by thick layers of dense corrosion products, including magnetite, or paint systems. Chloride contamination poses a greater threat to the preservation of chloride-contaminated wrought iron than sulphur dioxide attack.

2.10 The effect of temperature

Temperature not only affects rates of chemical reactions (figure 17), it also affects the hydration states of salts at given relative humidities (figure 16 and section 2.9). Ignoring other factors such as salt concentration, oxygen solubility etc. and considering temperature alone, the rate of corrosion of a metal will increase sharply with increase in metal surface temperature until the evaporation of its electrolyte occurs (Tidblad *et al.*, 2000). For uncontaminated wet iron, corrosion rate increases with increasing mean temperature. Once the moisture has been evaporated at elevated temperatures, a negative temperature effect on the annual corrosion rate is observed due to the overall reduced time of wetness (Tidblad *et al.*, 2000). Chloride-contaminated iron, contaminated by hygroscopic salts that prolong the time of wetness at the metal surface, prolong the time of wetness and the increase in corrosion with increasing temperature is maintained. In Great Britain, the summer months will be likely to tend to increase corrosion reaction rates due to increased ambient temperatures (and increased average relative humidity levels). Winter corrosion has been found to be more damaging where contamination from increased levels of combustion products in the air is experienced in or from urban or industrial areas (see section 2.9).

Tidblad *et al.* (*op. cit.*) found two attempts to describe the effect of temperature on atmospheric corrosion in the presence of chlorides (Morcillo *et al.*, 1998 & Panchenko *et al.*, 1984) but they studied its effect further. They cite the following equation which has been used for carbon steel. It indicates that the corrosion of carbon steel in marine atmospheres generally increases exponentially with temperature.

$$f(Cl^-) = A1 \cdot [Cl^-]^{B1} \cdot Tow^{C1} \cdot \exp(k \cdot T) \qquad [26]$$

Where $f(Cl^-)$ is the corrosion in the presence of chlorides, Tow is the time of wetness, T is temperature (°C) and $[Cl^-]$ is the chloride ion concentration. A1, B1 and C1 are experimentally observed.

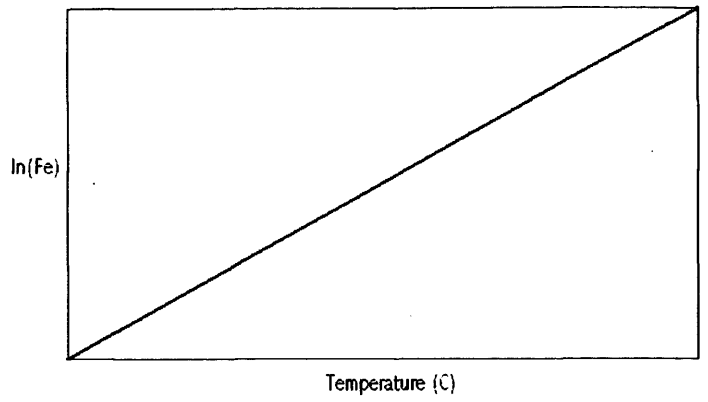

Figure 17. **Schematic representation of the observed temperature dependence of corrosion of carbon steel in marine atmospheres. After Tidblad *et al.* (2000: 25, *fig. 3*).**

Tidblad *et al.* (*op. cit.*: 30) also reported that increased temperature also increases the corrosive effect of chloride ions in contact with metallic iron.

When cited together with relative humidity, temperature provides a measure of the amount of water vapour in a given body of air and enables its dew point or frost point to be calculated. Dew formation can accelerate corrosion due to high sulphur dioxide levels near the ground in urban areas (Garverick, 1994: 5). Hemingway *et al.* (2002) (figure 16) show that [for iron sulphate hydrate] hydrate transition equilibria are temperature dependent and, whilst a corresponding equilibrium diagram for ferrous chloride hydrates has not been found during the literature searches for this research, it is anticipated that temperature will also affect the hydrate transitions for ferrous chloride (specifically with reference to the transformation of ferrous chloride tetrahydrate, $FeCl_2.4H_2O$, to ferrous chloride dihydrate, $FeCl_2.2H_2O$, and *visa versa*).

Ruby *et al.* (1971: 4560) constructed and published a phase diagram for the binary system $FeCl_2.nH_2O$ using existing data augmented by their own work (figure 18). It shows the water/ferrous chloride phases determined at different temperatures and ferrous chloride: water ratios. Percentage water will decrease with decreasing environmental relative humidity. Commensurately, weight % $FeCl_2$ will increase with the loss of water from the system as relative humidity falls. Figure 18 indicates that

weight % $FeCl_2$ *and* temperature influence phase stability and the location of the phase boundaries on the diagram. Compare the temperature ranges 0-5°C, 10-70°C and 75-650°C where five, four and three phases may be encountered respectively, each then determined by moisture availability/weight% $FeCl_2$.

Unfortunately, Ruby *et al.* (*op. cit.*) do not provide data for the dew point temperatures or relative humidities which favour each phase (i.e. weight % $FeCl_2$) at a given temperature and atmospheric pressure. These remain to be determined.

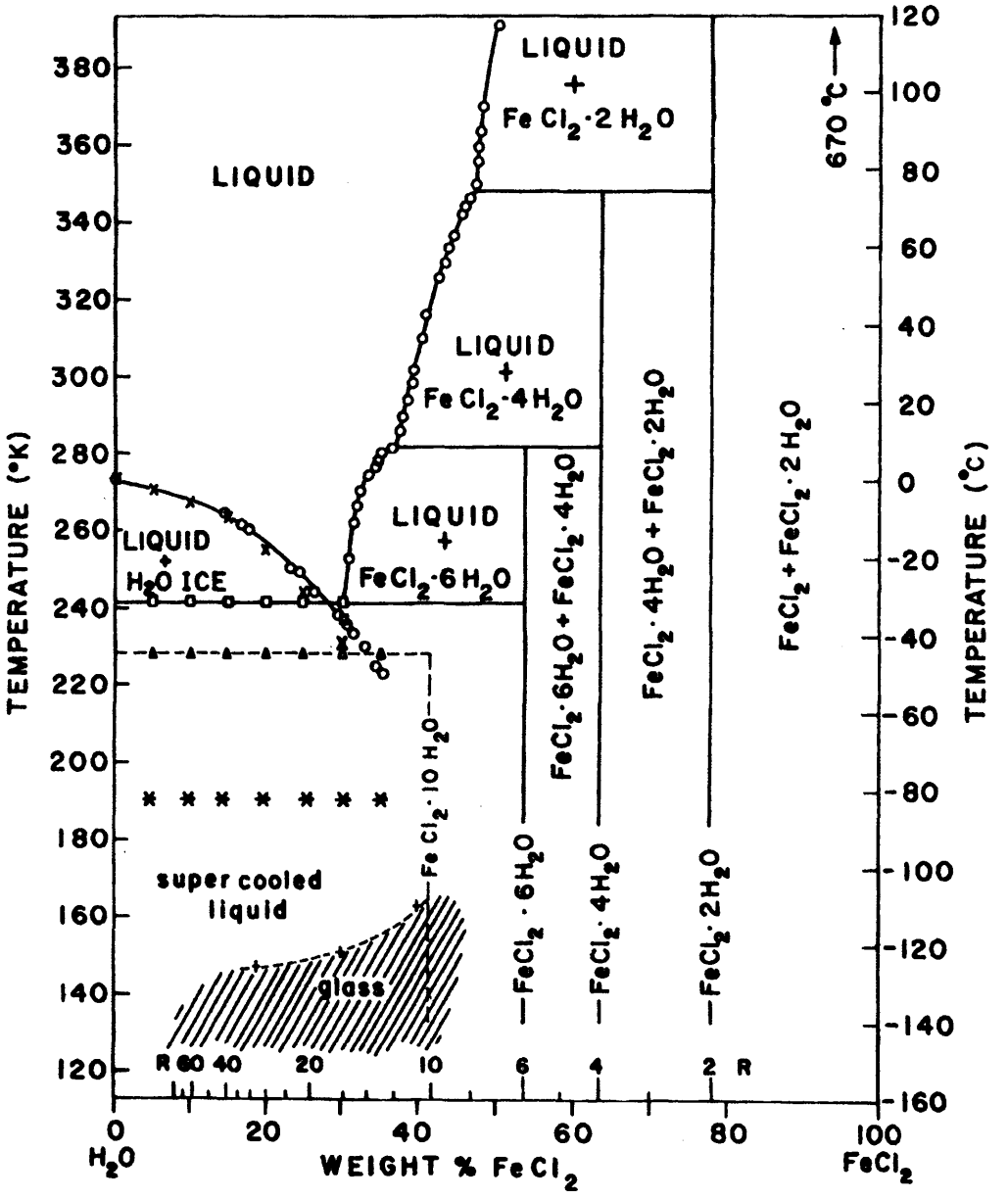

Figure 18. **Phase diagram for ferrous chloride hydrates including some metastable regions. After Ruby *et al.* (1971: 4560, *fig. 1*).**

3 Conserving chloride-contaminated iron

3.1 'Safe', dry, storage of chloride-contaminated iron: a brief review of recommendations

Corrosion of chloride-contaminated wrought iron in damp aerated environments is electrolyte based and chloride ions play a significant role (see section 2.6). Corrosion of chloride-contaminated wrought iron in dry aerated environments is linked to hydrated ferrous chloride (see section 2.8.1.).

Current dry-storage recommendations for chloride-contaminated wrought iron (Cronyn, 1990: 195-8; Watkinson & Neal, 1998: 16, *table 5* and 24) are based on results of experimental work carried out by Turgoose (1982b) that aimed to address the recognised problems encountered with post-excavation deterioration of archaeological chloride-contaminated wrought iron. Hydrated iron (ferrous) chloride ($FeCl_2.4H_2O$) is one of the products that can be formed as chloride-contaminated archaeological iron dries out after excavation (Thickett and Odlyha, 2007). This corrosion product is known to (a) attract water (it is hygroscopic) - Turgoose (1982b) showed that it will support the iron corrosion process, and (b) oxidise to form βFeOOH, whereas $FeCl_2.2H_2O$ is stable and does not oxidise (Turgoose, *ibid.*). Water can be supplied to the iron chloride from atmospheric moisture, which will be quantified here, conventionally, as relative humidity (%RH). Identifying the relative humidity value, below which iron chloride does not attract sufficient water to itself to corrode iron in contact with it, nor oxidises to form potentially harmful βFeOOH, provides a value for a corrosion threshold (akin to, but different to, the "critical humidities" cited in section 2.9 for iron/sulphate related mechanisms). Below this threshold humidity value iron contaminated with iron chloride should not corrode because the salt cannot attract sufficient water for an electrolyte. Conversely, above this threshold humidity value the moisture attracted by the iron chloride will support corrosion provided other essential corrosion parameters are active.

Turgoose (1982b) examined the relationship between iron chloride, iron and relative humidity. He reported that iron powder mixed with iron chloride tetrahydrate

($FeCl_2.4H_2O$) corroded in a sealed environment controlled to 20% relative humidity (by a saturated salt solution of $KC_2H_3O_2$ at 20 °C) while at 15% relative humidity (maintained in a sealed environment containing a saturated solution of $LiCl.H_2O$ at 20 °C) ferrous chloride dihydrate ($FeCl_2.2H_2O$) is the stable hydrate and the iron powder did not corrode. In summary, ferrous chloride tetrahydrate ($FeCl_2.4H_2O$) was found to promote corrosion when mixed with iron powder whereas ferrous chloride dihydrate ($FeCl_2.2H_2O$) was shown not to promote corrosion when mixed with iron powder.

The formation of ferrous chloride is thermodynamically possible as chloride-contaminated iron dries (figure 7). Turgoose concluded that anoxic damp storage [rather than desiccated or dehumidified storage] is ideal, but stated that "*...the chemical reactions occurring during the deterioration of excavated* [i.e. chloride-contaminated] *ironwork are not prevented in the presence of air unless the relative humidity is reduced below 20%...*". According to his results, at 15%RH, and below, $FeCl_2.2H_2O$ is the prevailing hydrate and is incapable of corroding iron, thereby preventing active corrosion. This newly identified storage "threshold" was much lower than the 60-70%RH and 40%RH thresholds for "appreciable" corrosion identified by earlier workers. It is unknown whether corrosion is still occurring between the recorded no corrosion point of 15% relative humidity and the corrosion point of 20% relative humidity. Despite this observation, 20% relative humidity has been cited by many conservators as the corrosion threshold, below which, chloride-contaminated wrought iron will be stable (Cronyn, 1990).

The accelerated corrosion of iron powder in the presence of solid ferrous chloride tetrahydrate had not been expected. Turgoose (1982b: 99) had expected corrosion to take place above the deliquescence point of ferrous chloride (the relative humidity above which ferrous chloride becomes a highly conducting aqueous solution) but not beneath it. Previous workers (Chandler, 1966; Chandler and Stanners, 1966; Evans and Taylor, 1974) that investigated the influence of solid and deliquesced salts (especially those containing chlorides) on iron also reported that corrosion was much more aggressive above the deliquescence point of a deliquescent salt, but that it was **not** prevented beneath this value.

Elsewhere, 20% RH (Cronyn, 1990; Green and Bradley, 1997), 18% RH (Knight, 1990: 40 and 1997: 37 & 38) and 15% relative humidity (Knight, 1990: 41 and 1997: 38; Watkinson and Neal, 1998) have been reported as the value below which chloride-contaminated wrought iron should be stored to prevent corrosion. These figures were not substantiated by research but are likely to have been interpretations of Turgoose's (1982b) data.

The origin of an 18% relative humidity corrosion threshold has been referenced to Turgoose (1982b) but Turgoose does not cite this figure in his work (Knight, 1990: 40). Re-examining Turgoose's published data (*ibid.*) produces a "no corrosion" threshold value at about 18% relative humidity by extrapolation of a plot of the data contained in his published table 3 (Turgoose, 1982b) (see figure 19 of this thesis). This is not recorded anywhere in the published literature. Despite the 18% corrosion threshold relative humidity being experimentally unproven, it is widely cited as the relative humidity below which chloride-contaminated archaeological iron should be stored. Since Turgoose (*ibid.*) showed that an iron chloride/iron powder mix did not corrode at 15% relative humidity, a logical assumption is that a safe storage threshold value must exist between 20%RH and 15%RH (corresponding with the highest relative humidity stability value for $FeCl_2.2H_2O$ before it converts to $FeCl_2.4H_2O$). The precise relative humidity at which ironwork containing ferrous chloride is stable has not been established.

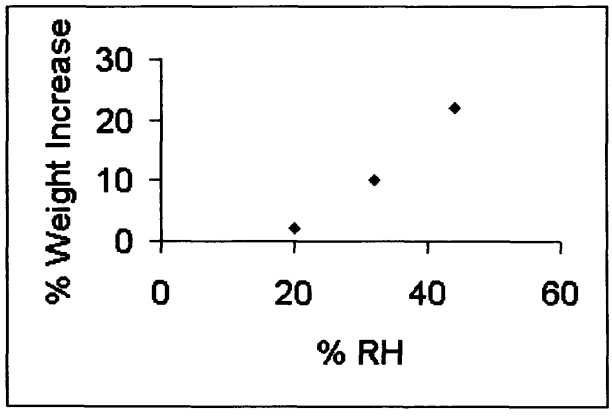

Figure 19. **A graphic representation of weight increase (corrosion) of iron in the presence of ferrous chloride at different relative humidities after a given (common) period of time (After Turgoose, 1982b, *table 3*).**

3.2 Discussion on the need for further work on the ferrous chloride/iron corrosion model

The response of iron chloride, either as $FeCl_2.2H_2O$ or $FeCl_2.4H_2O$, to relative humidity and the stability of iron in contact with it are potentially of great significance for the specification of an optimum environmental relative humidity level for the storage of chloride-contaminated iron. Re-examination of Turgoose's (1982b) experimental work raises a number of points that merit further investigation.

3.2.1. The method for control of relative humidity used by Turgoose (1982b)

Turgoose (1982b) used saturated salt solutions to maintain controlled relative humidity environments for his programme of experimental work. Literature searches reveal limited agreement with the equilibrium relative humidities of 15% and 20% (both at 20°C) cited by Turgoose (*ibid.*) for the salts he used (see table 3). The precision of the methodology used by Turgoose (*ibid.*), namely the specification of a single-point %RH value for a transition in hydration state measured over saturated salt solution, is cited as accurate to ±2%RH (Brown, 1994; Wexler, 1993). Martin (1965) demonstrated that saturated salt solutions can not be relied upon to produce and maintain known relative humidities where the other contents of the chamber (the substance(s) to be conditioned) absorb moisture themselves. At 20°C a rate of moisture absorption as low as 4mg/hour was found to be sufficient to depress the humidity by about 2%. This raises questions concerning both the actual values of relative humidity that Turgoose attained during his tests and their constancy during throughout the test period.

External temperature influences relative humidity within a sealed desiccator that lacks temperature control. Lowering or raising the temperature outside the glass desiccators would have raised or lowered the temperature inside them and affected the value of their internal relative humidity, which is temperature dependent. There is no record that Turgoose (1982b) artificially maintained the desiccator temperature at 20°C, nor that temperature or humidity levels within the desiccators were monitored throughout

his programme of work. It is possible that both the absolute value and the stability of the relative humidity within the test environments are open to question. His experimental programme should be reproduced to confirm its results.

Brown (1994), Thomson (1981), Martin (1965) and others have questioned the reliability of published RH values for saturated salt solution controlled environments and RH-measuring instruments. Using published data (see table 3) it is possible to estimate what the variation in range and absolute value of relative humidity might have been during the tests carried out by Turgoose (1982b). Relative humidity may have been as high as 23.11%±2%RH or as low as 11.1%±2%RH, rather than the 20% and 15% respectively reported by Turgoose (*ibid.*). The most recently reported values are considerably different to the values cited by Turgoose (see table 3); these might be considered to be more accurate than results reported over 70 years ago (Spencer, 1926). The relative humidity range within which corrosion occurs can be redefined using the published data.

Storage below an unidentified relative humidity lying between about 11.1% and about 23.11%, will prevent accelerated corrosion of chloride-contaminated iron as defined by the Turgoose (1982b) corrosion model. The identification of the relative humidity above which $FeCl_2.4H_2O$ is stable and beneath which $FeCl_2.2H_2O$ is stable is therefore identified as a primary aim of this study.

Reference	Relative Humidity (%) above saturated Lithium Chloride @ 20°C	Relative Humidity (%) above saturated Lithium Chloride @ 25°C	Relative Humidity (%) above saturated Potassium Acetate @ 20°C	Relative Humidity (%) above saturated Potassium Acetate @ 25°C
Greenspan, L. (1977)	11.31±0.31	11.30±0.27	23.11±0.25	22.51±0.32
CRC Handbook (1996)	11.31±0.31	11.30±0.27		
Lafontaine, R.H. (1984)	12.4	12		
Hickman, M.J. (1970)	12		23	
Anon (1973) & Anon (1964)	12		22	
Richardson & Malthus (1955)				22.7
Wink & Sears, (1950)	11.1 @ 22.8 °C		22.9 @ 22.8 °C	
Stokes & Robinson (1949)		11.1		22.5
Spencer, H.M. (1926)	15		20	
Obermiller & Goertz (1924)	15		20	
Turgoose, S. (1982b)	15		20	

Table 3. Relative humidities cited for saturated salt solutions of lithium chloride and potassium acetate.

3.3 Dehumidification as a means of preserving chloride-contaminated wrought iron: a contextual assessment

Support for the use of dry storage for metals as a general principle is widespread and has been acknowledged for many years. *"As previously indicated, corrosion usually will not occur at normal temperatures if access of water to the surface can be prevented"* (Greathouse and Wessel, 1954: 274). Military equipment has long been, and is currently, commonly stored and transported using desiccated or low humidity environments (MOD, 2004; U.S. Navy, Undated; Janecka, 1963; Wells, 1948a & b). US Military Specification MIL-P- 116B (1952) and guidelines for the preservation, packaging and packing of military supplies and equipment (U.S. Department of Defense, 1951) stated that a relative humidity of 40% would suffice to prevent corrosion, and this was about the lowest figure that could economically be achieved, monitored (using "cobaltous chloride" indicator) and maintained in warehouses at that time. During World War II, the American military Services took the view that on very highly finished parts no amount of corrosion was *'insignificant'* to the troops in the field and stipulated storage at no higher than 30%RH (Wells, 1948a).

The copper cables of the buried telephone lines in the UK were pressurised with dry air as early as 1963 (Gregory, 1969; The Post Office Electrical Engineers Journal, Jan./Apr./Jul./Oct. 1963; Post Office Telecommunications Journal, Autumn, 1963, Summer, 1965, Winter, 1965). The moisture content of the air was maintained below a dew point of -32°C (equivalent to between 4%RH and 9%RH at 1°C-9°C). Even chloride-free iron is acknowledged to be stable at relative humidities as high as 60%RH in the absence of particulate or other contaminants (Donovan, 1986: 192; Vernon, 1927 and 1935).

Since the 1970s the COWI Group consultancy has developed dehumidification systems for suspension bridge steel cables, anchor houses and abutment rooms (Bloomstine & Sørensen, 2006). Bloomstine & Sørensen (*ibid.*) cite the main advantages of dehumidification for steel where their critical humidity is that for uncontaminated metal i.e. 60%RH:

- *"Dehumidification is virtually 100% effective, providing a much higher level of protection than painting."*
- *"The initial cost of dehumidification is only a fraction of the cost of painting."*
- *"The maintenance costs of dehumidification are much lower than for painting."*
- *"The life cycle cost of dehumidification is much lower."*
- *"It is easy to monitor and verify effectiveness."*
- *Dehumidification is environmentally friendly, as it does not have the environmental problems which are caused by blasting and painting."*

The Messina bridge authority, Stretto di Messina, analysed the feasibility and life cycle cost of dehumidification compared with traditional corrosion protection systems for the Messina Bridge that will link Calabria with Sicily (Bloomstine & Sørensen, *op. cit.*). Their life cycle cost analysis indicated that the construction cost for a dehumidification system is 77% less and that the net present value of operation and maintenance over the first 60 years is 71% less than a traditional system. Indirect savings in construction costs included the ability to use lighter cables and that construction is less sensitive to weather conditions.

Steel components of suspension bridges are increasingly being preserved using dehumidification (Park *et al.*, 2006). All of the Honshu Shikoku suspension bridges in Japan, and three European bridges, use dehumidification of their cables as a means to preserve them. In 2006 work to wrap and dehumidify the suspension cables of the Forth Road Bridge and Severn Bridge in the U.K. was approved (Colford & Cocksedge, 2006; Waite, 2006; BBC, 2007). Pressurised dehumidified air with a relative humidity of 40%RH or lower will surround the enclosed steel (Waite, 2008; Park *et al.*, 2006). Clearly no chloride contamination of the steel cables has been identified, nor can it be expected, (given the target upper relative humidity of <40%RH) even though both bridges span saline or brackish water.

None of the examples cited refer to chloride-contaminated iron. They are operating below the critical humidity of 60%RH for the corrosion of uncontaminated iron (Donovan, 1986).

North and Pearson (1975a: 175) advocated desiccated storage of small marine iron objects using silica gel to absorb moisture from the artefacts and their sealed environment. Citing that corrosion cannot occur in the absence of moisture, they claimed that *"...an untreated marine iron object which is stored in a dry environment, e.g. in a closed container with a silica gel desiccant, will remain stable for an indefinite period. We have tested this method with samples containing up to 10% by weight chloride and, even with frequent exposure to the atmosphere for inspection purposes, no deterioration of samples has been noted in twelve months. If a glass container is used which is closed and sealed, the specimen will be stable as long as the seal remains intact."*

Archaeological conservators have also advocated the use of desiccated storage (most commonly through the use of sealed polypropylene or polyethylene containers containing a humectant such as conditioned silica gel) as a means of preserving chloride-contaminated wrought iron artefacts from terrestrial and marine contexts (Cronyn, 1990: 195-8; Watkinson & Neal, 1998: 16, *table 5* and 24). Geological conservators have also invoked desiccated storage for chloride-contaminated meteoric iron which has been shown to accumulate chloride ions in the ground and subsequently deteriorate via very similar mechanisms (Buchwald and Clarke, 1989; Howie, 1977 and 1992).

A successfully sealed enclosure would theoretically not only enable environmental conditions to be monitored closely (Cridland, 2000; Kapatou & Lyon, 2008) but controlled. Monitoring and control are not only of practical importance but also of ethical importance for a conservation treatment. It is desirable to be able to halt a negative treatment or adjust and optimise a positive conservation treatment following ongoing assessment of the implications of the changes effected on or around the artefact. Environmental control also facilitates continued access to the wrought iron. Since this approach is based on limiting ongoing corrosion by limiting the availability of water for the iron corrosion process, an understanding of the role of moisture in the corrosion of chloride-contaminated iron underpins the design and implementation of any environmental control scheme of this sort. The research reported here was

designed and conducted to examine the relationships between chloride bearing corrosion products and atmospheric moisture, thereby providing data that might be extrapolated to manage chloride-contaminated wrought iron cultural heritage.

Criticisms of the dehumidification approach to preserving chloride-contaminated wrought iron commonly cite the low relative humidity levels necessary to prevent ongoing corrosion, the complexity of macroscopic and microscopic processes, synergistic effects and other interactions, as obstacles to the identification of a model for the preservation of wrought iron in this way (e.g. Keene, 1994; Schrier 1976). Thickett (2005: *fig. 3*) demonstrated a range of synergistic effects by showing that iron in the presence of a mixture of ferrous chloride and copper chloride, and a mixture of ferrous chloride with humic acid, corroded more aggressively than in the presence of ferrous chloride alone. Conversely, he found that goethite reduced the akaganéite transformation rate. The relevance of each of these synergies (combined effects) to the corrosion of chloride-contaminated wrought iron is not equal and other synergies should also be considered in future work (e.g. with $MgCl_2$ which has relevance for marine and maritime wrought iron).

However, without water there is no electrolyte and electrochemical corrosion ceases. The hygroscopic nature of ferrous chloride and akaganéite means that water is retained at much lower relative humidities than would otherwise prevail and these have not been precisely established. Just as Brunel was criticised by contemporary professional engineers for his revolutionary new "model" for ship design when he constructed the ss Great Britain (Rowland, 1971 and section 1.1 of this thesis), the use of dehumidification as a means to preserve chloride-contaminated wrought iron has been criticised by professional conservators and engineers operating in this and related fields (various, pers. comm.; Keene, 1985 and 1991; Jolyon Gill, in Kitchen, 2005).

In all scientific endeavours, variables must be identified and studied individually (section 2.6). It is not possible to evaluate many unknowns in the same equation without finding solutions to each individually, leaving just one unknown for which the equation may be solved. Renowned corrosion scientist Ulick R. Evans (1972: iv) noted that someone who is not prepared to face difficulties is unlikely to become a great scientist. Whilst the

range of factors in the corrosion of chloride-contaminated wrought iron is acknowledged to be great, and their interactions and synergistic effects are potentially complex, it is essential to identify models for the individual corrosion processes that may be studied experimentally and replicated. Priority must be given to the most aggressive processes that are predicted or, preferably, proven to be active at any one time. Subsequent investigations into possible synergistic effects may then follow sequentially.

Importantly, critics of dehumidification as a means of preserving chloride-contaminated wrought iron have cited the failure of this method to effectively control the ongoing corrosion of corrosion-active artefacts in dehumidified (desiccated) storage in museum stores. This is a serious observation for, were this proven to be the case, it would remove the case for applying the method to preserve chloride-contaminated wrought iron. So far, none of the literature questioning the usefulness of desiccated storage of (archaeological) chloride-contaminated artefacts has demonstrated that the artefacts that suffered ongoing corrosion were stored successfully at the "desired" or sufficiently low level of relative humidity from the time of their discovery to the time of examination (Keene & Orton, 1985; Keene, 1994; Green & Bradley, 1995).

Thickett & Odlyha (2007) reported air exchange rate and permeability data for Stewart™ polyethylene and polypropylene boxes[2] and their modelling allows silica gel lifetime prediction when using these containers. New style, polypropylene, boxes have higher air exchange rates that the old style polyethylene boxes. 75% of the air exchange was found to occur at the lid seal (*ibid.*). Silica gel used to desiccate sealed Stewart™ boxes containing chloride-contaminated archaeological wrought iron can quickly become saturated when initially used to remove moisture from freshly excavated, damp, iron (Watkinson and Neal, 1998: 24). Upon saturation, the silica gel must be changed so that

[2] Stewart™ boxes became the accepted standard museum storage boxes for sealed environments following trials and their recommendation by the UKIC (1983) and Watkinson (1987). Originally of polyethylene, the manufacturer later switched to the denser, harder and less pliable polypropylene with reportedly less satisfactory seals (Thickett & Odlyha, 2007).

a dry equilibrium is created and maintained (Toishi, 1959; Weintraub, 2002). Failure to ensure that this is done will promote corrosion. Thickett and Odlyha (*op. cit.*) studied the drying kinetics of freshly excavated chloride-contaminated wrought iron and confirmed that *"...regular replacement of silica gel is required to minimise deterioration"* but they also found that the significant amount of water initially present takes up to two years to evaporate from the objects.

This highly significant data suggests that the iron remains at risk of ongoing corrosion in desiccated storage conditions until the water has evaporated from the artefact(s) (see section 6.6). This might account for the reported ongoing corrosion and break up of museum stored chloride-contaminated archaeological wrought iron which has been successfully maintained in a desiccated environment. The drying process will favour the crystallisation of solid corrosion products as the electrolyte present upon excavation becomes more concentrated upon drying. The formation of any solid crystal is potentially damaging so, by definition, the drying process itself is potentially damaging to the overlying corrosion products and any surface(s) contained therein. However, some crystals have geometry making them more voluminous than other products that may form. This is true of akaganéite (βFeOOH) and its formation (as ferrous chloride oxidises) is destructive.

The potential for the drying process to be inherently damaging via crystal growth upon loss of water from deep seated electrolyte is a serious consideration and will require study beyond the scope of this investigation. For the present it is sufficient to note that, ideally, the drying process would occur once, and long-term preservation would be optimised thereafter. However, the effect of failure to maintain the desiccated environment must be considered for artefacts within sealed containers must be exposed to ambient moisture levels when the containers are opened to examine the artefacts or to regenerate their silica gel. Building air handling plant, designed to dehumidify sealed spaces, must also experience down-time for maintenance, or as a result of failure, periodically. The rate of ingress and attraction of water vapour under these circumstances will contribute to the likelihood and rate of resulting/subsequent corrosion.

Self-indicating silica gel,[3] changes colour at a relative humidity of around 40%RH. The colour change does not provide a quantitative measure of the environmental conditions within the sealed container. The colour of self-indicating silica gel is not a satisfactory indicator of safe, i.e. successful, storage for chloride-contaminated iron although pink or yellow gel does indicate unsatisfactory storage conditions. A marginally more useful self-indicating silica gel for use with chloride-contaminated wrought iron is doped with orange-green, organic, methyl violet indicator which changes from dark orange at 10%w/w adsorption to green at 20%w/w (where >8%w/w at 25°C is at equilibrium with 20%RH, where >12%w/w at 25°C is at equilibrium with 35%RH and where >20%w/w at 25°C is at equilibrium with 50%RH). But orange is not an indication of guaranteed "safe" levels of moisture within the container (information from GeeJay Chemicals Ltd Product Information Sheets, 16th April 2002).

Indicator cards (usually cobalt chloride impregnated) are known to have limited accuracy and are known to become less reliable with time due to migration akin to bleeding from adjacent cells. Thickett and Odlyha (*op. cit.*) report evidence of the failure of RH indicator cards after seven years.

Notwithstanding the 'challenges' in maintaining and guaranteeing a low relative humidity environment *in perpetuity* noted above, it has not been possible to identify a single cause for the failure of dehumidified storage where failure to preserve the integrity of the wrought iron has been cited. For this reason, it has not been possible to discount dehumidified (or desiccated) storage as a method of preserving chloride-contaminated wrought iron.

[3] Self-indicating silica gel was formerly widely doped with blue-pink, cobalt chloride, indicator but, since 1st July 2000, it has been widely replaced in museums and elsewhere by orange-yellow inorganic iron compound indicator due to the toxicity reclassification of cobalt chloride.

4 Identified and prioritised areas for experimental research

4.1 Introduction

Turgoose (1982b) provides some results directly applicable to the atmospheric corrosion of archaeological iron but he does not expressly recommend a particular relative humidity below which chloride-contaminated wrought iron can be safely stored without corrosion. This study aims to qualify and extend Turgoose's (1982b) research. This research establishes an accurate corrosion threshold for chloride-contaminated iron based on an investigation of the interactions between iron, iron chloride and βFeOOH at various relative humidity values.

4.2 Research programme

Experimental work was subdivided according to the question(s) it was designed to answer and interrelationship between results.

4.2.1. Establishing an experimental methodology for studying corrosion and hygroscopicity of iron/iron corrosion products

A methodology for analysing relatively small weight changes of samples due to corrosion using salts and iron powder must be designed and tested. A high surface area to weight/volume ratio of reactants will favour measurable weight change upon corrosion. A sensitive balance will have to be enclosed in a controlled environment (temperature and relative humidity) without detriment to data collection through vibration or disturbing the environmental equilibrium at the point of weighing. Problems with the use of saturated salt solutions to maintain desired relative humidities have been identified (section 3.2.1.). An alternative methodology must be identified and proven. Work will be conducted to identify systematic error and eliminate operational error to establish the validity and reproducibility of results obtained.

4.2.2. Identifying a relative humidity value or "threshold" for the transition of $FeCl_2.4H_2O$ to $FeCl_2.2H_2O$

Ferrous chloride and its hydration state have been demonstrated to be important with respect to iron corrosion processes at low humidities. An accurate determination of the relative humidity at which $FeCl_2.4H_2O$ (iron chloride tetrahydrate) changes to $FeCl_2.2H_2O$ (iron chloride dihydrate) offers a no-corrosion point for iron in contact with this corrosion product (Turgoose, 1982b & 1985b). This value is central to identifying desiccation levels for the safe storage of chloride-contaminated iron.

4.2.3. Corrosion of iron powder mixed with iron chloride

The properties of ferrous (iron II) chloride (dihydrate and tetrahydrate) are determined by three distinct tests:

- Expose a mixture of $FeCl_2.4H_2O$ /iron powder to relative humidity values above the transition threshold relative humidity value established. This establishes whether crystalline $FeCl_2.4H_2O$ causes the corrosion of iron.
- Mix $FeCl_2.2H_2O$ /iron powder together and examine if iron corrodes within the relative humidity stability field of $FeCl_2.2H_2O$. This determines whether iron is stable in the presence of the dihydrate of ferrous chloride as suggested by Turgoose (1985b).
- Expose a range of $FeCl_2.4H_2O$ /iron powder samples to various relative humidities between the threshold value for conversion of $FeCl_2.2H_2O$ to $FeCl_2.4H_2O$ and the deliquescence point of $FeCl_2.4H_2O$. This determines whether increasing humidity increases the rate of iron corrosion in the presence of $FeCl_2.4H_2O$.

Overall these tests provide semi-quantitative data on the rate of iron corrosion in the presence of iron chloride.

4.2.4. The response of βFeOOH to changes in relative humidity and its effect on iron

A sequence of tests examines the effect of washing freshly produced βFeOOH. These provide information on the

- Response of washed βFeOOH to changes in relative humidity. This is investigated by studying any resulting weight changes to confirm whether βFeOOH is hygroscopic.
- Results for mixtures of washed βFeOOH and iron powder exposed to different relative humidities are compared with results of corresponding tests with unwashed βFeOOH and indicate whether the presence of either or both forms of βFeOOH cause iron to corrode at a lower relative humidity than the relative humidity corrosion threshold for iron mixed with ferrous chloride.

These tests:

- inform the model for the "safe" storage of marine (and archaeological etc.) wrought iron by assessing the relative contribution of βFeOOH and/or its adsorbed chloride in the corrosion of iron.
- confirm the effect of time and washing on the reported metastability of βFeOOH.

4.2.5. The response of βFeOOH/ Ferrous chloride/ iron mixtures to moisture

- Using results from experimental programmes 4.2.3. and 4.2.4. and with knowledge that some chloride-contaminated wrought iron will contain intimate mixtures of $FeCl_2.4H_2O$ and βFeOOH, a mixture of iron powder, $FeCl_2.4H_2O$ and βFeOOH are subjected to relative humidity changes. This offers a preliminary insight into any synergistic effects between these two corrosion products.

4.2.6. Examining the role of βFeOOH as a source of labile chloride

- Unwashed βFeOOH is placed in an open top container in the same sealed desiccator as a degreased and polished stainless steel sample (in this case a laboratory spatula) but not in physical contact with it and maintained at 41%RH using conditioned silica gel. This determines whether the labile surface chloride on unwashed βFeOOH is volatile.
- Wash solution from Soxhlet-washed βFeOOH is placed in a beaker covered by amphoteric aluminium foil. Aluminium is adversely affected by chloride ions and reacts to form water soluble aluminium chloride. This determines whether the labile surface chloride on unwashed βFeOOH is volatile.

4.2.7. The effect of elevated temperature on the ferrous chloride model

Temperature influences chemical reaction rates, relative humidity and its relationship to absolute humidity.

- Tests conducted at 20°C to identify the ferrous chloride transition threshold humidity are repeated at other temperatures. The effect of temperature is seen where the ferrous chloride transition threshold humidity changes at different temperatures.

These tests improve understanding of the effect of raising or lowering the environmental temperature where chloride-contaminated wrought iron is housed or stored. Heating is more efficient, and therefore less costly, than cooling. Thermal gain is identified as a potentially significant environmental parameter for chloride-contaminated wrought iron in unheated buildings or outdoors. Efficiency equates with financial savings. Identifying optimum conditions of temperature and humidity takes into account the chemical reactions at different temperatures and humidities. Cost, in terms of corrosion, can be weighed against benefit, in financial terms or *visa versa*.

4.2.8. Examining the role of sodium chloride

The high deliquescence point of sodium chloride (halite) (75-76%RH (Charlson *et al.*, 1978 / Michalski, 1993)) suggests that it is unlikely to influence corrosion as a solid in its own right (i.e. independently) at low relative humidities (Evans and Taylor, 1974). British outdoor and unheated indoor relative humidities can often exceed the deliquescence point of NaCl. This test confirms that the effect of discrete solid NaCl is less relevant at low relative humidities than other mechanisms. No corrosion of the iron powder is expected below the critical humidity of 75%RH so no weight change is anticipated. A constant mass balance reading will validate this prediction and contribute to validating the use of the balance within the environmental chamber for this type of research.

4.2.9. Examining the deliquescence of ferrous chloride tetrahydrate

Richardson and Malthus (1955) give 55.9%RH as the deliquescence point for ferrous chloride tetrahydrate.

- Ferrous chloride tetrahydrate ($FeCl_2.4H_2O$) is exposed to increasing relative humidity environments within the climatic chamber until deliquescence is observed.

This investigation confirms the behaviour of ferrous chloride in this region.

4.2.10. The effect of fluctuating relative humidity

The effect of sudden environmental changes on the corrosion processes taking place at different relative humidities is of importance where plant maintenance or failures are realities and where artefacts ordinarily stored in desiccated sealed containers are removed for examination or to change the desiccant. Votsch™ 4018 climatic chambers are programmable to allow relative humidity and temperature set-points to be

programmed to change at determined times during tests. This equipment enables the effects of changing environmental conditions to be modelled e.g. solar gain, plant failure, opening sealed storage boxes etc.

- The behaviour of ferrous chloride, βFeOOH and mixtures are recorded in relation to programmed changes in relative humidity within the climatic chamber.

4.3 The context for the experimental work

Extrapolation of the results from the above tests will provide useful data for setting parameters for the environmental control systems designed to meet the unique preservation needs of chloride-contaminated wrought iron. They will also provide a simple semi-quantitative understanding of the consequences of the failure of environmental controlled storage of chloride-contaminated iron, as well as support for the day to day management of these systems in areas such as:

- Understanding the implications of temporal and spatial differences (error) in relative humidity within the controlled area, which result from reaction and response times of the environmental management system used to dehumidify the space in which the chloride-contaminated wrought iron is stored.
- Assessing the risks of localised temperature differences through lighting, movement of visitors, solar gain, thermal bridging etc.

Additionally, working knowledge of the iron/chloride corrosion model mechanism at low relative humidity levels is greatly enhanced. A more predictive approach to environmental control is possible. The results will apply equally to the storage of chloride-contaminated archaeological iron, terrestrial meteoric iron in geological collections and to chloride-contaminated marine iron.

5. Experimental methodology

5.1 General principles and methodology

Experimental work centred on determining the stability of iron corrosion compounds and identifying the corrosion of iron by dynamic monitoring of their weight change in closely controlled relative humidity environments. Equal masses of iron and/or corrosion products were used in all experiments to ensure consistency and comparability of results. All samples and mixtures were thoroughly mixed and spread out across the full surface area of the Petri dishes to maximise their surface area in order to speed up responses to environmental change. A pure iron powder control was placed in the climatic chamber for all tests (see figure 92). The possibility of water adsorption on the Petri dishes themselves was tested but found to be repeatedly immeasurable or non-existent. Confirmation of the identity of compounds relied upon infra-red spectra (FTIR-ATR), X-ray diffraction (XRD) and visual appearance. The quality of the experimental work relied upon an accurate and stable control of relative humidity along with a sensitive weight measurement with quantified errors. The main body of work was conducted at a standardised temperature, maintained at 20°C by the chamber in order to ensure parity of resulting data. Different temperatures were subsequently employed to test the effect of changing temperature for a tested relative humidity. An outline of the experimental methodology is given here (section 5) whilst some specific issues are addressed where they arise in the Results section (section 6).

5.1.1. Absolute humidity and specific humidity

Environmental humidity is measured as relative humidity (RH) because this is the most meaningful measure for most practical situations. Air relative humidity controls the rate of evaporation from a moist surface (unless RH is 100%RH i.e. the air is saturated in which case no evaporation occurs). Relative humidity, through its effect on evaporation rate and cooling, therefore affects human comfort. High relative humidity causes

discomfort at high and low temperatures (Faber and Kell, 1957) and low relative humidity is associated with dryness of nasal passages and the skin.

Relative Humidity (t) = $\frac{\text{Actual Partial Water Vapour Pressure}}{\text{Saturated Vapour Pressure (t)}} \times 100\%$

This means that the amount of water held by the air is expressed as a percentage of the total amount of water the air could hold at saturation point, at a given temperature (t).

Percentage saturation is given by

$$\text{RH [\%]} = \frac{\text{mass of water-vapour in a given volume of atmosphere}}{\text{Mass of an equal volume of saturated water vapour at the same temperature}} \times 100\%$$

Absolute humidity and specific humidity are both measures of the actual quantity (concentration) of water vapour present in a given volume (kg/m^3) or mass (kg/kg) of air respectively. Elsewhere these definitions have been sometimes used interchangeably because they both describe actual, quantified, moisture content. Whilst related directly to relative humidity at any given temperature, absolute and specific humidity more directly relate to the reaction kinetics of water vapour during processes of adsorption, and for this study, the corrosion that may result. Conversely, RH is more important as an indication of water vapour gradient in desiccation and equilibrium moisture content processes. The reaction kinetics for the experimental programme studied here is determined by this gradient.

Percentage saturation and relative humidity are identical only for dry air (0%RH) and saturated air (100%RH). At ambient air temperatures the difference between percentage saturation and relative humidity is small. Under these conditions vapour pressure is proportional to specific humidity and the relative humidity may also be defined as approximating the ratio between the absolute humidity and the saturation humidity for a given (dry bulb) temperature. This ratio is called the percentage humidity. The relationships between RH, specific humidity and vapour pressure are approximately linear for a given temperature so RH may also be defined as the ratio

$$\text{RH} = \frac{\text{density of water vapour in the atmosphere}}{\text{density of saturated water vapour at the same temperature}}$$

Unsaturated vapour obeys Boyle's law, i.e. gas density is roughly proportional to pressure (as shown above). Relative humidity is temperature dependent because saturation vapour pressure varies with temperature (figure 20).

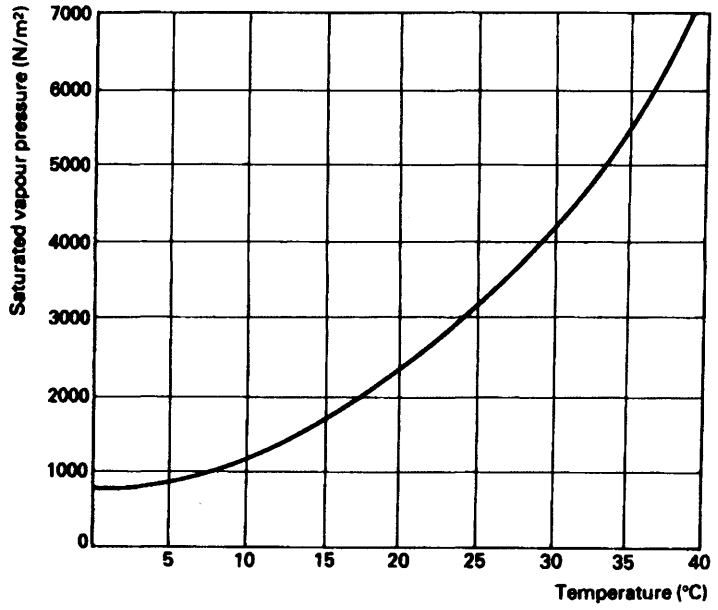

Figure 20. **Increase in saturated vapour pressure (akin to atmospheric moisture content/specific humidity) with increase in temperature for the ambient internal and external temperature range for the British Isles (after Smith et al. (undated) and Kaye and Laby (1966)).**

For a given temperature

$$\text{Relative Humidity [\%]} = \frac{\text{Absolute Humidity [kg/m}^3\text{] or Specific Humidity (kg/kg dry air)}}{\text{Quantity of Water Vapour in Air at Saturation Point [kg per m}^3\text{ or kg/kg dry air]}} \times 100\%$$

This shows that there is a direct linear relationship between relative and absolute or specific humidity at a given temperature. It is therefore possible to convert relative humidity data into absolute and specific humidities for a standardised temperature. This is made possible by monitoring temperature and keeping it constant throughout all

the tests. A fixed temperature of 20°C is used for most of the work conducted. The standardisation of the relative humidity tests at the fixed temperature of 20°C enables direct conversion to specific humidity values (see figure 41) to show how changes in specific or absolute humidity influence processes (dehydration in figure 41 - merely a linear transform of figure 40) at constant temperature.

Direct comparison of results would not be possible if temperature were not standardised for all of the relative humidity tests. The actual amount of water (kg/kg dry air or kgm^{-3} dry air) present at a given relative humidity is different at different temperatures. Data for 22%RH at 20°C and 30°C is presented in figure 74. Moisture content at 30°C is nearly double that at 20°C where the relative humidity is 22%RH in both cases (figure 74). The possibility that moisture content, rather than relative humidity, controls corrosion rates and salt hydrate transformation is considered. Comparison of just one experimental run at a previously tested relative humidity but at a different temperature will indicate the relationships between temperature, dehydration rate, relative humidity and absolute/specific humidity (figures 74, 76 and see section 6.8).

5.2 Customised Experimental Methods

5.2.1. Controlling relative humidity (moisture levels)

Traditionally, saturated salt solutions within closed temperature controlled environments have been used to regulate moisture levels in corrosion tests (Spencer, 1926; Richardson and Malthus, 1955; Martin, 1965; Greenspan, 1977; CRC, 1996). Their use presents disadvantages for research designed to answer the corrosion questions posed here. A saturated salt solution in a sealed environment provides a specific relative humidity whose value is influenced by a range of factors:

- Accurate temperature control e.g. environmental diurnal fluctuation.
- Salt creep up the sides of the salt containment vessel (Astrup & Hovin Stub, 1990).
- The presence of hygroscopic test compounds may depress or raise the environmental humidity through the contribution of their own equilibrium vapour pressure(s).
- Accurate monitoring of the prevailing relative humidity.
- Saturated vapour pressure values cited for the same saturated salt solution are commonly inconsistent (see table 3).
- Limited relative humidity options exist because the range of hygroscopic salts available does not cover all values of relative humidity (Wexler, 1996).

Each hygroscopic salt has a specific equilibrium saturated vapour pressure (Wylie, 1965; Marsh, 1987: 159; Wexler, 1996). Consequently the range of salts and their individual equilibrium saturated vapour pressures dictate both the actual relative humidities that can be achieved and the operational relative humidity range. There will be gaps in any relative humidity range because at a given temperature there is no salt available that can attain a particular humidity value. This prevents examination of the relative humidity range 13% to 23% in 1% increments. Neither is it possible to use saturated salts to simulate cyclic humidity changes that model fluctuations in air conditioning systems.

Maintaining a low relative humidity using a saturated salt solution in a closed container is not efficient (especially in large vessels). This is because diffusion in liquids is very slow and the surface layers of saturated salt solution rapidly become diluted upon absorption of water from the environment it is supposed to control (Padfield, 1966). Dilution means that the surface of the solution ceases to be saturated, altering its vapour pressure and the RH maintained above it. In a closed vessel, where the only movement of molecules is via Brownian motion, it is possible that some stratification might occur because water vapour is lighter than air.

Salt creep occurs on the sides of containers of saturated salt solutions and initiates at the container/solution interface (Astrup & Hovin Stub, 1990). Solid, crystalline, salt forms on the side of the container and this continues to grow in the direction away from the salt solution. The effect of salt creep is a dilution of the salt solution which can cease to be saturated and consequently cease to maintain the desired relative humidity within the sealed container.

The relative humidity maintained above a saturated salt solution in a sealed container is temperature dependent (CRC Handbook, 1996: 15-24). Slight changes in temperature result in small changes in relative humidity within a closed system. The effect of temperature change on relative humidity maintained above saturated solutions of lithium chloride and potassium acetate is demonstrated in table 3 (p86) for a 5°C difference.

The use of a climatic chamber addresses some of the shortcomings of saturated salts and provides data over an appropriate relative humidity range for the experiments, corrosion and corrosion control conducted here. A Votsch™ VC 4018 climatic chamber was chosen for the tests (figure 21). This chamber controls relative humidity to an accuracy of ± 3% over the temperature and humidity range to be tested (Votsch Manufacturer's Data). Measurements of relative humidity use wet and dry bulb temperatures at one location within the chamber and these consistently produced results with a reproducibility of ±1% relative humidity. This accuracy is used when discussing the results obtained from the test series reported here.

Figure 21. **The Votsch™ VC 4018 Climatic Chamber at Cardiff University.**

Using an experimental design that brackets and overlaps relative humidity values, it is possible to pinpoint specific corrosion thresholds for various iron/iron corrosion product mixtures. The similarity between the climatic chamber method of relative humidity control (using a humidification bath/cooling coil) and that of an air conditioning system (which both utilise a fan do deliver the conditioned air) favours transferability of results obtained experimentally within the chamber to iron and corrosion products within an environment maintained by a building management system. The chamber is programmable for cycling relative humidity and temperature, making the testing of worst case scenarios of environmental control failures and minimal target shortfalls possible in a way that would not be easy using saturated salt solutions.

5.2.2. Monitoring corrosion through weight change

5.2.2.1. Weight gain due to corrosion

In the corrosion model under investigation, dissolution of metallic iron produces ions which combine with water and oxygen from the atmosphere. The added weight of the water and oxygen means that mass increases as corrosion proceeds. The experimental method adopted relies upon monitoring these changes in mass and appearance to detect corrosion. Weight changes can be attributed to a range of factors and these have to be identified and their individual contribution to weight gain assessed.

5.2.2.2. Weight gain due to water adsorption

The stable weight of the reactants and products are recorded at the start and the end of each test. A proportion of any increase in mass of iron powder/ferrous chloride or βFeOOH mixtures may be due to adsorption of water other than solely the formation of oxide/oxyhydroxide minerals. It is not the aim of this research to quantify either the proportion of water adsorbed or the increase in mass through formation of corrosion product (although the increase in mass due to corrosion + water adsorption is known for every experiment because the mass of each mixture was recorded after initial mixing and again at the end of each relative humidity test). Corrosion is identified where there is an increase in mass *and* a visual transformation from metallic iron powder to corrosion product, seen as a colour and texture change and subsequently confirmed by XRD (appendices 3 and 4). Qualitative data for water adsorption and desorption is presented for ferrous chloride and βFeOOH in order to demonstrate their hygroscopic behaviour and their consequential contribution to the corrosion of iron.

The form of water on surfaces can be studied in various ways. Water adsorption may be studied qualitatively and semi-quantitatively using FTIR spectroscopy (Little, 1966). Hydrogen bonding (chemisorption) is a strong interaction similar to chemical reactions (Brunauer, 1943) and displaces the frequency of the hydroxyl stretching vibration to lower values whilst considerably broadening and intensifying the adsorption band. All solids in contact with the atmosphere attract part of the atmosphere's gases to their

surface because of unsatisfied molecular forces in their surface layers. The most condensable gases are adsorbed in the greatest quantities, so even at low relative humidities some water vapour is present on aerosol particles (Orr *et al.*, 1958: 473). Water vapour, being an abundant, highly polar, species with a high latent heat of vaporisation, is adsorbed in appreciable quantities (Amorosso and Fassina, 1983: 116). This physical adsorption or physisorption, where attractions are via weaker van der Waals type forces, produces spectral changes that more closely resemble those which result from a change of state (i.e. from a vapour to a liquid, or liquid to a solid). Loss of 3d rotational freedom to be replaced by vibrational or restricted rotational freedom is a feature of physical adsorption (*ibid.*). The fine structure of FTIR adsorptions observed in the vapour phase disappears in the adsorbed phase and asymmetry of the surface force field may give rise to new adsorption bands. Weakly adsorbed molecules have some degree of surface mobility.

FTIR-ATR data was one of the analytical techniques employed to confirm the nature of the corrosion products formed where a colour change was observed during and after tests. Water adsorption (and chloride adsorption) data will be present in the data collected but a systematic study and quantification of adsorbed species must await future work.

5.2.3. Data collection

A Mettler AJ100™ balance accurate to four decimal places (±0.0001g) was used to measure all weight changes in the tests. The balance reading was continuously logged at 5-minute intervals throughout the tests using Mettler's Balink™ software. Importantly, Balink™ software enables the reading of the balance to be logged whether it is stable or not. Balance performance within the chamber was monitored prior to any experimental work with corrosion products to establish whether it could be used in this way and to identify any recurrent or ongoing (systematic) errors, and quantify them.

It was anticipated that the balance would be influenced by vibration from the refrigeration plant supporting the chamber. This was confirmed by running the balance with a fixed weight and without a load. The observed balance vibration is mitigated by damping the shelf within the chamber on which the balance sits with closed cell polyethylene foam where it is supported by the chamber walls and by further damping the shelf by suspending lead weights on rubber tubing from the rungs of the same shelf (figure 21). The balance is also damped with closed cell polyethylene foam where it is supported by the shelf. The damping proves effective and produces a standard deviation for the balance reading data that is insignificant in relation to the magnitude of the mass changes being monitored (figure 24). The remaining vibration through the analytical balance contributes the "noise" visible on the plots of mass against time and reveals its lack of influence on the data produced (Figures 22-23).

Calibration of the balance was achieved by running chamber cycles with a standard mass on the balance (figures 22-24 and appendix 1). This showed a slight drift in balance reading and the mass recorded with the chamber running was usually different to the settled mass with the chamber off. This does not affect the validity of the results of the following experimental programme because they indicate the direction of weight change over time rather than absolute masses at given times. Repeated tests (appendix 1) showed that these factors were both measurable and reproducible, allowing them to be accounted for as systematic error in calculations and interpretation.

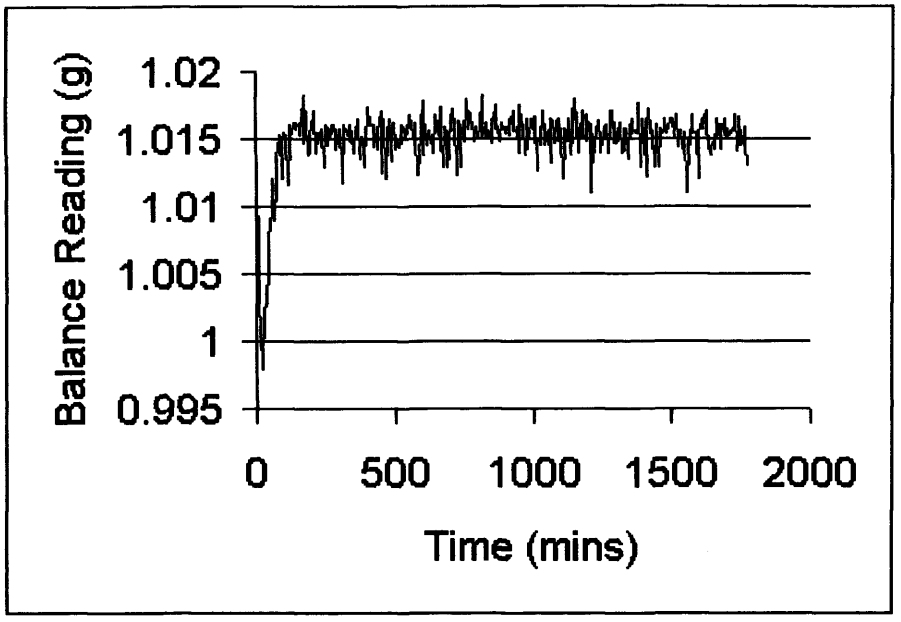

Figure 22. **1.0 gram standard mass showing influence of balance shake at the beginning of each test and "noise" due to vibration during the test (at 20°C and 23%RH).**

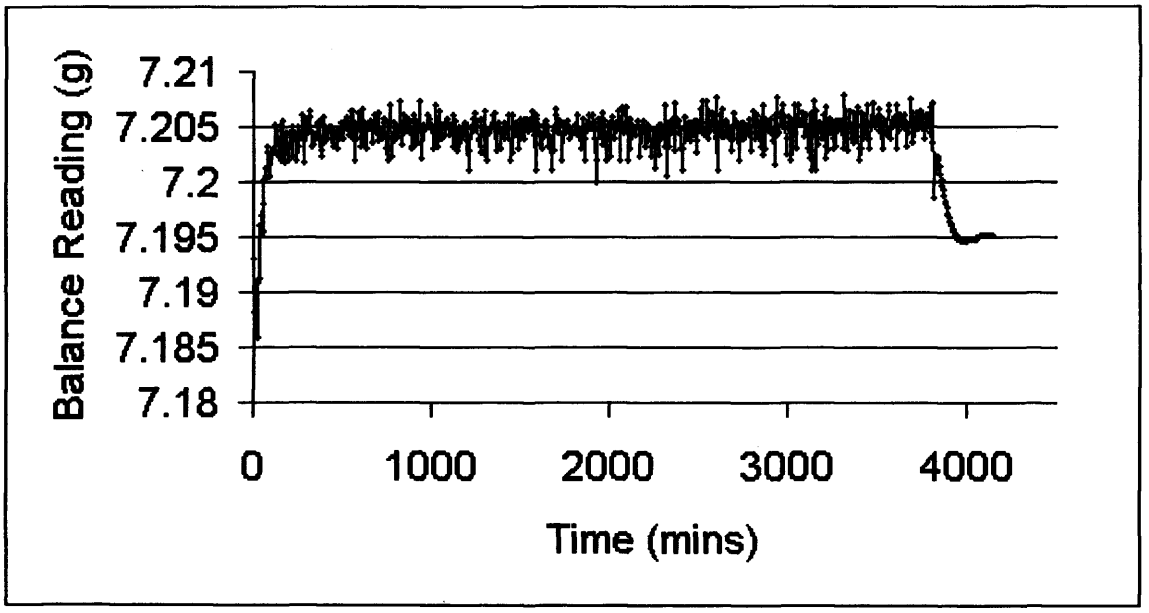

Figure 23. **Reproducible balance-drift for an empty Petri dish (at 20°C and 23%RH).**

Figure 23 shows reproducible balance-drift where an empty Petri dish weighing 7.1884g was placed on the balance and the chamber started at 0 minutes. Data show initial "root-sign" lurch followed by stabilisation at about 7.205g. Chamber turned off at 3700 minutes and the balance shows a slow return to the initial mass of the Petri dish (7.1884g) less the new "drifted" tare of the balance when the Petri dish is removed (0.0077g). The "drifted tare" (0.0077g) accounts for the magnitude of difference between the actual weight of the Petri dish (7.1884g) and the logged final balance reading (~7.195g) to within the precision of this method.

Initial balance readings result in a mathematical "root-sign" like plot for each test. The initial apparent gain or loss in weight due to this phenomenon is mirrored at the end of the test if the standard mass is left on the balance "at rest" with the chamber (and its vibrating refrigerator) off (figure 23). Any difference in logged start and end masses is attributable to "balance calibration drift" during the cycle. This is apparent as a discrepancy between the initial calibrated tare of the balance and the end "tare" reading when the sample is removed from the balance. For a complete data set, more balance drift and error test results are appended in appendix 1.

To avoid uncertainty when interpreting data, the reactants or products studied in each of the tests were used in quantities closely approximating 1 gram or 2 grams to provide changes in weight of a magnitude far in excess of any vibration or balance drift phenomena. All masses were weighed and recorded at four decimal places but the quantities always approximated 1.0000g or 2.0000g due to the difficulty in spooning out exact 1.0000g or 2.0000g quantities.

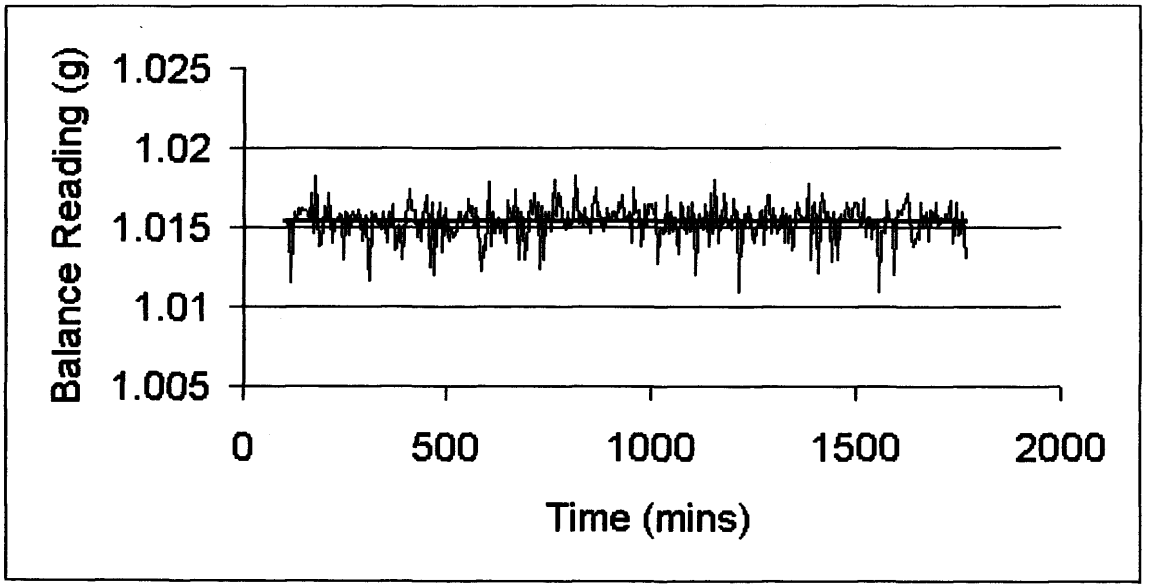

Figure 24. **The best-fit line (least squares) for data from a standard 1.0g mass placed on the balance during a climatic chamber cycle (at 20°C and 23%RH) shows good stability (indicating constant mass) within the vibration 'noise'.**

5.2.4. Environmental precision within the climatic chamber and environmental data collection using the chamber software

Figure 25 shows the climatic chamber temperature and wet/dry bulb relative humidity (%) plot against time (using Simpati™ software) for the 1.0 gram test in figure 22 run at set-points of temperature 20°C and relative humidity of 23%RH.

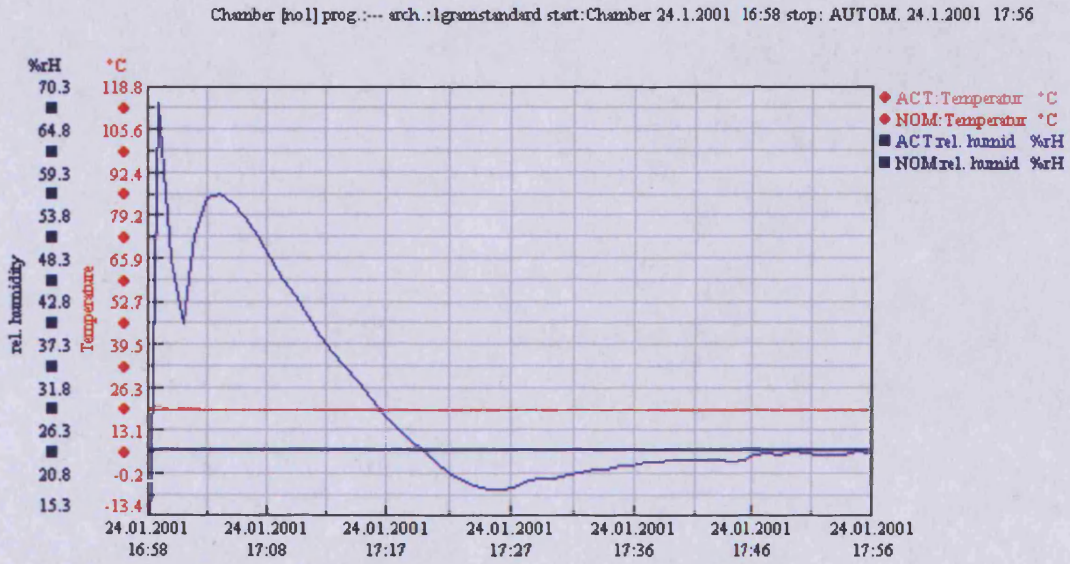

Figure 25. **Simpati™ software plot showing the relative humidity and temperature within the climatic chamber during the first hour of the standard 1.0g test for which the balance (Mettler™) data was reported in figure 22.**

The time taken for the climatic chamber to attain the programmed 'set-point' relative humidity and temperature is indicated where the horizontal set-point lines are joined by the matching coloured actual environmental reading taken within the chamber. The programmed temperature was achieved within 5 minutes. The programmed relative humidity was achieved by the chamber within an hour (time: *x*-axis).

It can be seen that the set-point temperature is achieved rapidly and the set-point relative humidity (shown as a horizontal bar at 23%) is attained after approximately one hour at this RH. Relative humidity set-point attainment was found to occur between half an hour and one hour after starting the climatic chamber programme in all cases (see also appendix 2).

Long periods at low relative humidities are difficult to maintain in the climatic chamber. Running at low relative humidity removes lots of water from the air within the chamber and this can lead to icing of the refrigeration coil used to remove it. Pre-dried compressed air must be supplied to the chamber to minimise icing during tests run at set-points of 20%RH to 10%RH. It was found that three oil filters in series had to be added to the incoming compressed air line to prevent oil carry over from the compressor and contamination of the experiments. Icing of the condensation coil results in a small, but undesirable, environmental RH drift away from the desired set-point (figure 26). This limits the length of tests that can be run at such low relative humidities to no more than two weeks. The condensation coil was checked for icing during and at the end of each test and compared with the data from the wet/dry bulb hygrometer to ensure that the environment within the climatic chamber was maintained at the desired set-point.

A potential source of error with this equipment is a dirty cotton sleeve covering the wet bulb thermometer of the hygrometer. The sleeve must be clean and uncontaminated in order to obtain reliable humidity data which is used by the computer controlling the chamber to control the humidity of the chamber space. It is necessary to replace the cotton wick regularly because it is contaminated by mould growth during use. It is important that the reservoir of deionised water is also cleaned and rinsed regularly to limit contamination to a minimum. The wick and the base of the chamber must not be contaminated by salts used for the experimental programme. The base of the chamber drains into the deionised water reservoir for the wick and contamination of either will result in erroneous relative humidity control and data.

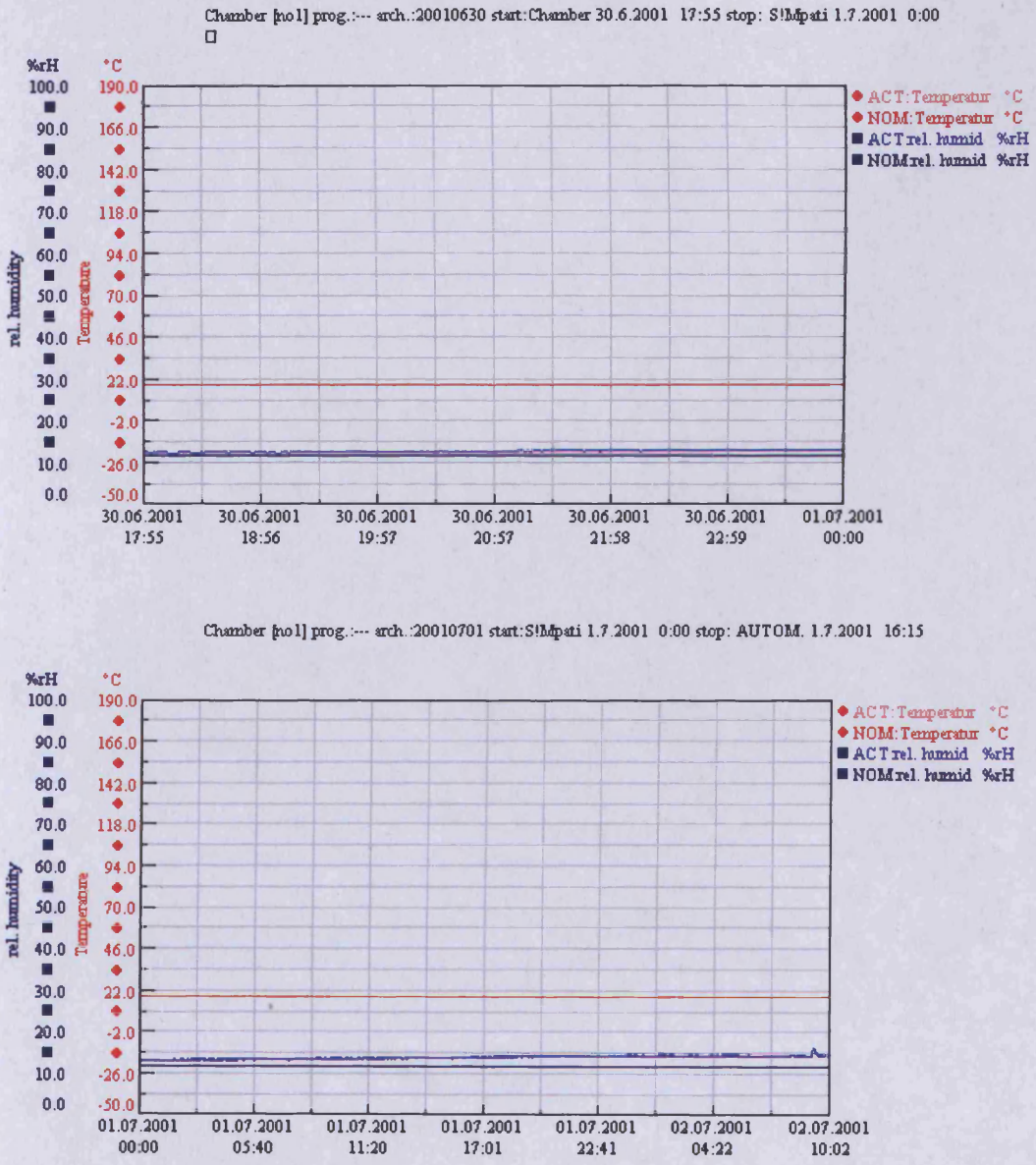

Figure 26. **Slow deviation from the climatic chamber set-point (shown as a horizontal bar) of 12%RH with time due to ice formation on the chamber condensation coil. The temperature within the chamber is maintained at its set-point throughout.**

5.2.5. The production of akaganéite (βFeOOH) for use in this study

Pure βFeOOH (akaganéite) has no commercial applications and is not retailed commercially as a graded compound (e.g. as laboratory grade, Analar or Aristar grades). Where available commercially (e.g. from Richard Taylor Minerals Ltd., see Thickett (2005)) akaganéite will be a potentially impure mineral of geological origin. It is necessary, and desirable, to synthesise any βFeOOH required for experimental research purposes.

Laboratory syntheses of βFeOOH using differing wet chemistry syntheses are known to precipitate different crystal structures e.g. larger spindle or cigar shaped somatoids and smaller rod shaped crystals (Atkinson *et al.*, 1977; Wolf *et al.*, 1966). βFeOOH can only be prepared at pHs below pH 5 because the hydroxyl ion is more competitive than the chloride ion for structural sites (Schwertmann & Cornell, 2000). The chloride content of βFeOOH varies widely with the conditions of preparation and subsequent wash treatments (Ishikawa and Inouye, 1975). Thickett (2005) reported that studies of akaganéite corrosion product and synthetic akaganéite using scanning electron microscopy (SEM-EDX) generally showed a higher chloride concentration in the corrosion products than in the synthesised akaganéite. Experiments using synthetic akaganéite might not accurately reflect reality if the chloride level it contains or the form in which it is present is different to that of akaganéite produced through corrosion.

Crystal size and morphology affect the properties (like colour) and surface chemistry of the resulting akaganéite. In common with ground artist's pigments, the finer crystals of βFeOOH have the more intense (often darker) colour. All crystals of βFeOOH are reported to be very small with a large surface area per unit volume (Buchwald and Clarke, 1989). A large overall surface area enables large amounts of surface adsorption to occur (e.g. adsorbed chloride and/or water molecules). This may promote and accelerate corrosion of iron in contact or close proximity to it. Mackay (1962) identified βFeOOH somatoids and tactoids. Studies of βFeOOH may be complicated by the possibility that crystal morphology is sometimes affected by the energy of the electron

beam of a Scanning Electron Microscope (SEM) (Mackay, 1960: 555; Galbraith *et al.*, 1979).

Most synthetic methods of production involve ferric (iron III) chloride solutions (not ferrous (iron II) chloride) at elevated temperatures with production via hydrolysis (Al-Zahrani, 1999: *table 8*). These methods of production tend to be far removed from the natural production of akaganéite (βFeOOH) during the corrosion of iron. Some reported syntheses produced βFeOOH via Fe (II) oxidation or from Fe (II) precipitation (Al-Zahrani, 1999: table 7). Atkinson *et al.* (1977) showed the properties of spindle form βFeOOH to be different from those of the rod form βFeOOH, which showed a greater capacity for adsorption due to its larger surface area. Interestingly, Cornell (1983) demonstrated that βFeOOH synthesis (according to the technique of Paterson & Tait, 1977) produced a cracked filter cake and did not have the ability to form a coherent film. βFeOOH is consequently likely to contribute to micro porosity and micro capillarity within cracks and corrosion products where they still adhere to the underlying metallic core. βFeOOH is certainly unlikely to passivate or stifle iron corrosion, irrespective of the action of its chloride.

βFeOOH formed on marine or on excavated archaeological material is likely to form under a range of conditions which are different to the synthetic methods reported above. Aerial oxidation of ferrous chloride, either in solution or as hydrated solid (Taylor, 1984b), in the presence of iron is one naturally occurring mechanism and this (using the hydrated solid) was chosen as the method of production of the βFeOOH synthesised for this study. This method of synthesis is particularly relevant to the existing Turgoose models for wrought iron i.e. oxidation of ferrous chloride tetrahydrate and ferrous chloride solutions. The weeping of supersaturated chloride solutions (effectively HCl with ferrous ions in solution) is commonly observed on chloride-contaminated wrought iron (Selwyn *et al.*, 1999). Crystal (βFeOOH) growth proceeds from this solution via nucleation and gradual loss of water of solution.

BDH GPR™ iron powder reduced by hydrogen was used in the synthesis of βFeOOH and for all tests. The advantage of this iron powder is its large surface area per unit volume due to its microscopic spherical form (spheres having the maximum possible surface area for reaction, see figure 27). Reactions being studied will occur more rapidly and, most importantly, measurably due to the large surface area of the iron available for chemical reaction (for chemical reaction will only take place at the surface of the iron).

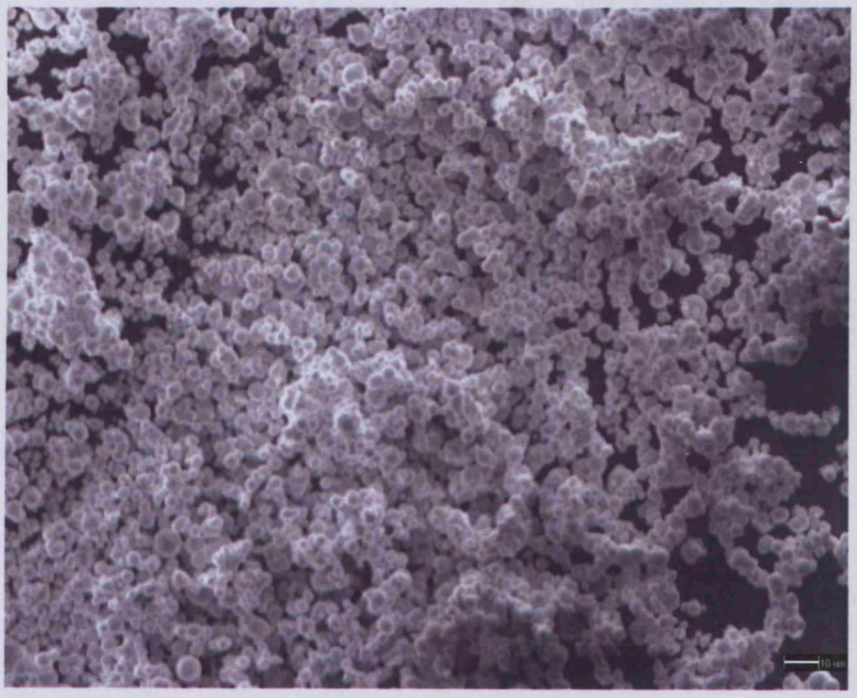

Figure 27. **SEM image of a sample of the iron powder used in this study. The scale bar represents 10μm.**

Analar grade ferrous chloride tetrahydrate (BDH) was used as supplied (figure 28) and, in desiccated form, to create ferrous chloride dihydrate.

Figure 28. **The green Analar grade ferrous chloride tetrahydrate (BDH) used for this study.**

The long history of the study of βFeOOH at Cardiff University has produced a wealth of accumulated experience in its production. Archives of previous syntheses of were researched in preparation for the synthesis necessary for the experimental programme reported here. An earlier worker noted important variations in the products formed using only slightly different equipment (Al-Zahrani, 1999). βFeOOH had been previously produced in two desiccators using identical mixtures of iron powder and ferrous chloride in environments maintained at ~92%r.h. in each case by a saturated solution of sodium carbonate to induce and support aerial oxidation. The aim then was to produce pure βFeOOH for further experimental work. The products of each desiccator were assayed at the time using X-ray diffraction (XRD). Whilst the product in one of the desiccators was assayed as pure akaganéite (βFeOOH) the product in the other desiccator was found to contain a mixture of akaganéite and magnetite. In order to understand why the two desiccators produced different products, and to avoid the production of a mixture rather than pure βFeOOH for use in this experimental programme, Al-Zahrani's syntheses were repeated using his original desiccators.

Refait & Genin (1997, and 1993 with Olowe) and Selwyn *et al.* (1999: 220) report that high chloride concentrations are necessary to enable the formation of βFeOOH. The concentration of chloride ions held (as counter ions) near the surface of iron is

determined by the ability of the metal core to corrode to produce Fe^{2+} ions. Electrolyte (water) is necessary for hydrated ferrous ions to form. Acidity is therefore determined by the Fe^{2+} concentration (see [5], p 49). Below pH6, Fe^{2+} ions do not readily oxidise to Fe^{3+} ions so low (more acidic) pH environments favour the formation of βFeOOH rather than magnetite (figures 7 - 10). A saturated solution of $FeCl_2$ is about 4.25M and has a pH of about pH4 (Selwyn *et al.*, 1999: 219).

Section 2.7 described how a saturated salt solution (e.g. $FeCl_2$) will continue to absorb atmospheric moisture from an environment maintained at a relative humidity much higher than the deliquescence point of that salt (Amorosso & Fassina, 1983: 115-117). The saturated salt solution will become more and more diluted as more and more atmospheric water is absorbed. This phenomenon could potentially decrease the chloride concentration sufficiently that it falls below the critical $[Cl^-]$:$[OH^-]$ ratio of 8:1 required for pure akaganéite formation as described by Refait & Genin (1997). However, below their ratio of 8:1 Refait & Genin reported goethite/akaganéite formation. Magnetite formation only began to occur when the $[Cl^-]$:$[OH^-]$ ratio fell to below 1.11:1 (Refait & Genin, 1993).

No goethite or lepidocrocite (the two products also formed at ratios between those given for magnetite and akaganéite formation) were reported as present in the contaminated sample of βFeOOH produced by Al-Zahrani (1999: 177). This suggests that low chloride concentration due to the very high relative humidity environment (~92%r.h.) was not the cause of the magnetite/ akaganéite product in the one desiccator. This is also demonstrated by the fact that uncontaminated βFeOOH was produced by Al-Zahrani using the same method in the other desiccator. It is likely that even at lower solution concentrations iron will retain a high chloride concentration near its surface.

Gilberg and Seeley (1981: 52) cite that βFeOOH is unstable to hydrolysis to αFeOOH but that in the presence of moisture and iron metal it will transform under moist conditions to magnetite. No detail of the mechanism for this transformation is given by them but this description would fit the description of the method of formation described by Al-

Zahrani (1999) and the results of his assay of the products formed. However, this does not account for the lack of magnetite in the other desiccator. It is therefore necessary to consider the other variable that would be a controlling factor in magnetite versus akaganéite formation: oxygen concentration. It may be inferred that where oxygen supply is limited it is this that is the controlling factor in akaganéite or magnetite formation. Low oxygen, reducing conditions, almost certainly prevailed in one of the two chambers and not in the other. It was decided to test this proposal experimentally.

The desiccators used by Al-Zahrani (1999) to produce his two batches of βFeOOH were traced in the laboratory, still containing their sodium carbonate saturated solutions. One desiccator was found to have a stopper with a channelled tap, which could have allowed entry of oxygen only if set to the open position. This desiccator and its stopper were sealed with silicone grease. The other desiccator was only sealed by loosely fitted cling-film wrapped around a 4cm hole in the top. The production of βFeOOH in the stoppered chamber as described by Al-Zahrani (*ibid.*) was repeated twice, once with the stopper open and once with the stopper closed.

With the stopper closed, after just one day the oxygen in the sealed desiccator had been consumed resulting in a strong partial vacuum. This sucked the top of the desiccator onto its base very strongly and resulted in an inward rush of air on opening the stopper after one day. The iron powder/iron chloride mixture within appeared olive green in colour. This compound was a green rust (Refait *et al.*, 1993; Misawa *et al.*, 1974: 132). Misawa *et al.* (1974) report the formation of "green rust I" by solid state oxidation of ferrous hydroxide or as a precipitate from solution upon aerial oxidation at near neutral or slightly alkaline pH. "Green rust I" was reported to form in the presence of Cl^- ions whereas "green rust II" was reported to form in the presence of SO_4^{2-} ions. Gilberg and Seeley (1981: 51) report lepidocrocite (γFeOOH) and slow conversion to magnetite (Fe_2O_3) as products of intermediary green rusts. Misawa *et al.* (1974) also cite green rusts as intermediates with further oxidation producing magnetite (cited in connection with the aerial oxidation of ferrous hydroxide), lepidocrocite (γFeOOH), δFeOOH or goethite (αFeOOH) via amorphous ferric oxyhydroxide. After opening the stopper it was left open and the green rust had oxidised to a bright orange product

within hours (figure 29). This then slowly converted to dark brown product with the stopper open and the product aerated over the next few weeks. The dark brown product was assayed and found to be akaganéite (appendix 3, samples 3 and 4). No γFeOOH was reported by Al-Zahrani (1999) either. Had the stopper not been opened to oxygenate the desiccator and the green rust within it, the green rust would probably have slowly converted to magnetite.

Figure 29. **The green rust to βFeOOH (Akaganéite) transformation in progress upon aeration after oxygen within the sealed vessel had been consumed in forming the green rust. Dark areas near the edges are green rust. Surface oxidation of the green rust to βFeOOH (Akaganéite) is most advanced at the centre.**

Limited oxygen supply was responsible for the magnetite found in the one batch of Al-Zahrani (1999) akaganéite. It is therefore likely that the desiccator that produced the βFeOOH and magnetite mixture was the desiccator with the stopper and that the stopper was closed. The desiccator which was ineffectively sealed with cling-film was probably the one that produced the pure βFeOOH because a partial vacuum due to the exhaustion of oxygen could never have occurred. Oxygen used up during oxidation

could easily have been replaced through diffusion. No other differences between the two desiccators were observed. Once formed, the stable magnetite would not have subsequently been oxidised on exposure to high oxygen levels (Misawa et al, 1974: 134-149). The result of this experiment was used to inform the synthesis methodology for the βFeOOH used in this research. To avoid the production of magnetite the desiccation vessels used for βFeOOH synthesis for use in this research were opened daily (Monday to Friday) to allow oxygen exchange, but with insignificant, short term, affect on the environmental RH within. βFeOOH formation (see figure 29) was observed to proceed directly from the admixture of ferrous chloride and iron powder via a *green rust* (GR1) phase (Taylor, 1984; Kassim *et al.*, 1982; Refait & Genin, 1997, 1993 with Olowe and 1993 with Rezel).

For interpretation of later experimental work it was desirable to confirm the presence or absence of unreacted iron powder, residual ferrous chloride tetrahydrate and/or other iron corrosion products within the synthesis product. Microscopic examination of the synthesis product revealed it to be microcrystalline with orange to reddish internal reflections intermediate between those of goethite and lepidocrocite (Buchwald and Clarke, 1989). No opaque iron powder was detected using optical microscopy (figure 30) and the product sampled was not attracted to a magnet. The product exhibited birefringence under crossed polars (figure 31).

X-ray diffraction (XRD) performed independently at the Department of Earth Sciences, Cardiff University, did not reveal any residual solid, crystalline, ferrous chloride after equilibration of the product to 41%RH (appendix 3 and appendix 4, sample 8). These XRD analyses revealed βFeOOH as the only crystalline solid present (figure 32). Equilibrium to 41%RH means that ferrous chloride should not be present in an amorphous (non-crystalline) form, deliquesced and in solution. XRD can only identify solid crystalline substances because the diffraction angle measured and diagnostic to this technique requires crystal lattice planes which diffract the x-ray beam. Solid, crystalline ferrous chloride hydrate ($FeCl_2.4H_2O$) was also submitted for XRD analysis along with $FeCl_2.4H_2O$ crystals which had visibly partially oxidised at their surfaces during long-term storage and comprised $FeCl_2.4H_2O$ with a small amount of βFeOOH

(appendix 4, samples 5 and 6). The diffractogram for $FeCl_2.4H_2O$ matched the international powder diffraction file reference pattern 16-0123 [appendix 5] for monoclinic ferrous chloride hydrate ($FeCl_2.4H_2O$). The diffractogram of partially oxidised $FeCl_2.4H_2O$ is included here for comparative purposes (figure 33). Colour and general appearance were noted carefully throughout the syntheses to inform later experimental observations during corrosion tests utilising iron powder.

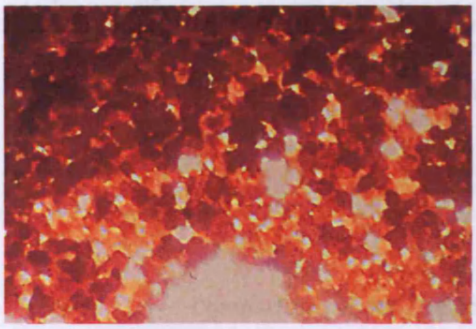

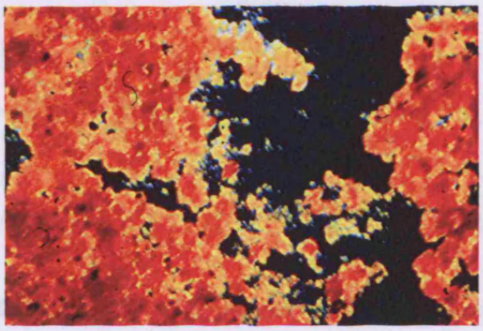

Figure 30 **(left) Photomicrograph of translucent laboratory synthesised βFeOOH (transmitted light).**

Figure 31 **(right) Photomicrograph of birefringent laboratory synthesised βFeOOH (transmitted light with crossed polars).**

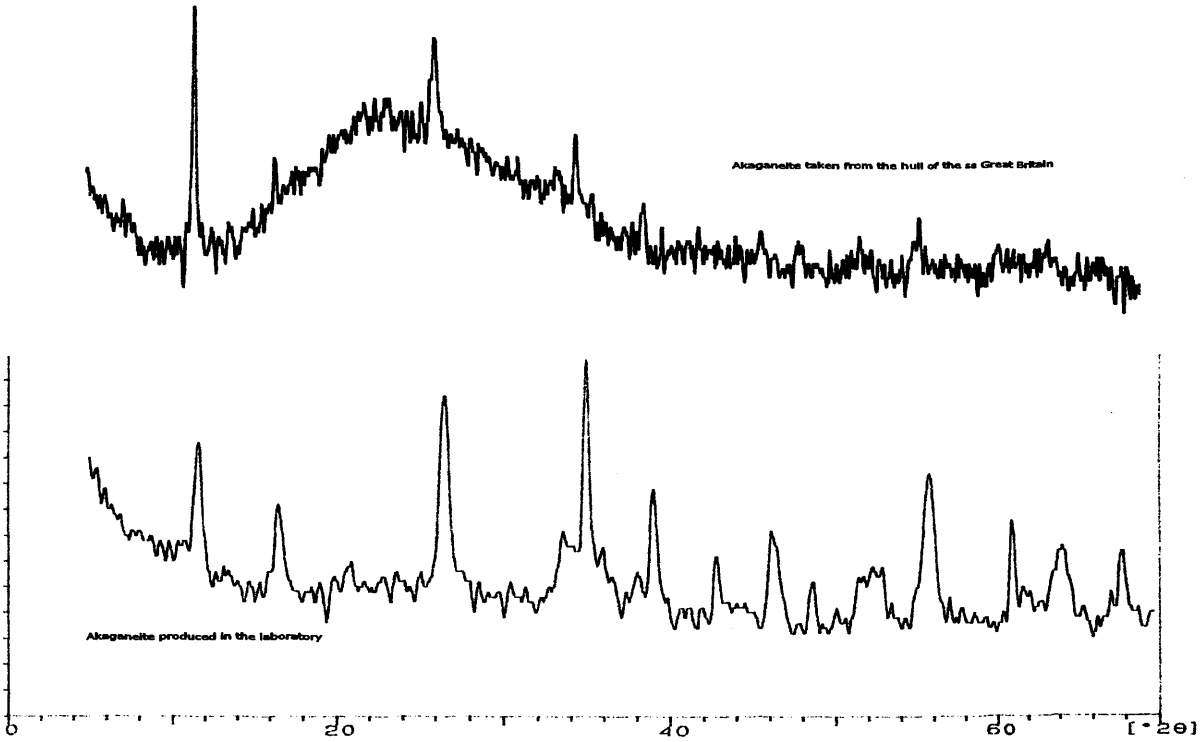

Figure 32. **Comparison of XRD spectra for βFeOOH (Akaganéite) produced in the laboratory (bottom) and a sample taken from the hull of the ss Great Britain (top). XRD conducted by Dr. A. Oldroyd, Department of Earth Sciences, Cardiff University.**

(Note that the broad hump in the upper sample was due to mounting that sample on a glass plate. The presence of all of the major peaks in both samples gives a positive match i.e. a positive identification as compared with the international powder diffraction files JCPDS 42-1315 and 34-1266.)

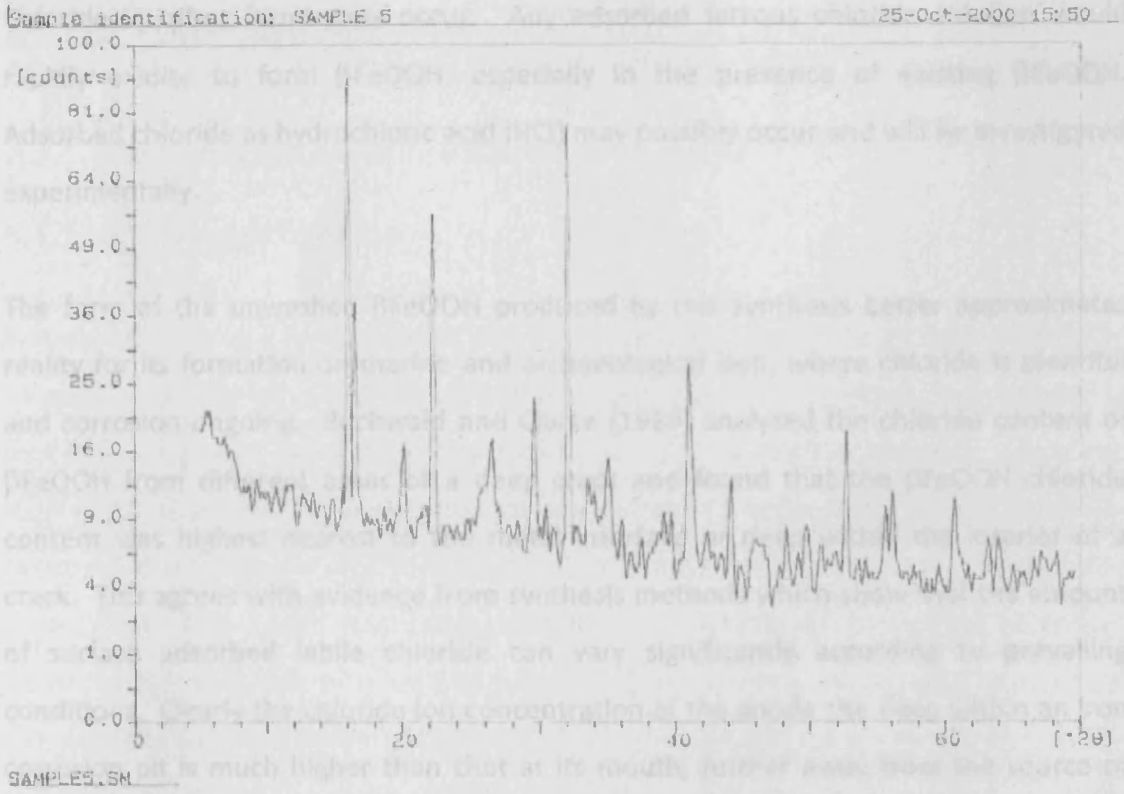

Figure 33. XRD spectrum for partially [surface] oxidised ferrous chloride tetrahydrate. XRD conducted by Dr. A. Oldroyd, Department of Earth Sciences, Cardiff University.

The βFeOOH synthesised via slow aerial oxidation for this study will have excess adsorbed chloride present because stoichiometrically chloride is in excess of that required for βFeOOH alone when 25g of Fe powder are mixed with 25g of $FeCl_2.4H_2O$ and oxidised at high RH. The βFeOOH synthesised via slow aerial oxidation for this study was divided. Half was washed with water until the filtrate was chloride free. The rest was not washed and was anticipated to have excess surface adsorbed chloride as a result.

XRD analysis (figure 32 and appendix 4, sample 8) showed no crystalline $FeCl_2.4H_2O$ peaks. XRD of the $FeCl_2.4H_2O$ used was conducted successfully as a control and confirmed the absence of these peaks in the βFeOOH product (appendix 4, samples 5 and 6; see also figure 33). The excess or adsorbed chloride is not crystalline.

Chloride in other forms may occur. Any adsorbed ferrous chloride solution would rapidly oxidise to form βFeOOH, especially in the presence of existing βFeOOH. Adsorbed chloride as hydrochloric acid (HCl) may possibly occur and will be investigated experimentally.

The form of the unwashed βFeOOH produced by this synthesis better approximates reality for its formation on marine and archaeological iron, where chloride is plentiful and corrosion ongoing. Buchwald and Clarke (1989) analysed the chloride content of βFeOOH from different areas of a deep crack and found that the βFeOOH chloride content was highest nearest to the metal interface or deep within the interior of a crack. This agrees with evidence from synthesis methods which show that the amount of surface adsorbed labile chloride can vary significantly according to prevailing conditions. Clearly the chloride ion concentration at the anode site deep within an iron corrosion pit is much higher than that at its mouth, further away from the source of ferrous (Fe^{2+}) ions.

Aqueous washing of βFeOOH reduces chloride content. This reflects Cl^- bound in the hollandite structure (only for any βFeOOH that breaks down) and any residual surface chloride until a low, fixed, chloride content is reached (North, 1982). If βFeOOH causes corrosion of iron as reported (Turgoose, 1982b) and this is due to mobile surface adsorbed chloride, the βFeOOH synthesised here can be said to offer a 'worst case' scenario for the corrosion of associated iron (especially iron in finely divided powder form as used here) because of the enormous surface area and contact area of the reactants and the higher levels of labile chloride on unwashed βFeOOH than on washed βFeOOH. This is desirable to provide timely results in corrosion experiments at low humidities.

6. Results and discussion

6.1 Dehydration of $FeCl_2.4H_2O$ to $FeCl_2.2H_2O$

6.1.1. Data and discussion

In order to verify and further Turgoose's threshold humidity work with ferrous chloride, samples of green $FeCl_2.4H_2O$ (figure 34) approximating 1 gram in mass, but weighed to four decimal places, were subjected to a range of fixed relative humidity values and their mass measured against time. If conversion to white $FeCl_2.2H_2O$ (figure 35) occurred at a particular relative humidity the balance records the loss of water as a weight loss. The weight loss can be predicted because it will be equivalent to two waters of hydration per mole for a known mass of ferrous chloride tetrahydrate. This is calculated to be 0.1812g for 1.0000g of ferrous chloride tetrahydrate according to the molecular formulae. Turgoose (1982b) also cites an expected weight loss of 18.1% for the reaction

$$FeCl_2.4H_2O \leftrightarrows FeCl_2.2H_2O + 2H_2O \qquad [27]$$

Using the above formula where Fe has an atomic weight of 55.850, Cl has an atomic weight of 35.457, H has an atomic weight of 1.008 and O has an atomic weight of 15.999, the molecular weight (M_r) of $FeCl_2.4H_2O$ is calculated as 198.828 and the molecular weight (M_r) of $FeCl_2.2H_2O$ is calculated as 162.796.

Using the unitary method,

Let 198.828 = 100%

Dividing both sides by 198.828, gives 1 = 100/198.828

Therefore 162.796 = (100/198.828) x 162.796 = 81.88%

The two waters of hydration therefore represent 100% - 88.88% of the mass of ferrous chloride tetrahydrate, i.e. 18.12% by weight. For 1.0000g of $FeCl_2.4H_2O$, a loss of

0.1812g (18.12%wt) is predicted on conversion to $FeCl_2.2H_2O$, representing weight loss corresponding with the mass of two waters of hydration.

Figure 36 records weight change as a function of time for the dehydration of green $FeCl_2.4H_2O$ to white $FeCl_2.2H_2O$ at a range of humidities expected to promote this phase change based upon Turgoose's (1982b) data. The colour change was observed in each case (figures 34 and 35). Results show that the time taken to achieve the full weight loss of 0.1812g/g varies according to the relative humidity at which it occurs (figure 36). A correlation between the rate of conversion to $FeCl_2.2H_2O$ and the relative humidity of the chamber is evident. The lower the relative humidity the faster the dehydration rate will be.

Figure 34. **(left) Green/yellow $FeCl_2.4H_2O$, as supplied by BDH.**

Figure 35. **(right) White $FeCl_2.2H_2O$ after desiccation of green $FeCl_2.4H_2O$.**

The reduction in weight recorded at 14%RH and 12%RH corresponds well with the theoretical reduction in weight of 0.1812g to 0.8188g associated with the loss of two waters of hydration. These results also validate the data obtained from the balance within the climatic chamber and its use in this way for this type of study.

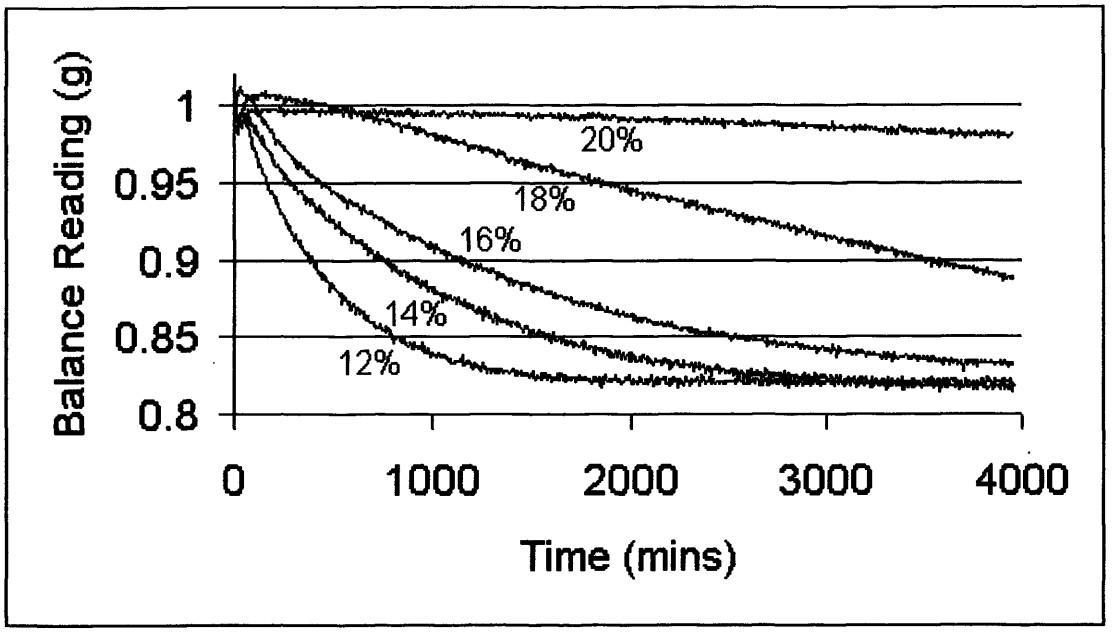

Figure 36. **Changes in mass of samples of $FeCl_2.4H_2O$ during transition to $FeCl_2.2H_2O$ at various relative humidities as a function of time (published in Watkinson and Lewis, 2005a).**

The results presented in figure 36 show that the stable hydrate of ferrous chloride at 20%RH, and lower RHs, at 20°C is the white dihydrate, which does not corrode iron. As the slope of the 20%RH curve tends towards zero and the time taken for it to dehydrate is tending towards infinity it is predicted that a threshold relative humidity for ferrous chloride dihydrate lies above a little above 20%RH. This can not be established by a 21%RH test because of the time that would be necessary to provide useful data. The reaction of ferrous chloride tetrahydrate with iron powder at relative humidities above 20%RH was tested instead.

6.1.2. Diffusion mechanisms

The possibility that a diffusion mechanism influences the measurements taken (so that statements regarding reaction rate would need to take this into account) must be considered. The samples are placed on a glass-enclosed balance pan. The balance chamber door opposite the climatic chamber fan is left open a standardised amount (1mm) to ensure that any affect is common to all the experiments. This gap minimises "noise" from the climatic chamber fan due to air flow disturbing the balance pan.

Each test was run at a programmed set-point of 20°C to ensure parity of results with various RH set-points depending on the test being run. Each started from an ambient chamber temperature and RH. The environment within the balance chamber will come into equilibrium with the environment within the climatic chamber via air exchange by diffusion through the one open balance chamber door (Thomson, 1977; Brimblecombe and Ramer, 1983). The transfer of humidity across the gap by diffusion will occur at an exponential rate according to Fick's law [28] & [29] (Padfield, 1966: 15; and see figure 37 of this thesis).

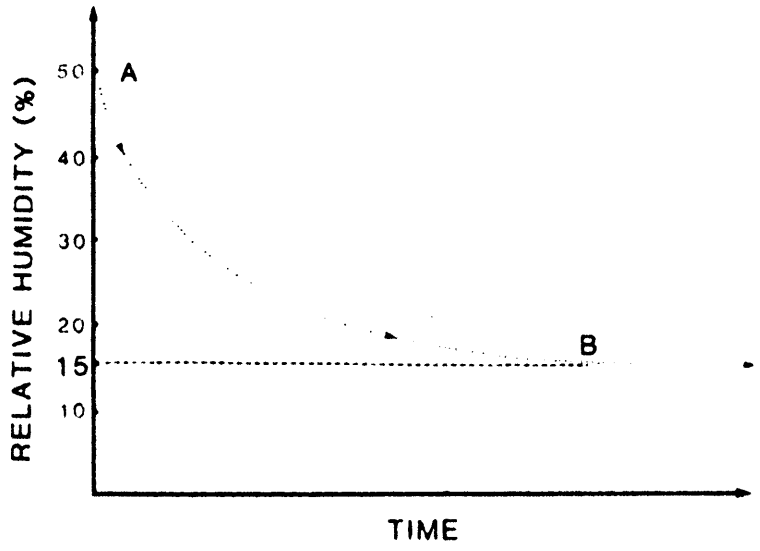

Figure 37. **Exponential decrease of relative humidity inside a leaky museum display case at 50%RH initially (A) in a room with a relative humidity of 15%RH (after Lafontaine, 1984).**

$$\frac{dc}{dt} = -A D \frac{dc}{dx} \quad [28]$$

$$C = C_0\left(1 + e^{\frac{-DAt}{Vx}}\right) \quad [29]$$

Where *c* is the quantity of material (water vapour) passing through the plane,

dc/dx is the concentration gradient

A is the area of the plane,

D is the diffusion coefficient,

C is the concentration within the balance chamber,

C_0 is the concentration of water vapour in the climatic chamber,

V is the volume of the balance chamber.

The quantity *Vx/DA* is the time taken for the concentration to drop from C_1 to C_0 at the initial rate. It is also the time at which $C = 1.37C_0$.

Equation [29] confirms that the change of RH with time is exponential and equation [28] shows that as RH difference becomes smaller the rate of change diminishes.

The results are exponential in figure 36. As expected for a gradient-controlled mechanism, the fastest changes in mass are experienced where the difference between the ambient (start) humidity and operating humidity is greatest, whether humidifying or dehumidifying the samples. Other factors also influence the set up. The climatic chamber fan is set at a standardised speed for all reported tests. It aggressively disturbs and redistributes air in the chamber and is likely to greatly reduce the exponential "time lag" that would be expected if diffusion (due to Brownian motion) were the only factor in the equilibration of the balance environment and the chamber environment.

As the time lag between the climatic chamber and the balance chamber is negligible, the difference in water vapour pressure within the balance chamber and the climatic chamber should also be negligible which means that balance glass enclosure effects on the rates given by the slopes of the plots of data reported here are also negligible. This

was confirmed by simultaneously running a relative humidity test with one RH data logger within the balance enclosure, one data logger in the climatic chamber and comparing their data with the climatic chamber's own RH data logger (appendix 2). The rate of change in weight (the slope) of each plot of data reported here records corrosion rate *and* diffusion effects, which are real and present but are negligible relative to the rate of corrosion. Importantly, diffusion effects only influence the first few hundred minutes of each test.

Figure 36 illustrates this point. Tests began with both the climatic chamber and the balance chamber at the same, ambient RH. The Cardiff University Conservation Laboratories tend to be dry and the βFeOOH was stored at 41%RH so the region 30%RH-60%RH can be used as a very broad starting RH range. According to Fick's law, the rate of transfer of water vapour to or from the balance chamber is proportional to the concentration gradient across the gap [28]. The rate of transfer will therefore be slowest for the tests run near the ambient range of humidities and fastest for the lowest humidity tests (i.e. 22%RH, 23%RH and 25%RH). Weight increases for corroding samples can be clearly seen as early as 170 minutes from the beginning of the higher humidity tests. The chamber and balance take about 30-60 minutes and 170 minutes respectively to settle at the start of each test (figures 23, 24 and 25). Dehydration of ferrous chloride tetrahydrate at 12%RH is rapid due to the large moisture (relative humidity) gradient between the balance enclosure and the climatic chamber enclosure. The balance rapidly attains equilibrium with the climatic chamber.

Additionally, the results presented in figure 36 are similar to those reported by Turgoose (1982b) and illustrated graphically in figure 19. Turgoose's results can not have been affected by balance enclosure diffusion effects because they were obtained from samples over saturated salt solutions within closed desiccators. All the reported tests were conducted at the same temperature (20°C) which eliminates any increased rate of diffusion that occurs with an increase in temperature for a given concentration gradient. In summary, the influences of diffusion effects identified for the tests reported here on weight changes, are negligible and can be ignored.

6.1.3. Towards a threshold humidity for the dehydration of $FeCl_2.4H_2O$ to $FeCl_2.2H_2O$

The nearer the threshold humidity for the dehydration of $FeCl_2.4H_2O$ to $FeCl_2.2H_2O$, the more time it takes to achieve complete loss of excess water of hydration (figures 36 and 38). Chamber limitations at low relative humidities [due to icing on the cooling apparatus used to remove moisture from the chamber to maintain that low humidity] meant that time was not available to run every test to completion. Very low humidity studies using the climatic chamber are limited to about two weeks because of the icing on the condensation coil and loss of humidity control (section 5.2.4. and figure 26).

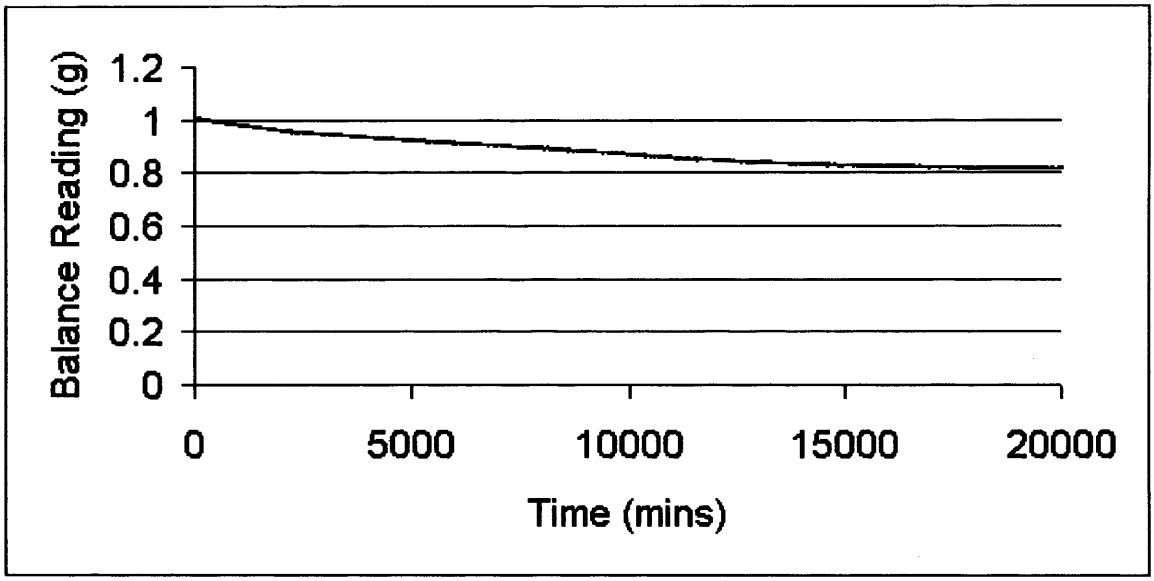

Figure 38. **Dehydration of ferrous chloride tetrahydrate to ferrous chloride dihydrate at 18%RH. Run to near complete desiccation. The slight irregularity (hump) in the line is attributable to balance drift over this period of time and would introduce a small margin of error in measured half-life. The magnitude of weight loss corresponds with the theoretical loss of two waters of hydration (0.1812g/g).**

To avoid the need to run all of the tests to completion (a mass reduction of 0.1812g/g) regression analysis (r^2) of the initial 20-24 hours of each relative humidity cycle was carried out. This provided good support for exponential mass change during this initial dehydration time period for all the relative humidities shown in figure 36 (see table 4).

R.H.(%)	Initial r^2	For whole period	For linear correlation
12	0.911986	0.527219	
14	0.972936	0.614204	
16.5	0.98551		0.985974
18	0.941934		0.942287

Table 4. **Exponential change in mass correlations.**

The r^2 values for the full dehydration period at 12% and 14% are less convincing than those recorded for the initial 24 hours. This can be explained by the presence of long periods with no net change in weight (once the end point has been reached) within the full dehydration period and a possible, small, contribution from balance drift.

6.1.4. An equation for rate of dehydration

An equation [30] to describe each curve in figure 36 can be derived given the good correlation supporting the graphic evidence that the rate of change in weight loss (mass) with time (*t*) *is* exponential (at least initially) for all the humidities tested.

$$Mass = (Initial\ Mass - Final\ Mass)e^{-\Lambda t} \qquad [30]$$

where Λ is a constant for a given temperature and RH.

It is possible to simplify this equation for the experiments reported here where the initial mass of $FeCl_2.4H_2O$ is always about 1.0000g [i.e. as close to 1.0000g as possible but weighed and recorded to four decimal places]. The theoretical final mass is calculated by subtracting theoretical mass of lost water of hydration, which is two water molecules per mole of $FeCl_2.4H_2O$ or 0.1812g, from the starting weight of 1.0000g (see section 6.1.1.). Thus the final mass should always be 0.8188g. These values can be inserted into equation [30] to produce equation [31].

$$Mass = (1 - 0.8188)\, e^{-\Lambda t} \qquad [31]$$

$Mass = 0.1812\, e^{-\Lambda t}$ [32]

In equation [32] t is a given time elapsed since the start of the drying cycle and Λ is a constant hereafter referred to as the *exponential hydrate conversion rate constant*. This constant will be different for each relative humidity tested. It is the element of the equation that determines the time necessary for conversion of a set mass of ferrous chloride tetrahydrate to ferrous chloride dihydrate at a given relative humidity.

Weight loss resulting from loss of water of hydration can be expressed in terms of "half life". The "half-life" is defined as the time required for half the expected total change in mass to occur, which is the time for the mass 0.9094g to be reached or for 0.0906g of water of hydration to be lost.

The "half-life" may either be calculated using a standard equation for half life [33] or read from the relative humidity curves on the graph showing the rate of weight loss (see figure 36).

$$\text{Half-life } (t_{0.5}) = \frac{\text{Mass at start} - \text{Theoretical Final Mass}}{2} = \frac{1}{\Lambda} \times \ln 2 \quad [33]$$

$$t_{0.5} = \frac{0.693}{\Lambda} \quad [34]$$

Values for the constant Λ are obtained by inserting half life readings from figure 36 into equation [34] (see table 5). Where the halfway point of a dehydration test is not reached the line is extrapolated to the halfway point in weight loss (0.9094g). Error is expected to be greatest for the higher humidities.

Table 5. Derived *exponential hydrate conversion rate constants (Λ)* for each of the curves in figure

6.1.5. Plotting a rate constant for dehydration of $FeCl_2.4H_2O$ against relative humidity

Since Λ is a rate constant then plotting its value against the relative humidity value produced it will indicate the relative humidity at which conversion of $FeCl_2.4H_2O$ to $FeCl_2.2H_2O$ will tend towards zero. This is shown in figure 39.

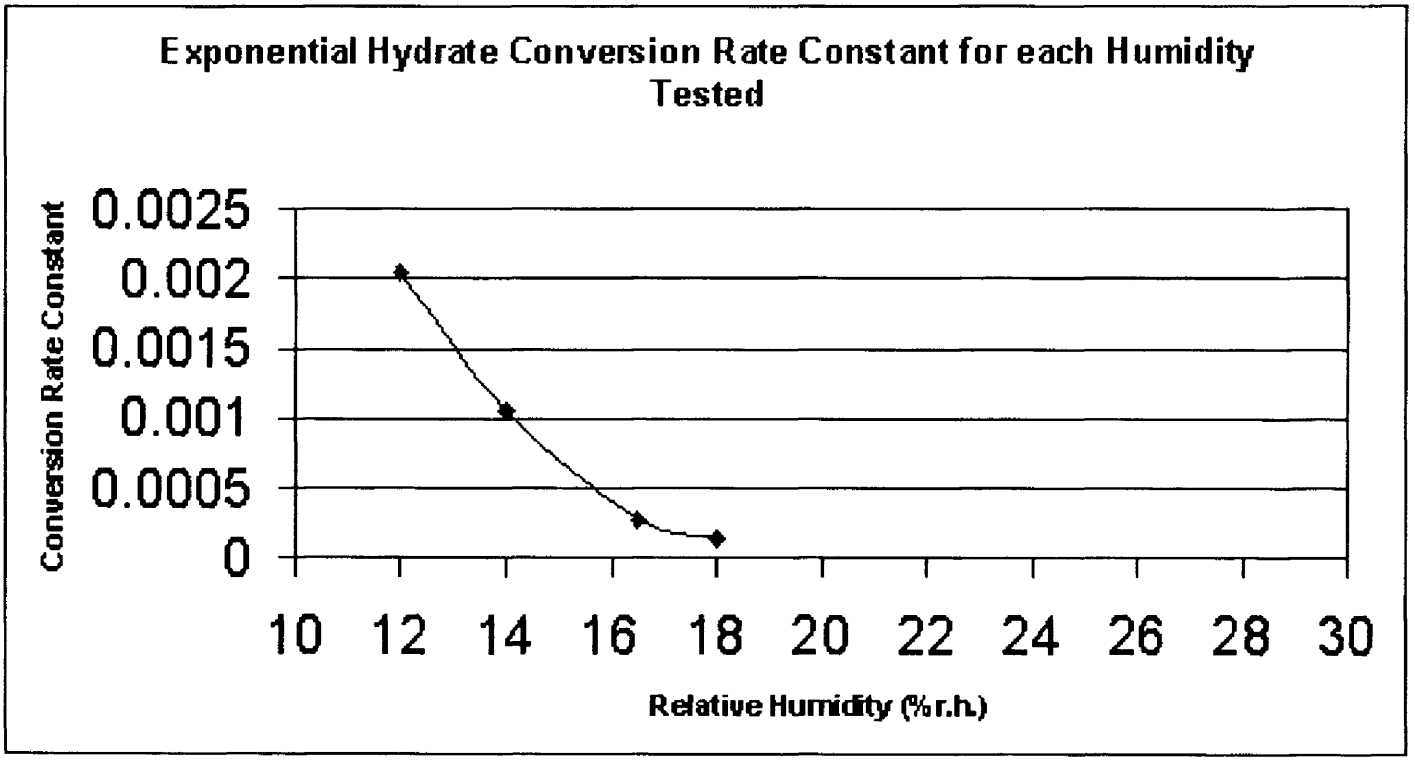

Figure 39. Rate constant for the conversion of $FeCl_2.4H_2O$ to $FeCl_2.2H_2O$ plotted against relati humidity.

It would have been fortuitous if the above chart revealed a linear relationship, for would have provided an intercept on the x-axis for the relative humidity at w

conversion of $FeCl_2.4H_2O$ to $FeCl_2.2H_2O$ ceased to occur. Further evidence for a non-linear relationship is obtained by examining where each curve in figure 36 would intercept a vertical line drawn from a mass of 0.9094g (half-life). There would be a different interval distance between the intercept points of each curve, showing that the relationship between the half-lives of the curves is not linear.

Plotting the "half-life" of each curve against the relative humidity at which they were obtained did not reveal a linear relationship between dehydration and half life (see figure 40). The time to reach the half-life (0.9094g) will tend towards infinity above 20% relative humidity, somewhere in the region of 21% relative humidity.

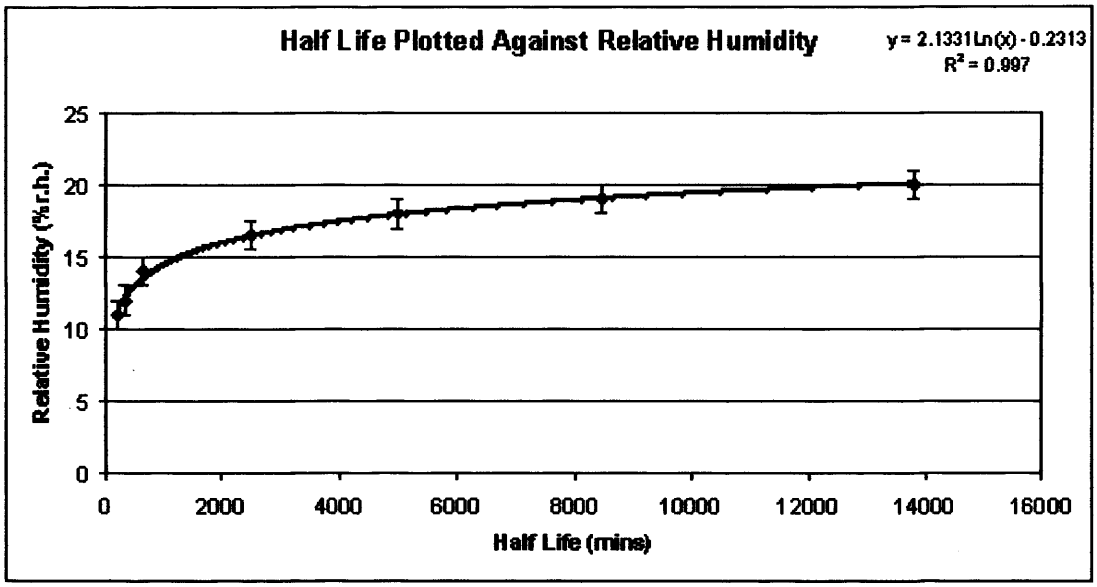

Figure 40. **The relationship between half-life of partially desiccated $FeCl_2.4H_2O$ and relative humidity (published in Watkinson and Lewis, 2005a).**

The logarithmic correlation r^2 for the above relationship is good (0.997) but there must come a point (which will be described here as the threshold relative humidity), where the gradient in figure 40 tends towards zero as time tends towards infinity. This will be followed by a point where the gradient is zero, where no change occurs - $FeCl_2.4H_2O$ stops converting to $FeCl_2.2H_2O$. The logarithmic relationship is expected to be asymptotic to this limiting threshold relative humidity, above which no loss of water of

hydration takes place. A value for this limiting relative humidity cannot be obtained by extrapolating a log relationship because, whilst these tend towards zero, they never reach it. The limiting relative humidity must be determined experimentally.

6.1.6. Mathematical notes

The plot of the half-life against relative humidity gives a very good correlation of r^2 = 0.997 (figure 40). The equation for the curve in figure 40 is provided by Excel ™ [35].

$$y = 2.1331\ ln(x) - 0.2313 \qquad [35]$$

Differentiating the equation of the curve gives the gradient at any given point

$$\frac{dy}{dx} = \frac{2.1331}{x} \qquad [36]$$

(As x, which is the half-life, tends towards infinity, the gradient, which is the reaction rate, tends towards zero. This is clearly visible in the shape of the curve in figure 40). The general equation describing a horizontal asymptote for an exponential relationship is

$$y = K_1 [1 - e^{-K2\,t}] \qquad [37]$$

(K_1 is the value of the asymptote.)

This equation describes the function controlling the exponential change in mass for the loss of water of hydration for each curve in figure 36. So for the curves in figure 36:

$$mass\ (g) = 0.8188(1 - e^{-\Lambda t}) \qquad [38]$$

(Equation [38] is valid at a given time t where Λ is the rate constant for that particular relative humidity [and temperature])

As $e^{-\Lambda t}$ is a fraction $\frac{1}{e^{\Lambda t}}$ whose reciprocal is $e^{\Lambda t}$ it does not follow that this is substituted in [38] for a horizontal asymptote because the figure within the brackets must always be less than or equal to 1.

Similarly when a horizontal asymptote is zero the equation is as for simple exponential decay [39].

$$y = k_0 e^{-\Lambda t} \qquad [39]$$

6.1.7. An equation for the relationship between 'half life' and relative humidity

The asymptotic behaviour observed in figure 40 can be described as the exponential decrease in the rate of conversion of $FeCl_2.4H_2O$ to $FeCl_2.2H_2O$ for a unit increase in humidity (see figure 39), rather than a logarithmic increase in half life (time) for a unit increase in relative humidity.

The rate of increase in relative humidity decreases exponentially as half-life increases. At the limiting relative humidity (the asymptote) the rate of change of relative humidity is equal to zero. It occurs where the half-life tends towards infinity. The equation describing this type of asymptotic behaviour is shown by equation [40].

$$y = K_1 [1 - e^{-K2\,t}] \qquad [40]$$

(Where K_1 gives the limiting value of the asymptote i.e. the relative humidity above which no change takes place). For figure 40 this gives

$$relative\ humidity = limiting\ relative\ humidity\ [1 - e^{-K2\,t}] \quad [41]$$

Where t is the half-life for that given relative humidity and K_2 is the constant for the curve in figure 40 that describes its transform from a purely natural logarithmic form.

6.2 *Results for ferrous chloride dehydration expressed as a function of specific humidity*

6.2.1. Specific humidity data

Standardisation of test temperature at 20°C for all of the ferrous chloride dehydration tests allows their results to be expressed as a function of absolute or specific humidity as well as relative humidity (figure 41). Conversion of data from relative humidity to specific humidity is effected by means of a simple linear transform (see section 5.1.1.).

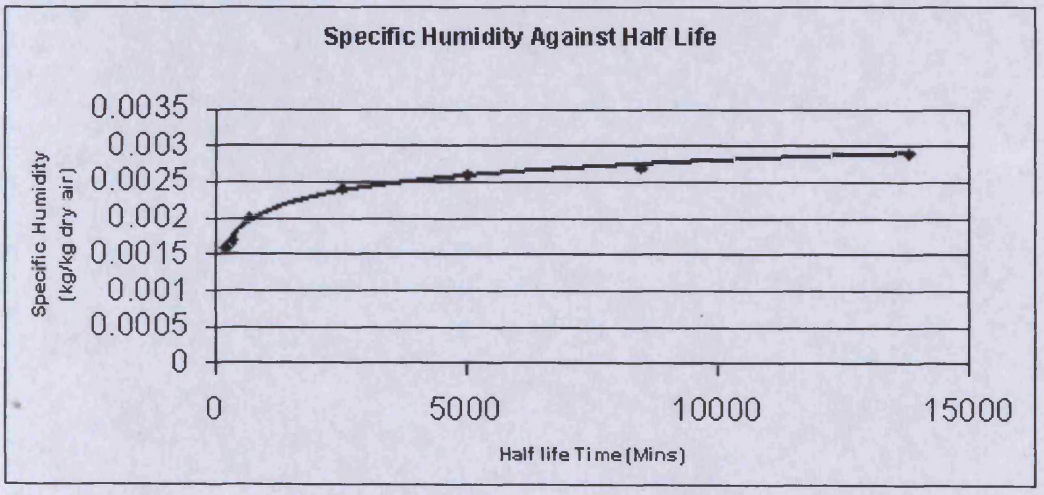

Figure 41. **The relationship between half-life and specific humidity for the dehydration of $FeCl_2.4H_2O$ at 20°C.**

At any given air temperature, the concentration of water vapour in the atmosphere can not exceed a saturation limit called the saturation vapour pressure (Vp) [its saturation point or dew point, i.e. 100%RH]. Saturation vapour pressure (Vp) is a function of temperature and obeys the exponential function

$$Vp_{(t)} = V_o \exp(-E/RT) \qquad [42]$$

Where E is the activation energy for water absorption, R is the gas constant and T is temperature (K).

The water vapour absorbed by hygroscopic materials (W) increases with absolute water concentration in the atmosphere (expressed as vapour pressure (mmHg or mbar)). Assuming linearity (Cuddihy, 1987),

$$W_{(t,v)} = k_{(t)} V \qquad [43]$$

Where W = adsorbed water content at a given temperature and vapour pressure (t,v),

k = adsorption isotherm, the slope of the line at a given temperature (t)

V = atmospheric water vapour concentration

The temperature dependence of $k_{(t)}$ is generally an Arrhenius relationship i.e. the rate of the reaction or process is proportional to a function involving two variables: temperature and activation energy (*c.f.* table 9).

$$k_{(t)} = k_{(0)} \exp(E/RT) \qquad [44]$$

where T is absolute temperature (K)

E is the activation energy for water vapour absorption in units of cal/mol or kcal/mol

R = 1.987 cal/mol.

For constant V, the absorbed water vapour content of hygroscopic materials decreases with increasing temperature (t or T).

For a given body of air, containing a given (fixed) quantity of water vapour, the temperature where condensation first begins to occur is the dew point temperature or dew point (or frost point below 0°C). At this temperature atmospheric water vapour molecules fail to possess sufficient kinetic energy to prevent them being attracted to each other and condensing (Lawrence, 2005; Horstmeyer, 2008). If the same body of air is then heated, the amount of available energy for evaporation increases. If a source of extra moisture is available more water may evaporate and the saturation vapour pressure (Vp) and dew point temperature of the body of air may rise (figure 20). If no source of extra moisture exists, the dew point temperature of the body of air will remain constant whilst its relative humidity falls. The greater the difference between the temperature of the air and its dew point temperature, the lower its relative humidity. Unlike relative humidity, if dew point temperature increases it is only because the amount of moisture in the air (Vp) increases (figures 20 and 74). If the relative humidity level of a body of air changes, it can be due to moisture level changes, temperature changes or both.

For the study of phase changes of hydrated salts such as ferrous chloride specific humidity, absolute humidity, dew point temperature or Vp of an enclosed, sealed, space are less ambiguous measures of environmental moisture levels than relative humidity if temperature is not also cited. At a given barometric pressure, independent of temperature, the dew point indicates the mole fraction of water vapour in the air and therefore determines the specific humidity of the air. Conversely, relative humidity is a useful expression of the quantity of water vapour in the atmosphere as a function (%) of the possible maximum level of atmospheric moisture (Vp) at saturation (i.e. the amount of available thermal energy used in evaporation as a function of the amount of thermal energy available to do the work of evaporation) (Lawrence, *op. cit.*; Horstmeyer, *op. cit.*).

6.2.2. Barometric pressure

The quantity of water vapour which can exist in a given volume of air varies significantly with temperature but it varies only slightly with changes in (barometric) pressure over the range normally encountered in atmospheric conditions. At low pressure the volume of vapour required for saturation is slightly less than at high pressures (Faber and Kell, 1957). Brown (1994) states, for a variation of 101.3±3.7kPa for Cardiff (collected taking noon readings over a ten-year period (99.7% confidence limit)), maximum errors will occur at 0%RH (±2%RH at 0°C, ±1% at 30°C), falling linearly towards zero at 100%RH. Pressure was not standardised during these experiments but its effects are negligible through its lack of influence (as random 'error') in the results. Cardiff University is located at sea-level (with relative air density of 1.0) for these purposes.

6.3 *The behaviour of iron powder mixed with $FeCl_2.2H_2O$*

Mixing $FeCl_2.2H_2O$ with iron powder and exposing it to a relative humidity value at which $FeCl_2.2H_2O$ is the stable iron chloride phase, will indicate whether iron corrodes in the presence of $FeCl_2.2H_2O$. A ferrous chloride dihydrate/iron powder mixture at 19% relative humidity showed no weight gain and no visible change over a period of two weeks (figures 42 and 43). These results *strongly support* the premise on which desiccated storage of chloride-contaminated wrought iron is based; namely that ferrous chloride dihydrate (and iron) are stable to oxidation at low relative humidities (which has been experimentally demonstrated at 19%R.H. and below).

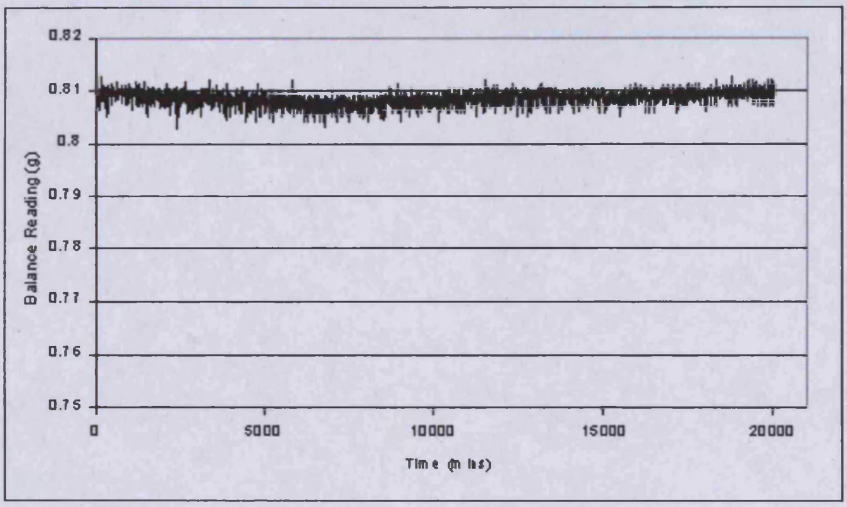

Figure 42. **The behaviour of 0.31g $FeCl_2.2H_2O$ mixed with 0.50g iron powder at 19% relative humidity over a 14 day period.**

Figure 43. **$FeCl_2.2H_2O$ mixed with iron powder at 19%RH after 14 days.**

Minor fluctuations in mass are suggested by the data in figure 42. An initial fall in mass up to 6000 minutes is apparently followed by a minor increase in mass from 6000 minutes to 22000 minutes. The lack of visible colour change (figure 43) after two weeks indicates that corrosion has not taken place. The minor fall in mass suggested by the data between 13000 and 15000 minutes also suggests that corrosion is not occurring over that time. The magnitude and sinusoidal character of this balance data (although peaks and troughs are additive and not sequential, i.e. for this plot: trough [0-3000 minutes], trough [3000-6000 minutes], peak [6000-9000 minutes], peak [9000-13000 minutes], trough [13000-15000 minutes], peak [15000 minutes onwards]) is typical of a balance drift phenomenon observed for standard masses and iron powder alone (control), where no corrosion takes place, over very long periods of time. The balance used has a self-calibrating capacity and this phenomenon is thought to be a result of that function of the balance. This sinusoidal drift phenomenon has only been identified for data where no change or very slow changes in mass occurred (*c.f.* figure 38). Data sets where dehydration or corrosion had occurred with their commensurate weight changes did not exhibit this phenomenon.

The data presented in figures 42 and 43 indicate that no corrosion took place during this two week experiment.

6.4 *Corrosion of iron in the presence of $FeCl_2.4H_2O$*

Figure 48 shows weight change of matched weight mixtures of ferrous chloride tetrahydrate and iron powder (figure 44) exposed to a range of fixed relative humidities in the stability region for ferrous chloride tetrahydrate ($FeCl_2.4H_2O$). Over a period of about 3 days (4320 minutes), most samples increased in weight and there were visible signs of corrosion of the iron powder (figures 45-47). The greatest weight increase occurred at the highest humidity.

Figure 44. **Approximately 2.0000g of $FeCl_2.4H_2O$ (BDH) mixed with approximately 2.0000g of iron powder. Photographed upon mixing.**

Figure 45. **Active corrosion of iron in the presence of $FeCl_2.4H_2O$ above the threshold relative humidity (35%RH in this case).**

In contrast, one control sample consisting of pure iron powder and another of pure $FeCl_2.4H_2O$ did not increase in weight at any of the relative humidity values tested. This suggests that iron alone does not corrode measurably at these relative humidities over the time-scales tested.

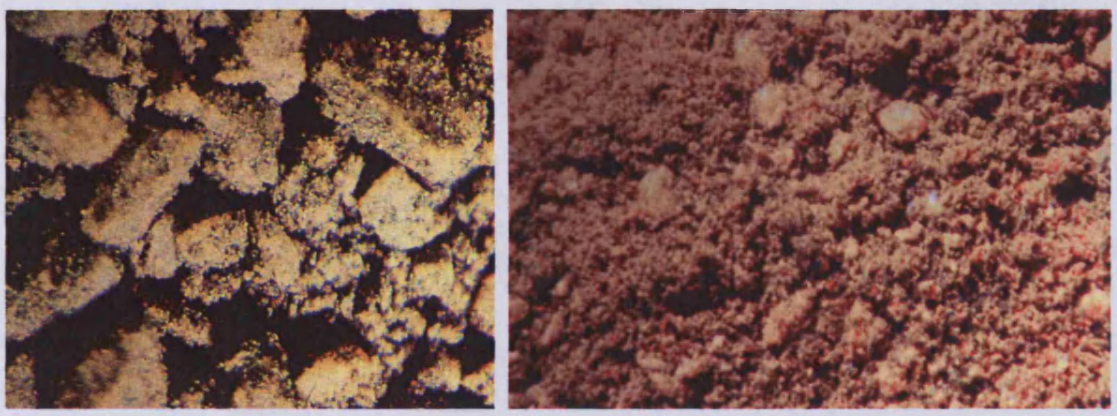

Figure 46. **(left) Active corrosion of iron in the presence of $FeCl_2.4H_2O$ above the threshold relative humidity (25%RH in this case). Dark brown βFeOOH can be seen forming on the surface of the iron powder coated (grey) $FeCl_2.4H_2O$ (green/yellow) crystals.**

Figure 47. **(right) Active corrosion of iron in the presence of $FeCl_2.4H_2O$ above the threshold relative humidity (35%RH in this case). Dark brown βFeOOH can be seen forming on the surface of the iron powder coated $FeCl_2.4H_2O$ crystals, rapidly obscuring and eventually replacing them.**

The increase in weight is due to incorporation of atmospheric oxygen and water during corrosion product formation. The lack of weight change of the ferrous chloride tetrahydrate control suggests that weight gain is not attributable to water uptake due to hygroscopicity.

Relative humidity influences the rate of corrosion – essentially the higher the relative humidity the faster the corrosion rate for $FeCl_2.4H_2O$/iron powder mixtures – and the amount of corrosion formed. This is reflected by plotting weight gain (corrosion) against test relative humidity (figure 48).

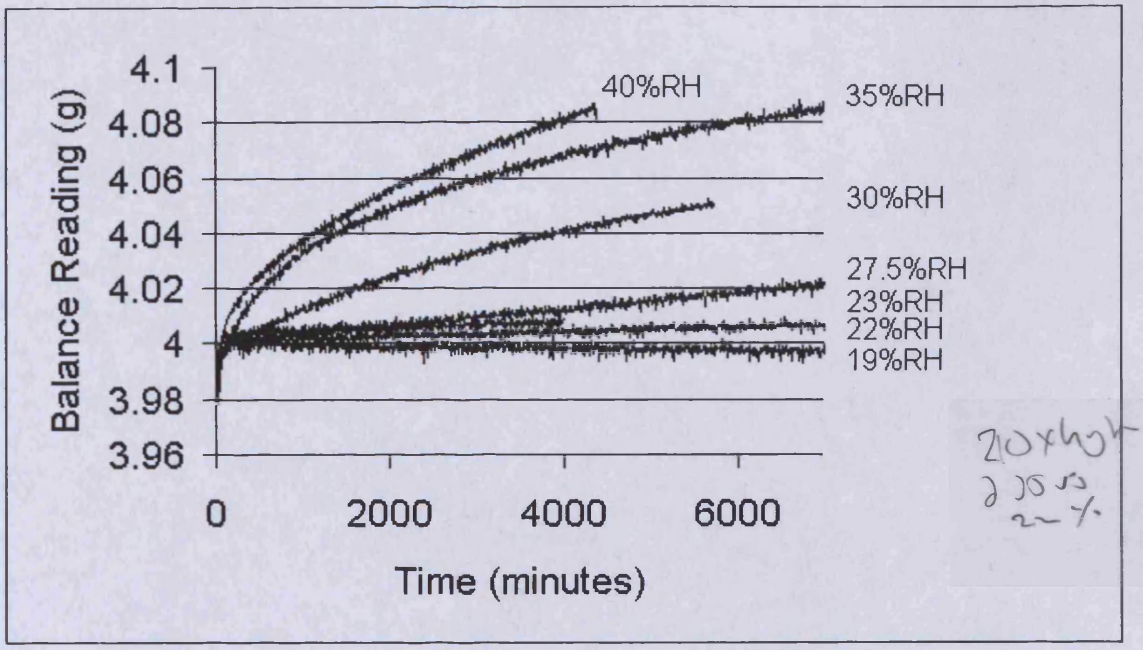

Figure 48. **Results showing active corrosion of iron in the presence of $FeCl_2.4H_2O$ at various relative humidity values above the threshold relative humidity, with data for 19%RH for comparative purposes.**

All tests were conducted with approximately 2.0000g of $FeCl_2.4H_2O$ mixed with approximately 2.0000g of iron powder.

Examination of the rates of corrosion in figures 48 and 49 show that corrosion is slow in the region 22% to 25% relative humidity, as compared to 30% relative humidity and above. For chloride-contaminated marine iron or archaeological iron in store containing solid ferrous chloride, which continue to corrode via the $FeCl_2.2H_2O$ to $FeCl_2.4H_2O$ transformation, it is likely that brief excursions in environmental humidity levels above 19% relative humidity, which will not support corrosion, into the 22% - 25% relative humidity region which does support corrosion, would result in corrosion at a very slow rate. Ferrous chloride will need to pick-up water and convert to its tetrahydrate form to support corrosion of the iron. This hydration may be slow, depending on whether hysteresis effects occur, and this effect might further limit the damage occurring during short periods of loss of environmental control. Experimental data was collected using programmed relative humidity set-point changes over time to establish any hysteresis effects.

The production of βFeOOH as a product of iron corrosion in the presence of ferrous chloride tetrahydrate means that the influence of this oxyhydroxide also requires investigation.

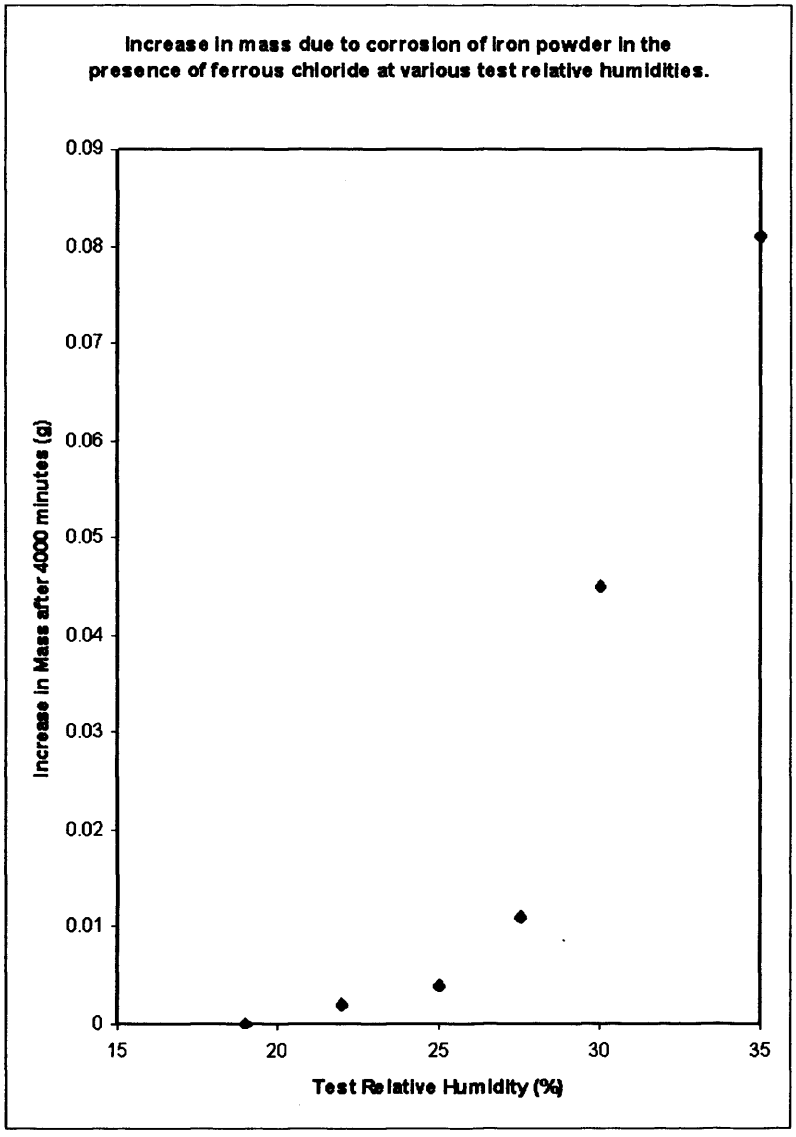

Figure 49. **Increase in mass of iron powder mixed with $FeCl_2.4H_2O$ as a result of corrosion at various humidities over a three day period (4000 minutes).**

6.5 The role of βFeOOH (β–iron oxyhydroxide) in the corrosion of iron

6.5.1. Hygroscopicity of unwashed βFeOOH

The βFeOOH used (termed unwashed βFeOOH for the reasons outlined) was that which was synthesised using the methodology described in section 5.2.5., and stored in a closed desiccator maintained at 41% relative humidity by conditioned silica gel. It was independently assayed using XRD, found to be a match for a marine wrought iron sample (taken from the hull of the ss Great Britain) and was confirmed as the only crystalline solid present after its synthesis in the laboratory (figure 32). Production using this methodology, without washing and filtering the product, was chosen to replicate as closely as possible (under laboratory conditions) the raw material and agencies of deterioration of chloride-contaminated wrought iron after excavation or recovery from the sea.

The βFeOOH was removed from the desiccator (maintained at 41% relative humidity) and exposed to a 19% relative humidity in the climatic chamber before returning the environment back to 41% relative humidity. Moisture release produced a loss in weight at 19% relative humidity followed by weight gain as moisture was adsorbed when the atmosphere was altered to 41% relative humidity (figure 50). Another sample was conditioned to 41%RH and exposed to 13%RH followed by 19%RH and 40%RH. The changes in weight corresponded with increases and decreases expected to occur as a result of water adsorption and desorption (figure 51).

Although their relative magnitudes may reflect the weights of water lost or gained, it is uncertain to what extent the balance was affected by the cessation of vibration if the refrigerator of the chamber stopped or started during the changes in relative humidity set point. Estimates of masses of water held, gained or lost, and %wt water information have not been extracted from this data. Further tests using multiple climatic chamber environmental set points in the same cycle, produced logical data for the changes in

programmed relative humidity and the data-logged balance readings obtained. Any change in weight and the direction of change of weight indicated by the data-logged balance readings would appear to be real and informative.

In order to establish the validity of the weight changes suggested by the balance readings within the chamber during multiple RH set-point tests, and to unequivocally establish the capacity for βFeOOH to attract atmospheric moisture, a further sample of unwashed βFeOOH was placed in the climatic chamber during a series of other tests. Its initial mass upon removal from the 41%RH storage environment was recorded and it was reweighed after each test (figure 52). The data obtained here corresponds with the weight changes expected through changes in adsorbed water due to the hygroscopicity of unwashed βFeOOH.

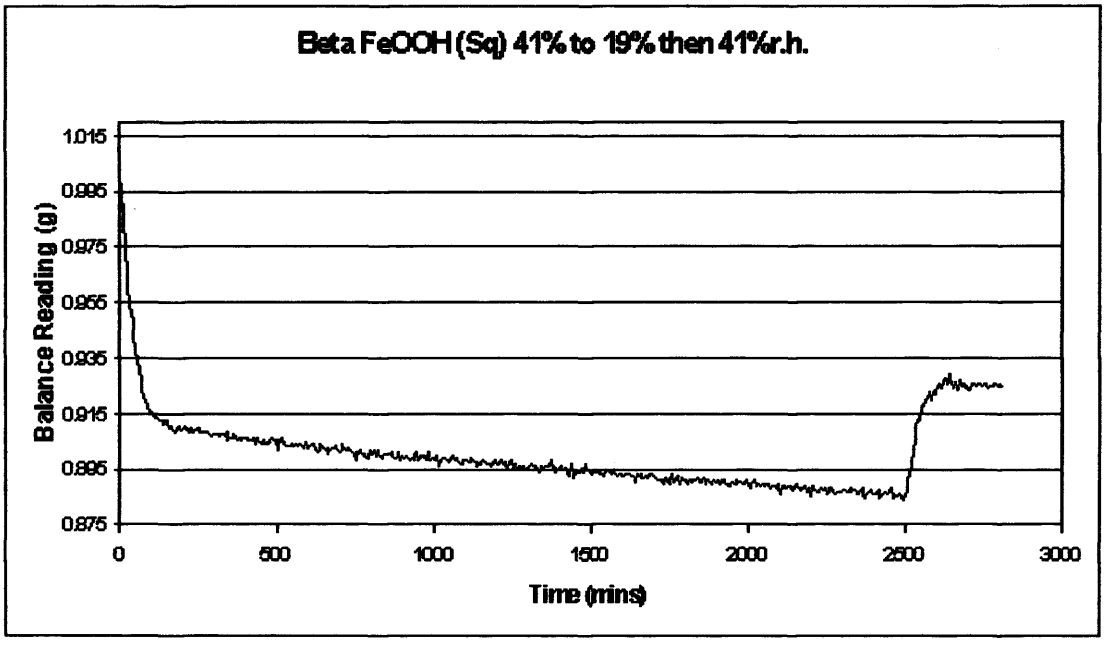

Figure 50. **The response of unwashed βFeOOH to changes in humidity. (βFeOOH stored in a desiccator at 41% relative humidity was placed in the chamber at 19% relative humidity and after 2500 minutes (1.7 days) the humidity was raised to 41%RH).**

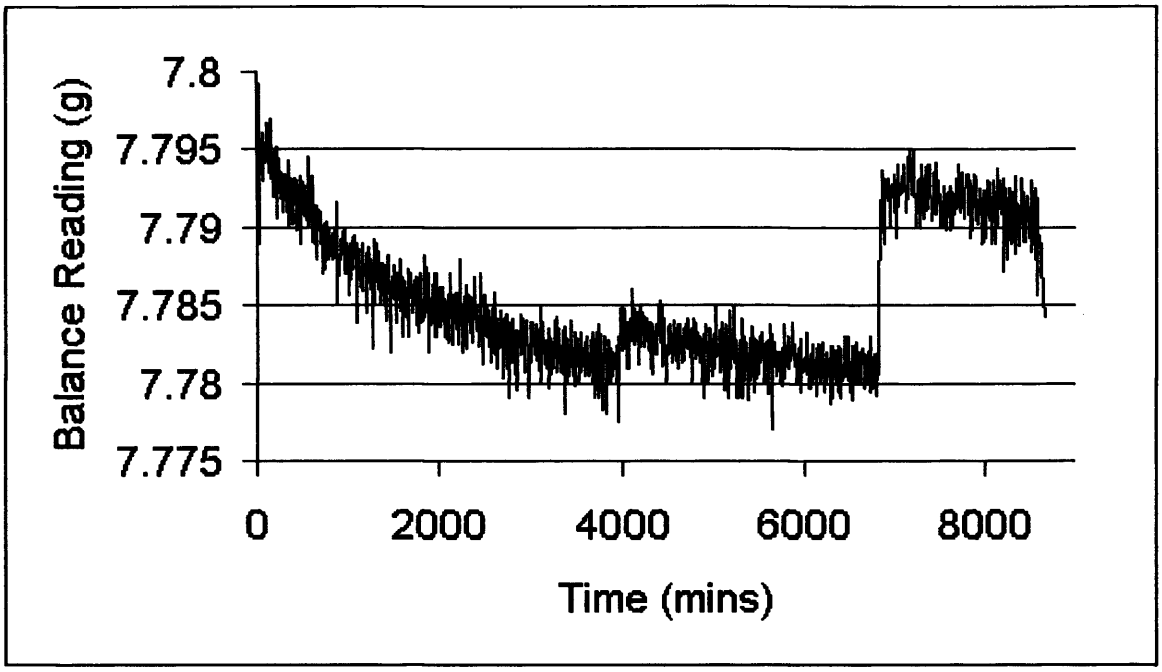

Figure 51. **The response of unwashed βFeOOH to changes in humidity. (βFeOOH stored in a desiccator at 41% relative humidity was placed in the chamber at 13% relative humidity. After 4000 (~3 days) minutes the humidity was raised to 19%RH and at 7000 minutes (~5 days) the humidity was raised to 40%RH).**

The hygroscopicity demonstrated by these tests is in accord with thermogravimetric data published by Micale *et al.* (1985) and Stahl *et al.* (2003). The implications of this hygroscopicity merit comment but it should be noted that these workers washed their synthetically produced βFeOOH. In an unwashed scenario where βFeOOH has adsorbed surface chloride and could be present with unoxidised iron chloride dihydrate and iron, the hygroscopic nature of the βFeOOH may attract greater quantities of water to the system, even though ambient relative humidity favoured the stability of iron chloride dihydrate. Corrosion could be exacerbated by surface-adsorbed, labile, chloride on βFeOOH, which may be released by the action of sufficiently high relative humidities to produce an electrolyte for the corrosion of iron. Turgoose's (1982b: 100) hypothesis that naturally produced βFeOOH could potentially hold a thin film of hygroscopically adsorbed water at relative humidities below 44%RH, thus providing the necessary aqueous phase for corrosion, is supported by the data presented in figures 50 and 51 which show its adsorption and desorption.

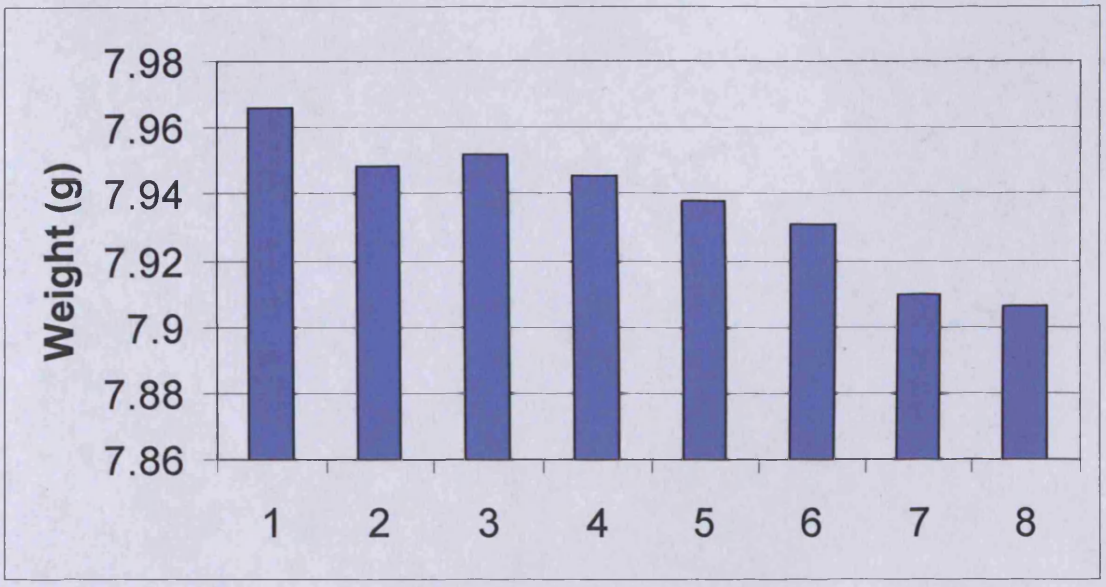

Figure 52. **Unwashed βFeOOH removed from storage in a desiccator conditioned to 41%RH (1) and weighed after exposure to (2) 25%RH, (3) 30%RH, (4) 27.5%RH, (5) 23%RH, (6) 22%RH, (7) 21%RH and (8) 19%RH. The data is presented, left to right, in the order in which the individual exposures took place. The drop from 41%RH to 25%RH followed by exposure at 30%RH produces the expected weight decrease and increase respectively but the mass recorded at 27.5%RH is less than that recorded for 25%RH and is probably indicates hysteresis which is direction dependent (Amorosso and Fassina, 1983: 115; Orr *et al.*, 1958).**

6.5.2. Hygroscopicity of washed and unwashed synthetic βFeOOH: a comparison

The relative hygroscopic properties of washed and unwashed βFeOOH were examined experimentally (see figures 62, 67, 83, 85 and 87). This was to confirm the extent of the likely contribution to corrosion from βFeOOH washed free of labile chloride compared with that from βFeOOH having labile surface-adsorbed chloride. This establishes (i) the validity of claims (Turgoose, 1982b) that βFeOOH is likely to contribute water and facilitate the corrosion of iron in close proximity to itself at high humidities, (ii) whether desiccation affects the amount of water adsorbed, and (iii) the hygroscopic contribution of the adsorbed chloride.

Fourier-transform infrared attenuated reflectance spectroscopy (FTIR-ATR) analyses of freshly prepared unwashed βFeOOH (figure 53), freshly prepared (Soxhlet, see Scott and Seeley, 1987) hot water-washed βFeOOH (figures 54 and 56) and a sample of Turgoose's βFeOOH (figure 55) were conducted and compared. They suggest that Turgoose washed his βFeOOH at the conclusion of his production process. Washing the product when βFeOOH is produced synthetically is the norm in the chemistry literature (Atkinson *et al.*, 1977; Wolf *et al.*, 1966; Schwertmann & Cornell, 2000). This is a logical conclusion to a laboratory synthesis where βFeOOH is precipitated from solution.

FTIR absorption bands for washed βFeOOH and Turgoose's βFeOOH are similar, and do not exhibit the broad bands and general absorption associated with non-crystalline adsorbed chloride seen for fresh, unwashed βFeOOH. The surface adsorbed chloride clearly depresses the overall reflectance of the attenuated IR beam resulting in a greatly reduced %T (the equivalent of % transmission for FTIR analysis in transmission mode) compared with the analyses of washed βFeOOH. The adsorbed chloride is partially scattering the IR beam due to its very different refractive index to that of βFeOOH, especially in the liquid state.

The unwashed βFeOOH shows a sharper absorption at about 1600cm^{-1} in common with ferrous chloride dihydrate (figure 57). The characteristic ferrous chloride diffraction spacing (d-spacing) was absent from the XRD analysis of the same sample (figures 32 and 66a). This suggests that the chloride producing the chloride absorption peak in the FTIR absorption curve is non-crystalline. It is either amorphous, surface-adsorbed or present as aqueous (ferrous/hydrogen) chloride. Askey (1993) and Turgoose (1985b) suggest that the surface adsorbed labile chloride could be present in solution – possibly as hydrochloric acid (HCl), albeit with dissolved ferrous and ferric ions in solution. Kiyama and Toshio (1972) reported free HCl acid in each filtrate following the repeated aerial oxidation of ferrous chloride solutions. They reported that the free HCl concentration in each filtrate, and its Fe^{3+}/Fe^{2+} ratio, increased with repeated oxidation. The replication of the natural process leading to the formation of βFeOOH (aerial oxidation of ferrous chloride) means that tests using unwashed βFeOOH will produce

data which should have relevance for archaeological iron, marine iron and terrestrial meteorites. Results of tests using unwashed βFeOOH are the product of a mixture of βFeOOH and surface adsorbed, labile, chloride.

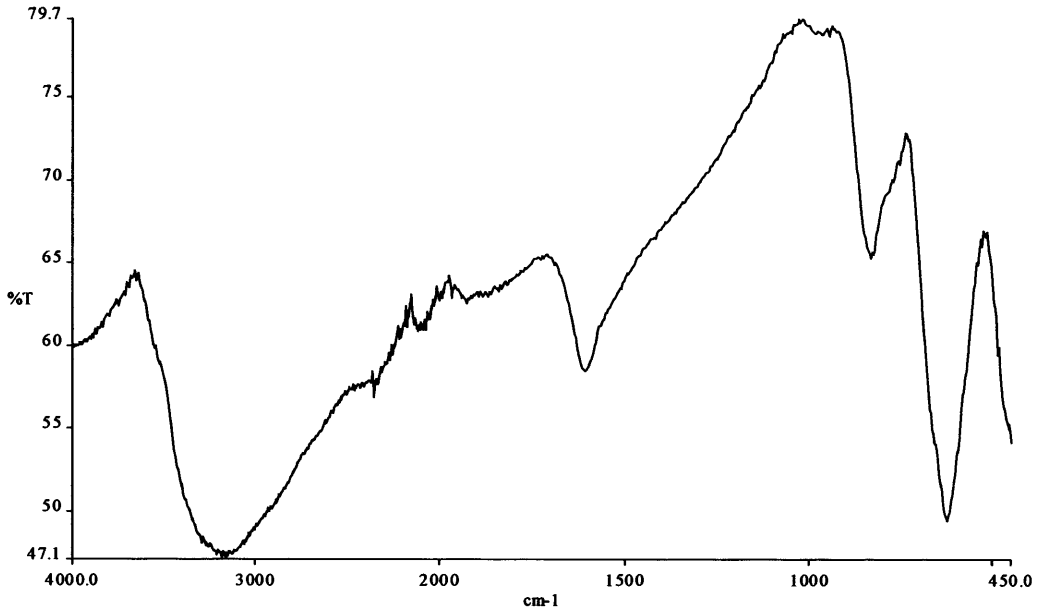

Figure 53. **FTIR spectrum for unwashed βFeOOH (sq) (acquired by attenuated reflectance [ATR]). Note the excessive broad –OH absorptions in the 3000cm^{-1} and 1600 cm^{-1} regions. A sloping baseline may also occur where the sample particle size is large.**

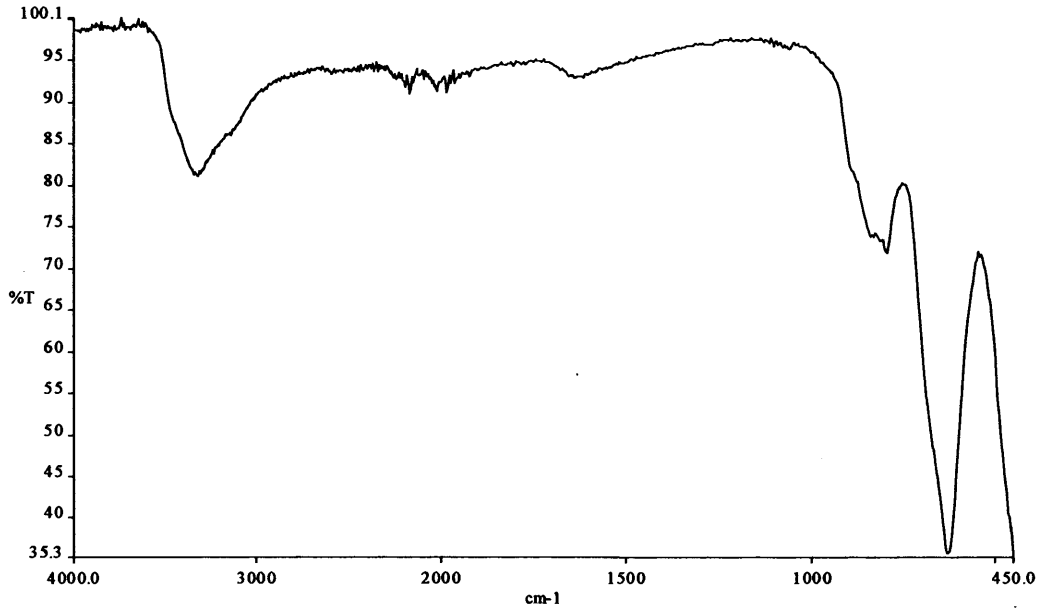

Figure 54. **FTIR spectrum for Soxhlet washed βFeOOH (acquired by attenuated reflectance [ATR]).**

Figure 55. **FTIR spectrum for Turgoose's 25 Year Old βFeOOH (acquired by attenuated reflectance [ATR]).**

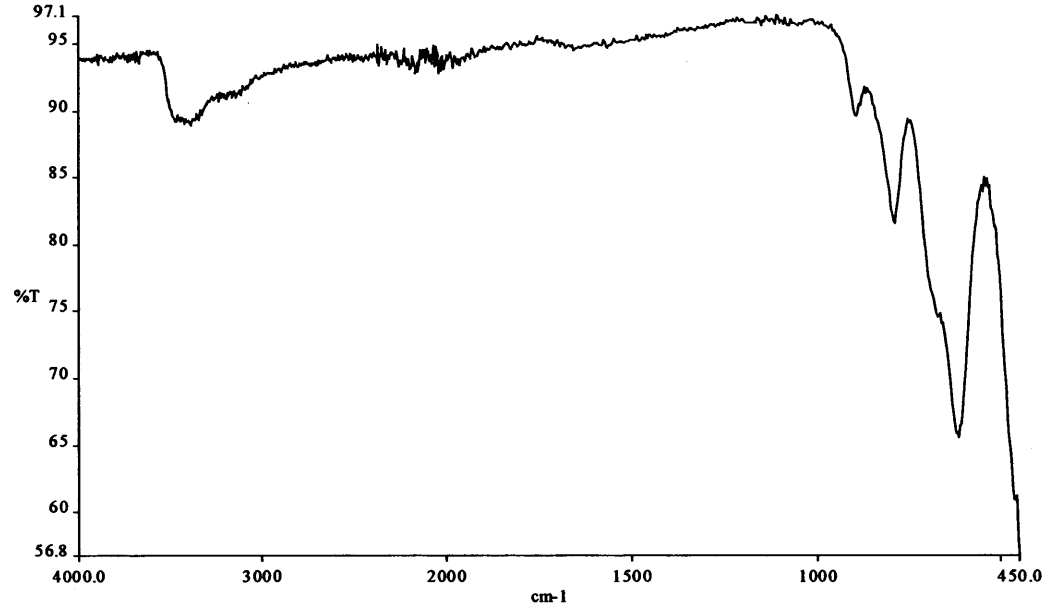

Figure 56. **FTIR spectrum for Soxhlet washed βFeOOH (04/06/04) (acquired by attenuated reflectance [ATR]). Partial hydrolysis to another oxyhydroxide polymorph possibly accounts for the extra OH-bending absorption at ~900 cm^{-1} (but *c.f.* figure 59 for somatoidal and rod-like akaganéite) and a shoulder at ~700 cm^{-1}.**

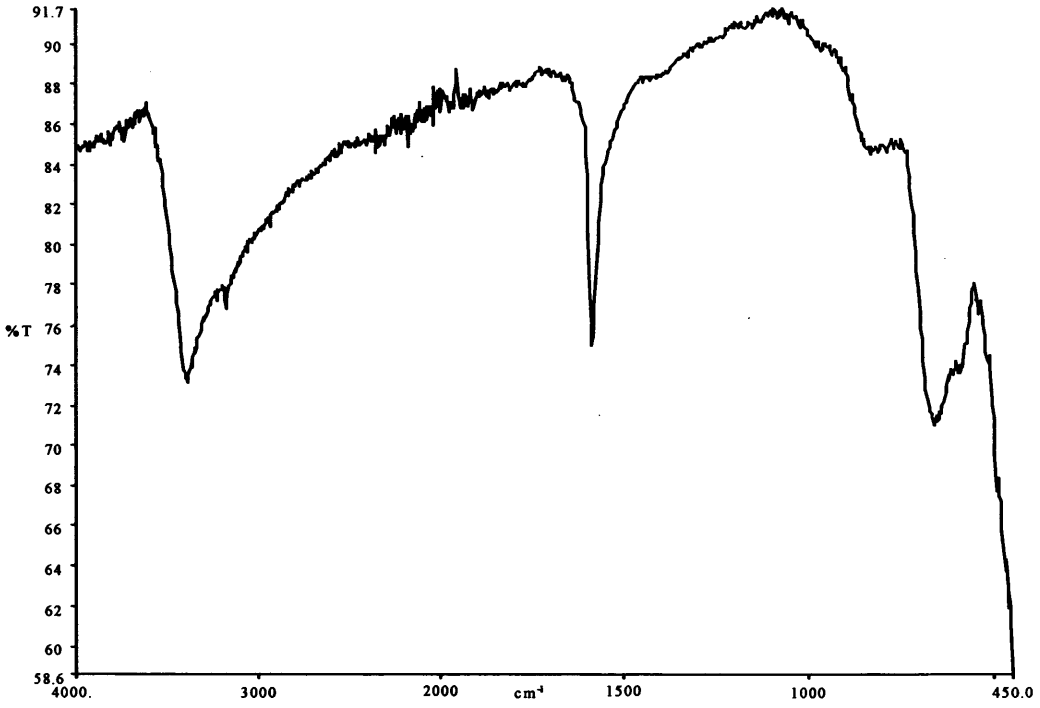

Figure 57. **FTIR spectrum for 10%RH partially oxidised $FeCl_2.2H_20$ (acquired by attenuated reflectance). The sharp absorption at about 1600cm^{-1} is characteristic of the –Cl bond. The broad absorption band around 3200 cm^{-1} is due to –OH bonds (stretching), here from water of hydration. See Derrick *et al.* (1999) and Skoog *et al.* (1998).**

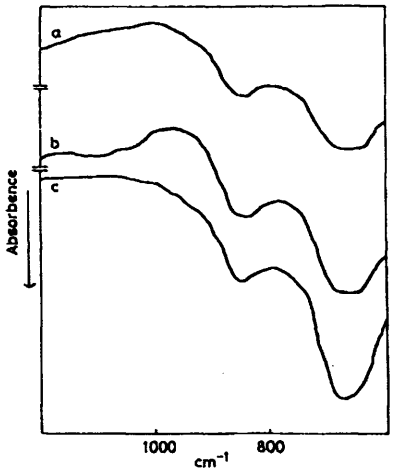

Figure 58. **Infrared spectra of βFeOOH: *a* = archaeological iron corrosion product, b = product from ferrous chloride + iron + moist air, c = product from ferrous chloride and moist air. After Turgoose (1982b: 97, *fig. 1*)**

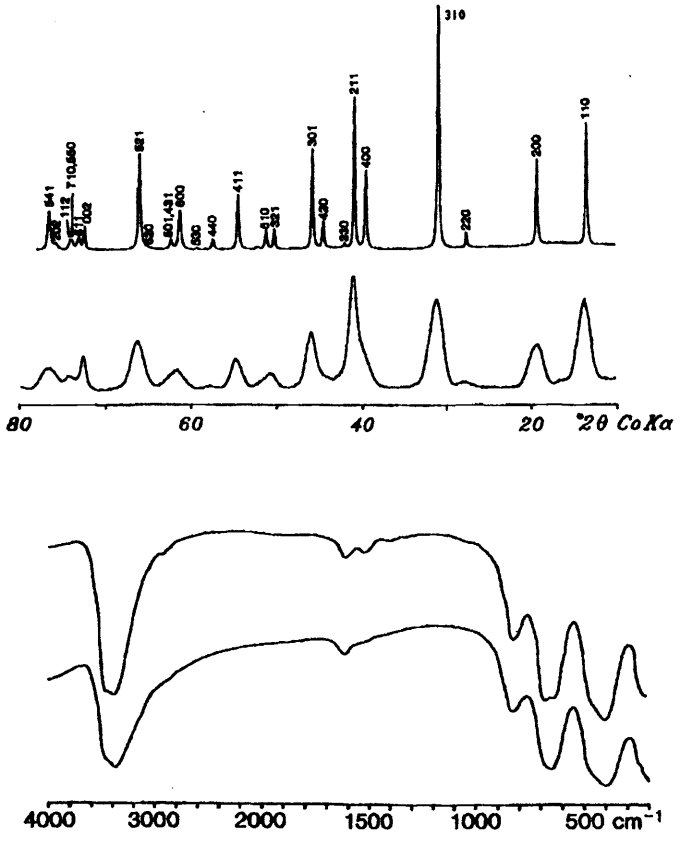

X-ray diffractogram and IR spectrum of somatoidal (upper) and rod-like (lower) akaganeite.

Figure 59. **X-ray diffractogram and infrared spectra of βFeOOH (Somatoidal (upper) and rod-like (lower) . After Schwertmann & Cornell (2000).**

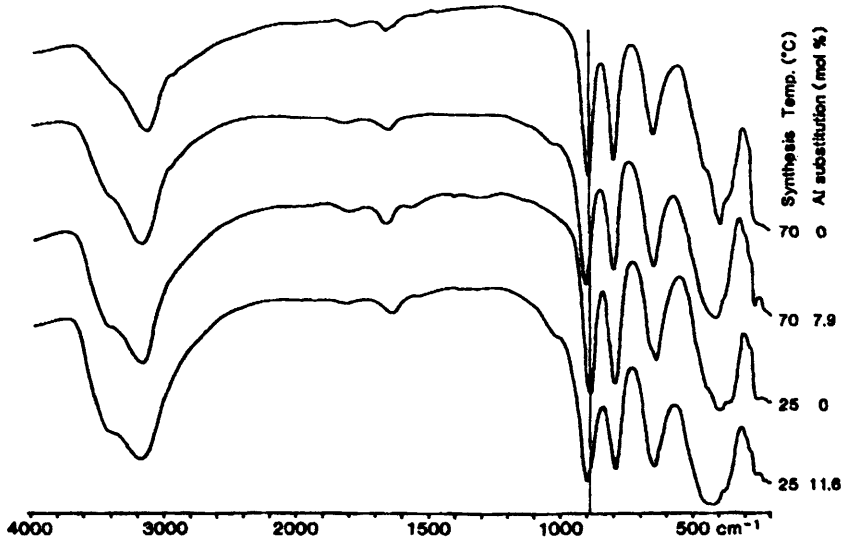

Infra red spectra of pure and Al-substituted goethites prepared at 25 and 70 °C. The vertical line illustrates the shift in the position of the OH bending mode due to Al-for Fe substitution.

Figure 60. **Infrared spectra of goethite (αFeOOH) for comparison. After Schwertmann & Cornell (2000).**

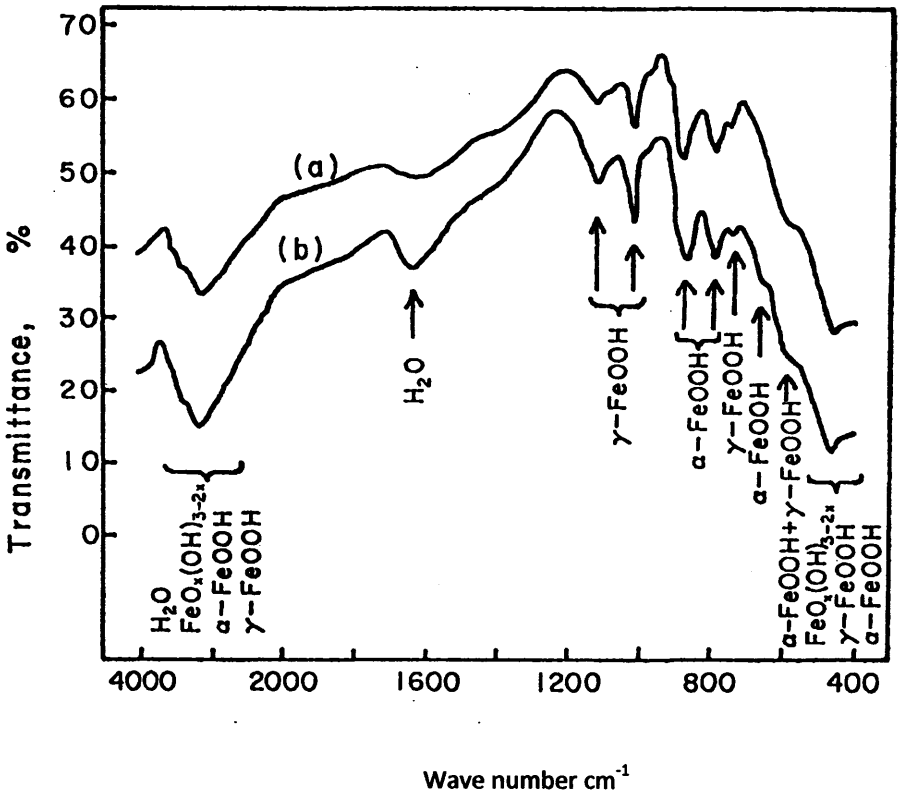

Figure 61. **Infrared spectra of iron oxyhydroxides (FeOOH) for comparison. After Misawa *et al.* (1974).**

Turgoose (figure 58) identifies diagnostic βFeOOH absorptions at 850cm^{-1} to 820cm^{-1} and ~650cm^{-1}. Thickett (2005) has developed a method of quantifying amounts of βFeOOH present in a sample based upon the length (rather than area) of its 852cm^{-1} absorption using FTIR in transmission mode with KBr discs.

Ishikawa *et al.* (1986 and 1988) reported four kinds of hydroxyl group for βFeOOH. Three are on the surface and are responsible for hydrogen bonding with water by chemisorption: 3723cm^{-1}, 3686cm^{-1} and 3659cm^{-1}. The other hydroxyl group was reported to be within the tunnel of the hollandite structure: 3485cm^{-1}. Murad and Bishop (2000) studied the Fourier-transform infrared (FTIR) spectra of a synthetic akaganéite (somatoids prepared by slow hydrolysis of an $FeCl_3$ solution) and listed its bands as 3480 + 3390 (doublet), 1630, 850 + 820 (doublet), 650, 490 and ~420 cm^{-1}. They also confirmed that ATR spectra (surface only) and transmittance spectra (absorbance only) showed compatible trends above and below ~1000cm^{-1}. However, measurements taken on pellets prepared by pressing the sample with alkali halides (KBr or CsI) displayed bands at 1096, 1050 and 698 cm^{-1} that were not observed in spectra of the pure akaganéite and must therefore be considered to be artefacts (*ibid.*: 716).

The –OH and H_2O stretching region is characterised by two intense bands near 3388cm^{-1} and a weaker band near 3486cm^{-1}. The H_2O bending band is weaker than the –OH and H_2O stretching bands at around 1630cm^{-1}. A band at 847cm^{-1} has been attributed to H_2O molecules within the hollandite tunnels or to O-H...O bending vibrations. Murad and Bishop (2000: 719) studied the influence of heating βFeOOH to 100°C for different periods of time and reported the reduction of intensity of the 3391cm^{-1} band whilst the 3487cm^{-1} band remained unchanged. The latter band was therefore ascribed solely to structural –OH whereas the 3391cm^{-1} band was ascribed to –OH and molecular H_2O. The H_2O bending band at ~1627cm^{-1} showed an even more marked relative decrease in intensity and a shift from ~1627cm^{-1} to 1618cm^{-1} indicating the existence of minor amounts of adsorbed molecular water bound to different structural sites. These conclusions agree with Ishikawa *et al.* (1986) and indicate a potential source of water to form an electrolyte for electrolytic corrosion or to support hydrolysis of the βFeOOH itself. Differences in the published data were ascribed to differences in the βFeOOH

synthesis methods used by different workers and their failure to discount the presence of other oxyhydroxides in their samples in many cases.

The FTIR-ATR spectrum of Turgoose's sample shows that it still comprises stable βFeOOH after 25 years (see also XRD data, figure 66b). Whilst βFeOOH is known to be thermodynamically less stable than goethite (αFeOOH) and magnetite (Fe_3O_4) claims of its **inherent** "metastability" with time (Gilberg and Seeley, 1981: 52) must be questioned under dry storage conditions (see Cornell and Giovanoli, 1990 for elevated temperature and alkaline conditions). Murad and Bishop (2000: 717) report the analysis of a synthetic akaganéite (somatoids prepared by slow hydrolysis of an $FeCl_3$ solution) in 1979 and again in 1999 using X-ray diffraction (XRD) and report that the sample had not suffered any alteration since its synthesis two decades earlier. These observations have important implications for the desiccated storage of chloride-contaminated wrought iron. Chloride bound within the βFeOOH structure is not likely to become freed up as labile chloride as long as moisture is absent. However, βFeOOH is known to be unstable to hydrolysis to αFeOOH or, in the presence of metallic iron, hydrolysis to magnetite under moist conditions e.g. during aqueous (including Soxhlet) washing (Keller, 1969; Cornell and Giovanoli, 1990). Without environmental control, βFeOOH will release chloride which will promote further corrosion under humid conditions.

FTIR-ATR spectra for Soxhlet washed βFeOOH (figures 54 and 56) show additional adsorptions in the fingerprint region (below frequency 1000cm^{-1}) and these suggest that partial hydrolysis of βFeOOH has taken place as a result of the wash. Whilst this will have released chloride ions formerly bound in the hollandite lattice of the βFeOOH which could potentially promote further corrosion, it is possible that (at least in part) these could be removed by this washing process (Al-Zahrani, 1999: *table 30*). Keene and Orton (1985: 141) and Keene (1991: 259) advocated the use of aqueous washing techniques. They reported that aqueous washing had been observed to enhance the stability of contaminated wrought iron artefacts in museum stores, having a greater effect on survival than controlled storage at low relative humidity. The most effective treatments were found to be those removing the greatest quantity of chloride.

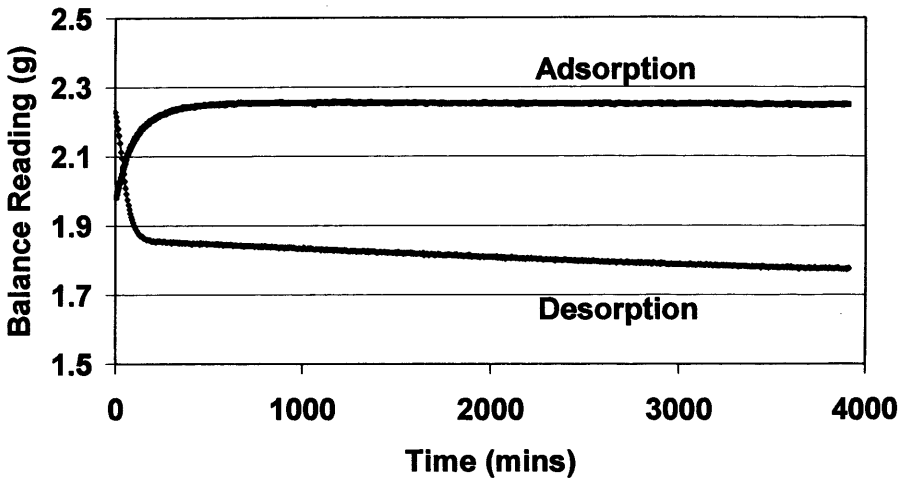

Figure 62. **Adsorption curve for 2g unwashed βFeOOH conditioned to 41%RH and placed in the climatic chamber with its environmental set-point at 80%RH. Desorption curve for unwashed βFeOOH conditioned to 80%RH within the climatic chamber (weighing 2.257g) and set point changed to 18%RH.**

Results shown in figures 62, 67, 83, 85 and 87 are useful although they are not directly comparable because they were obtained under different environmental parameters. Figure 62 (unwashed βFeOOH) clearly shows a measurable increase in weight when the sample is removed from a desiccator maintained at 41%RH and placed in the climatic chamber at a set-point of 80%RH. Figure 62 (unwashed βFeOOH) also clearly shows a measurable loss in weight when the 80%RH set-point is changed to, and maintained at 18%RH. Although minor balance effects are expected to be present (appendix 1), the trends observed are those that would be expected for adsorption and desorption of water vapour by a hygroscopic material i.e. weight increase on exposure to a higher relative humidity and weight decrease on exposure to a lower humidity. Figure 67 (washed βFeOOH) also exhibits weight change trends associated with adsorption and desorption of water but the magnitude of the trend (the amount of water surface adsorbed) on washed βFeOOH significantly less than for unwashed βFeOOH. The findings reported here initially appear to be contradictory because Ishikawa and Inouye (1975) reported that their thermogravimetric analyses of [precipitated and washed] laboratory synthesised βFeOOH showed that weight loss due to adsorbed water occurred between 200°C and 600°C but that chloride content influenced the degree of

loss: Low chloride content corresponded with higher water content and greater weight loss up to 270°C. An explanation of the increased water adsorption measured in these experiments for unwashed βFeOOH is that the significant surface adsorbed chloride is present mostly as aqueous hydrochloric acid rather than surface-bonded chloride as would have been the case for Ishikawa and Inouye (*ibid.*).

Because washing removes surface adsorbed, labile, chloride and is advantageous, significantly reducing the hygroscopicity of βFeOOH, washed βFeOOH is likely to play much less of a role in the ongoing corrosion of wrought iron maintained within a dry atmosphere than unwashed βFeOOH; attracting less water to the surfaces and providing less chloride for the electrolyte. This was tested experimentally and the results are presented in section 6.5.3.

6.5.3. Unwashed βFeOOH mixed with iron powder at different relative humidities

The results of exposing a mixture of equal quantities (approximately 2.0000g) of unwashed βFeOOH conditioned to 41%RH and (approximately 2.0000g) iron powder (figure 64) at different relative humidities between 12%RH and 35%RH for up to 16,000 minutes (216 hours or 9 days) are shown in figure 63. The result of active corrosion is shown in figure 65.

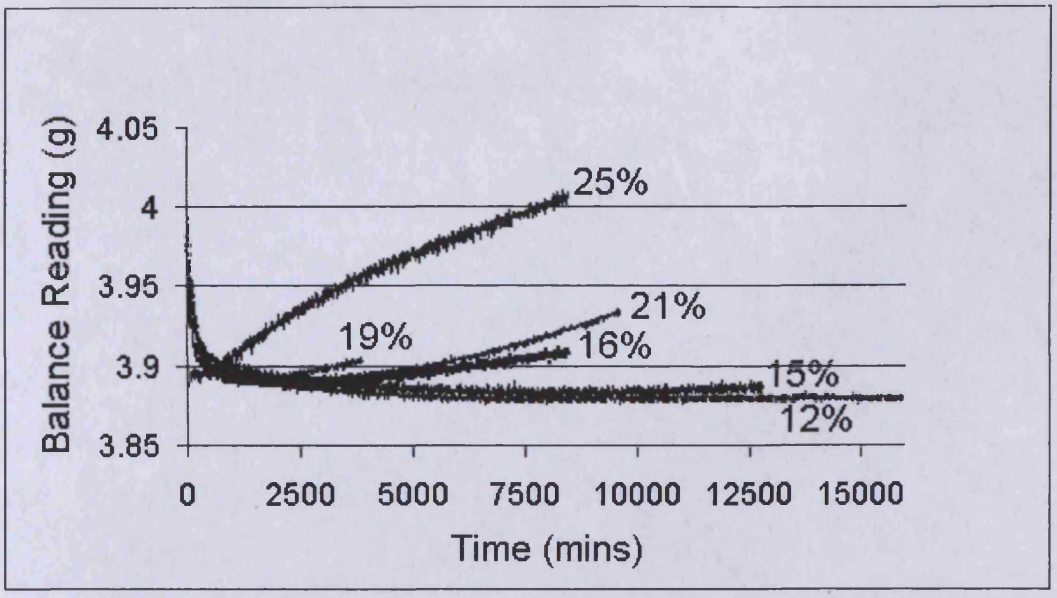

Figure 63. **Changes in mass of unwashed βFeOOH mixed with iron powder at different relative humidities.**

Examination of figure 63 shows an initial period of desiccation for low humidity tests during which the βFeOOH loses adsorbed water at a greater rate than any corrosion can increase the mass of the mixture. After approximately 3,000 minutes for tests at 15%RH and above corrosion contributes a greater increase in weight than the small decrease in weight through continued loss of adsorbed moisture. After 3,000 minutes the net result is an increase in weight attributable to active corrosion of the iron powder. Visual examination suggested the formation of more βFeOOH (figure 65). At 25%RH and 35%RH corrosion of the iron caused an increase in weight in excess of any loss in weight through desiccation from the start of these tests.

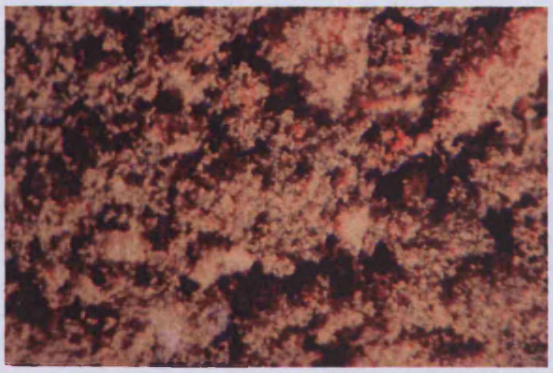

Figure 64. **(left) βFeOOH and iron powder upon mixing.**

Figure 65. **(right) Active corrosion of iron in the presence of βFeOOH (at 35%RH in this case).**

The results reveal that corrosion of iron in the presence of unwashed βFeOOH occurs at least as low as 15%RH. No measurable increase in weight occurred at 12%RH after 16,000 minutes (11 days). No visible change was observed. Some icing of the climatic chamber condensing coil led to the loss of RH control to ±1%RH towards the end of the 12%RH test in figure 63. This time scale is at the operational limit of the Votsch™ 4018 climatic chamber at relative humidities between 10%RH and 20%RH, even with dried compressed air. The recorded RH deviation from the set-point 12%RH was recorded as ±3%RH at the end of the test. Examination of the sample mixture at the end of the test (~16,000 minutes = 11 days) was inconclusive. There was possibly a small amount of colour change (corrosion) of the iron powder but this would be expected for the period of poor set-point attainment as shown by the 15%RH data set. If corrosion had occurred it was so slight that no weight change was recorded over and above the balance "noise".

Results suggest a considerable quantity of adsorbed chloride on the surface of the βFeOOH produced in the laboratory and used in this test. This chloride can not be present as solid ferrous chloride dihydrate which would be expected below 20%RH at 20°C, for this would not support corrosion (sections 6.1 – 6.3). XRD analyses of the laboratory-synthesised βFeOOH used did not show the presence of solid ferrous chloride (figure 32 and appendix 3). An explanation for the behaviour of the mixture observed in figure 63 is that adsorbed chloride on the surface of the βFeOOH is present either as hydrochloric acid (HCl) or initially as adsorbed ions that become mobile in moisture supplied by the ambient relative humidity to the hygroscopic βFeOOH (Ishikawa and Inouye, 1972 and 1975; Atkinson, 1977; Galbraith *et al.*, 1979; Childs *et al.*, 1980; Ishikawa *et al.*, 1988). This chloride solution provides an electrolyte that promotes increased ferrous ion production (corrosion) at the surface of the metal. These ferrous and chloride ions can ultimately combine with atmospheric oxygen to form fresh βFeOOH (figure 65). If chloride ion concentrations are sufficiently low (i.e. diluted), αFeOOH may also form but this polymorph was not identified by XRD on marine wrought iron samples analysed for this study (appendix 4). It is not expected that the original βFeOOH used in the test will have degraded and broken down to

release its internally bound chloride unless it is dissolved by an acidic aqueous solution, possibly HCl. βFeOOH assayed over 20 years after it was produced in Cardiff by Turgoose (using the $FeCl_2.4H_2O$/iron powder/high relative humidity synthesis process) was still found to be virtually pure βFeOOH (with **possibly** up to 1%wt goethite indicated by XRD but not FTIR-ATR analyses – see figures 55 and 66b). This sample had been stored in a sealed, dry, jar for this time and will not have had access to sufficient atmospheric moisture for slow hydrolysis to αFeOOH (Watkinson and Lewis, 2005b).

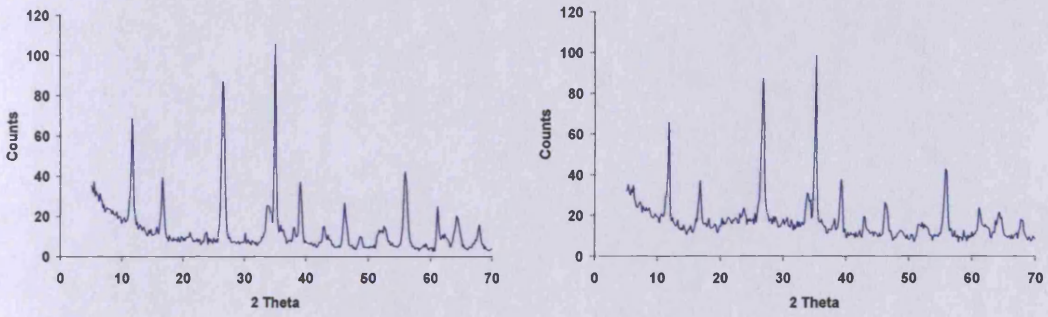

(a) (b)

Figure 66. **Results of XRD analysis of (a) recently synthesised unwashed βFeOOH and (b) βFeOOH synthesised by aerial oxidation of ferrous chloride with iron powder in 1980 by Turgoose and submitted for independent XRD analysis in 2005.**

Results of these tests, using synthesised, unwashed, βFeOOH, represent a worst case scenario in terms of corrosion. This is due to its chloride-rich surface caused by adsorption of chloride from the large chloride reservoir used in its production.

The implications of these results for the aqueous washing of chloride-contaminated wrought iron have been considered and informed further tests. Washing would remove large quantities of loosely adsorbed surface chloride (and loosely adhering corrosion products, including βFeOOH) potentially enhancing its preservation. Rates of increase in weight (corrosion) in figure 63 suggest that storage of chloride-contaminated iron containing βFeOOH in low relative humidity environments is beneficial and, the lower the environmental RH the more beneficial the environment will be.

6.5.4. Comparison of iron powder behaviour in the presence of washed βFeOOH and unwashed βFeOOH

A sample of Soxhlet washed βFeOOH was mixed with an equal mass of iron powder and was exposed to 19% relative humidity. When compared with results for a similar mixture comprising equal masses unwashed βFeOOH and iron powder exposed to 19%RH (figure 67), it is clear that removal of surface chloride has eliminated the immediate aggressive corrosive effects of the βFeOOH on iron (figure 63). The lack of weight loss by the sample suggests that surface adsorbed chloride is responsible for the majority of the hygroscopic behaviour observed for unwashed βFeOOH in these tests. This may be due to the association of chloride with water and subsequent production of HCl on the surface of the βFeOOH, which then attracts more water. Once chloride has been removed surface sites are occupied by hydroxyl ions from the wash solution. More research is required to substantiate this theory.

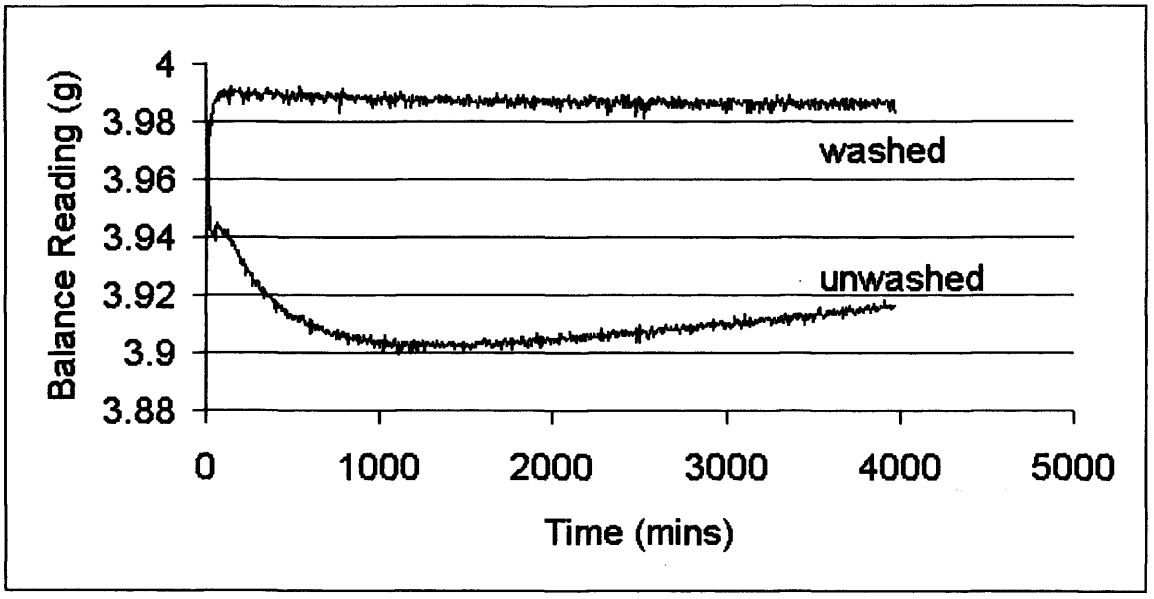

Figure 67. **The change in mass of a mixture of washed βFeOOH and iron powder exposed to 19% relative humidity compared with a mixture of unwashed βFeOOH and iron powder exposed at the same RH.**

6.5.5. The nature of the surface adsorbed labile chloride on βFeOOH.

The nature of the surface adsorbed chloride on βFeOOH determines its degree of mobility and this is relevant to its ability to act as a contaminant, and to its removal. Two observations were made which are informative regarding the presence and volatility of adsorbed chloride ions on unwashed βFeOOH and/or their ability to become volatile hydrochloric acid (HCl) at ambient temperatures and relative humidities. A degreased stainless steel spatula was placed in a sealed desiccator (conditioned to 41%RH with silica gel) on a clean Petri dish over an open jar containing unwashed βFeOOH. Over a period of months long thread-like dark-brown crystals of corrosion grew from the spatula (figure 68). XRD and SEM-EDX analysis confirmed that this was a mixture of βFeOOH (~38%) and probably a βFeOOH-like nickel-containing corrosion product (figure 69). Chromium and nickel were present in the EDX data and would be expected in a modern stainless steel.

Buchwald and Clarke (1989) reported analyses of corrosion from chloride-contaminated meteoric kamacite (bcc iron with 4-7% Ni) that gave βFeOOH of the composition 5.5%wt Ni, 3.1%wt Cl and 5.0%wt Ni, 4.4%wt Cl, 0.5%wt S. They noted that the broad XRD peaks for βFeOOH are characteristic of small crystal size and found that Ni could be present in βFeOOH in quantities up to 19%wt, but that 3-5%wt was most common. They concluded that the composition of βFeOOH depends upon the composition of the parent metal. The findings of this study agree with this observation. The actual quantity of chloride-containing corrosion on the spatula is anticipated to be significantly higher than 38%. The spatula was not in contact with any of the other components of the desiccator. Moisture and chloride for the thread-like crystal growth (corrosion) must have come from the vapour phase.

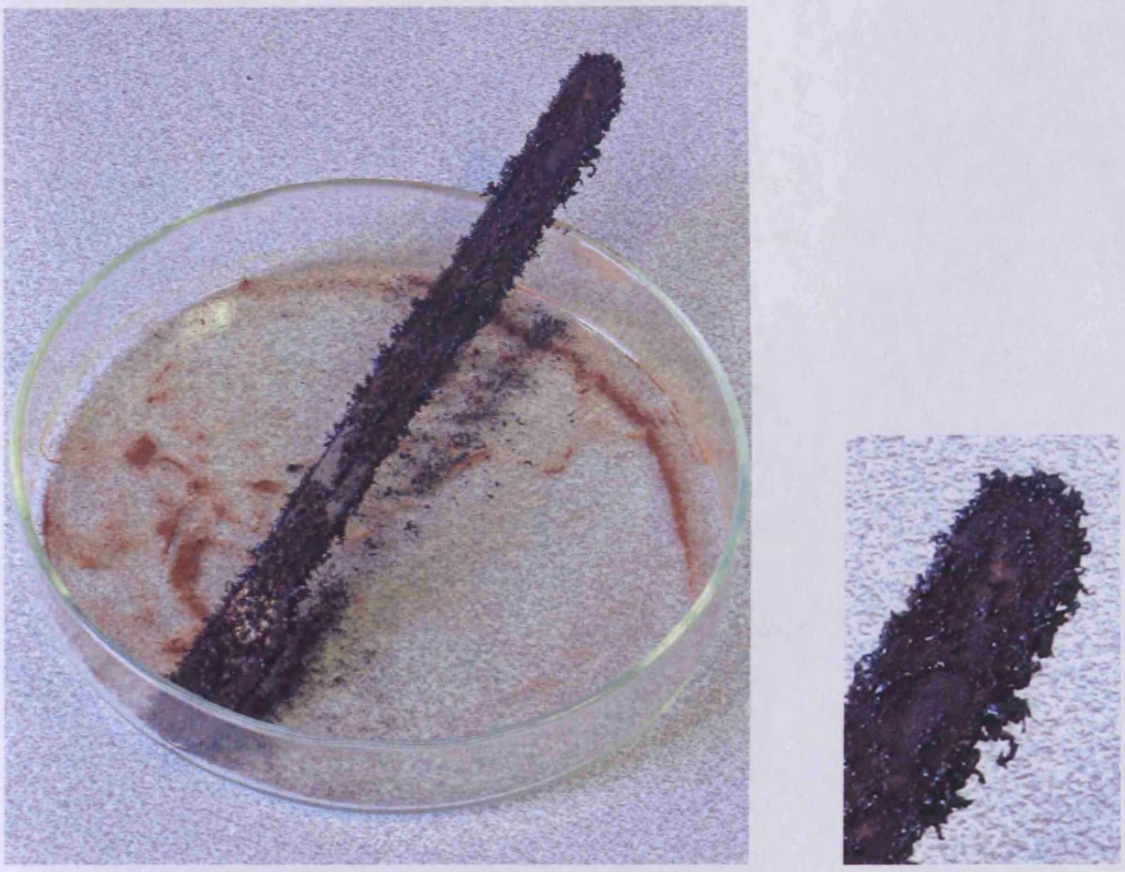

Figure 68. **Thread-like crystals of iron corrosion on a steel spatula exposed to volatile chloride, possibly HCl, from unwashed βFeOOH (left) with close up (right).**

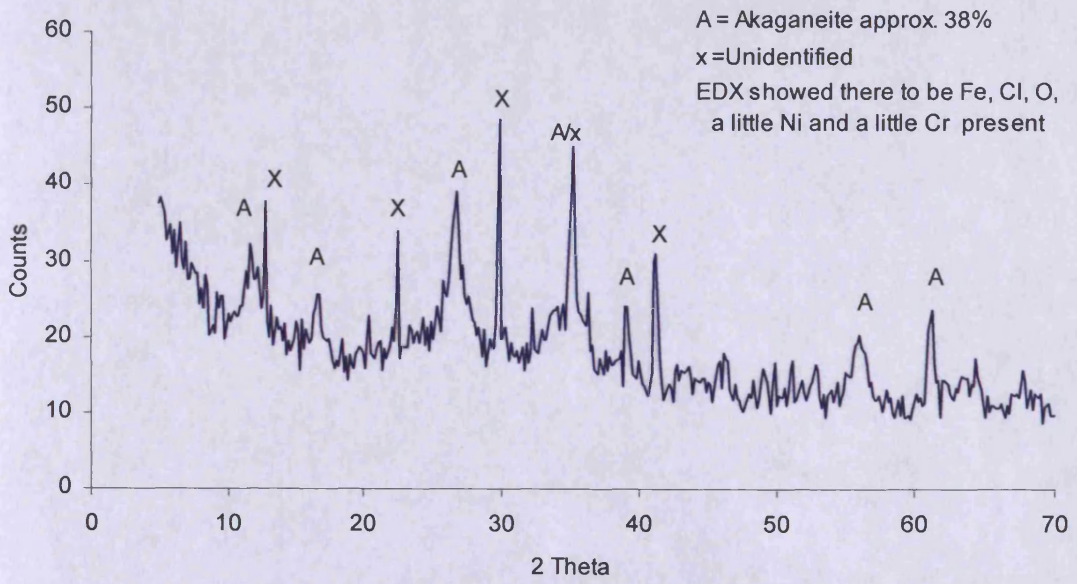

Figure 69. **XRD data for a sample of the thread-like crystals of iron corrosion shown in figure 68.**

A sample of unwashed βFeOOH was Soxhlet washed until wash solutions were chloride free (Scott & Seeley, 1986). The wash solution from the bulb containing the labile chloride from the washed βFeOOH was placed in a beaker covered with aluminium foil. The aluminium foil was observed to oxidise rapidly forming grey aluminium oxide at the edges with the greater portion of the foil disintegrating as a fluffy white powder (figure 70). Analysis of this white powder by XRD (figure 71) confirmed an amorphous (non crystalline) structure suggestive of aluminium chloride ($Al_2Cl_6.6H_2O$).

Figure 70. **Aluminium chloride resulting from attack of aluminium foil by volatile chloride, possibly HCl, from a βFeOOH Soxhlet wash solution.**

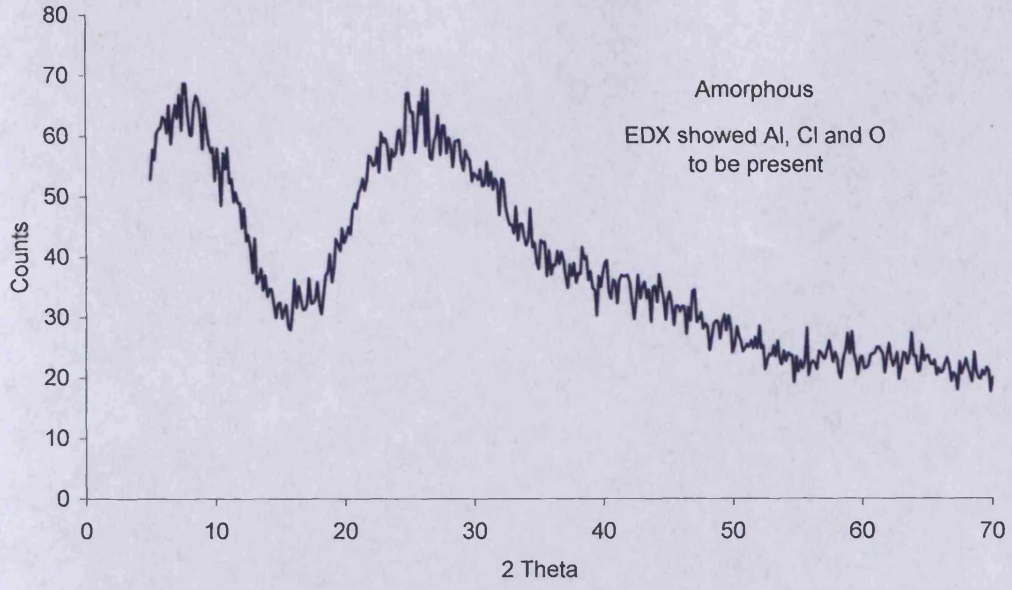

Figure 71. **XRD and EDX analysis show amorphous white substance to be aluminium chloride with some grey aluminium oxide.**

Ferrous chloride tetrahydrate was dissolved in deionised water to form a concentrated but not saturated solution, and left in a beaker covered with aluminium foil in the same way as for the Soxhlet solution shown in figure 70. A skin rapidly formed on the surface of the ferrous chloride solution as it oxidised from yellow to dark green/brown with orange brown oxidation product forming a ring around the beaker at the meniscus matching that visible on the edges of the beaker in figure 70. The aluminium foil formed a dull grey oxide layer on its underside within a few days and after two weeks very localised filiform dark grey and white areas of corrosion formed on the upper surface of the aluminium foil in contact with the atmosphere. The underside of the aluminium foil remained unaltered after the initial formation of the dull grey oxide layer.

The observations for the ferrous chloride solution suggest that the high humidity and ambient oxygen levels within the beaker promoted the rapid formation of a protective layer of aluminium oxide on the underside of the aluminium foil. The protective oxide layer on the underside of the aluminium foil made it cathodic to the upper surface of

the foil in contact with the atmosphere. Corrosion then proceeded at anodic sites on the upper surface. The foil did not break up or form white fluffy corrosion products over a period of one month and the deterioration of the foil covering it over that time was markedly less than had been observed for the foil covering the Soxhlet wash solution. The presence of volatile chloride was not demonstrated for the ferrous chloride solution arrangement over the period of observation. Ideally the test would be run for a longer period and until the water had evaporated leaving a solid residue. A more concentrated solution of ferrous chloride may produce a different effect on the aluminium foil. This will be investigated systematically as future work and the oxidation products (of the aluminium foil and the ferrous chloride solution) will also be submitted for XRD and FTIR-ATR analyses.

These preliminary observations suggest that the labile chloride on βFeOOH could exist as surface adsorbed, mobile - even volatile, hydrochloric acid (HCl) at relative humidities at least as low as 41%RH. Aqueous washing removes this potentially highly corrosive chloride solution/hydrochloric acid from βFeOOH. The orange/brown colour of the wash solutions and their solid residue upon evaporation suggest that Fe^{2+} and/or Fe^{3+} ions are also present in the wash water. If hydrochloric acid remains in proximity to metallic iron it could perpetuate ongoing corrosion via the "acid regeneration cycle" model proposed by Askey *et al.* (1993). A potential risk for wrought iron stored in sealed containers has been identified and is discussed in section 7.3.

Goethite, lepidocrocite and akaganéite are soluble in HCl, which is used commercially to remove corrosion products from iron which is to be galvanised (Donovan, 1986: 145). The rate law and mechanism of the dissolution of goethite, lepidocrocite and akaganéite in HCl have been published (Cornell *et al.,* 1976; Cornell & Giovanoli, 1988) and are similar. Dissolution of βFeOOH in hydrochloric acid proceeds via the ends of its chloride-containing tunnels, which are hollowed out, destabilising the structure and releasing their Cl^- ions. HCl will prevent the formation of these insoluble corrosion products and will continue to attract water hygroscopically as long as there is sufficient atmospheric moisture available to it. XRD and FTIR-ATR analyses conducted as part of this study indicate that insufficient hydrochloric acid is present on the surface of the

unwashed βFeOOH studied to initiate its dissolution or transformation (appendices 3 and 4). The surface adsorbed chloride *is* probably aqueous at ambient relative humidities for it has been shown (by XRD) that it is not crystalline. These results suggest that the surface of the βFeOOH has adsorbed chloride ions (Cl^-) with ferrous ions (Fe^{2+}) and probably ferric ions (Fe^{3+}) in aqueous solution. The Fe^{2+} ions possibly act as counter ions in this solution and the Cl^- ions are fully dissociated. The results show that the chloride is volatile and upon evaporation it is possible that the chloride ions leave the solution as HCl.

The silica gel maintaining the environment within the desiccator continued to maintain a stable 41%RH even though it could have been contaminated by absorbing HCl vapour [silica gel was patented in 1919 for use in the adsorption of vapours and gases in gas mask canisters during World War I (Weintraub, 2002)]. Any absorption by the silica gel was insufficient to prevent chloride or HCl vapour corroding the stainless steel spatula. Future analyses of the silica gel will be informative.

6.6 Oxidation of $FeCl_2.4H_2O$ to βFeOOH

During a 20% relative humidity drying cycle ferrous chloride turned from green to white, signalling the transition from $FeCl_2.4H_2O$ to $FeCl_2.2H_2O$. After five days at 20% relative humidity a distinct change in colour towards brown was observed. This may indicate that dehydration of ferrous chloride tetrahydrate at 20% relative humidity is too slow to prevent some of it oxidising to βFeOOH. This is a change that might have implications for the iron corrosion process as the small amount of βFeOOH formed has the potential to contribute to the corrosion of the iron powder. Ideally $FeCl_2.4H_2O$ would be desiccated to $FeCl_2.2H_2O$ without oxidation to the potentially harmful, disruptive, voluminous βFeOOH, especially at the metal/DPL interface.

Since no browning of $FeCl_2.4H_2O$ was observed at relative humidity cycles below 20%RH, i.e. during or post-transformation to $FeCl_2.2H_2O$ (figure 36), this may represent the threshold for βFeOOH formation via oxidation of $FeCl_2.4H_2O$. [Chamber

environmental conditions fluctuate ±1% relative humidity from the central, quoted, relative humidity value for short periods of time (appendix 2) so an error of at least this order should be quoted e.g. 20% ±1% relative humidity. See error bars, figure 40].

6.7. Corrosion of iron powder in the presence of $FeCl_2.4H_2O$ and βFeOOH at 20% relative humidity: Synergistic behaviour?

Figure 72 shows the result of a test examining the effect of combining $FeCl_2.4H_2O$, unwashed βFeOOH and iron powder at 20% relative humidity and 20°C.

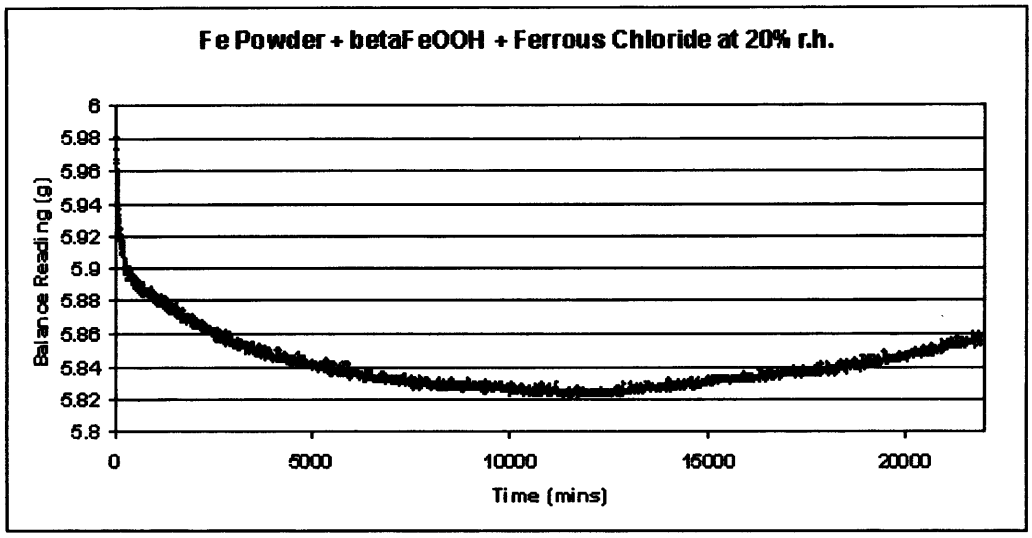

Figure 72. **Changes in mass of a mixture of iron powder, $FeCl_2.4H_2O$ and unwashed βFeOOH over a period of 15 days at 20% relative humidity and 20°C.**

Before 12500 minutes decrease in overall mass through loss of bound and adsorbed water was greater than the increase in mass through βFeOOH formation. After 12500 minutes the increase in mass due to incorporation of oxygen during βFeOOH formation is greater than any continued loss of water from βFeOOH or from ferrous chloride.

The initial rapid fall in balance reading (mass) in figure 72 (from time = 0 minutes to time = 300 minutes [5 hours]) is identified to be dominated by the loss of adsorbed water from the βFeOOH present in the mixture. The continued gradual (almost exponential) fall in balance reading (from time = 300 minutes [5 hours] to time = 12500 minutes [208 hours or 8.7 days]) is ascribed to the dehydration $FeCl_2.4H_2O$ to

$FeCl_2.2H_2O$ combined with the continued loss of a small amount of water from the βFeOOH present.

From approximately 12500 minutes (8.7 days) the rise in balance reading (increase in mass) is ascribed to the now dominant contribution of the increase in mass due to active corrosion of the iron powder. Visual examination of the mixture at the end of the experimental run suggests that βFeOOH formation was occurring. The corrosion recorded as mass increase after 12500 minutes was almost certainly occurring throughout the period leading up to 12500 minutes, but was masked by the greater loss in mass caused by water leaving the mixture.

The desiccation of the $FeCl_2.4H_2O$ to $FeCl_2.2H_2O$ may be slow enough to allow some oxidation of $FeCl_2.4H_2O$ to βFeOOH and some corrosion of iron powder in contact with $FeCl_2.4H_2O$ whilst the water is being removed (see also section 6.6). In reality the amount of loss of wrought iron during this period will be negligible compared with that resulting from corrosion occurring above 21%RH because it ceases when full desiccation to $FeCl_2.2H_2O$ is achieved. Below 21%RH it is the βFeOOH that is then responsible for the corrosion of the iron, which is recorded in figure 72 as a weight gain (from 12500 minutes), once desiccation of iron chloride is complete. The corrosion evident from 12500 minutes is probably due to the labile surface-adsorbed chloride on the βFeOOH used in the test (sections 6.5.4. and 6.5.5.).

The rate of increase in mass recorded in figure 72 for 20%RH and 20°C may be compared with that for the corrosion of iron powder in the presence of unwashed βFeOOH alone at 20%RH and 20°C over the same period of time (*c.f.* figure 63). The results are of the same magnitude and show that the presence of ferrous chloride dihydrate does not accelerate the corrosion of iron powder in the presence of unwashed βFeOOH synergistically under the test conditions used. If $FeCl_2.2H_2O$ acted as a desiccant, it was not sufficient to prevent corrosion (it would be unlikely to be an effective desiccant where the environmental RH is maintained) but may have slowed it.

6.8 *The effect of temperature*

6.8.1. Dehydration of ferrous chloride tetrahydrate to form ferrous chloride dihydrate at an elevated temperature (30°C)

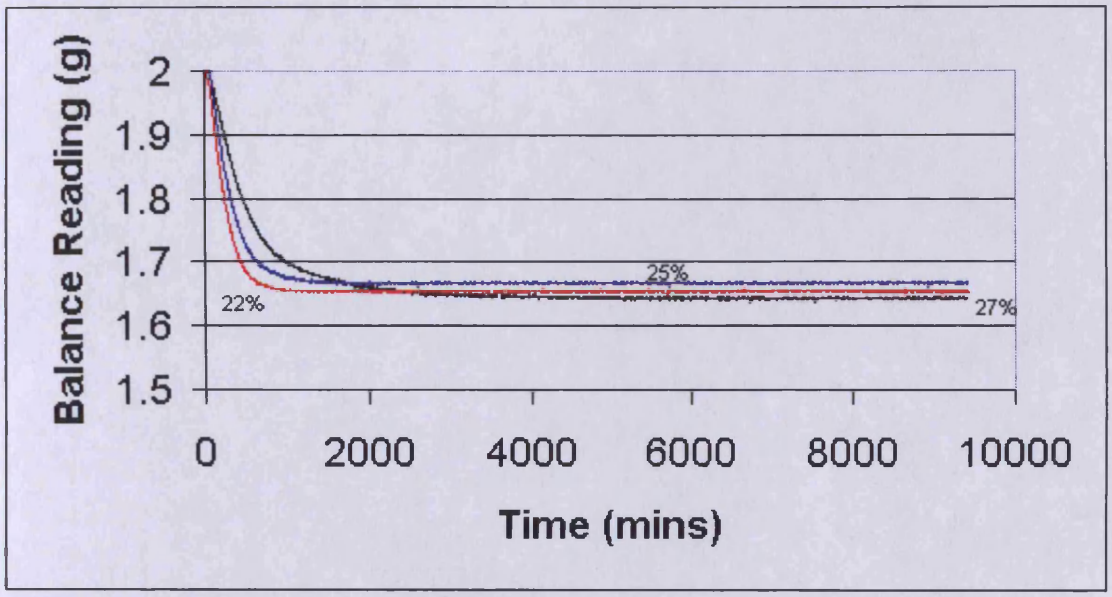

Figure 73. **Dehydration of ferrous chloride tetrahydrate to form ferrous chloride dihydrate at different relative humidities, at 30 °C.**

It is clear that the loss in weight exhibited in figure 73 corresponds well with the theoretical loss of 0.3624g corresponding with the loss of two waters of hydration upon conversion from 2g ferrous chloride tetrahydrate to 1.6376g ferrous chloride dihydrate see calculation in section 6.1.1.). It should be noted that the initial mass of ferrous chloride tetrahydrate was not exactly equal to 2.0000g. This accounts for the uncorrected differences in stable end mass but this is fortuitous for visual acuity of all three data sets. In all three cases the green crystals of ferrous chloride tetrahydrate were also visually observed to have converted to the white crystals of the dihydrate.

These results have major implications for the theoretical threshold humidity for the storage of chloride-contaminated wrought iron based upon the ferrous chloride dihydrate model. At 30°C the dihydrate becomes the stable hydrate at relative humidities at least as high as 27%RH.

Further work is necessary to quantify the rate-determining factor at elevated (or lower) temperatures. Corrosion reactions are generally expected to proceed more rapidly at elevated temperatures (figure 17) as predicted by the Arrhenius equation (equations [26] & [44]). Conversely, the stability range (%RH) of ferrous chloride dihydrate is extended at elevated temperature of 30 °C (*c.f.* figure 16 for rozenite-melanterite equilibria). In theory the ferrous chloride dihydrate is stable, acts as a desiccant preventing corrosion and will not oxidise to form fresh βFeOOH (Turgoose, 1982b; Knight, 1997). This was tested and confirmed during prolonged tests at 20 °C. If the inability of ferrous chloride dihydrate to promote the corrosion of iron is established at other temperatures, the results shown in figure 73 suggest that storing chloride-contaminated wrought iron at a relative humidity of 27%RH and a temperature of 30°C would prevent corrosion (Turgoose, *ibid.*). Iron powder in the presence of ferrous chloride was exposed to a range of environmental relative humidities at 30 °C to establish whether corrosion does or does not occur in the presence of $FeCl_2.2H_2O$ where this is the stable hydrate of ferrous chloride at this elevated temperature (section 6.8.2.).

6.8.2. Corrosion of iron powder in the presence of ferrous chloride dihydrate at an elevated temperature (30°C)

Tests for the corrosion of iron powder in the presence of ferrous chloride tetrahydrate run at 20°C (reported in section 6.1.1. and figure 36) were repeated but at a set-point temperature of 30°C to show the effect of elevated temperature on the corrosion process (figures 76 and 77). Very similar masses of reactants (approximately 2.0000g of iron powder and 2.0000g of analar ferrous chloride tetrahydrate) were used in at each relative humidity so that when the results for each test were plotted directly from the data the three data sets converged graphically making their trends relative to one another difficult to see. The 19%RH data and the 22%RH data, as presented in figure 76, were therefore deliberately separated from the 15%RH data set, and each other, by moving their positions on the y axis for clarity. This was achieved by addition of a fixed figure to every balance reading in the data set for each test and plotting the resulting data. It may be seen that corrosion occurs at 22%RH *and* at 19%RH but still does not occur at 15%RH. The corrosion threshold has shifted to a lower relative humidity (*c.f.* figures 36 and 48) with increased temperature.

The model that iron powder will not corrode in the presence of ferrous chloride dihydrate appears to require modification as a result of the tests run at 30°C. Visually, the white ferrous chloride dihydrate was observed to form during the tests reported in figure 73. Corrosion of iron powder was observed visually to form at 19%RH and 22%RH at 30°C (figure 76) in the presence of ferrous chloride dihydrate so the interpretation of the plotted weight changes is not in doubt. An amended model must be sought.

A given relative humidity (take for example 22%RH) at a given temperature (take for example 30°C) will represent a larger quantity of environmental water vapour than the same relative humidity (22%RH) at a lower temperature (e.g. 20°C) (figure 74 and section 5.1.1.). More water vapour (kg/kg dry air) is present in the tests run at 30°C than the tests run at 20°C, i.e. specific or absolute humidity has increased even though the relative humidity is the same (figure 74). It is possible that this increased quantity of water vapour and/or the effect of increased temperature may be responsible for the corrosion observed at low relative humidities and 30°C. In the collision theory of

reactions, reactant molecules must meet and have (or acquire from their surroundings) sufficient minimum energy for reaction to ensue (Atkins, 1990: 841). Not surprisingly, collision theory in gases is governed by an equation of the Arrhenius [44] form and is exponentially temperature dependent where sufficient energy for reaction is present.

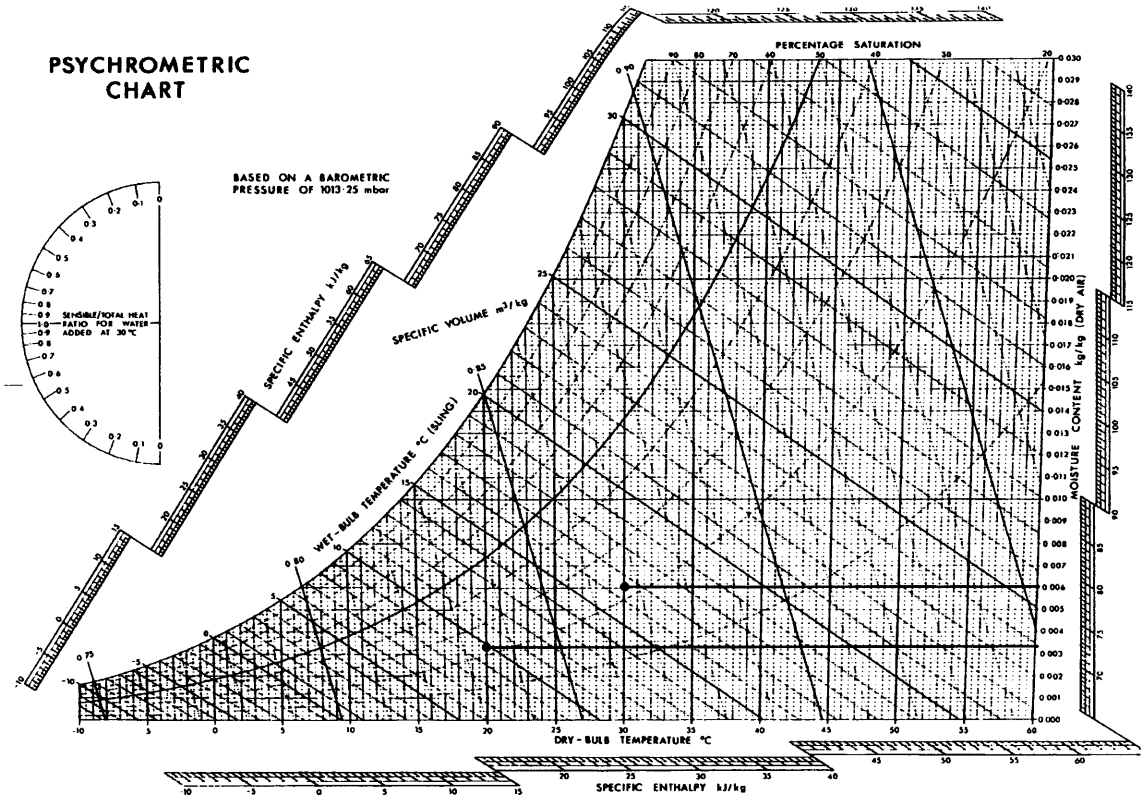

Figure 74. **Psychrometric chart showing the moisture content of air at 22%RH for temperatures of 20°C and 30°C. The moisture content of air (its specific humidity) at 30°C is significantly greater than (nearly double) the moisture content of air at 20°C for a relative humidity of 22%RH in both cases.**

Non-annotated psychrometric chart after Thomson (1986: *figure 66*) with reproduction credit to the Chartered Institute of Building Services, 22 Balham High Road, London SW12 9BS.

As predicted, the increase in reaction rate with increase in temperature (figure 77) corresponds well visually with the Arrhenius relationship [44]. Temperature has a major bearing on the specification of a threshold *relative* humidity for the "safe" storage of chloride-contaminated iron. Further work is being conducted (Lewis & Watkinson) to examine the relationship between threshold relative humidity and temperature. This

will establish whether environmental specification should be given as specific (or absolute) humidity or cited as relative humidity for a cited temperature for metals. A review of existing literature points towards an Arrhenius type relationship for reaction rate as a function of temperature.

Desombre (1980) and Cuddihy (1987) reported that experimental ageing studies produced an empirically derived mathematical ageing correlation for electrochemical corrosion in photo-voltaic cells. The rate of corrosion is logarithmically related to the summation term RH +t, where RH is relative humidity (%) and t is temperature (^{o}C).

$$\delta = \exp [A+B(\theta^{o}C+\%RH)] \qquad [45]$$

and

$$\ln r (t,RH) = A - k(t + RH) \qquad [46]$$

Cuddihy (1987) noted that the resistivity (r) of polyvinyl butyral (PVB) was related to RH and concluded that its resistivity must therefore be a function of the absorbed water vapour in the PVB. Water absorption in a polymer increases with **absolute water vapour concentration** in the atmosphere **at any constant temperature** *and* **with increasing temperature** (figure 75).

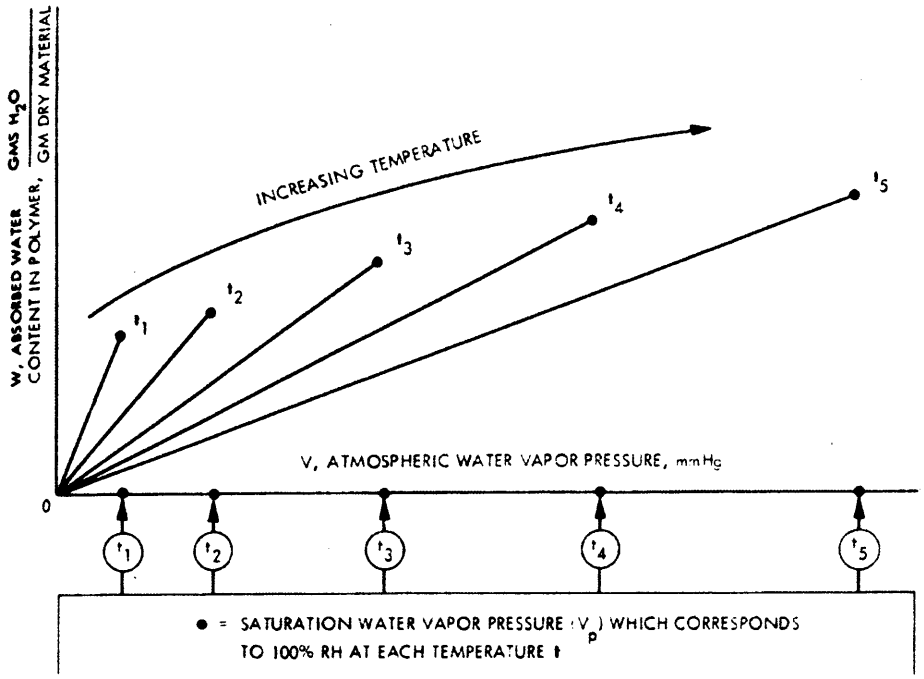

Figure 75. Generalised hygroscopic behaviour of polymeric materials (from Cuddihy, 1987).

Cuddihy (1987) demonstrated that exponentially less water vapour is absorbed by PVB with increasing temperature at constant absolute water vapour concentration. The values of the slopes of each constant temperature line obeyed an Arrhenius (temperature dependent) relationship. A similar temperature dependent trend may be applicable to adsorption of moisture by deliquescent salts and the rate of corrosion of wrought iron in contact with them. It is not currently clear whether the change in the relative humidity value (threshold relative humidity) for the transformation of $FeCl_2.4H_2O$ to $FeCl_2.2H_2O$ follows a similar trend. This is being investigated experimentally at Cardiff University (Lewis and Watkinson) and is critical to the question of whether the iron in contact with ferrous chloride will corrode or not.

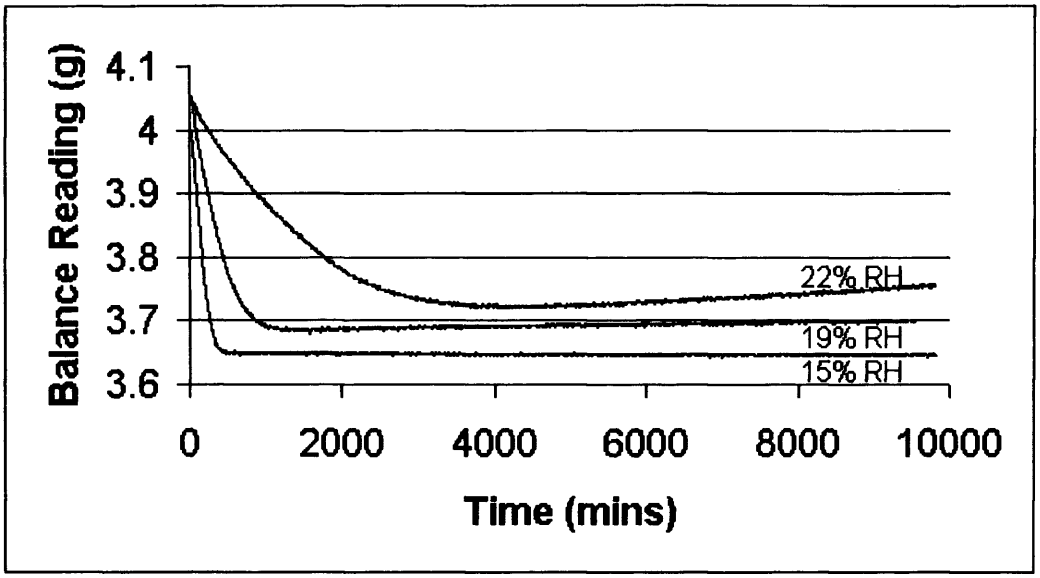

Figure 76. **The behaviour of mixtures of approximately 2.0000g ferrous chloride tetrahydrate and approximately 2.0000g of iron powder at different relative humidities at 30°C. Corrosion of iron powder was observed in the presence of ferrous chloride dihydrate at 22%RH and 19%RH but desiccation of ferrous chloride tetrahydrate to ferrous chloride dihydrate at 15%RH was observed without corrosion.**

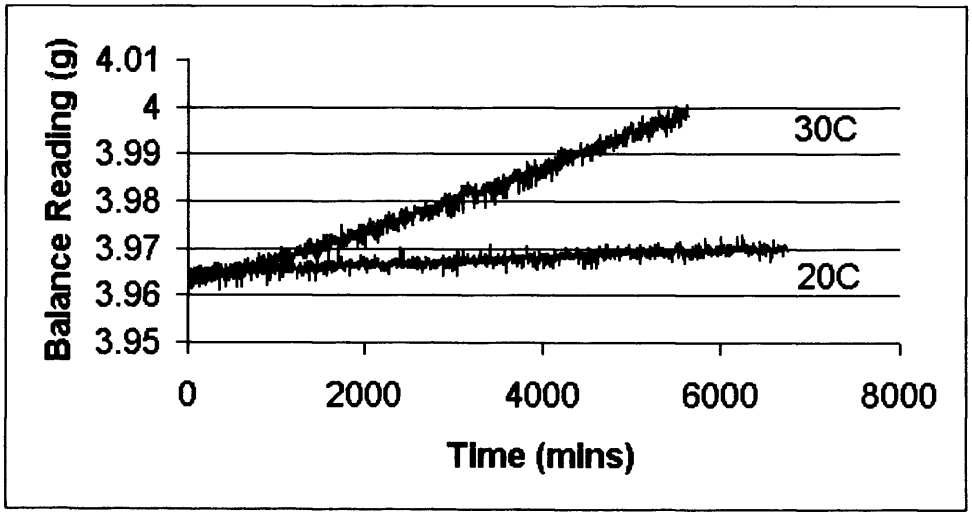

Figure 77. **Comparison of data for the corrosion of iron powder in the presence of ferrous chloride tetrahydrate at 22%RH at different temperatures (20°C and 30°C). The exponentially increased rate of reaction observed at the higher temperature is due to the combined effects of higher levels of available moisture and increased temperature (figure 17). The atmosphere contains twice the moisture (kg/kg dry air) at 30°C and 22%RH than it does at 20°C and 22%RH (figure 74).**

Note that each data set in figure 77 was plotted from the point where increase in weight (due to corrosion) exceeds any balance or dehydration contributions for comparative purposes.

6.9 *Sodium Chloride*

Turgoose (1982b) reported that the corrosion of iron in the presence of solid $FeCl_2.4H_2O$, i.e. below its deliquescence point, was unexpected. The corrosion of iron in the presence of NaCl (common salt) was not expected to occur below its deliquescence point (Chandler, 1966; Evans and Taylor, 1974) but this was tested to ensure that no corrosion takes place (rather than inappreciable corrosion).

The potential role of solid sodium chloride in the corrosion of iron at low relative humidities was investigated at 30%RH and 20 °C by mixing analar NaCl (BDH) with the same type of iron powder used for the other tests reported here (figure 78). As expected, $NaCl_{(s)}$ does not exhibit hygroscopicity leading to corrosion at this relative humidity (deliquescence is cited as 75-76%RH). Over a period of 15,000 minutes (250 hours or 10.4 days) there is no net weight gain. Visually, no colour change was observed. An initial minor downward weight trend (weight loss) is attributed to balance drift where no weight change occurs rather than a slow loss of adsorbed water which would have supported corrosion (appendix 1). This result supports Evans and Taylor (1974) and Chandler (1966) who reported a significant reduction in corrosion below the deliquescence point of sodium chloride and the lowering of corrosion rate below the critical humidity for any given deliquescent salt.

After a year and a half in a covered Petri dish, left on the open laboratory bench at ambient temperatures and humidities, no change in mass of the NaCl/Fe powder mixture or change in its appearance occurred (on 09/02/04 weight = 4.0922g, on 05/09/05 weight = 4.0917g). This test involved mixing solid phase components, whereas Evans and Taylor (1974) and Chandler (1966) immersed mild steel in sea water and then exposed them to test environments after merely shaking them. The parameters of time (length of study) and phase (solid or liquid) are likely to influence the interpretation of experimental results such as those demonstrated here.

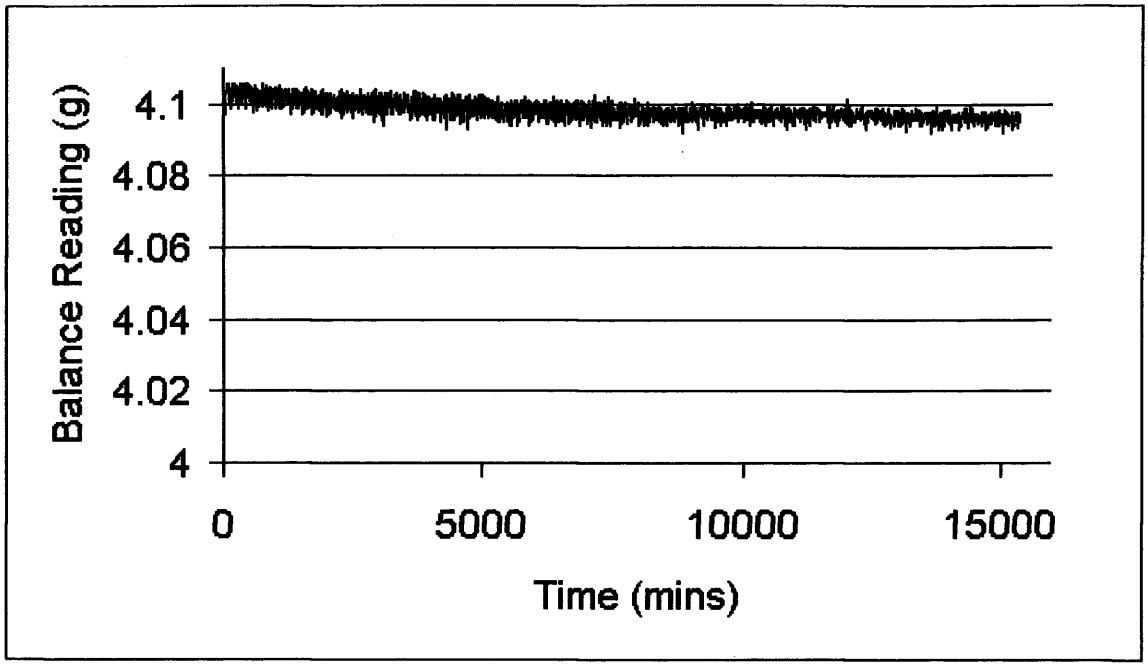

Figure 78. **Iron powder mixed with solid sodium chloride at 30%RH, 20°C.**

6.10 *Ferrous chloride tetrahydrate deliquescence*

Approximately 2.0000g of analar ferrous chloride tetrahydrate (BDH) was removed from its supplier's container and placed in a Petri dish in the climatic chamber with a set-point of 75%RH in order to observe the change in weight during deliquescence (figure 79). Deliquescence occurred and a golden brown liquid was formed at 75%RH (20°C).

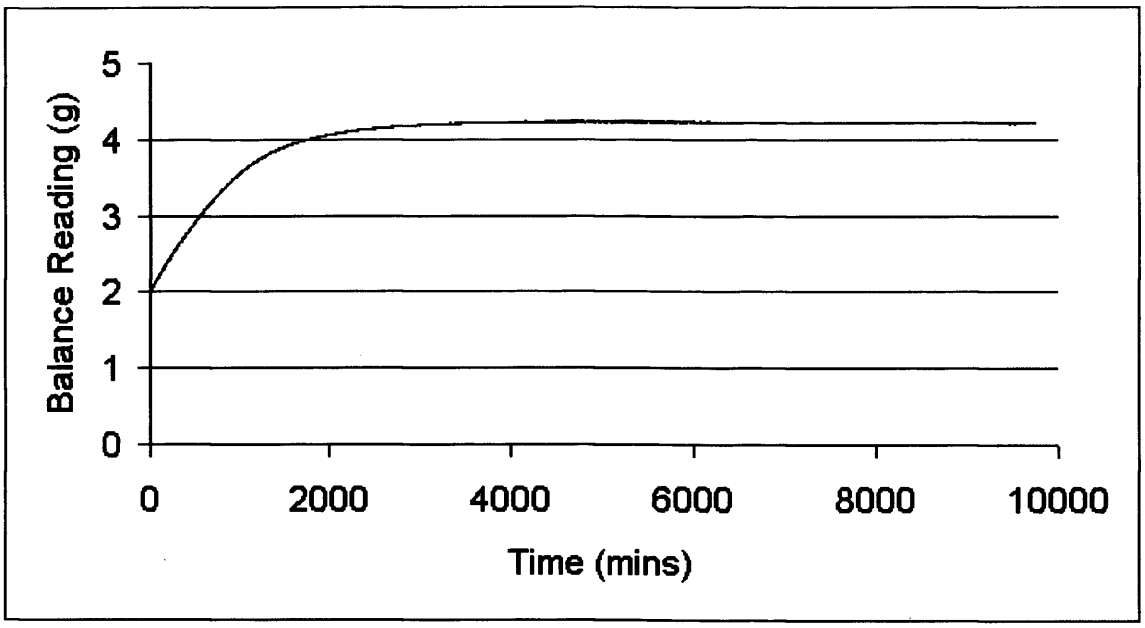

Figure 79. **2.0000g of solid ferrous chloride tetrahydrate exposed to a relative humidity set at 75%RH.**

Compare the data in figure 79 with that for a mixture of approximately 2.0000g of iron powder and 2.0000g of solid ferrous chloride tetrahydrate exposed to an environmental humidity of 65%RH and 20 °C (figure 80). Although the test set-point was maintained above the deliquescence point of 55.9%RH at 25 °C cited by Richardson and Malthus (1955) the mixture remained solid at 65%RH but did appear to be moist. Figures 85 and 86 illustrate that the uptake of water and any solid/liquid transformation is not instantaneous at a particular relative humidity for this system. There is no sudden uptake of water. The process is logarithmic with time and gradual above the deliquescence RH. This (monotonic) behaviour and differences in the apparent

observed weight of water adsorbed in figures 79 and 80 also agree with the fact that a saturated solution can hold more moisture, becoming more diluted, at higher relative humidities (Carlson, 1978 and see figures 5 and 6 of this thesis). The two sets of results (figures 79 and 80) show that in each case the salt and salt solution reached equilibrium with the environmental humidity.

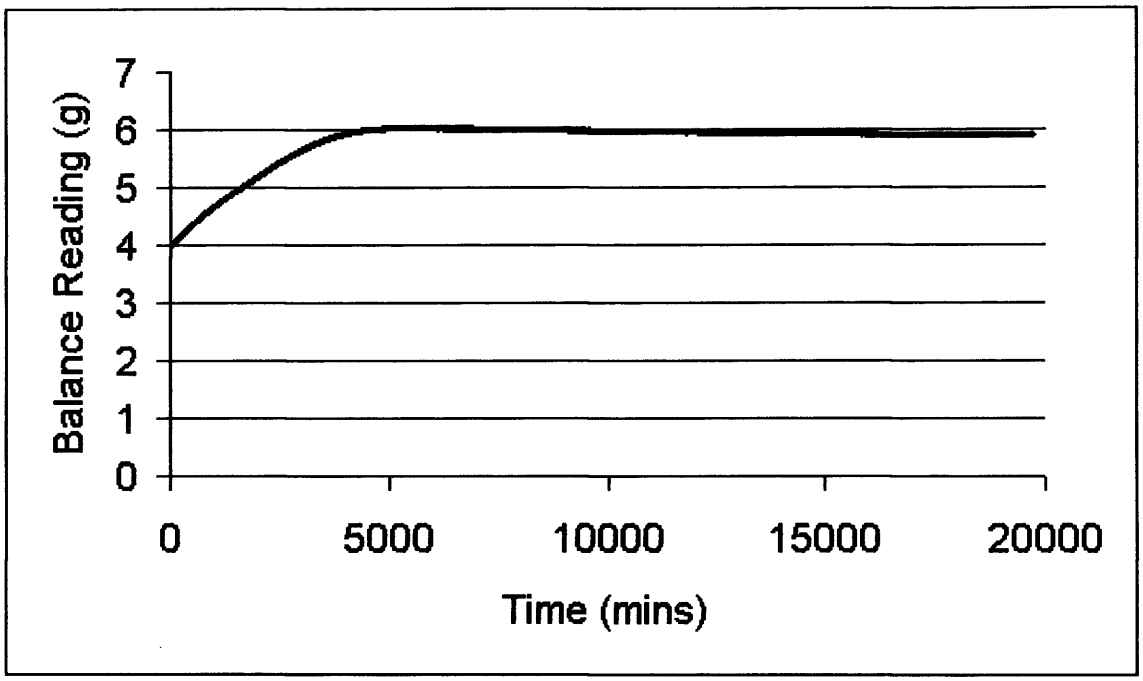

Figure 80. **Approximately 2.0000g of solid ferrous chloride tetrahydrate mixed with approximately 2.0000g of iron powder exposed to a relative humidity set at 65%RH.**

The upward trend levels off by 5,000 minutes (3.5 days) because all of the iron had oxidised to form βFeOOH (observed to have occurred via the green rust phase) by then, with no green rust remaining. A slight and constant downward trend after 5000 minutes (3.5 days) could be a result of balance drift or may reflect the changing composition of the mixture due to oxidation and its changing hygroscopicity as a result. A detailed study of this relationship over longer periods of time will be informative.

6.11 Modelling sudden environmental change

The experimental results reported here were collected to investigate the effect of sudden environmental change on ferrous chloride, βFeOOH and mixtures of these corrosion products with iron powder. The rates of adsorption and desorption of water and the rates of corrosion of iron in contact with these corrosion products upon sudden environmental change have relevance for opening a sealed, desiccated, Stewart™ box to examine the artefacts within and to environmental air conditioning failure in a building or supplying conditioned (dehumidified) air to the storage space in which chloride-contaminated wrought iron is stored.

Tests were conducted using the climatic chamber where the set-point relative humidity was cyclically changed in order to observe the response of different samples to environmental change. All of the tests reported in this section were conducted at 20°C. Balance effects (appendix 1), due to the vibration of the refrigeration plant of the climatic chamber during cooling of the condensation coil (to lower RH) and the absence of vibration when the refrigeration plant is off (to raise RH), were studied for cyclical set-point relative humidity climatic chamber tests. Periodic cessation of balance vibration due to the chamber refrigeration plant turning off and on for different set-points was expected to have an affect on the magnitude of the balance readings but not their direction. The results obtained support this statement and are considered to be indicative of genuine changes in mass and valid.

6.11.1. Ferrous chloride tetrahydrate hygroscopicity behaviour

Approximately 2.0000g of ferrous chloride tetrahydrate was placed in the climatic chamber with a set-point humidity of 15%RH (figure 81). After 48 hours at 15%RH the set point was changed to 65%RH for 6 hours before returning to 15%RH. The cycle was then repeated.

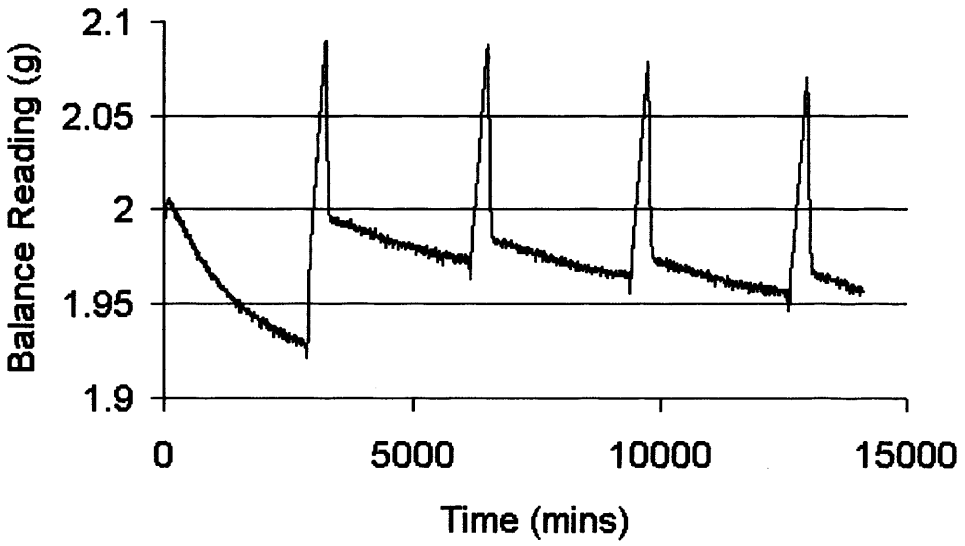

Figure 81. **Ferrous chloride tetrahydrate cycled between 15%RH (48 hours) and 65%RH (6 hours).**

The results in figure 81 suggest that the mixture shows initial dehydration of the ferrous chloride tetrahydrate at 15%RH. Rapid water adsorption occurs during periods at 65%RH, followed by water desorption upon return to 15%RH. The slowing of the dehydration at 15%RH after each 65%RH cycle suggests a level of hysteresis or indicates a balance phenomenon at play. In reality, surface morphology, especially corrosion layers, will play a significant role in determining the rate of uptake of water during short periods exposed at higher relative humidities. Whilst the results presented here suggest that water uptake will be rapid, water desorption and weight stabilisation occurs at a reasonable rate once the humidity is lowered.

6.11.2. Ferrous chloride tetrahydrate and iron powder

Approximately 2.0000g of ferrous chloride tetrahydrate and 2.0000g of iron powder were mixed and placed in the climatic chamber with set-point 15%RH (figure 82). After 48 hours at 15%RH the set-point was changed to 30%RH for 6 hours before returning to 15%RH. The cycle was then repeated.

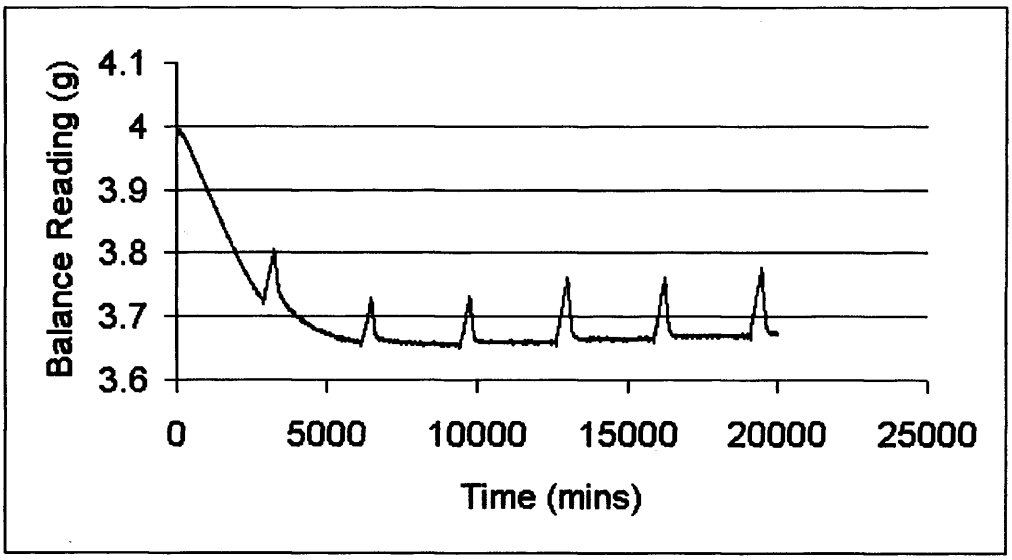

Figure 82. **Ferrous chloride tetrahydrate and iron powder cycled between 15%RH (48 hours) and 30%RH (6 hours).**

The results in figure 82 show initial dehydration of the ferrous chloride tetrahydrate at 15%RH. Rapid water adsorption is indicated during periods at 30%RH followed by water desorption upon return to 15%RH. The slight increase in the weight recorded by the balance at 15%RH after each 30%RH cycle may indicate a small amount of corrosion of the iron powder at 30%RH, which would form βFeOOH. An increased rate may be expected as βFeOOH is produced.

6.11.3. Unwashed βFeOOH and iron powder

Approximately 2.0000g of unwashed βFeOOH and 2.0000g of iron powder were mixed and placed in the climatic chamber with set-point 15%RH (figure 83). After 48 hours at 15%RH the set-point was changed to 30%RH for 6 hours before returning to 15%RH. The cycle was then repeated.

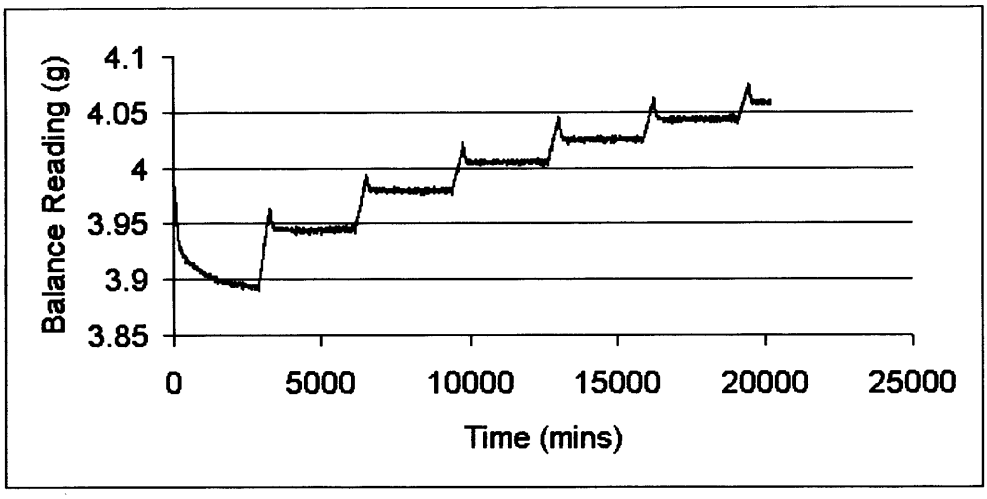

Figure 83. **Unwashed βFeOOH and iron powder cycled between 15%RH (48 hours) and 30%RH (6 hours).**

The results in figure 83 suggest that the mixture shows initial dehydration of the unwashed βFeOOH at 15%RH. Rapid water adsorption is indicated during periods at 30%RH followed by water desorption upon return to 15%RH. The significant increase in the weight of the sample at 15%RH following each 30%RH cycle indicates corrosion of the iron powder during periods exposed at 30%RH. Comparing this with figure 82 indicates that the contribution of unwashed βFeOOH to the corrosion of wrought iron would appear to be far greater that that of ferrous chloride under similar environmental conditions.

6.11.4. Ferrous chloride tetrahydrate and iron powder at higher humidities

Approximately 2.0000g of ferrous chloride tetrahydrate and 2.0000g of iron powder were mixed and placed in the climatic chamber with set-point 22%RH (figure 84). After 48 hours at 22%RH the set-point was changed to 65%RH for 6 hours before returning to 22%RH. The cycle was then repeated.

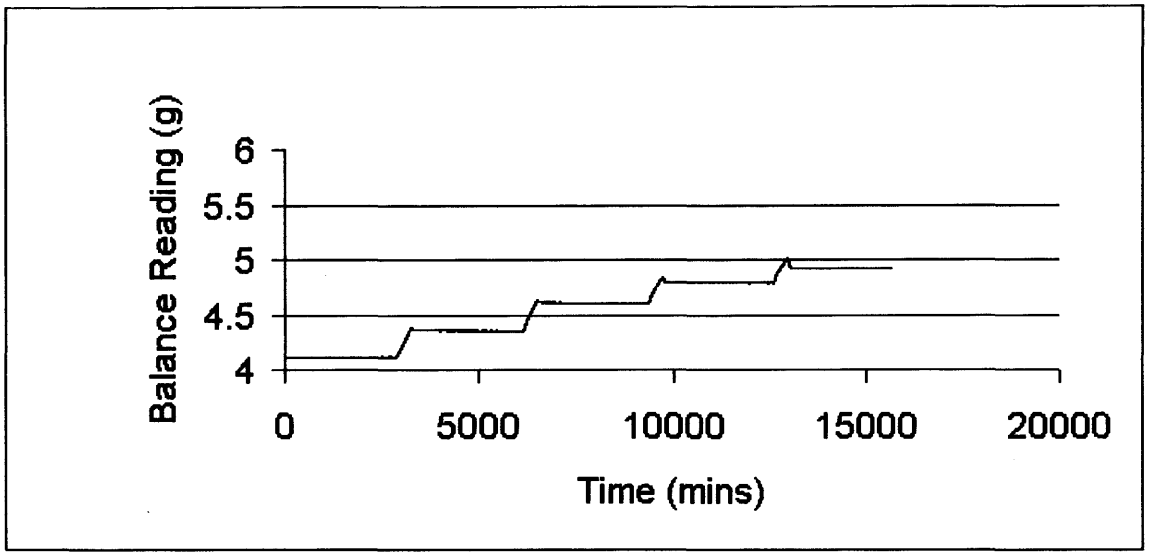

Figure 84. **Ferrous chloride tetrahydrate and iron powder cycled between 22%RH (48 hours) and 65%RH (6 hours).**

The results presented in figure 84 suggest that the mixture shows stability without initial dehydration of the ferrous chloride tetrahydrate at 22%RH. This compares well with the data presented in figure 48 for a similar period of time. Rapid water adsorption *and* corrosion is indicated during periods at 65%RH followed by a small level of water desorption *and* inappreciable corrosion upon return to 22%RH. The slight increase in the balance reading at 22%RH after each 65%RH cycle indicates an increase in weight due to a small amount of corrosion of the iron powder at 65%RH. The results suggest that corrosion slows, and becomes comparatively negligible, rapidly once the environment is returned to 22%RH, but this may indicate error in the cited set-point within the chamber itself which was experimentally determined as 22%RH±1%RH but

cited by the manufacturer as ±3%RH. These experimental results dictated the detailed consideration of potential balance effects on the data due to intermittent vibration during variable set point tests (appendix 2).

6.11.5. βFeOOH and iron powder at lower relative humidities

Approximately 2.0000g of unwashed βFeOOH and 2.0000g of iron powder were mixed and placed in the climatic chamber with a set-point of 15%RH (figure 85). After 48 hours at 15%RH the set-point was changed to 22%RH for 6 hours before returning to 15%RH. The cycle was then repeated.

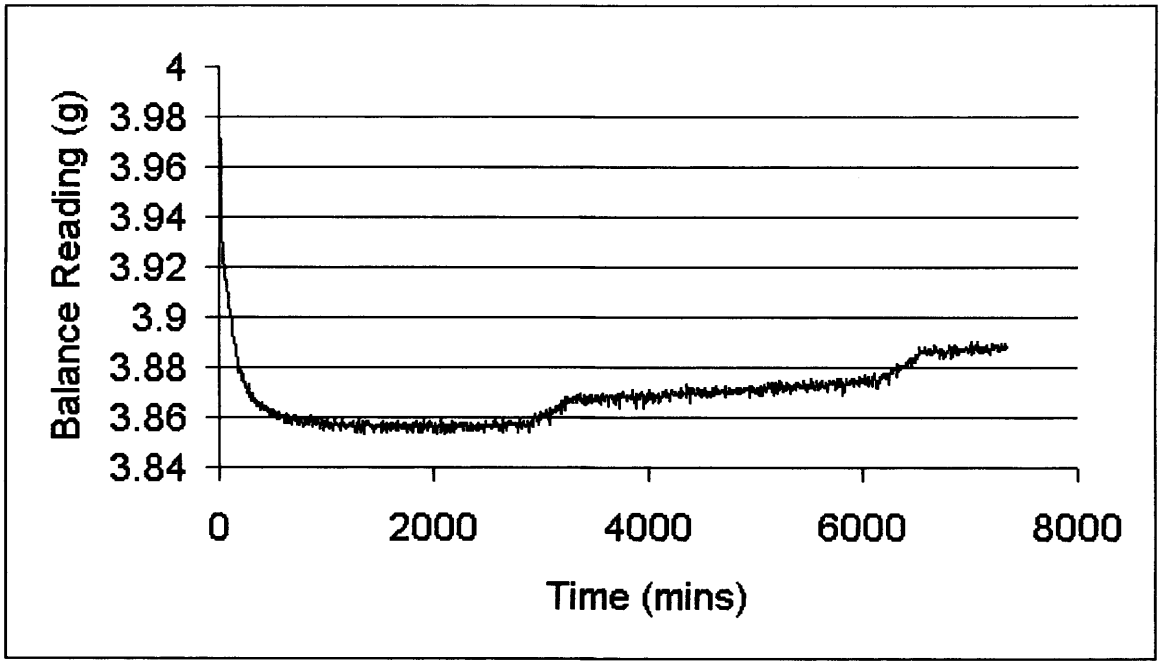

Figure 85. **Unwashed βFeOOH and iron powder cycled between 15%RH (48 hours) and 22%RH (6 hours).**

The results in figure 85 suggest that the mixture shows initial dehydration of the unwashed βFeOOH at 15%RH. Some water adsorption is indicated during periods at 22%RH followed by water desorption upon return to 15%RH but rather less than shown in figure 83. This result is logical. As expected, the level of water adsorption appears to be directly related to the difference in environmental relative humidity. The quantity of hygroscopically surface adsorbed water reaches equilibrium with the moisture in the

surrounding environment according to its vapour pressure. The small increase in the level of the balance reading at 15%RH after each 22%RH cycle indicates an increase in weight increase due to corrosion of the iron powder at 22%RH. Slow corrosion appears to be occurring, and outweighing any continued dehydration, between 3,000 and 6,000 minutes at 15%RH. This agrees with the results presented in figure 63.

6.11.6. Dehydration of a saturated solution of ferrous chloride

1.0002g of ferrous chloride tetrahydrate was placed in a desiccator at 92%RH maintained by a saturated solution of sodium carbonate until it had completely deliquesced to form a yellow solution weighing 2.6235g (an increase of 1.6233g or 162%) after two weeks [*c.f.* weight gains observed at 65%RH (figure 80) and 75%RH (figure 79) which broadly agree]. This Petri dish was then removed to the climatic chamber with an initial set-point of 75%RH. After 72 hours (and for each subsequent increment) the relative humidity within the chamber was then reduced to 70%RH, 60%RH, 50%RH and 20%RH before being allowed to return to 75%RH and then reduced to 70%RH once more (figure 86).

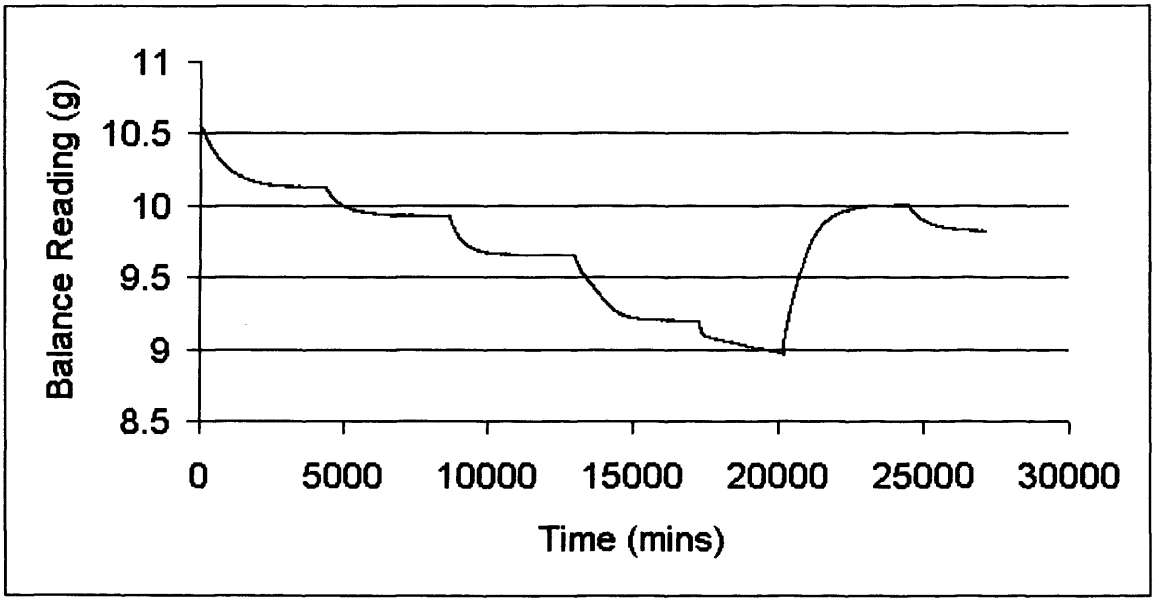

Figure 86. **Dehydration of a saturated solution of ferrous chloride sequentially from 92%RH to 75%RH, then 70%RH, 60%RH, 50%RH and 20%RH before returning to 75%RH and 70%RH again.**

The results in figure 86 show the relationship between deliquesced ferrous chloride and relative humidity at 20°C. Crystallisation is a gradual process, taking place in solution as concentration increases and water is lost from solution. The loss in weight due to evaporation is also gradual (and expectedly exponential). The shape of the curve during the 50%RH section is interesting and may indicate the loss of the last liquid water to evaporation and waters of hydration in the solid state. For decreasing humidities the solutions become supersaturated but this branch of the curve is influenced by nucleation phenomena and is not reproducible (Winkler & Junge, 1972: 622). Dehydration at 20%RH then represents loss of adsorbed water and probably water of hydration (water of crystallisation). Uptake of water and deliquescence is again rapid at 75%RH. The original deliquesced mass was not regained but some oxidation to βFeOOH had been observed and surface tension effects may also be significant. There is a hysteresis for adsorption and desorption. It will take longer for water to be lost from the hydrated/adsorbed/absorbed phases than initial uptake on the basis that deliquescence occurs at a higher relative humidity than crystallisation (Amorosso & Fassina, 1983). This gives a slight buffer in terms of time of exposure to higher relative humidity environments before deliquescence reoccurs and rapid electrochemical corrosion recommences.

6.11.7. The effect of washing βFeOOH until wash solutions are chloride free

The effect of washing βFeOOH was investigated by cycling the relative humidity in the climatic chamber between 22%RH and 65%RH (figure 87).

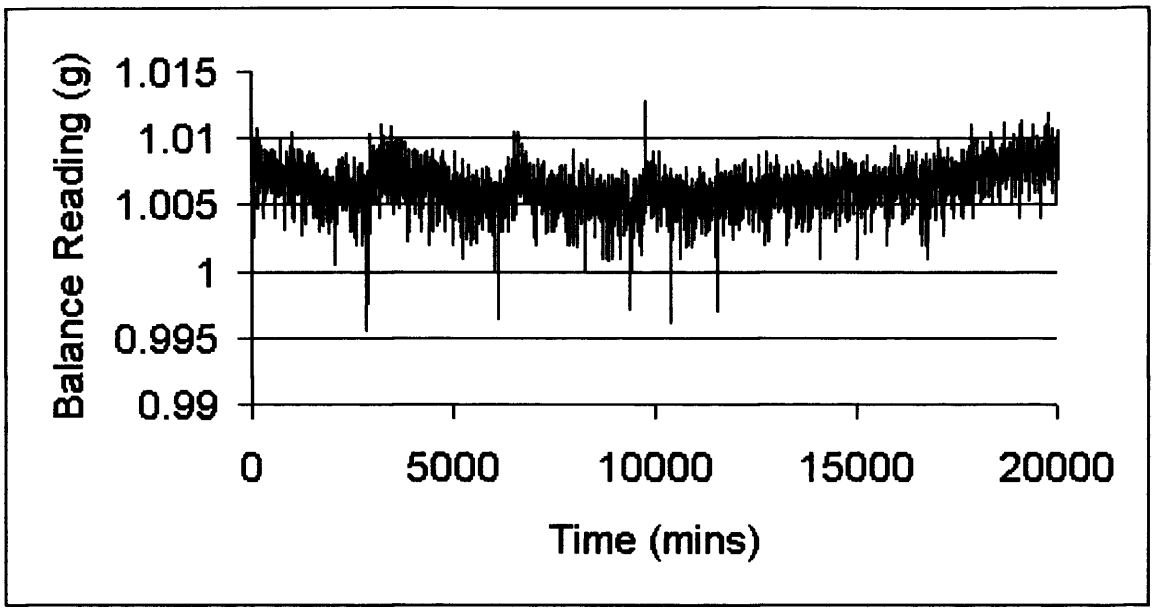

Figure 87. **Washed βFeOOH cycled between 22%RH and 65%RH to 10,000 minutes then set at 65%RH from 10,000-20,000 minutes.**

Note the high precision of the balance reading scale (as compared with other results presented) which is indicative of how small the observed changes in mass were during this experiment.

The effect of washing βFeOOH very greatly reduces its hygroscopic properties compared with unwashed (freshly prepared) βFeOOH (figures 83 and 85). Weight increase and decrease due to adsorption and desorption in figure 87 is so small that it is of a similar magnitude to the balance vibration after damping; which is the limit of the weight change that may be observed using this method over short periods of time. This results in the particularly high levels of "signal noise" for the data in figure 87 and accounts for its balance reading (g) scale at three decimal places. Any aqueous ferrous chloride (or HCl) will have been removed by aqueous Soxhlet washing (and possibly some of the βFeOOH transformed into other FeOOH polymorphs or magnetite). Hygroscopicity is demonstrated for washed βFeOOH but is of significantly lower magnitude and less significant than suggested for unwashed βFeOOH (figures 83 and 85).

7. Conclusions: The influence of atmospheric moisture on the corrosion of chloride-contaminated iron.

7.1 Comparing corrosion as a function of relative humidity

Table 6 and figure 88 allow comparison of selected experimental corrosion rate results from this research for iron powder mixed with different combinations of corrosion products at different relative humidities at 20°C. In each instance approximately 2.0000g of each reactant was present other than for the 19% relative humidity test (see caption, figure 42) where this is irrelevant to weight increase because none occurs. βFeOOH is unwashed for the data presented here.

Test Relative Humidity	Admixture	Increase in Mass over 4000 minutes
16%	Fe + Ferrous chloride	0.000g
16%	βFeOOH + Fe powder	0.005g
19%	Fe + Ferrous chloride	0.000g
20%	βFeOOH + Fe powder + Ferrous chloride	0.011g
21%	βFeOOH + Fe powder	0.016g
22%	Fe + Ferrous chloride	0.002g
25%	Fe + Ferrous chloride	0.004g
25%	βFeOOH + Fe powder	0.065g
27.50%	Fe + Ferrous chloride	0.011g
30%	Fe + Ferrous chloride	0.045g
35%	Fe + Ferrous chloride	0.081g

Table 6. **Comparative summary of results of selected corrosion tests.**

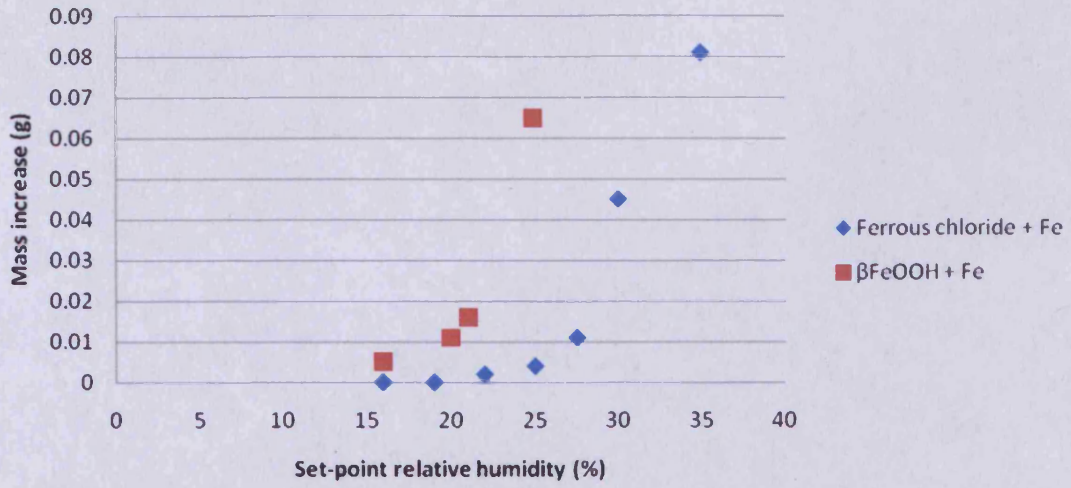

Figure 88. **Comparative summary of selected corrosion tests from data presented in table 6.**

The data in figure 88 is not presented as quantitative for corrosion but as indicative of corrosivity and rate. The following observations may be made:

- The concept of a threshold relative humidity for the stability of $FeCl_2.2H_2O$ between 20% and 22% relative humidity at 20°C is shown by the small increase in mass at 22% relative humidity and a nil increase in mass at 19% and 16% relative humidity because iron in contact with $FeCl_2.2H_2O$ at 20°C does not corrode (see also the results presented in sections 6.1.1. and 6.4).

- Unwashed laboratory-produced βFeOOH causes iron corrosion each time it is present above 12%RH (see also results section 6.5.3.).

- Corrosion rate is determined by the amount of atmospheric moisture for a given temperature for iron powder in contact with both $FeCl_2.4H_2O$ and βFeOOH.

- The rate of corrosion of iron powder in the presence of unwashed laboratory-produced βFeOOH at 20% and 21% relative humidity is comparable to the rate of corrosion of iron powder in the presence of $FeCl_2.4H_2O$ alone at around 27.5% relative humidity. However, the rate of corrosion of iron powder in the presence of unwashed laboratory-produced βFeOOH at 20% and 21% relative humidity is far

lower than in the presence of $FeCl_2.4H_2O$ alone at relative humidities above 30% relative humidity. Desiccation or dehumidification is beneficial because it slows both processes.

Thickett (2005) independently studied the behaviour of 3mg samples of ferrous chloride mixed with iron powder at different relative humidities. Glycerol solutions were used to control the relative humidity in small jars. The relative humidities of sealed environments controlled by glycerol solutions are not as temperature-sensitive as those above saturated salt solutions. Corrosion resulting in βFeOOH was confirmed analytically and quantified using FTIR (in transmittance through KBr disks) or using Raman spectroscopy to double check if none was identified by FTIR. Deliquescence was observed between 58%RH and 65%RH in a refrigerated oxygen-free enclosure, depending on temperature [Wang (2007b) reported deliquescence of ferrous chloride tetrahydrate on iron foil at 54%RH within a month of exposure but used saturated salt solutions for her experimental programme]. No corrosion was observed at relative humidities below 20%RH in agreement with the experimental results reported in this thesis. Between 20%RH and 30%RH *"minor"* corrosion was observed. A big increase in corrosion was reported between 30%RH and 35%RH leading Thickett (*ibid.*) to conclude that a sensible threshold relative humidity for the storage of chloride-contaminated wrought iron lies at 30%RH (Thickett, 2005 and 2008).

For unstable archaeological iron *"Keeping the air dry, below 30 per cent relative humidity, will almost stop the reaction"* (Thickett, 2008b: 17; see also Thickett, 2008a: 98). Thickett (2008a: 98) recognises that *"some archaeological iron is sensitive to RHs above 16%..."* and this has also been demonstrated (for iron in the presence of unwashed βFeOOH) by this study where corrosion also occurred at 15%RH (section 6.5.3., figure 63). Wang (2007b) reported that *"pitting was hardly observed"* on iron foil in the intimate presence of ferrous chloride tetrahydrate after one year at 33%RH and concluded that *"these findings indicate that keeping iron at RH levels below 35%RH can slow deterioration significantly"*. Wang (*ibid.*: 65) reported that akaganéite was formed on ferrous chloride tetrahydrate on iron foil after one year at 23%RH, but that pitting

was not observed on the foil. After three months, pitting was observed on the iron foil exposed at 44%RH.

Thickett's (2005) independent results confirm those obtained in this study using the Votsch VC 4018™ climatic chamber. Thickett's (*ibid.*) rapid increase in corrosion of iron powder in the presence of ferrous chloride [tetrahydrate] above 30%RH is confirmed by the data reported here in figures 49, 88 and schematically in figure 91. This data was published prior to the Thickett (2005) data becoming available (Watkinson and Lewis, 2004). Whilst Thickett's work correctly identifies the rapid increase in corrosion above 30%RH, the data reported here confirms that (i) corrosion continues to occur below this value and that (ii) the decrease in rate is sigmoidal about ~30%RH. The rate and amount of corrosion at 27.5%RH is nearly one quarter of that at 30%RH and corrosion at 25%RH is nearly 1/8 that at 30%RH. Desiccation or dehumidification of chloride-contaminated wrought iron to relative humidities lower than 30%RH will be advantageous in the short term. Dehumidification or desiccation to a relative humidity below 21%±2%RH is necessary to prevent βFeOOH formation through the oxidation of solid ferrous chloride and further iron corrosion as a result.

7.2 βFeOOH and wrought iron

The corrosion of chloride-contaminated wrought iron is complex and involves a large number of corrosion reactions, which together produce the overall corrosion rate. At high relative humidity values it is chloride ion solutions that provide the major contribution to the corrosion rate, which will be fast. In contrast, at relative humidity values of 20% and below iron chloride solutions will crystallise to produce solid $FeCl_2.2H_2O$. Tests have shown that this corrosion product mixed with iron powder does not cause the iron to corrode at 20°C. Dehydrating chloride-contaminated wrought iron to 21%±2%RH or less at 20°C will prevent ferrous chloride solutions contributing to the corrosion of the iron.

βFeOOH is formed through the aerial oxidation of damp $FeCl_2.4H_2O$ or as a product from the electrolytic corrosion of iron in chloride-rich environments. Whereas $FeCl_2.4H_2O$ undergoes slow aerial oxidation to βFeOOH, which can potentially contribute to further corrosion of the iron, $FeCl_2.2H_2O$ does not (Knight, 1997: 38). Desiccation to a relative humidity beneath the established threshold humidity for $FeCl_2.2H_2O$ stability will prevent the formation of fresh βFeOOH from either ferrous chloride solutions or solid $FeCl_2.4H_2O$, which might be present. This would significantly enhance the stability of the remaining metallic iron.

Past corrosion in the presence of high concentrations of chloride ions means that βFeOOH has already formed on much chloride-contaminated wrought iron (Figures 3, 12-15 and 32) and will attract water which could promote ongoing corrosion or provide suitable conditions for the conversion of the βFeOOH to other iron oxyhydroxide polymorphs, releasing its bound chloride in the process. The release of the previously lattice-bound chloride ions will enable aggressive, chloride counter-ion driven, hydrolysis of ferrous ions producing a highly acidic environment in which electrochemical corrosion will proceed. This could potentially occur cyclically. α-FeOOH, γ-FeOOH and other oxide/oxide-hydroxide polymorphs will also be present and adsorb water. Ishikawa *et al.* (1992a) report that the relative permitted number of

water molecules adsorbed on γ-FeOOH is 3.5 times higher than for α-FeOOH or β-FeOOH, citing entropy values of

Polymorph	Entropy value
α-FeOOH	-3.2 $JK^{-1}cm^{-2}$
β-FeOOH	-3.8 $JK^{-1}cm^{-2}$
γ-FeOOH	-0.59 $JK^{-1}cm^{-2}$

Table 7. Water adsorption entropy values for different iron oxyhydroxide polymorphs (after Ishikawa *et al.*, 1992a).

Physisorption of water occurs by a double hydrogen-bond in the first layer (Kaneko 1975 and 1979; Ishikawa *et al.*, 1992a). The second layer is mobile but the next few layers of adsorbed water form an ice-like formation (*ibid.*). Ardizzone *et al.* (1983) also demonstrated that, unlike αFe_2O_3, αFeOOH and γFeOOH, magnetite shows significant (but slow, pH dependent) adsorption of chloride anions.

Because α and γ polymorphs do not **cyclically** promote corrosion in the ways proposed for the chloride-bearing ferrous chloride or βFeOOH they need not be considered in detail here other than to note their hygroscopic nature – their ability to attract water – and the ability of magnetite to adsorb chloride anions, both of which will promote ongoing electrolytic corrosion. Thickett and Odlyha (2007) reported that damp archaeological iron raised the moisture content of silica gel to over 40% in the first three weeks and, through further monitoring, concluded that the iron originally held approximately 1.5% of its own weight as water. Chandler and Stanners (1963: 328) reported the weight of moisture in an air-formed rust as 6% by weight (compared with 85%wt $Fe_2O_3.H_2O$ and 4%wt sulphate) and they reported the weight of moisture lost during heating rust, giving an indication of the ability of other corrosion products to provide water for ongoing corrosion at ambient relative humidities (table 8).

Temperature (°C)	Loss in weight of sample (%)		
100	4.9	5.5	4.1
110-130	1.2	1.0	4.1
130-150	1.3	1.1	0.8

Table 8. **Weight of moisture lost during the heating of rust. After Chandler and Stanners (1963: 328, *table 2*)**

Weight loss on heating reported by Chandler and Stanners (1963), and reproduced in table 8, compares well with weight loss of 6.46%wt for an archaeological nail with a remaining metal core and 4.75%wt for a lump of mineralised iron (Heated at 70°C for 1.5 months after previous ambient indoor storage) measured by Wiltshire (1982). Wiltshire's (*ibid.*) results suggest hygroscopicity in both cases but with increased water absorption in the case of chloride-contaminated iron (where a metal core remains and holds chloride ions as a counter ion). Wiltshire's (*ibid.*) reported increased water adsorption in the presence of chlorides agrees with the greater adsorption and desorption of water for unwashed βFeOOH than for washed βFeOOH observed in this study (section 6.11.7.).

βFeOOH may be present on chloride-contaminated wrought iron in 2 forms:

i. freshly formed βFeOOH, which will have a lot of adsorbed surface chloride (this adsorbed chloride would be mobile in water as $Cl^-_{(aq)}$ and/or HCl),
ii. long-lived βFeOOH which may have been rain-washed or laboratory-washed. Although βFeOOH is insoluble, this process will probably have removed some of the mobile chloride on its surface.

It is feasible that some of the surface adsorbed chloride will be volatile and this chloride may be lost to the environment (section 6.5.5.). Rain-wash or aqueous washing of the βFeOOH could reduce its potency as a corrosion accelerator by freeing its adsorbed surface chloride, to be washed away. However, surface tension, especially deep within

corrosion product cracks and micro capillaries will help to retain chlorides. Where present in a counter-ion capacity the chloride will not be lost.

The βFeOOH synthesised for the tests here was of type (i) and has been termed "unwashed". Unwashed laboratory-produced βFeOOH will have chloride concentrations greatly in excess of those required to occupy the tunnels of the βFeOOH formed because the chloride content of the mixture used is in excess of the iron present. The Petri dish method of βFeOOH production is a closed system, so excess chloride not utilised in βFeOOH formation will remain as adsorbed chloride ($Cl^-_{(aq)}$ and/or HCl). Post-production assay by XRD showed the presence of βFeOOH, but no crystalline iron chloride was detected (appendix 3). This type of βFeOOH has the potential to be particularly aggressive and produce more corrosion than an equivalent amount of washed βFeOOH due to the chloride on its surface which is available to produce a conducting electrolyte (and/or HCl) for corrosion.

According to Cornell & Schwertmann (1996: 19) the amount of chloride within, and adsorbed on, βFeOOH can vary between about 0.5mmol per mol and 7mmol per mol. North and Pearson (1975: 175) cite 10% by weight Cl^- within wrought iron objects recovered from the sea, Gilberg & Seeley (1981) cite 2%wt to 6.5%wt, North (1982) cites chloride contents of 2-3% in the solid βFeOOH after washing, Stahl *et al.* (2003) indicate 5.6%wt Cl^- bound within the βFeOOH structure, Réguer *et al.* (2007) cite $8\%_{mass}$ Cl^-, Thickett (pers. comm.) reported 12% by weight and Al-Zahrani (1999) reported chloride levels as high as 13%wt although his average for six washed laboratory-synthesised samples was 4.5%w/w ±0.12% (See also Watkinson & Al-Zahrani, 2008). Keller (1970) prepared synthetic βFeOOH with chloride ion contents of 2.3 to 6.4%wt. A sample of βFeOOH synthesised for this study was cold washed and another was Soxhlet washed in order to examine their chloride content, to examine the effect of aqueous washing on βFeOOH in this way, and to produce samples of washed βFeOOH for the hygroscopicity and corrosion tests. Figures 89 and 90 show progressive chloride extraction, wash by wash.

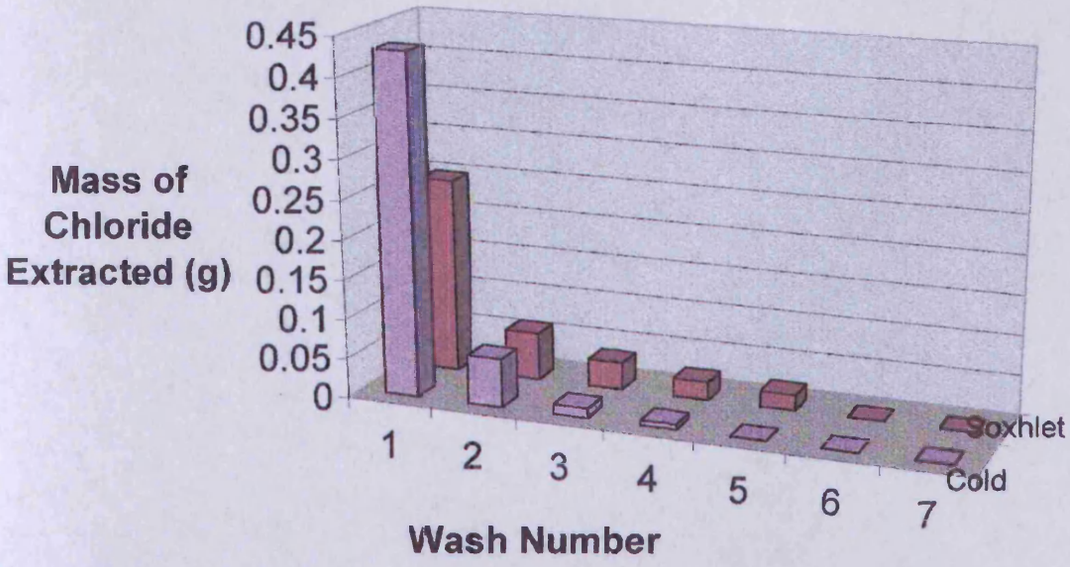

Figure 89. Comparative chloride extraction data for cold and Soxhlet washed βFeOOH expressed as mass of chloride extracted per wash.

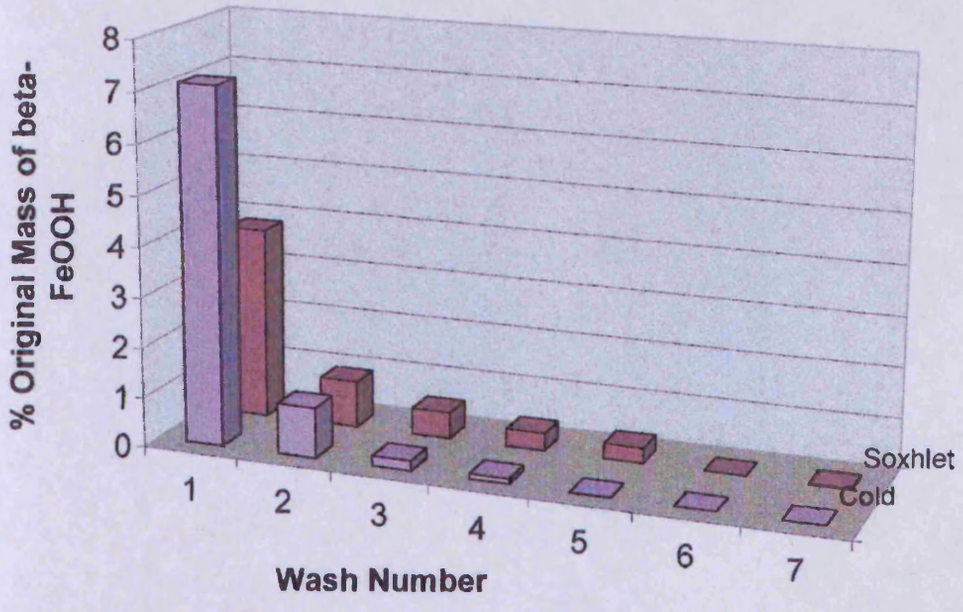

Figure 90. Comparative chloride extraction data for cold and Soxhlet washed βFeOOH expressed as the amount of chloride extracted per wash as a percentage of the original mass of the laboratory-synthesised βFeOOH.

The initial apparent comparative success of cold washing compared wash number by wash number with hot, Soxhlet, washing in figures 89 and 90 should be ignored because the volume of Soxhlet wash water was much smaller than the volume of water used for each cold wash. Watkinson and Al-Zahrani (2008: 83) note that it is labile chloride that is removed from the βFeOOH in non-alkaline washes. Variation in the amount of labile chloride in each sample here (figures 89 and 90) is apparent when the sum of chloride removed over all seven washes is calculated for each wash method.

It is expected that some βFeOOH will be more aggressive than other βFeOOH, according to its chloride content. Tests conducted here (section 6.5.5.) support a model where at least a significant amount of the adsorbed chloride is aqueous in the presence of atmospheric moisture and volatilises, possibly as (dilute aqueous) hydrochloric acid (HCl).

βFeOOH not washed after synthesis (as used here) can be paralleled with the initial formation of βFeOOH from iron chloride solutions on chloride-contaminated wrought iron. Adsorbed chloride on newly formed βFeOOH will be mobile and contribute to corrosion. A large volume of wrought iron relative to the amount of mobile chloride on the metal surface will nevertheless be adversely affected by the acid regeneration cycle and labile chloride. Mobile chloride may come into contact with anodic metallic iron and oxidise to form βFeOOH (figure 12). Whilst some chloride will be attracted back to the metal surfaces and retained as counter ions accelerating ongoing corrosion, some could volatilise. Any chloride bound as counter ions will be firmly retained.

Using unwashed laboratory synthesised βFeOOH can be considered as a worst case scenario for the contribution of βFeOOH (and adsorbed chloride) to corrosion of chloride-contaminated wrought iron. The claimed long-term [ambient, dry] metastability of washed βFeOOH and its capacity to release internally bound chloride on breakdown may be questioned (section 2.8.5.). The corrosion threat posed by any washed βFeOOH on chloride-contaminated wrought iron is likely to be limited, and insignificant, as compared with corrosion sustained by labile chloride ($Cl^-_{(aq)}$ and/or HCl)

associated with βFeOOH where unwashed (sections 6.5.2. & 6.5.3.). Aqueous washing of chloride-contaminated wrought iron will enhance its preservation by removing labile, surface adsorbed chlorides. This agrees with Keene (1991) and Keene & Orton (1985) who reported that objects that had been treated by aqueous washing techniques fared better than those that had not during long-term museum storage.

7.2.1. Synergistic effects

Other, synergistic, relationships are anticipated (see sections 2.8 and 2.9). Kaneko (1989) and other workers showed that akaganéite (βFeOOH) has great affinity for chemisorption of atmospheric gases, including sulphur dioxide that can be converted to sulphuric acid by reaction with atmospheric water molecules (Kaneko & Inouye, 1981 and 1984; Kaneko, 1989; Waqif *et al.*, 1992). The chemisorbed sulphur dioxide and any resultant sulphuric acid are likely to accelerate corrosion of any associated metallic iron. The amount of chemisorbed sulphur dioxide depends upon the number of chloride-occupied sites on the surface of the βFeOOH (Ishikawa and Inouye, 1975). The results of this programme of research provide a basis for the future study of various synergistic relationships and their effects on corrosion rate.

7.3 Implications drawn from, and recommendations based upon, variable relative humidity set-point moisture adsorption/desorption behaviour

The results from variable set-point tests show that water adsorption is rapid and can reactivate corrosion during brief (6 hour) periods at a higher relative humidity (section 6.11). Water desorption is less rapid but corrosion appears to cease or slow reasonably quickly once environmental equilibrium at the lower relative humidity is regained. Fortunately, RH exchange in a building can be slowed by closing doors and windows and limiting access whilst any problems with air conditioning are rectified. Temperature will be slow to change in heavily built structures that are well insulated.

Thickett and Odlyha (2007) found that the time taken for the environment within a silica gel conditioned Stewart™ box to reach 16%RH was between 4 and 8 days in agreement with data proposed by Thomson (1977), Weintraub (2002) and Tetrault (2005). The results of this study suggest that artefacts in Stewart™ or other sealed boxes should be placed at the bottom of the boxes within pierced bags, beneath crumpled acid free tissue paper and, importantly, beneath the silica gel desiccant that requires regular regeneration. Any ingress of moisture into the Stewart™ box through a leaky lid will reach the absorbent gel before the artefacts and the gel can be quickly removed and replaced without disturbing the artefacts (without removing them from the box to the environment at large). The lid should be placed back on the box whilst the desiccant is being replaced. This is relevant because Thickett and Odlyha (*ibid.*) reported that approximately 75% of the air exchange between a sealed Stewart™ box and the environment occurs through the lid seal. Furthermore, water vapour is lighter than air so, in the event of any stratification of vapour within the box, the gel would be best placed at the top of the box and the artefacts beneath. However, moisture content differences are likely to average out quickly because the diffusion coefficient of water vapour in air is twice that of oxygen or nitrogen (Brown, 1994: 41). The packaging and support of the objects should be such that the weight of the silica gel presents no danger to them. The granular or bead forms of silica gel will not exert point pressure on the artefacts if placed loosely in large enough bags.

7.4 The influence of atmospheric moisture on the corrosion of chloride-contaminated wrought iron - Conclusions from this programme of research

It is clear from corrosion studies and the body of evidence from the tests reported in this work that corrosion rate varies according to a very wide range of factors. All efforts at corrosion prevention aim to significantly reduce corrosion rate or, less realistically, totally prevent corrosion. Attaining these goals is heavily influenced by the nature of the material in question, as well as environmental parameters. For archaeological conservation the stated conservation goal is to retain corrosion layers both for ethical reasons, and often because of the significant conversion of the original artefact to corrosion product. This means that interest lies in the microclimate created at the interface between the hard thick corrosion layer (DPL) and the wrought iron core of the object. It is here that corrosion will occur and fresh, voluminous, products will form. These products will not form a continuous layer that builds to produce a barrier to reduce moisture and oxygen ingress, as often occurs on iron in the atmosphere. In effect this barrier already exists as the outer corrosion layer, but it is cracked and defective and allows oxygen and moisture access to the metal surface. This illustrates why the tests carried out in this study are reasonable simulations of what will occur at the metal/DPL interface.

This study confirms that atmospheric moisture has a pronounced affect on the corrosion rate of chloride-contaminated iron and offers a new and detailed account of the activity of corrosion processes in relation to the moisture content of the atmosphere. Controlling moisture levels will contribute to preservation and it is important to examine the extent to which this could contribute to reducing corrosion rate. Primarily this study showed that reducing the moisture content of the ambient atmosphere can produce very significant reductions in corrosion rate of iron/chloride/chloride-bearing corrosion systems. Furthermore, it identified the influence of particular relative humidities on corrosion rate.

The corrosion process for chloride-contaminated wrought iron has been identified as consisting of a number of reactions that contribute towards the overall corrosion rate:

- Corrosion in high relative humidities – above the deliquescence point of ferrous chloride – where chlorides are in solution and solid iron chlorides have dissolved. Generally the wetter the surface of the metal and the greater the concentration of chloride (electrolyte) the faster the corrosion rate. The corrosion of the iron by the electrolyte solution will be the major contributor to corrosion rate.

- Corrosion over the stability field for $FeCl_2.4H_2O$ at 20°C (currently thought to be in the region of 50% relative humidity and 21%±2% relative humidity as determined by this study). As in higher humidities, oxidation may produce fresh β-FeOOH, which may then contribute towards the corrosion process. Corrosion is much slower at these relative humidities as compared to above the deliquescence point. This is because the major contribution to corrosion rate (that was provided by the large volume of chloride bearing electrolyte) is no longer present.

- The contribution of $FeCl_2.4H_2O$ to the corrosion process ceases when it converts to $FeCl_2.2H_2O$ at low humidities (20% relative humidity and below) at 20°C. In the absence of β-FeOOH that contains mobile surface chloride, corrosion would then cease. The presence of β-FeOOH in its chloride-rich form will allow corrosion to continue below 20%RH. Below 20%RH the corrosion rate will be reduced as the β-FeOOH provides the only reaction contributing to corrosion within the chloride corrosion model examined here.

Further observations can be made on corrosion rate that illustrate just how much the corrosion rate can be reduced by lowering relative humidity to the point where $FeCl_2.2H_2O$ is the stable form of chloride (see figure 88) and these are presented schematically in figure 91.

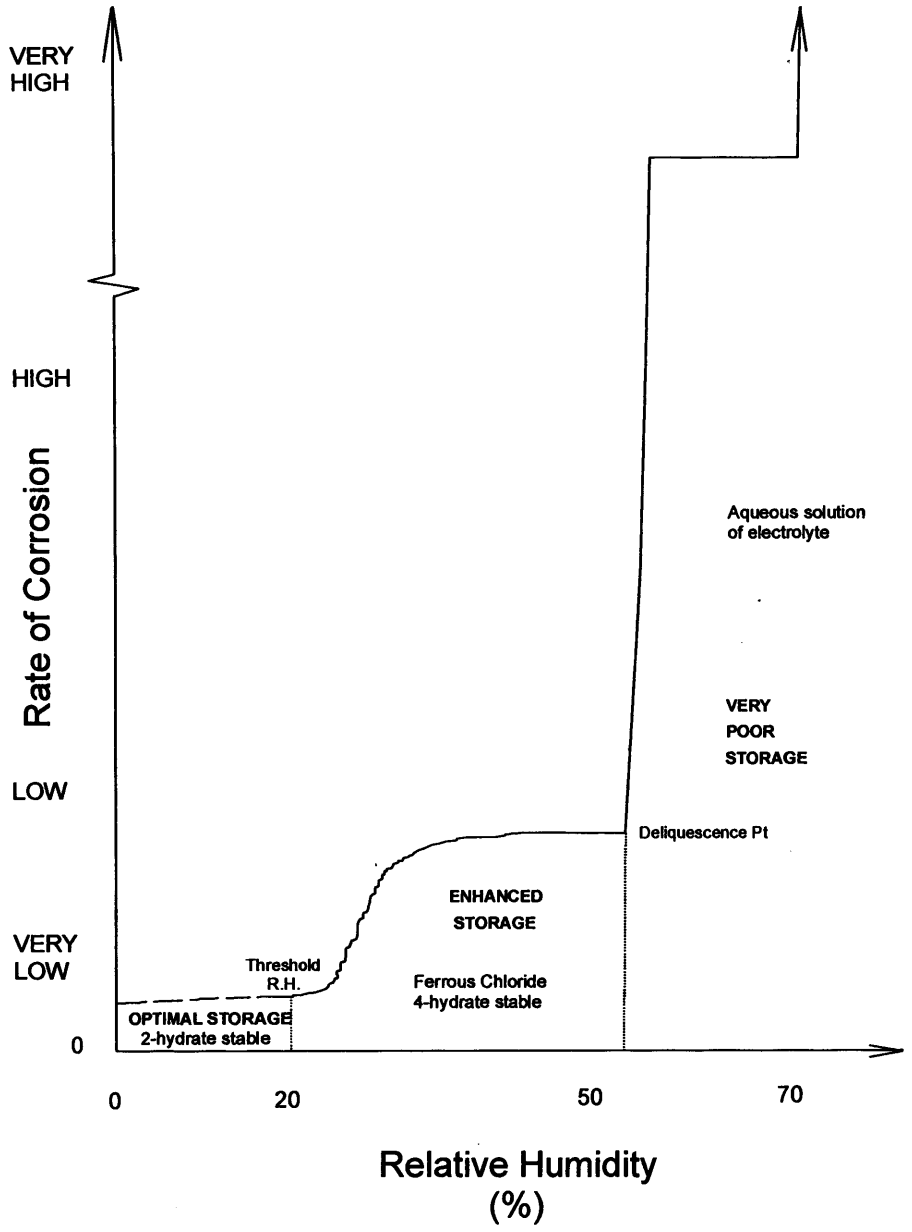

Figure 91. **Schematic diagram showing relative corrosion rates against environmental relative humidity (See Watkinson and Lewis, 2004). This diagram incorporates data from this report generated at 20°C (see figures 36, 48, 49 and 88) and Chandler (1966: *figure 1*).**

The change in corrosion activity caused by varying relative humidity for the chloride/iron system can be represented on a schematic diagram (figure 91), which presents the results from this study (published in Watkinson and Lewis, 2004: 99, *fig. 11*) and the work of Chandler (1966). Figure 91 represents the pragmatic outcome and summary of the results of this study and may be used to inform the preservation of

chloride-contaminated wrought iron. It is also relevant to the deterioration of meteoric iron in geology collections where chloride contamination is the cause.

Figure 91 provides a management tool that may be used by the conservation profession to perform cost benefit analyses based upon corrosion rate and environmental control costs (Watkinson & Lewis, 2004; Watkinson *et al.*, 2006; Watkinson and Tanner, 2008). Figure 91 shows that the rate of corrosion above the deliquescence point of ferrous chloride (which produces a highly conducting electrolyte solution of ferrous and chloride ions) is significantly higher than at any relative humidity below this point. Workers in the 1960s and early 1970s described corrosion rates beneath the deliquescence point of salts such as ferrous chloride as *"inappreciable"* (Chandler, 1966). In comparison to the rate of corrosion above the iron chloride deliquescence point, corrosion below it could be described as *"relatively inappreciable"*. Chandler's work (1966) is of value in estimating the likely increased rate of corrosion at relative humidities above the deliquescence point of ferrous chloride even though he studied the effects of NaCl in his work. Corrosion of iron above the iron chloride deliquescence point is likely to be between, or in **excess** of, 4 to 10 times greater than corrosion of iron below the deliquescence point, depending on salt concentration (Chandler, 1966: *fig. 1*).

Beneath the deliquescence relative humidity for ferrous chloride, where the rate of corrosion is governed by the additive contributions of $FeCl_2.4H_2O$ and the βFeOOH it produces, the rate of corrosion induced by the presence of $FeCl_2.4H_2O$ alone is less than that induced by unwashed βFeOOH alone. This was shown for all humidities in the range between the stability threshold humidity and the deliquescence point of ferrous chloride (figure 88). The contribution of $FeCl_2.4H_2O$ to iron corrosion through its stability range (see figure 88) is proportional to the relative humidity of its environment (see also figures 36, 48 & 49). Corrosion of iron powder in the presence of $FeCl_2.4H_2O$ takes place (initially) about ***forty*** times faster at 35% relative humidity than at 22% relative humidity. No accelerated iron corrosion takes place in the presence of $FeCl_2.2H_2O$ alone at 20°C.

Beneath the threshold relative humidity for the corrosion of iron in the presence of ferrous chloride only βFeOOH contributes to corrosion. Compared to the rates of corrosion at relative humidities where $FeCl_2.4H_2O$ is stable, corrosion at relative humidities where $FeCl_2.2H_2O$ is stable will be minimal at 20°C.

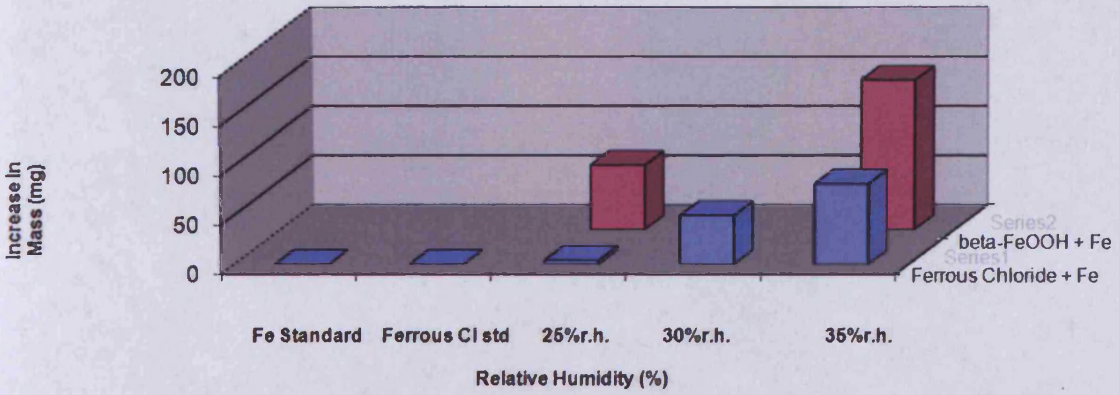

Figure 92. **A comparison of the relative levels of weight increase of iron (indicative of corrosion and moisture adsorption) in the presence of ferrous chloride tetrahydrate and in the presence of unwashed βFeOOH after 3 days at different relative humidities at 20°C.**

The contribution of βFeOOH to iron corrosion at low relative humidities (i.e. where $FeCl_2.2H_2O$ is stable ferrous chloride phase; below 22%RH), requires further examination but initial weight for weight results reported here (figure 88) suggest that it is ***much less significant*** than the contribution of $FeCl_2.4H_2O$ at 35% relative humidity, especially where it has been washed. Future work should assess mole for mole ratios also because ferrous chloride hydrate is heavier than βFeOOH. Stahl *et al.* (2003: 2573) give a tentative chemical formula for βFeOOH from which its molecular weight (M_r) can be calculated [$FeO_{0.833}(OH)_{1.167}Cl_{0.167}$].

Adsorbed water will have contributed to the weight data presented in figure 92 as indicative of corrosion. This has not been quantified and the data can not be represented as quantitative for that reason. There will be a relationship between water adsorption and the quantities of different corrosion products. The data presented here

represent weight increases as a function of corrosion + adsorbed moisture which is a combined indicator of corrosivity.

In summary, the results of this study mean that storage environments for chloride-contaminated wrought iron can be classified according to their aggressiveness to the iron.

STORAGE CATEGORY	RELEVANCE FOR CHLORIDE-CONTAMINATED WROUGHT IRON
VERY POOR	Outdoor storage conditions in Great Britain for much of the year or storage conditions within unheated damp buildings. Humidity lies above the deliquescence point of ferrous chloride (~50% relative humidity). Corrosion will be accelerated very greatly due to the presence of the very strongly conducting electrolyte (see figure 91).
ENHANCED	Humidities below the deliquescence point for iron chloride and above the corrosion threshold established for ferrous chloride and iron mixtures in this research. Within this region the rate of corrosion increases significantly with increases in relative humidity (see figures 48, 49 and 91).
EXCELLENT/ OPTIMAL	Any relative humidity beneath the threshold humidity for the corrosion of ferrous chloride and iron powder mixtures. Ferrous chloride no longer contributes directly to the corrosion of the iron and no longer oxidises to produce βFeOOH (see figures 38, 49, 88 and 91).

Table 9. **Categories of storage for chloride-contaminated wrought iron based on the findings of this research.**

In conclusion (table 9), the results of this study provide further evidence-based support for low humidity storage as an enhanced conservation option for chloride-contaminated wrought iron. Figure 88 shows that storage in an environment with a relative humidity

beneath the threshold relative humidity for corrosion of iron/ferrous chloride mixtures (21%±2% relative humidity at 20°C) would be optimal, minimising the amount of continued deterioration.

Attaining and maintaining the low humidity environments supported by the results of this study is likely to present challenges for the heritage sector. The capital and running costs of the air handling plant necessary to achieve the low humidities discussed here are likely to be significant (Watkinson & Tanner, 2008). Maintaining micro-environments for chloride-contaminated wrought iron in sealed containers presents challenges of its own (Thickett and Odlyha, 2007). Issues surrounding the logistics of maintaining the environmental parameters proposed as a result of this study have not been its primary focus. This study is process-feasibility focused, examining only the corrosion of chloride-contaminated iron and iron in the presence of carefully selected chloride-bearing corrosion products at low relative humidities.

The results of this study have contributed to the following published conservation papers and have significantly improved understanding of the control of levels of atmospheric moisture as a means of preserving chloride-contaminated wrought iron.

- Watkinson, D.E. & Lewis, M.R.T. (2004) ss Great Britain Iron Hull: Modelling corrosion to define storage relative humidity. **Metal'04 Proceedings of the International Conference on Metals Conservation, Canberra, 4-8 October 2004.** [ed. J. Ashton and D. Hallam]. Canberra: National Museum of Australia pp88-103.

- Watkinson, D.E. & Lewis, M.R.T. (2005a) Desiccated Storage of Chloride-contaminated Archaeological Iron Objects. **Studies In Conservation 50,** pp1-12. London: IIC.

- Watkinson, D.E. & Lewis, M.R.T. (2005b) The role of β-FeOOH in the corrosion of archaeological iron. **Materials Issues in Art and Archaeology VII** edited by Vandiver, P.B., Mass, J.L. and Murray, A. **(Materials Research Society of America Symposium Proceedings 852, Fall Meeting (2004), OO1.6** Boston, Mass. Warrendale, PA.

- Watkinson, D.E. and Lewis, M.R.T. (2007) ss Great Britain: Science and Technology Underpin Enclosure Design. **Conservation Matters in Wales. On Display: Showcases and Enclosures.** Post prints of a one day conference held on 14 June 2007 at the Oakdale Institute, St. Fagan: National History Museum, Cardiff, pp 13-17. Cardiff: Federation of Museums and Art Galleries in Wales and the National Museum of Wales, supported by Cymal.

- Watkinson, D.E., Tanner, M., Turner, R. and Lewis, M.R.T. (2006) ss Great Britain: Teamwork as a platform for innovative conservation. **The Conservator 29**, pp73-86. London: The Institute of Conservation (ICON).

- Watkinson, D. and Tanner, M. (2008) ss Great Britain: Conservation and Access – Synergy and Cost. **Conservation and Access.** Contributions to the London Congress 15-19 September, 2008. London: IIC, pp109-114.

One major consideration remains to be discussed. Desiccation (dehumidification or low humidity storage) aims to lock chlorides within solid ferrous chloride dihydrate or immobilise them as surface adsorbed chloride on βFeOOH. During desiccation the concentration of ferrous chloride solutions will rise (pH will fall) and solid, crystalline ferrous chloride tetrahydrate will form. Some will oxidise to solid βFeOOH. As relative humidity falls below 20%RH (assuming a temperature of 20°C) ferrous chloride tetrahydrate will transform to crystalline ferrous chloride dihydrate at the metal surface. The location and volume increase issues for ferrous chloride dihydrate will be similar to those for βFeOOH, being approximately three times that of metallic iron (Selwyn *et al.*, 1999).

Loss of overlying corrosion layers can be expected to occur during the desiccation process. The reported failure to preserve the integrity of archaeological iron using desiccated storage, including the use of Stewart™ boxes conditioned with silica gel to very low relative humidities (Keene, 1994; Keene & Orton, 1985), may reflect the significant length of time necessary to desiccate archaeological iron sufficiently in this way, rather than the failure to maintain a permanently low relative humidity within the box (see section 6.6)? The length of time required to desiccate archaeological iron was reported to be substantial (over two years) by Thickett and Odlyha (2007) where a weight loss of ~1.5%wt of its own weight is indicated for the "freshly excavated" iron used in their study. Oxidation with corrosion product formation at the metal surface, commonly beneath overlying corrosion products containing the "original" surface of the artefact is likely to proceed during this time at low relative humidity with undesirable results.

The response of chloride-contaminated wrought iron to slow [or more rapid] drying must be established by future research but a preliminary indicator of ongoing corrosion during slow desiccation is reported in section 6.6. It is anticipated that most chloride-contaminated wrought iron will take at least two years to fully dry out if the environmental parameters necessary can be maintained for that time. Ongoing corrosion can be expected to continue during the drying period. Any spalling of DPL during truly desiccated storage should be used as an opportunity to mechanically clean (using air abrasion) the evident underlying βFeOOH from the corrosion pit in the metal's surface, and the underside of the spalled DPL. Re-corrosion could be encouraged followed by repeated removal of βFeOOH until no more growth is observed. The DPL spall may then be re-adhered and the artefact returned to desiccated storage. This technique has been successfully employed on unstable Roman chloride-contaminated wrought iron artefacts from Usk stored at the Roman Legionary Museum, Caerleon – National Museum of Wales.

7.5 Relative humidity or specific humidity for corrosivity prediction?

The results of this study support models where

(i) the phase transformation of $FeCl_2.4H_2O$ to $FeCl_2.2H_2O$ (section 6.8.1.)

and

(ii) the corrosion or non-corrosion of iron powder in the presence of $FeCl_2.2H_2O$ (section 6.8.2.).

are a function of vapour pressure/specific humidity (sections 5.1.1., 6.8.2. and *c.f.* section 2.8, figure 20) or (RH + t) (Cuddihy, 1987; see section 6.8.2.) rather than relative humidity independent of temperature. Deliquescence is also governed by vapour pressure (Amorosso & Fassina, 1983: 122).

Future work at Cardiff University (Lewis &Watkinson) will examine these models.

8 Future work

8.1 The effect of temperature on ferrous chloride hydrate phase transformation and iron corrosion in its presence

Preliminary results resulting from ongoing experimental work to investigate the threshold relative humidity values for the transformation of $FeCl_2.4H_2O$ to $FeCl_2.2H_2O$ agree with data obtained at 30°C (reported in section 6.8.2.) which indicated that this hydrate transformation is temperature dependent for any given relative humidity (section 7.5).

From 0°C to 40°C the water content of saturated air doubles with each 11°C rise in temperature (an Arrhenius type relationship). Each 11°C reduction in temperature halves the saturated vapour pressure (water content) of the saturated air, with the difference in moisture condensing on surfaces or forming frost (Donovan, 1986: 194, *fig.14.1*). At 50%RH within the same temperature range each 22°C rise or fall in temperature doubles or halves the water content (saturated vapour pressure). This relationship between temperature and moisture content of the air (saturated vapour pressure) is shown by the steeper 100%RH percentage saturation curve and the shallower 50%RH percentage saturation curve in figure 74. For any given environmental condition, a change in temperature only, results in a horizontal change in the position on the psychrometric chart. Moisture content (specific humidity) will remain unaffected. A useful rule of thumb observes that air at 50%RH within this range cooled by 11°C will reach saturation (100%RH). Conversely, air at 100%RH (the dew-point) cooled by 11°C will fall to 50%RH (Donovan, 1986: 194-5).

Ordinarily, maintaining the temperature within an enclosed space at 10°C above the mean external temperature will have a significant drying effect in terms of relative humidity and a significant effect on the equilibrium moisture content (EMC) of organic hygroscopic materials within it. Water vapour content is not sensitive to temperature change and for the changes in relative humidity cited here for 11°C changes in

temperature it will remain constant. The results of the experimental research conducted for this study show that the rate of corrosion of iron (when it occurs) is a function of the moisture content of the air (figures 48, 49 and 91, and see section 7.5).

Further work is necessary to establish the nature of the ferrous chloride hydrate phase trend, its reproducibility and its relationship as a function of specific humidity or vapour pressure (which can be plotted horizontally on figure 74 as for moisture content kg/kg dry air (Wallert, 1996: 200, *fig.4*) where vapour pressure 0-15 Torr is equivalent to approximately 0.000-0.013kg/kg dry air on this scale).

Results could have important implications for air conditioning plant heating parameters, and running costs. Cold storage could be advantageous, not just thermodynamically but also if it influences the formation of different corrosion compounds. Conversely, current research by Kuhn (2008) aims to establish the corrosion stability of chloride-contaminated iron below the freezing point of water. Iron archaeological finds in Baden-Württemberg have been deep-frozen since the 1970s and 16 tonnes of artefacts currently occupy the freezer chamber of the newly built laboratory of the State Monument Protection Office (Landesdenkmalamt). Kuhn (*ibid.*) reports that despite good results in the short term, the artefacts do not appear to be stable over decades. She cites experience of corrosion of iron in Antarctic huts of polar researchers which also raises questions over the stability of iron at low and sub-zero temperatures (Maxwell & Viduka, 2004).

8.2 Quantifying experimental corrosion based upon molar calculations and thermogravimetric analyses

The data reported for the results of the experimental programme conducted for this research are based on weight change (increase) as an indicator of corrosion. The molecular weight of ferrous chlorides is greater than that for βFeOOH. This means that a like-for-like increase in mass will not indicate a like-for-like increase in the number of molecules of each form of corrosion product. Similarly, a like-for-like increase in mass will not indicate a like-for-like volume increase upon production of corrosion product at the metal – DPL interface. A study of experimental corrosion based upon molar calculations will enable the relative volumes of corrosion products to be estimated.

The weight changes measured and used to indicate corrosion will also contain a component mass of adsorbed or absorbed water. This was not quantified during this study. Thermogravimetric analyses of the products of these experiments would enable the water content to be quantified and its relative contribution to the corrosion process assessed.

8.3 Analyses of Soxhlet wash condensate

The observed volatility of chloride (section 6.5.5.) may partly contribute to the reported inability to remove all chloride from archaeological and marine objects in the laboratory by aqueous Soxhlet washing (section 2.8.7.). The analysis of chloride content of wash solutions from the basal distillation flask of the Soxhlet apparatus (contaminated with chloride following siphoning from the wash chamber) is standard practice and is used to monitor the progress and effectiveness of the treatment. The same (boiling) wash solution is the source of the wash water, which condenses from its steam in a Graham condenser in reflux. Analysis of the condensate from this boiling wash solution will establish whether volatile chloride is condensed to return to the siphon chamber where the object is treated.

8.4 *Volatile labile chloride on βFeOOH*

The amount and nature of surface adsorbed labile chloride on βFeOOH requires further study. Wang (2007b: 69) reported the formation of akaganéite on her control foils without a source of chloride in the chamber. Her other tests used ferrous chloride tetrahydrate and iron foil which formed akaganéite in all the tests she conducted. If the control tests were conducted after the main series then volatile, labile, chloride from the ferrous chloride/akaganéite must be suspected although Askey *et al.* (1993: 233 & 235) do cite levels of HCl in an urban area as 1-10μg m^{-3}, with the highest encountered presentation rate at 2.5 x 10^{-6} mg cm^{-2} s^{-1}. HCl reacts with Mg, Zn and Fe to form its respective chlorides (Askey *et al.*, 1993). Exposure of stainless steel within a sealed environment in the presence of unwashed βFeOOH successfully produced tower and thread-like crystal growth of βFeOOH (section 6.5.5. and figure 68). Repeat exposures, but for Zn and Mg in place of stainless steel, should produce their respective chlorides (liberating hydrogen which can be collected and confirmed by ignition) which may subsequently be assayed.

Askey *et al.* (*op. cit.*: 246) reported that mild steel reacts directly with gaseous atmospheric HCl giving $FeCl_2$ which then oxidises to give FeO(OH), Fe_3O_4 or Fe_2O_3, liberating its chloride as HCl, depending on humidity and oxygen access, which is itself dependent on scale thickness. $FeCl_2$ in the presence of lepidocrocite (γ-FeO(OH)) were identified as the corrosion products by X-ray diffraction (*ibid.*). βFeOOH was not identified. It would be useful to clarify these products of HCl attack on iron by repeating their experiment. This would confirm the expected presence, or absence, of βFeOOH as a corrosion product.

Exposure of damp blue litmus within a sealed environment containing unwashed βFeOOH would result in a colour change to red in the presence of HCl. Similarly, methyl orange would change from yellow to pink and alkaline phenolphthalein from pink to colourless. Exposure of a silver nitrate solution or lead nitrate solution would confirm the presence of HCl by forming white precipitates of silver chloride or lead chloride respectively. These tests may be used semi-quantitatively (Semczak, 1977). Ammonia

will also form a white precipitate in the presence of halide ions, a common classroom demonstration of the kinetic theory of gases in the form of Graham's Law of diffusion or effusion. HCl can be identified using FTIR where HCl stretch bands occur around 2704cm^{-1} and rotational bands at around 2900cm^{-1}. Preliminary FTIR-ATR analyses of unwashed βFeOOH, where any adsorbed HCl is aqueous, are not informative due to masking due to a broad adsorption resulting from –OH bond adsorption in this region. Diffusion tubes for hydrochloric acid quantification are commercially available (Drager® direct-reading Hydrochloric Acid 10/a-D and 20/a-D diffusion tubes or Gradco Environmental® DIF 900 RTU – Acid gases) and will quantify levels of atmospheric HCl.

The current practice for the storage of chloride-contaminated wrought iron in museums is to desiccate it in sealed containers using conditioned silica gel or beads etc. (Cronyn, 1990; Green and Bradley, 1997; Watkinson and Neal, 1998; Thickett & Odlyha, 2007). Where volatile labile chloride (as HCl) is either present or forms on chloride-contaminated wrought iron objects in sealed storage containers levels of chloride/HCl vapour in the sealed container could rise to dangerous levels and promote corrosion of remaining iron within the container. The potential for this has been demonstrated at a relative humidity as low as 41%RH (section 6.5.5.). The presence of HCl vapour (or otherwise) within sealed storage boxes containing archaeological iron needs to be established by future work.

If HCl vapour is found within sealed boxes of archaeological iron at relative humidities around 41%RH and lower, this is in the region that the old cobalt chloride doped "self indicating" silica gel changed colour (from blue to pink) to show that it needed regeneration (section 3.3). The possibility that desiccated storage of archaeological iron has reportedly failed (Keene, 1994) partly due to the presence of chloride/HCl vapour should be investigated. Clearly silica gel has been ineffective in preventing some of the accelerated corrosion mechanisms long before the observed indicator colour change. Levels of chloride/HCl vapour within boxes are expected to be low as compared with levels within the pores and corrosion layers of artefacts themselves.

That the silica gel may adsorb chloride/HCl vapour and provide a reservoir for ongoing environmental pollution within the sealed container remains a possibility. Paradoxically the act of sealing chloride-contaminated artefacts in containers in order to effect desiccation may enable a build up of harmful environmental contaminants within the container. HCl vapour within sealed containers could be tested for simply with moist litmus paper. Further research is this area has been identified. It may be found to be advantageous to include an alkaline buffer within sealed polypropylene/polyethylene boxes of chloride-contaminated wrought iron. Alkaline residues from alkaline wash treatments may have implications for long-term stability in storage (Watkinson, 1996). Costs for bulk storage in this way would need to be assessed against costs for RP/ESCAL™ enclosures with and without an oxygen scavenger (Mathias *et al.,* 2004). Treatment (washing) will be costly and any preventive measure reducing this cost would meet with widespread interest. The results of the tests conducted for this study support the washing of chloride-contaminated wrought iron (especially in de-oxygenated environments) to remove as much labile chloride (possibly HCl) as possible prior to desiccated storage (especially in sealed containers) thereby "enhancing" their stability through the removal of a significant agency of deterioration. Keene and Orton (1985) reported that most aqueous washing treatments of wrought iron assessed in their study of past treatments had improved the stability of the objects to some extent.

Atmosphere characterisation within Stewart™ boxes containing chloride-contaminated wrought iron should also be conducted in order to verify the presence or absence of atmospheric volatile chloride/acid. None has been reported.

The use of aluminium foil to cover a beaker containing a solution of ferrous chloride (section 6.5.5.) should be repeated using a solution of known concentration and allowed to fully evaporate. Products should be analysed using XRD and FTIR-ATR. The results should be compared with those reported in section 6.5.5. and data resulting from tests suggested here as future work.

A programme of adsorbed chloride characterisation and quantification will inform future storage parameters and methods for chloride-contaminated wrought iron.

8.5 A corrosion monitoring programme for desiccated chloride-contaminated wrought iron

A detailed environmental monitoring programme combined with corrosion current monitoring for chloride-contaminated wrought iron maintained in desiccated storage would be a valuable way of measuring the low humidity environments for corrosion prevention (Cole *et al.*, 2004: 12-13). The Vaisala Drycap™ sensor is a low-cost thin film polymer sensor optimised for use in dry ambients, where moisture is usually measured as a dew point temperature (Cridland, 2000). Low end accuracy of ±0.1%RH is claimed for this humidity/temperature sensor which operates on the principle of a change in capacitance across the polymer sensor with varying atmospheric moisture levels (Cuddihy, 1987). This type of sensor can also withstand condensation. It is ideal where dry air has to be continuously monitored.

Data for periods of air conditioning plant failure or the opening of sealed containers (to examine their contents or renewal of their desiccant) would identify the effect of changes in relative humidity and identify changes in rate of corrosion during that time. The slow drying of chloride-contaminated wrought iron is expected to cause ferrous chloride crystallisation and some βFeOOH formation with possible spalling as a result. Study of newly identified areas of spalling occurring in desiccated storage should be sampled and analysed for $FeCl_2.4H_2O$ or $FeCl_2.2H_2O$.

Appendix 1

Systematic Error

The following tests established the behaviour of the Mettler AJ100™ balance in terms of balance vibration and balance drift using standard masses. It can be seen that the vibration and drift phenomena were found to be systematic i.e. predictable and reproducible. Although the direction and magnitude of the vibration induced lurches that were found to vary, they could be accounted for in the following way for each test.

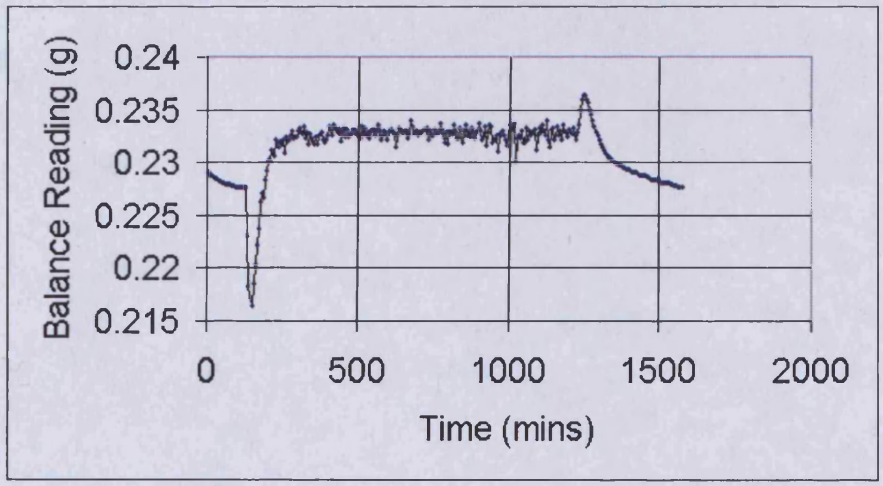

i **Initial mass = 0.2291g. Balance drift (~0.0015g) observed at rest until chamber turned on at ~100mins. Lurch to around 0.233g. Final end tare upon removal of mass = -0.0015g (corresponding with the initial balance drift).**

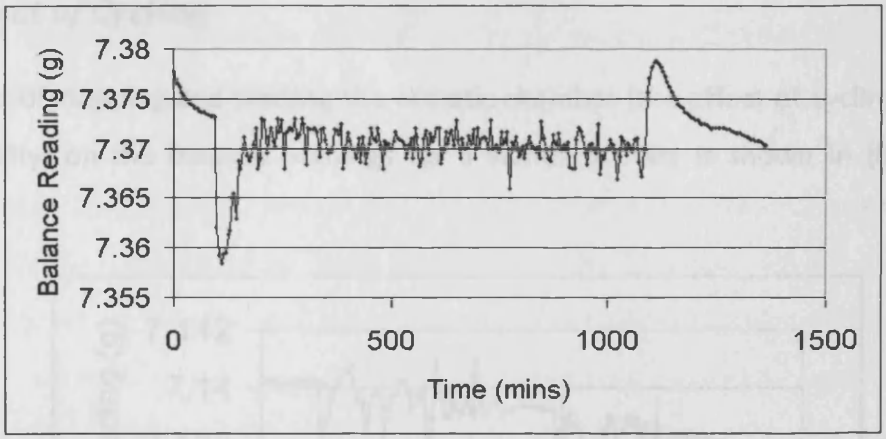

ii **Reproducibility test. Initial mass = 7.3777g. Chamber activated after 95 minutes. Drift before chamber activated = 0.0046g in 1hr 35 minutes. Assumed value is about 7.3705g ± $3x10^{-4}$g. End mass = 7.3704g at 1365 minutes. End Tare = - 0.0073g.**

Whilst the balance data is recorded to four decimal places, results should only be interpreted to three at most due to error introduced through balance vibration (the 'noise').

Weight change to the sample during a test superimposes its trend on that of the phenomena above rather like a Fourier transform. This was confirmed for every test conducted by calibrating the balance with a 100g mass standard at the beginning of each test. The weight of the empty Petri dish was then recorded. Any change to the balance tare was also recorded. The mass of the sample was recorded before the test was run. This data was compared with the recorded stable mass of the sample at the end of each test and the balance tare when this sample was removed. The initial tare and end tare were compared to find the magnitude of the balance drift during the tests. In all cases this was of the expected magnitude. Stable weight data was compared with the data-logged and plotted data (accounting for balance drift using the tare comparison) and was found to agree in all instances.

The Effect of Cycling

The effect of stopping and starting the climatic chamber (the effect of cycling vibration and stability) on the balance readings for a standard mass is shown in (iii) and (iv) below.

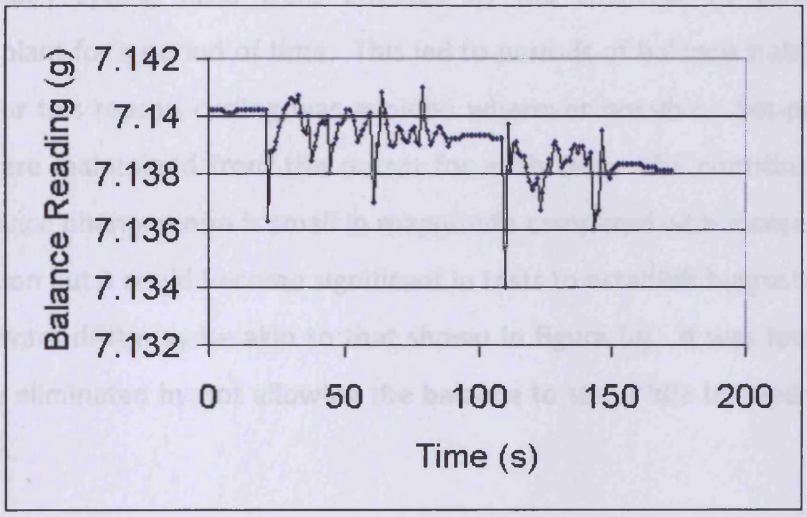

iii **The effect of climatic chamber cycling on the balance reading.**

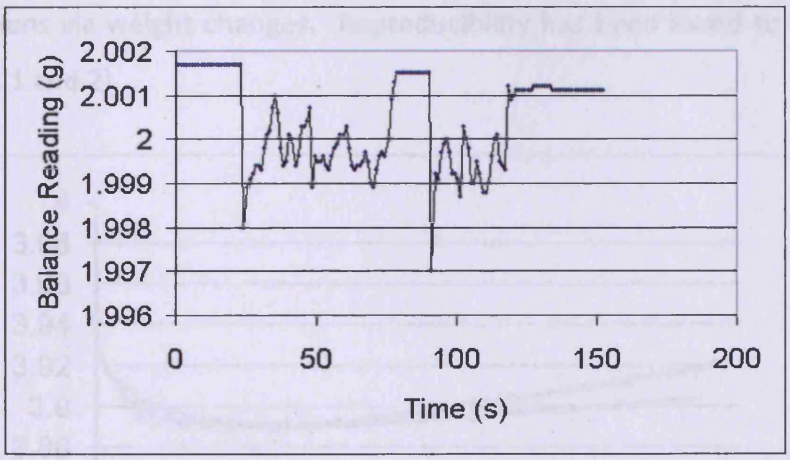

iv **Further testing of climatic chamber cycling effects on the balance.**

Periods at rest and periods with the climatic chamber activated may clearly be seen. It should be noted that the balance shows a slight downward drift each time the climatic chamber (vibration) stops and starts.

It was found that changes to the test set-point humidity during climatic chamber relative humidity cycling tests were effected by the chamber by turning off the refrigeration plant for a period of time. This led to periods of balance stability (with no vibration). For this reason cycling was avoided wherever possible. Set-point relative humidities were maintained from the outset for each test. The contribution of drift from this balance phenomenon is small in magnitude compared with increase in weight due to corrosion but it could become significant in tests to establish hygroscopicity. The overall downward drift may be akin to that shown in figure (ii). It was found that this drift could be eliminated by not allowing the balance to stand idle between calibration and operation.

Reproducibility of Results

The Votsch™ 4018 climatic chamber has been established as a means of investigating corrosion reactions via weight changes. Reproducibility has been found to be good (v and appendices 1 and 2).

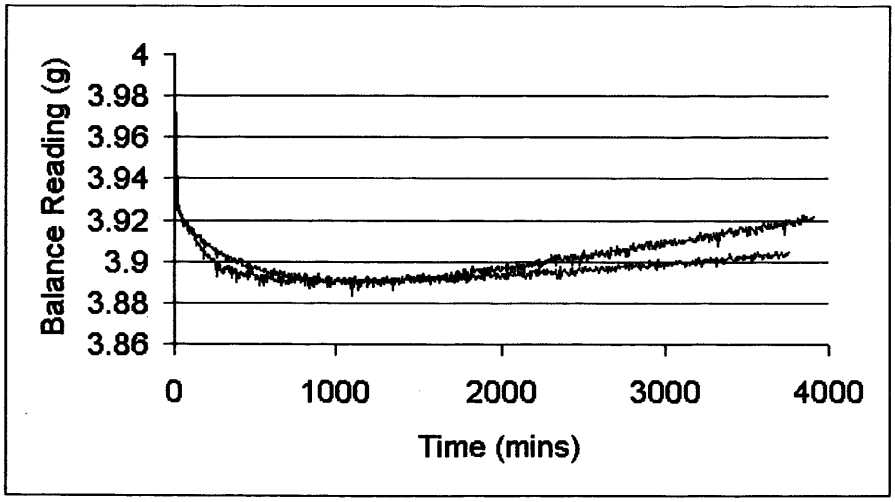

v. **Reproducibility for replicated beta-FeOOH and iron powder corrosion at 19%RH and 20°C.**

Figure (v) shows good reproducibility of data for iron corrosion in the presence of βFeOOH. For any non-linear relationship (such as the example shown here) a small discrepancy will be magnified by the trend. What is important for our purposes is not the actual change in weight of the sample or its actual rate of change of weight during the test, but the trend exhibited and its relationship with the trends exhibited by the other related tests.

Appendix 2

Quantifying Balance Diffusion Effects

A Rotronic™ data-logger at ambient temperature and RH was placed on an upturned Petri dish within the balance in the exact position of the test samples and the door of the balance was positioned exactly as it was for all of the other tests. The climatic chamber set-point was set to 20°C and 20%RH. The temperature and relative humidity changes within the balance were compared with those within the chamber in order to assess balance enclosure diffusion lag effects.

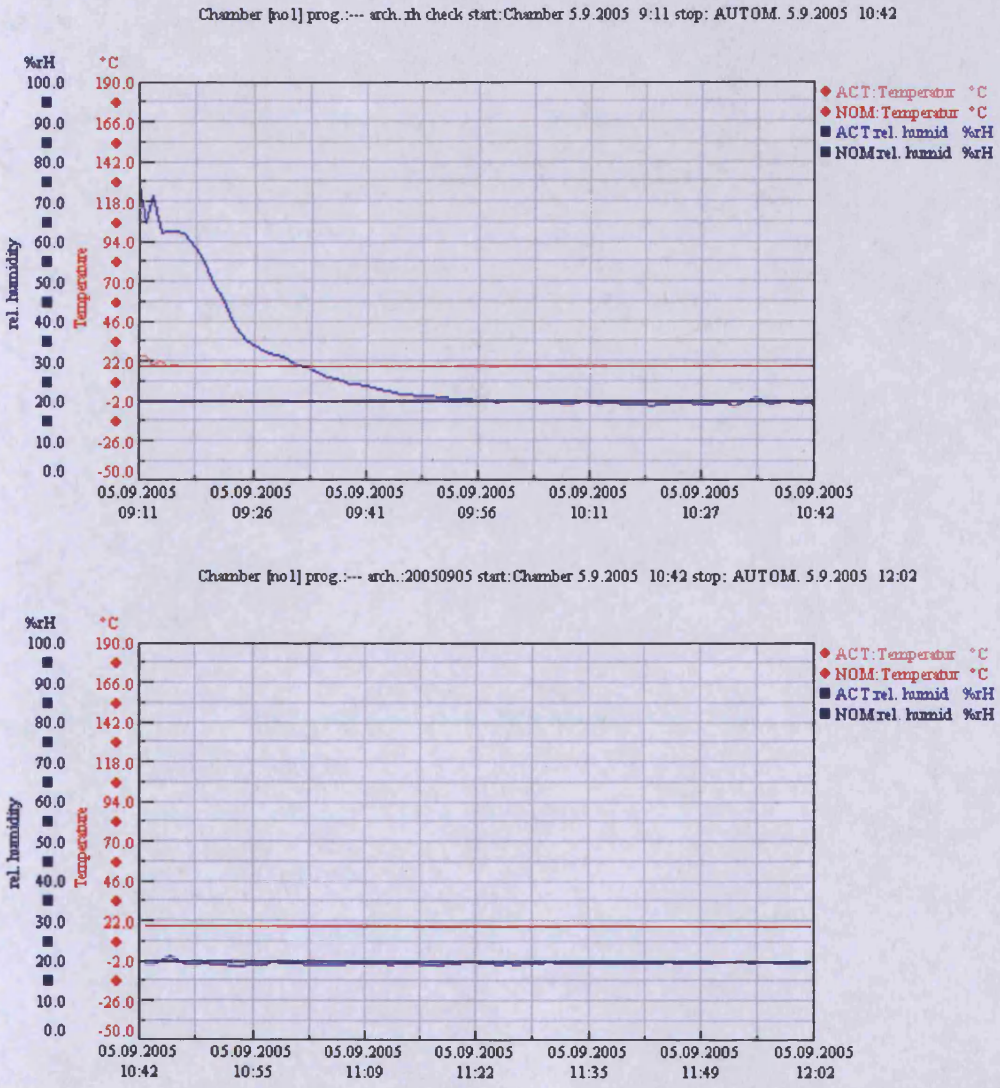

v **Environmental data for the climatic chamber.**

The chamber data (v) clearly shows that the set point temperature was attained and maintained within 5 minutes. The chamber RH was attained and maintained from 55 minutes.

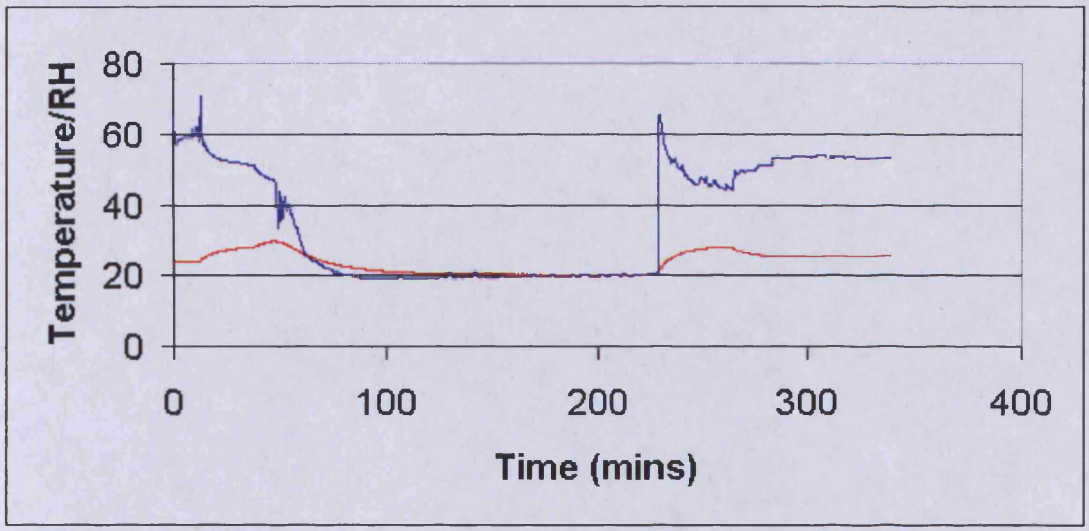

vi **Environmental data for the balance enclosure as logged by the Rotronic™ data-logger. This independently verified the chamber set point and data i.e. 20%RH at 20°C. The logger was placed in the balance enclosure at about 20 minutes and was removed to the ambient from the chamber at about 230 minutes on this chart.**

Within the balance enclosure it can be seen that the temperature was finally attained by 150 minutes and that the exponential nature of the temperature plot is indicative of the loss of (radiant) heat from the balance body itself (cooling). Within the balance enclosure it can be seen that the RH is attained and maintained at the set-point from approximately 90 minutes.

A small time lag within the balance enclosure has been identified but it is not significant enough to greatly influence the results reported in this study. All of the reported experimental data sets ran for thousands of minutes so that the environment within the balance will have come into equilibrium with that of the chamber well before the end of each test.

Appendix 3

X-Ray Diffraction Data for Ferrous Chloride and the βFeOOH Synthesised and Used for this Study

The following pages contain the XRD spectra and powder diffraction file data for the ferrous chloride and for the βFeOOH used in this study. The analyses and identifications were conducted by Dr A. Oldroyd at the Department of Earth Sciences, Cardiff University, without prior knowledge of their likely composition. The samples submitted were as follows,

Sample 1 βFeOOH synthesised by the author in a large, cuboid, Perspex™ desiccator maintained at 92%RH via the aerial oxidation of iron powder and ferrous chloride tetrahydrate. This sample was taken from the surface of the synthesised mass.

Sample 2 βFeOOH synthesised by the author in a large, cuboid, Perspex™ desiccator maintained at 92%RH via the aerial oxidation of iron powder and ferrous chloride tetrahydrate. This sample was taken from beneath the surface of the synthesised mass.

Sample 3 βFeOOH synthesised by the author in a conventional glass laboratory desiccator maintained at 92%RH via the aerial oxidation of iron powder and ferrous chloride tetrahydrate. This sample was taken from the surface of the synthesised mass.

Sample 4 βFeOOH synthesised by the author in a conventional glass laboratory desiccator maintained at 92%RH via the aerial oxidation of iron powder and ferrous chloride tetrahydrate. This sample was taken from beneath the surface of the synthesised mass.

Sample 5 $FeCl_2.4H_2O$ which had visibly oxidised at the crystal surfaces during long-term storage. Likely to comprise a mixture of $FeCl_2.4H_2O$ and βFeOOH.

Sample 6 βFeOOH synthesised by the author in a conventional glass laboratory desiccator maintained at 92%RH via the aerial oxidation of iron powder and ferrous chloride tetrahydrate. This sample was taken from the very bottom of the desiccator and the very bottom of the synthesised mass. This sample was taken to investigate whether oxygen was sufficiently plentiful throughout the mass during production.

Summary

Samples 1,2,3,4 and 6 were identified as βFeOOH (akaganéite).
Sample 5 was confirmed as mostly ferrous chloride tetrahydrate ($FeCl_2.4H_2O$) with a small amount of βFeOOH (akaganéite).

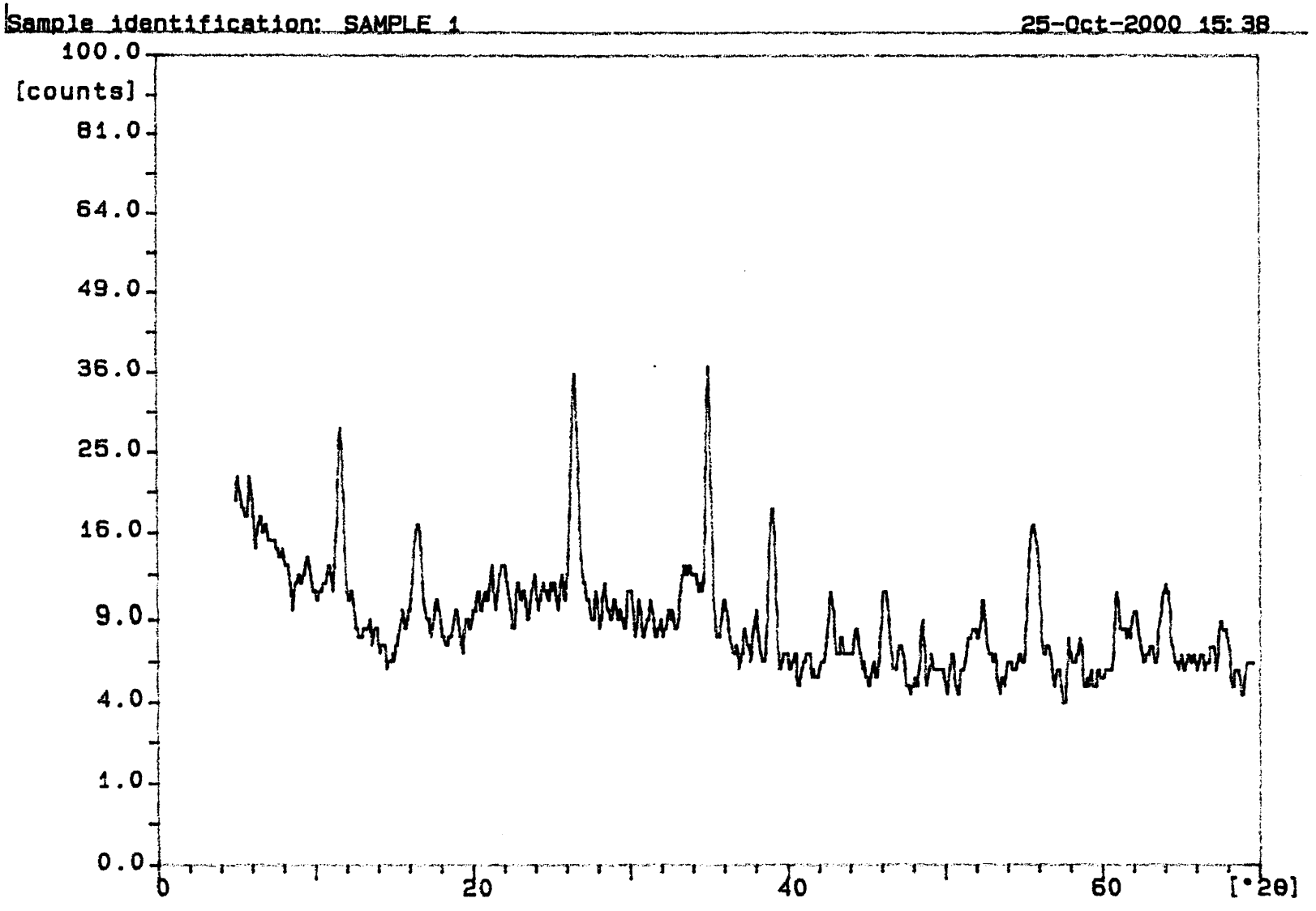
Sample identification: SAMPLE 1
25-Oct-2000 15:38
100.0
[counts]
81.0
64.0
49.0
36.0
25.0
16.0
9.0
4.0
1.0
0.0
0
20
40
60
[°2θ]

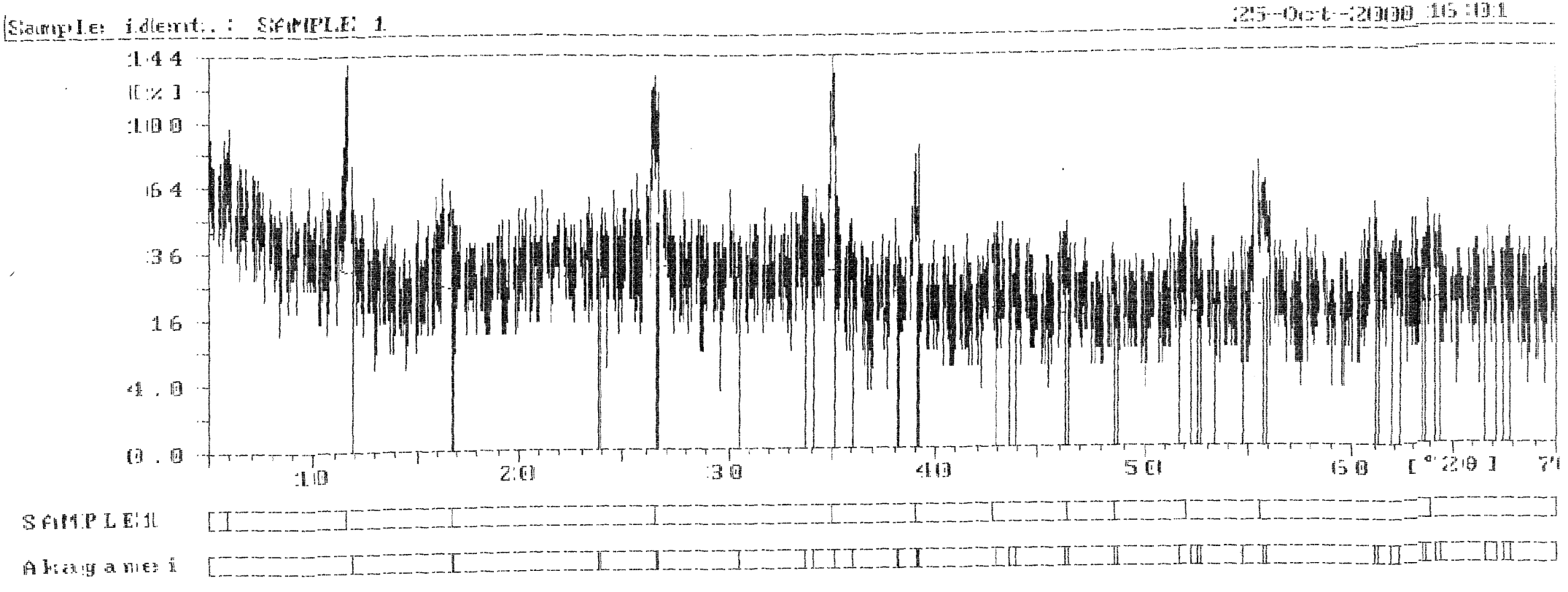
Sample identif. : SAMPLE 1
25-Oct-2000 16:01
144
[x]
100
64
36
16
4.0
0.0
10
20
30
40
50
60
[°2θ]
SAMPLE1
Akagane1

File: SAMPLE1.DI 25-Oct-2000 11:29

Philips Analytical PC-APD Diffraction Software

Sample identification: SAMPLE 1
Data measured at: 25-Oct-2000 11:02:00

Diffractometer type: PW1710 BASED
Tube anode: Cu
Generator tension [kV]: 35
Generator current [mA]: 28
Wavelength Alpha1 [Å]: 1.54056
Wavelength Alpha2 [Å]: 1.54439
Intensity ratio (alpha2/alpha1): 0.500
Divergence slit: 1°
Receiving slit: 0.1
Monochromator used: YES

Start angle [°2θ]: 5.000
End angle [°2θ]: 70.000
Step size [°2θ]: 0.020
Maximum intensity: 32.4900
Time per step [s]: 0.500
Type of scan: CONTINUOUS

Minimum peak tip width: 0.00
Maximum peak tip width: 1.00
Peak base width: 2.00
Minimum significance: 0.75
Number of peaks: 12

Angle [°2θ]	d-value α1 [Å]	d-value α2 [Å]	Peak width [°2θ]	Peak int [counts]	Back. int [counts]	Rel. int [%]	Signif.
5.915	14.9293	14.9664	0.320	6	14	19.2	0.78
11.695	7.5606	7.5794	0.120	32	10	100.0	1.00
16.685	5.3090	5.3222	0.480	9	8	27.7	1.37
26.515	3.3589	3.3672	0.400	23	10	70.9	2.88
34.955	2.5648	2.5711	0.160	25	10	76.9	0.81
39.070	2.3036	2.3093	0.400	10	7	31.5	2.27
42.740	2.1139	2.1191	0.480	5	6	14.9	0.90
46.315	1.9587	1.9636	0.560	5	5	14.9	2.07
48.600	1.8718	1.8765	0.240	4	5	11.1	0.84
52.130	1.7531	1.7574	0.960	3	5	10.0	2.19
55.500	1.6543	1.6584	0.480	10	6	31.5	1.31
63.965	1.4543	1.4579	0.640	4	6	13.6	1.22

Sample identification: SAMPLE 2 25-Oct-2000 15:41

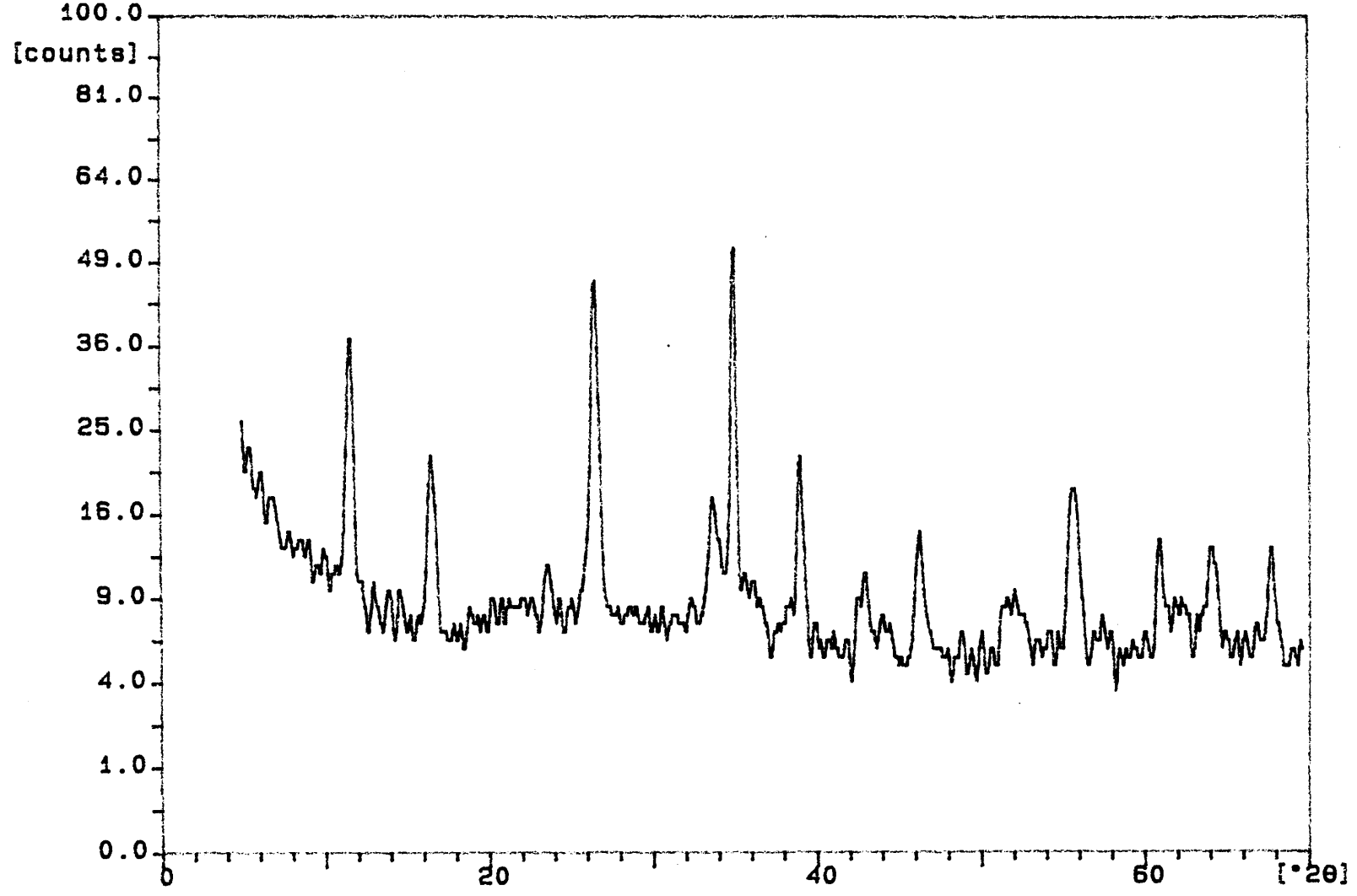

SAMPLE2.SM

File: SAMPLE2.DI 25-Oct-2000 12:34

Philips Analytical PC-APD Diffraction Software

Sample identification: SAMPLE 2
Data measured at: 25-Oct-2000 12:07:00

Diffractometer type: PW1710 BASED
Tube anode: Cu
Generator tension [kV]: 35
Generator current [mA]: 28
Wavelength Alpha1 [Å]: 1.54056
Wavelength Alpha2 [Å]: 1.54439
Intensity ratio (alpha2/alpha1): 0.500
Divergence slit: 1°
Receiving slit: 0.1
Monochromator used: YES

Start angle [°2θ]: 5.000
End angle [°2θ]: 70.000
Step size [°2θ]: 0.020
Maximum intensity: 51.8400
Time per step [s]: 0.500
Type of scan: CONTINUOUS

Minimum peak tip width: 0.00
Maximum peak tip width: 1.00
Peak base width: 2.00
Minimum significance: 0.75
Number of peaks: 14

Angle [°2θ]	d-value α1 [Å]	d-value α2 [Å]	Peak width [°2θ]	Peak int [counts]	Back. int [counts]	Rel. int [%]	Signif.
11.645	7.5929	7.6118	0.200	34	9	64.9	1.20
14.030	6.3071	6.3228	0.400	1	7	1.9	0.79
16.495	5.3697	5.3830	0.320	15	7	29.3	0.98
26.455	3.3663	3.3747	0.360	37	8	71.8	3.85
33.690	2.6581	2.6647	0.640	10	8	18.5	1.49
34.990	2.5623	2.5687	0.240	52	8	100.0	4.10
38.955	2.3101	2.3159	0.320	15	6	29.3	1.52
42.740	2.1139	2.1191	0.800	3	6	6.2	1.75
46.235	1.9619	1.9668	0.400	8	5	16.2	1.24
51.885	1.7608	1.7651	0.960	3	5	6.2	1.95
55.615	1.6512	1.6553	0.640	13	6	25.0	2.12
60.835	1.5214	1.5252	0.320	8	7	15.1	1.00
64.160	1.4503	1.4539	0.480	6	6	12.1	1.88
67.675	1.3833	1.3867	0.320	7	5	14.1	0.82

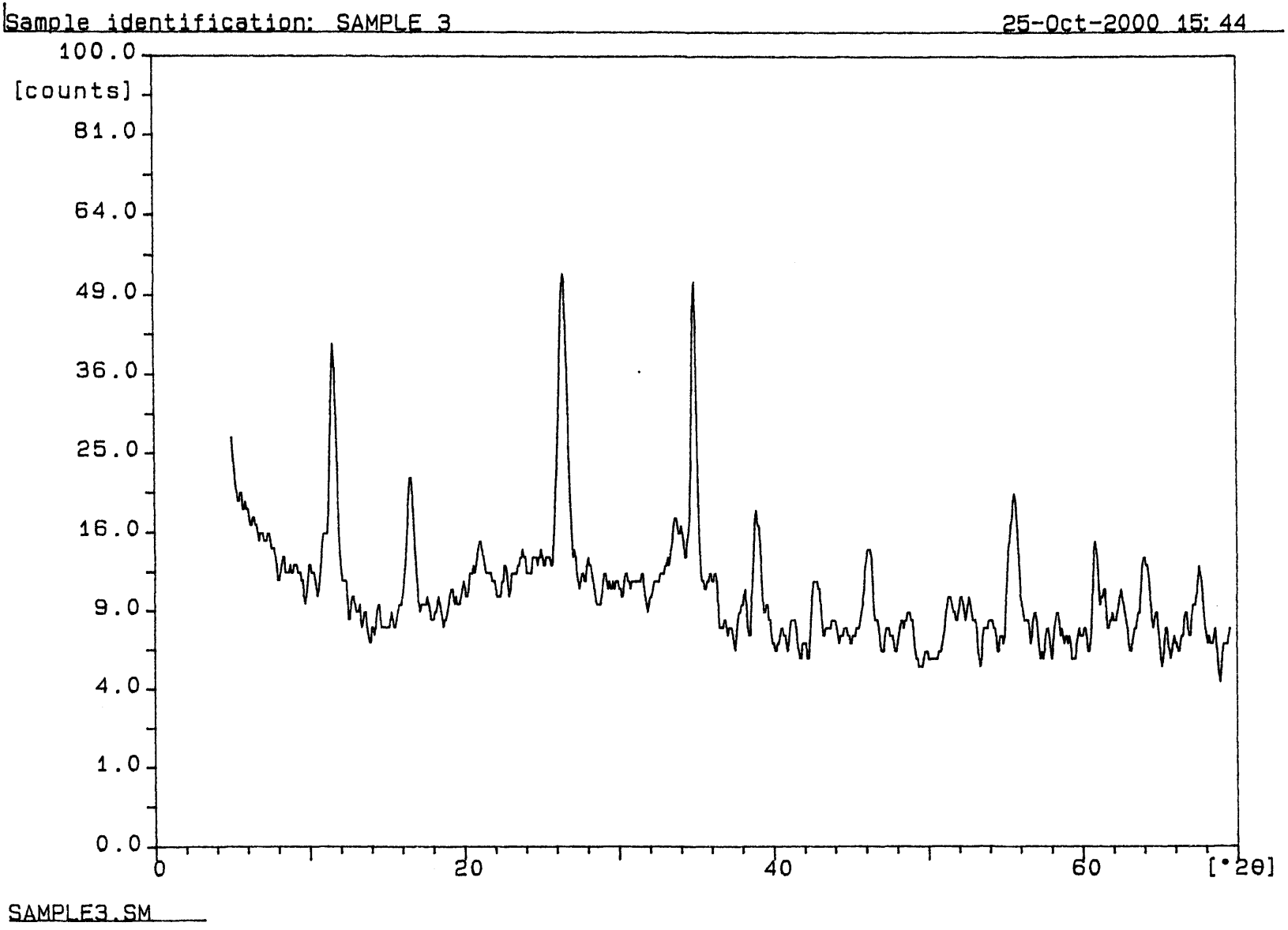
Sample identification: SAMPLE 3
25-Oct-2000 15:44
100.0
[counts]
81.0
64.0
49.0
36.0
25.0
16.0
9.0
4.0
1.0
0.0
0
20
40
60
[°2θ]
SAMPLE3.SM

File: SAMPLE3.DI 25-Oct-2000 13:56

Philips Analytical PC-APD Diffraction Software

Sample identification: SAMPLE 3
Data measured at: 25-Oct-2000 13:28:00

Diffractometer type: PW1710 BASED
Tube anode: Cu
Generator tension [kV]: 35
Generator current [mA]: 28
Wavelength Alpha1 [Å]: 1.54056
Wavelength Alpha2 [Å]: 1.54439
Intensity ratio (alpha2/alpha1): 0.500
Divergence slit: 1°
Receiving slit: 0.1
Monochromator used: YES

Start angle [°2θ]: 5.000
End angle [°2θ]: 70.000
Step size [°2θ]: 0.020
Maximum intensity: 43.5600
Time per step [s]: 0.500
Type of scan: CONTINUOUS

Minimum peak tip width: 0.00
Maximum peak tip width: 1.00
Peak base width: 2.00
Minimum significance: 0.75
Number of peaks: 13

Angle [°2θ]	d-value α1 [Å]	d-value α2 [Å]	Peak width [°2θ]	Peak int [counts]	Back. int [counts]	Rel. int [%]	Signif.
11.645	7.5929	7.6118	0.160	34	10	77.2	0.96
16.595	5.3376	5.3508	0.400	15	8	34.9	1.79
22.150	4.0099	4.0199	0.140	3	11	6.6	0.86
26.460	3.3657	3.3741	0.480	40	13	91.1	4.13
34.890	2.5694	2.5758	0.240	44	13	100.0	3.22
38.880	2.3144	2.3202	0.320	9	7	20.7	0.78
42.775	2.1122	2.1175	0.320	5	7	11.1	1.43
46.340	1.9577	1.9626	0.480	8	7	18.0	1.46
48.645	1.8702	1.8748	0.960	3	6	6.6	0.78
55.680	1.6494	1.6535	0.400	12	7	28.1	1.09
60.805	1.5221	1.5259	0.200	8	7	19.3	0.91
64.075	1.4521	1.4557	0.480	7	7	15.5	1.80
67.570	1.3852	1.3886	0.480	7	6	15.5	1.38

Sample identification: SAMPLE 4 25-Oct-2000 15:47

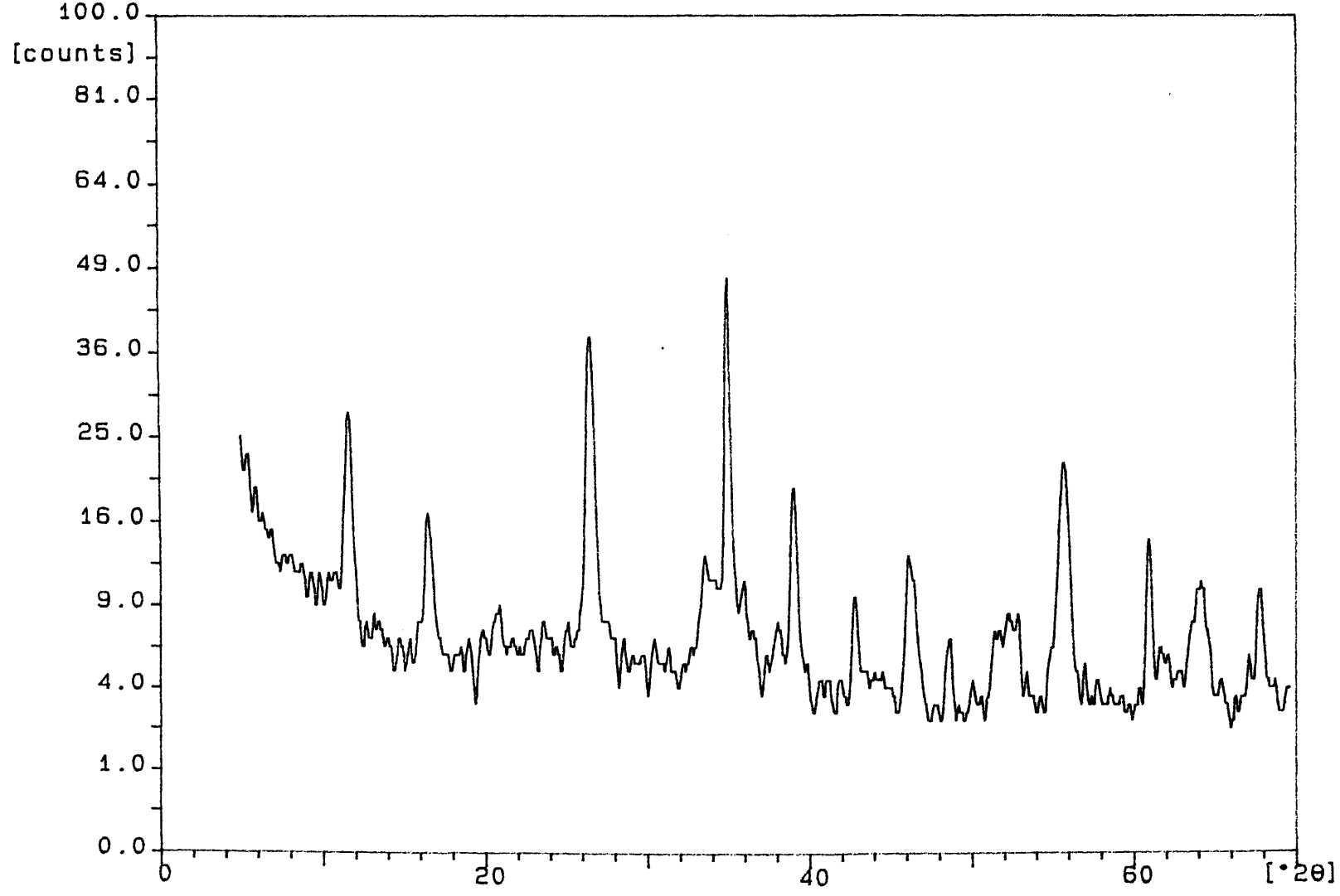

SAMPLE4.SM

File: SAMPLE4.DI 25-Oct-2000 14:49

Philips Analytical PC-APD Diffraction Software

Sample identification: SAMPLE 4
Data measured at: 25-Oct-2000 14:21:00

Diffractometer type: PW1710 BASED
Tube anode: Cu
Generator tension [kV]: 35
Generator current [mA]: 28
Wavelength Alpha1 [Å]: 1.54056
Wavelength Alpha2 [Å]: 1.54439
Intensity ratio (alpha2/alpha1): 0.500
Divergence slit: 1°
Receiving slit: 0.1
Monochromator used: YES

Start angle [°2θ]: 5.000
End angle [°2θ]: 70.000
Step size [°2θ]: 0.020
Maximum intensity: 46.2400
Time per step [s]: 0.500
Type of scan: CONTINUOUS

Minimum peak tip width: 0.00
Maximum peak tip width: 1.00
Peak base width: 2.00
Minimum significance: 0.75
Number of peaks: 15

Angle [°2θ]	d-value α1 [Å]	d-value α2 [Å]	Peak width [°2θ]	Peak int [counts]	Back. int [counts]	Rel. int [%]	Signif.
11.650	7.5897	7.6086	0.120	27	8	58.5	1.46
16.475	5.3762	5.3895	0.400	12	5	25.0	1.32
26.480	3.3632	3.3716	0.560	31	6	67.8	6.78
33.530	2.6704	2.6771	0.480	7	5	15.8	0.92
34.975	2.5634	2.5697	0.240	46	6	100.0	3.09
38.055	2.3627	2.3685	0.480	3	4	5.5	0.79
39.045	2.3050	2.3107	0.320	17	4	36.4	1.43
42.840	2.1092	2.1144	0.120	13	4	28.0	0.79
46.085	1.9679	1.9728	0.320	9	3	19.5	0.91
48.575	1.8727	1.8774	0.480	3	3	7.0	1.72
52.700	1.7354	1.7398	0.960	4	4	8.7	1.31
55.705	1.6487	1.6528	0.640	18	4	38.1	4.49
60.885	1.5203	1.5240	0.160	14	4	31.2	0.80
64.100	1.4516	1.4552	0.960	7	4	14.6	2.82
67.725	1.3824	1.3858	0.400	8	3	18.2	1.59

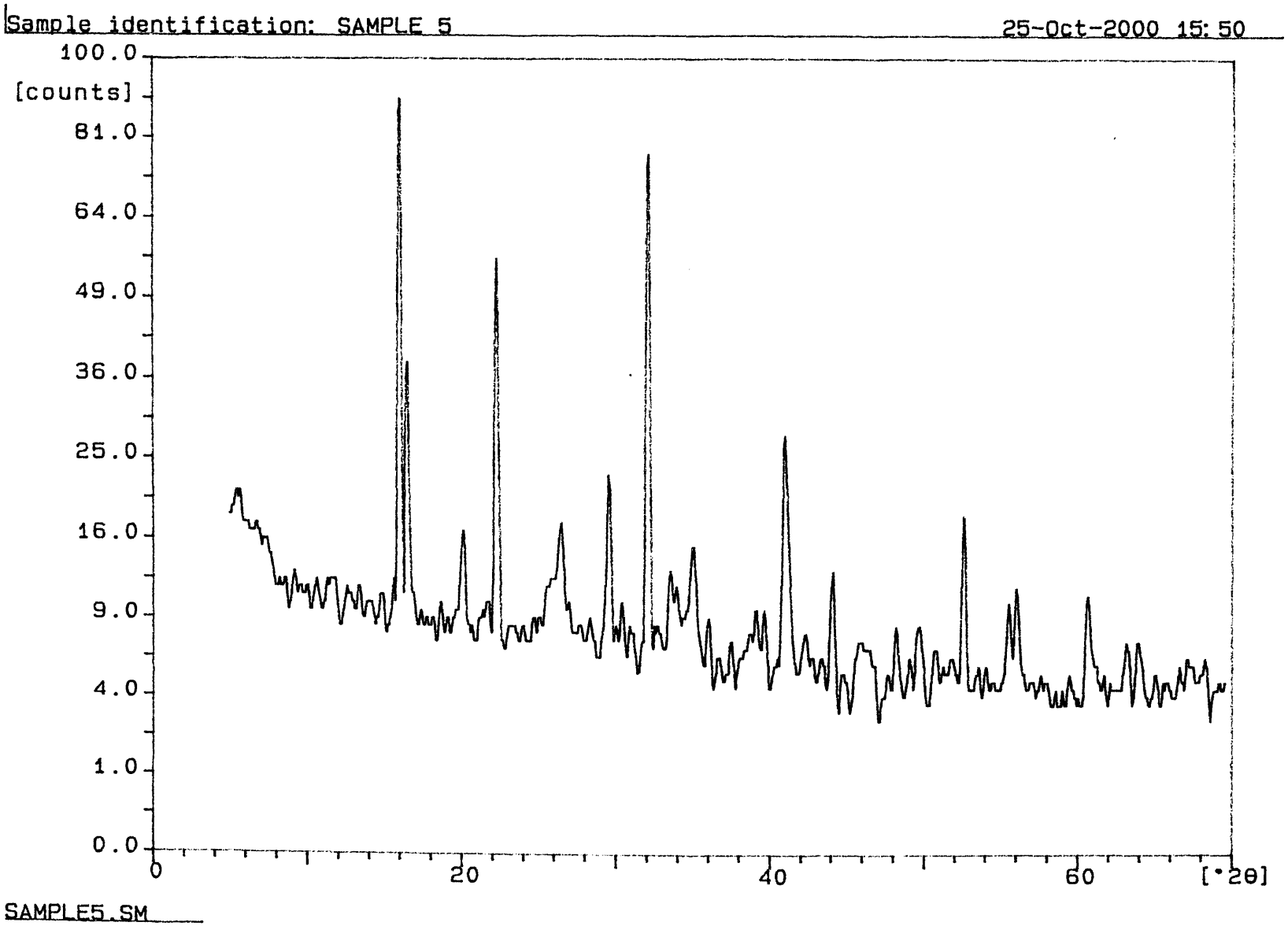
Sample identification: SAMPLE 5
25-Oct-2000 15:50
100.0
[counts]
81.0
64.0
49.0
36.0
25.0
16.0
9.0
4.0
1.0
0.0
0
20
40
60
[°2θ]
SAMPLE5.SM

Sample identif. : SAMPLE 5

25-Oct-2000 16:56

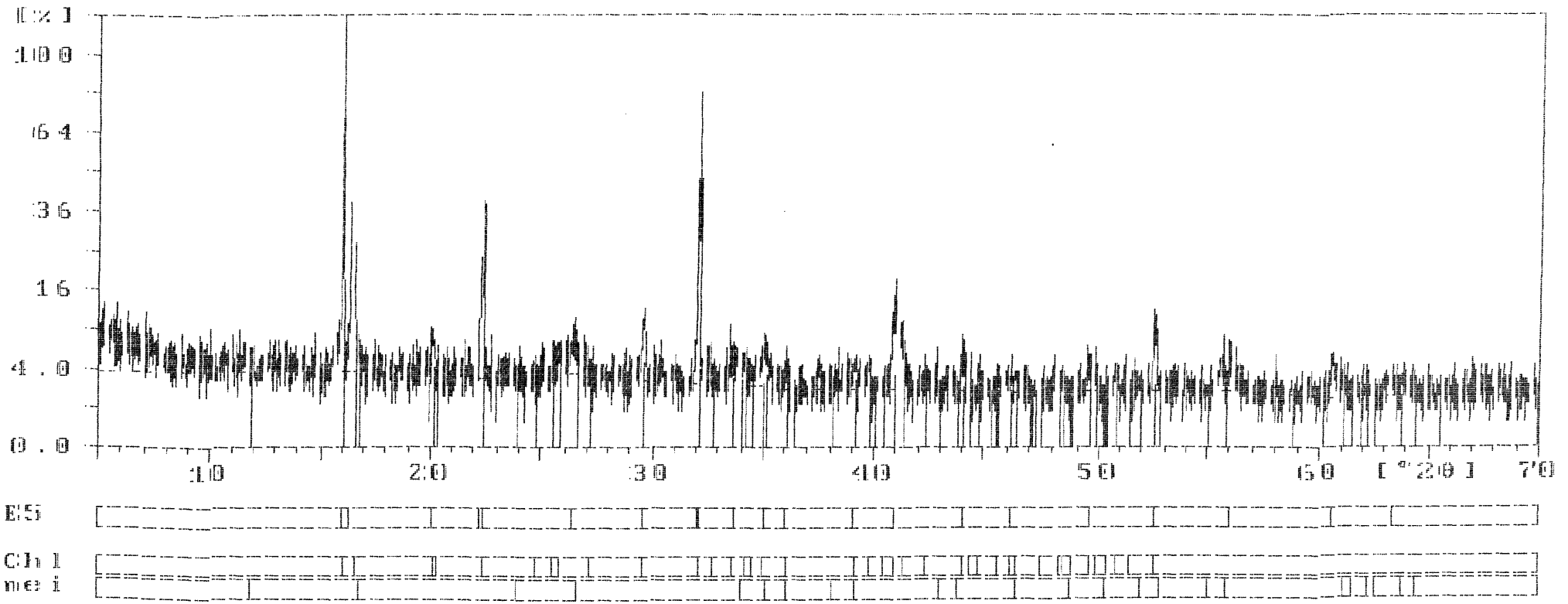

File: SAMPLE5.DI 25-Oct-2000 10:10

Philips Analytical PC-APD Diffraction Software

Sample identification: SAMPLE 5
Data measured at: 25-Oct-2000 9:43:00

Diffractometer type: PW1710 BASED
Tube anode: Cu
Generator tension [kV]: 35
Generator current [mA]: 28
Wavelength Alpha1 [Å]: 1.54056
Wavelength Alpha2 [Å]: 1.54439
Intensity ratio (alpha2/alpha1): 0.500
Divergence slit: 1°
Receiving slit: 0.1
Monochromator used: YES

Start angle [°2θ]: 5.000
End angle [°2θ]: 70.000
Step size [°2θ]: 0.020
Maximum intensity: 237.1600
Time per step [s]: 0.500
Type of scan: CONTINUOUS

Minimum peak tip width: 0.00
Maximum peak tip width: 1.00
Peak base width: 2.00
Minimum significance: 0.75
Number of peaks: 21

Angle [°2θ]	d-value α1 [Å]	d-value α2 [Å]	Peak width [°2θ]	Peak int [counts]	Back. int [counts]	Rel. int [%]	Signif.
16.040	5.5210	5.5347	0.080	237	9	100.0	4.67
16.475	5.3762	5.3895	0.060	85	9	35.7	0.91
20.070	4.4206	4.4315	0.200	12	8	5.2	1.39
22.190	4.0028	4.0127	0.060	49	7	20.7	1.94
22.335	3.9771	3.9870	0.080	86	7	36.5	1.70
26.475	3.3638	3.3722	0.480	9	8	3.8	1.53
29.615	3.0139	3.0214	0.240	21	7	8.9	2.73
32.085	2.7873	2.7943	0.060	185	6	78.0	1.33
32.190	2.7785	2.7854	0.040	83	6	34.9	1.31
33.735	2.6547	2.6613	0.480	5	6	2.0	0.92
35.055	2.5577	2.5640	0.400	10	6	4.1	1.42
36.060	2.4887	2.4949	0.240	5	5	2.2	0.85
39.160	2.2985	2.3042	0.960	3	5	1.2	1.15
41.005	2.1992	2.2047	0.060	37	5	15.7	0.79
44.120	2.0509	2.0560	0.320	7	5	3.1	1.61
46.210	1.9629	1.9678	0.960	3	4	1.1	0.98
49.755	1.8310	1.8356	0.480	3	5	1.2	1.15
52.570	1.7394	1.7437	0.240	22	5	9.3	2.91
56.080	1.6386	1.6427	0.240	8	5	3.5	1.32
60.655	1.5255	1.5293	0.240	8	4	3.3	1.50
63.330	1.4673	1.4710	0.400	3	4	1.2	0.83

Sample identification: SAMPLE 6 25-Oct-2000 15:53

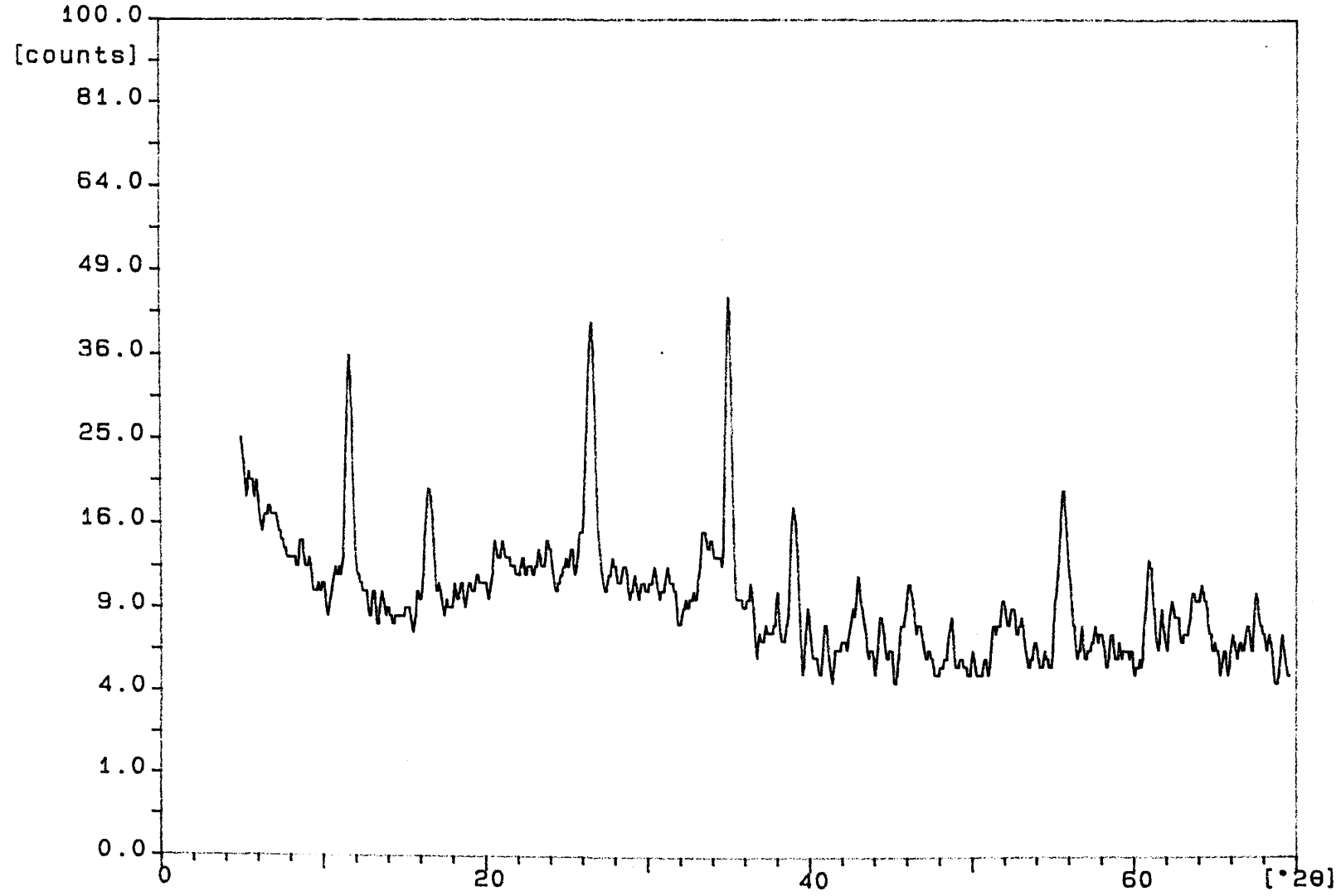

SAMPLE6.SM

File: SAMPLE6.DI 25-Oct-2000 15:30

Philips Analytical PC-APD Diffraction Software

Sample identification: SAMPLE 6
Data measured at: 25-Oct-2000 15:03:00

Diffractometer type: PW1710 BASED
Tube anode: Cu
Generator tension [kV]: 35
Generator current [mA]: 28
Wavelength Alpha1 [Å]: 1.54056
Wavelength Alpha2 [Å]: 1.54439
Intensity ratio (alpha2/alpha1): 0.500
Divergence slit: 1°
Receiving slit: 0.1
Monochromator used: YES

Start angle [°2θ]: 5.000
End angle [°2θ]: 70.000
Step size [°2θ]: 0.020
Maximum intensity: 38.4400
Time per step [s]: 0.500
Type of scan: CONTINUOUS

Minimum peak tip width: 0.00
Maximum peak tip width: 1.00
Peak base width: 2.00
Minimum significance: 0.75
Number of peaks: 10

Angle [°2θ]	d-value α1 [Å]	d-value α2 [Å]	Peak width [°2θ]	Peak int [counts]	Back. int [counts]	Rel. int [%]	Signif.
11.750	7.5253	7.5440	0.160	27	10	70.3	0.79
16.700	5.3042	5.3174	0.560	8	9	20.4	2.66
26.500	3.3607	3.3691	0.240	31	12	81.6	1.12
34.970	2.5637	2.5701	0.240	38	12	100.0	2.69
39.010	2.3070	2.3127	0.480	13	6	33.7	2.48
43.055	2.0992	2.1044	0.480	5	6	13.8	1.08
46.145	1.9655	1.9704	0.640	5	6	12.6	0.77
55.665	1.6498	1.6539	0.400	14	6	35.6	1.58
60.940	1.5190	1.5228	0.320	6	6	15.0	0.88
64.105	1.4515	1.4551	0.960	4	7	9.4	0.81

Appendix 4

X-Ray Diffraction Data for Samples of Marine Corrosion Products from the Wrought Iron Hull of the ss Great Britain, Laboratory Ferrous Chloride and Laboratory-Synthesised βFeOOH

The following pages contain the XRD spectra and powder diffraction file data for samples of iron corrosion products removed from the hull of the ss Great Britain and laboratory ferrous chloride that was stored in ambient and desiccated conditions. The analyses and identifications were conducted by Dr A. Oldroyd at the Department of Earth Sciences, Cardiff University, without prior knowledge of their likely composition.

The samples submitted were as follows,

Sample 1 Clear crystals removed from a peculiar area of one-time seepage on the underside of the ss Great Britain Hull. The crystals were insoluble in tepid water. Sampling attempted to avoid areas possibly contaminated with iron staining. The sample identification was gypsum ($CaSO_4.2H_2O$).

Sample 2 Corrosion product removed from scales of corrosion within the hull of the ss Great Britain. Only the orange/brown products were of interest but it was difficult to avoid sampling magnetite also (using a scalpel). This sample was taken to confirm the presence of ferrous chloride and/or βFeOOH (akaganéite). The sample was confirmed as βFeOOH (akaganéite).

Sample 3 Corrosion product removed from scales of corrosion from the exterior starboard side of the hull of the ss Great Britain. Only the orange/brown products were of interest but it was difficult to avoid sampling magnetite also (using a scalpel). This sample was taken to confirm the presence of ferrous chloride and/or βFeOOH (akaganéite). The sample was confirmed as βFeOOH (akaganéite).

Sample 4 Corrosion product removed from scales of corrosion from the exterior port side of the hull of the ss Great Britain. Only the orange/brown products were of interest but it was difficult to avoid sampling magnetite also (using a scalpel). This sample was taken to confirm the presence of ferrous chloride and/or βFeOOH (akaganéite). This sample was confirmed as Fe_3O_4 (magnetite) after a second analysis using the Debye-Scherrer camera diffractometer.

Sample 5 $FeCl_2.4H_2O$ which had been stored with archaeological iron in a silica gel desiccated environment. Likely to comprise $FeCl_2.2H_2O$ and no βFeOOH. The sample was confirmed as iron chloride hydrate ($FeCl_2.4H_2O$).

Sample 6 $FeCl_2.4H_2O$ which had been stored under ambient conditions in the laboratory over the same period as for sample 5. Partial oxidation may have occurred at the crystal surfaces during long-term storage. Likely to comprise $FeCl_2.4H_2O$ and possibly βFeOOH. The sample was confirmed as iron chloride hydrate ($FeCl_2.4H_2O$).

Sample 7 Ferrous chloride crystals were placed in a desiccator at 92%RH and deliquesced. The saturated solution was subsequently desiccated and the evaporate residue was analysed. Likely to comprise ferrous chloride as crystalline $FeCl_2.4H_2O$, amorphous ferrous chloride or with some βFeOOH if partially oxidised. The sample was found to be amorphous. This represents potentially important data for the identification of ferrous chloride using XRD. Any amorphous ferrous chloride will not be identified using this technique. XRD analyses of iron corrosion products where the presence of ferrous chloride is suspected should also be analysed by SEM-EDX and/or FTIR-ATR in order to confirm the presence of chloride and its form.

Sample 8 βFeOOH synthesised by the author in a conventional glass laboratory desiccator maintained at 92%RH via the aerial oxidation of iron powder and ferrous chloride tetrahydrate. This sample was taken from beneath the surface of the synthesised mass. On this occasion the sample was desiccated until placed in the XRD unit in an attempt to identify any solid crystalline ferrous chloride present due to desiccation of an otherwise amorphous, aqueous solution at higher, ambient, humidities. None was identified and the sample was confirmed to be pure βFeOOH.

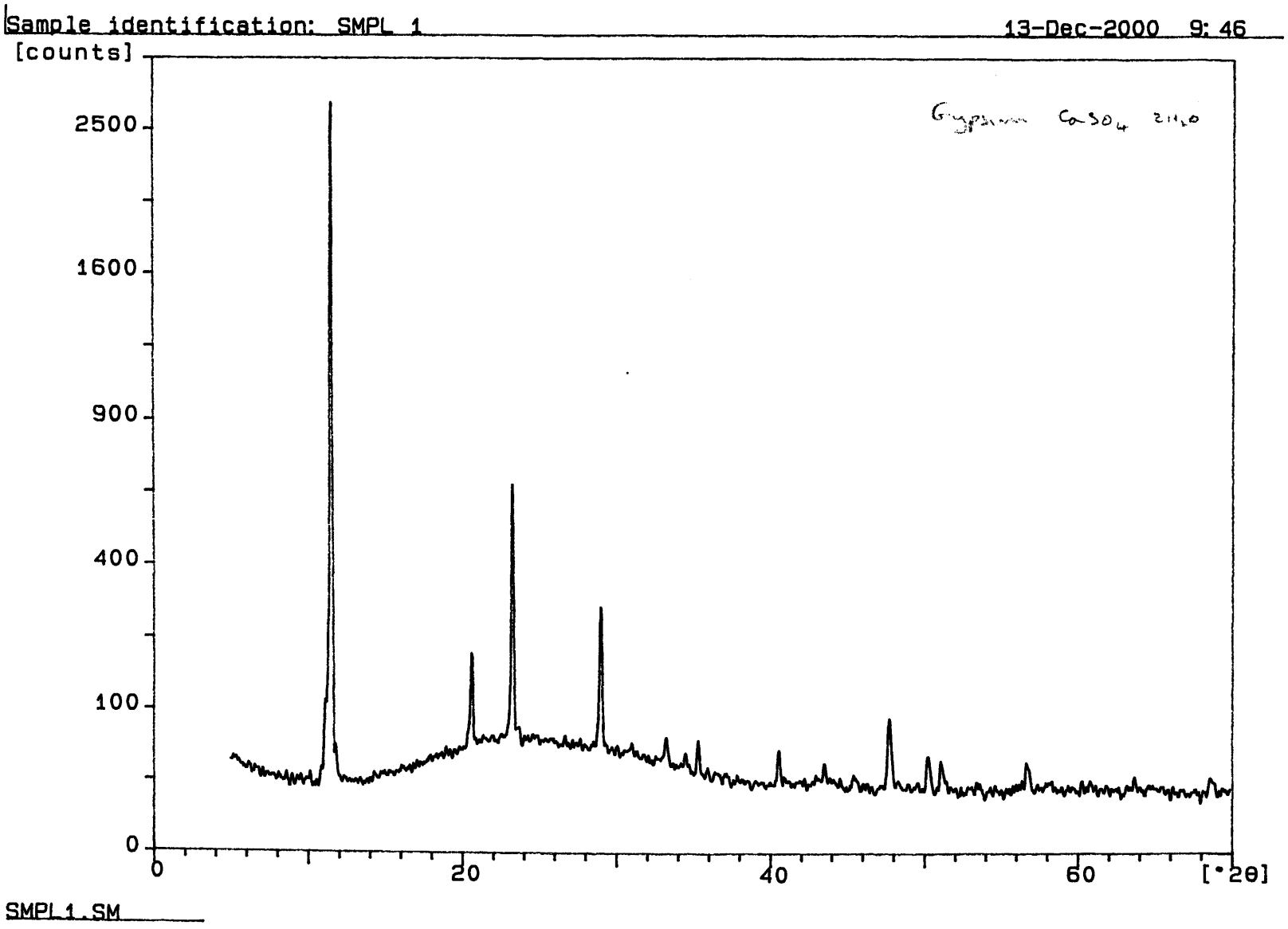
Sample identification: SMPL 1
13-Dec-2000 9:46
[counts]
2500
1600
900
400
100
0
0
20
40
60
[°2θ]
Gypsum CaSO4 2H2O
SMPL1.SM

File: SMPL1.DI 12-Dec-2000 10:48

Philips Analytical PC-APD Diffraction Software

Sample identification: SMPL 1
Data measured at: 12-Dec-2000 10:20:00

Diffractometer type: PW1710 BASED
Tube anode: Cu
Generator tension [kV]: 35
Generator current [mA]: 28
Wavelength Alpha1 [Å]: 1.54056
Wavelength Alpha2 [Å]: 1.54439
Intensity ratio (alpha2/alpha1): 0.500
Divergence slit: 1°
Receiving slit: 0.1
Monochromator used: YES

Start angle [°2θ]: 5.000
End angle [°2θ]: 70.000
Step size [°2θ]: 0.020
Maximum intensity: 4096.000
Time per step [s]: 0.500
Type of scan: CONTINUOUS

Minimum peak tip width: 0.00
Maximum peak tip width: 1.00
Peak base width: 2.00
Minimum significance: 0.75
Number of peaks: 17

Angle [°2θ]	d-value α1 [Å]	d-value α2 [Å]	Peak width [°2θ]	Peak int [counts]	Back. int [counts]	Rel. int [%]	Signif.
11.090	7.9717	7.9915	0.060	137	23	3.3	0.99
11.530	7.6684	7.6875	0.080	4096	24	100.0	16.21
20.630	4.3018	4.3125	0.080	196	52	4.8	2.04
23.280	3.8178	3.8273	0.100	790	58	19.3	7.45
29.005	3.0759	3.0836	0.160	282	52	6.9	9.12
33.230	2.6939	2.7006	0.160	27	40	0.7	0.82
34.540	2.5946	2.6011	0.240	12	35	0.3	0.80
35.320	2.5391	2.5454	0.160	29	32	0.7	1.39
40.520	2.2244	2.2300	0.060	38	23	0.9	1.43
43.505	2.0785	2.0836	0.160	18	22	0.5	0.97
45.495	1.9921	1.9970	0.400	6	21	0.1	1.17
47.700	1.9050	1.9097	0.080	77	20	1.9	0.99
50.190	1.8162	1.8207	0.200	32	19	0.8	1.55
51.045	1.7878	1.7922	0.160	22	19	0.5	1.39
56.735	1.6212	1.6252	0.240	17	20	0.4	0.92
63.710	1.4595	1.4631	0.640	5	20	0.1	0.76
68.565	1.3675	1.3709	0.320	11	18	0.3	0.86

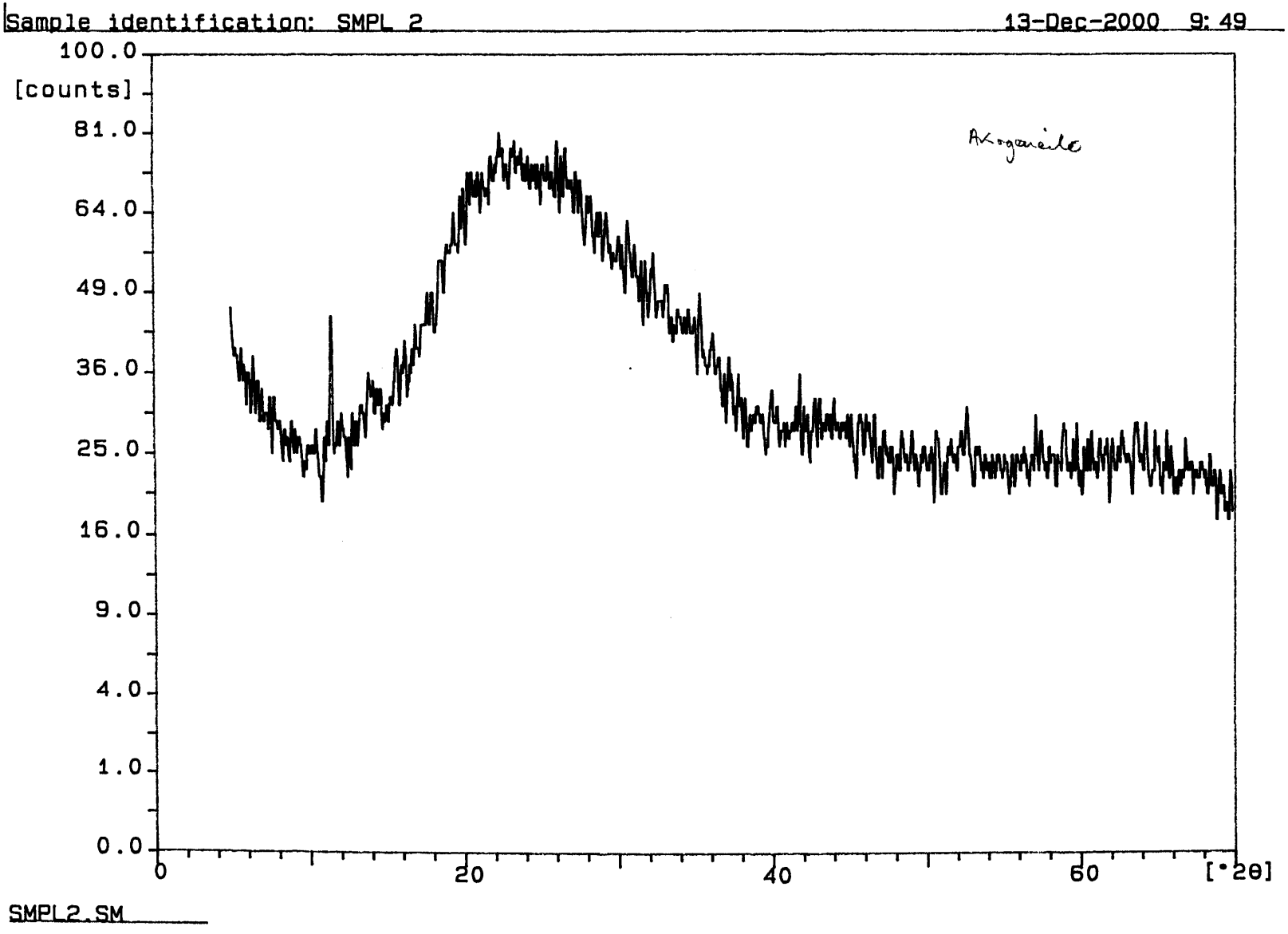
Sample identification: SMPL 2
13-Dec-2000 9:49
100.0
[counts]
81.0
64.0
49.0
36.0
25.0
16.0
9.0
4.0
1.0
0.0
0
20
40
60
[°2θ]
SMPL2.SM

File: SMPL2.DI 12-Dec-2000 11:53

Philips Analytical PC-APD Diffraction Software

Sample identification:	SMPL 2
Data measured at:	12-Dec-2000 11:26:00
Diffractometer type:	PW1710 BASED
Tube anode:	Cu
Generator tension [kV]:	35
Generator current [mA]:	28
Wavelength Alpha1 [Å]:	1.54056
Wavelength Alpha2 [Å]:	1.54439
Intensity ratio (alpha2/alpha1):	0.500
Divergence slit:	1°
Receiving slit:	0.1
Monochromator used:	YES
Start angle [°2θ]:	5.000
End angle [°2θ]:	70.000
Step size [°2θ]:	0.020
Maximum intensity:	32.4900
Time per step [s]:	0.500
Type of scan:	CONTINUOUS
Minimum peak tip width:	0.00
Maximum peak tip width:	1.00
Peak base width:	2.00
Minimum significance:	0.75
Number of peaks:	1

Angle [°2θ]	d-value α1 [Å]	d-value α2 [Å]	Peak width [°2θ]	Peak int [counts]	Back. int [counts]	Rel. int [%]	Signif.
11.485	7.6984	7.7175	0.060	32	24	100.0	0.83

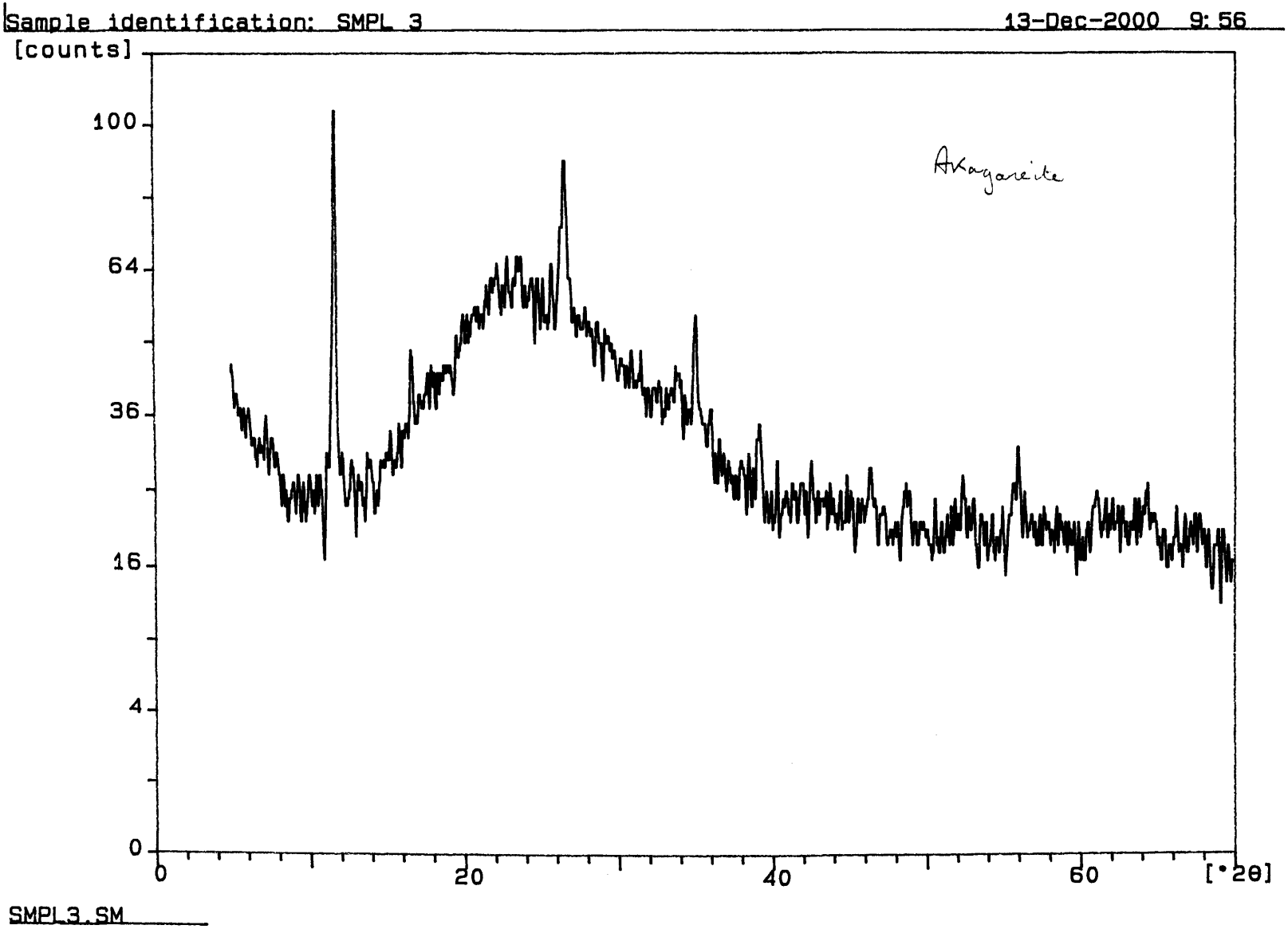
Sample identification: SMPL 3
13-Dec-2000 9:56
[counts]
100
64
36
16
4
0
0
20
40
60
[°2θ]
Aragonite
SMPL3.SM

File: SMPL3.DI 12-Dec-2000 12:25

Philips Analytical PC-APD Diffraction Software

Sample identification:	SMPL 3
Data measured at:	12-Dec-2000 11:58:00
Diffractometer type:	PW1710 BASED
Tube anode:	Cu
Generator tension [kV]:	35
Generator current [mA]:	28
Wavelength Alpha1 [Å]:	1.54056
Wavelength Alpha2 [Å]:	1.54439
Intensity ratio (alpha2/alpha1):	0.500
Divergence slit:	1°
Receiving slit:	0.1
Monochromator used:	YES
Start angle [°2θ]:	5.000
End angle [°2θ]:	70.000
Step size [°2θ]:	0.020
Maximum intensity:	92.1600
Time per step [s]:	0.500
Type of scan:	CONTINUOUS
Minimum peak tip width:	0.00
Maximum peak tip width:	1.00
Peak base width:	2.00
Minimum significance:	0.75
Number of peaks:	8

Angle [°2θ]	d-value α1 [Å]	d-value α2 [Å]	Peak width [°2θ]	Peak int [counts]	Back. int [counts]	Rel. int [%]	Signif.
11.745	7.5285	7.5472	0.100	92	24	100.0	1.85
26.580	3.3508	3.3591	0.200	42	55	45.8	0.95
35.100	2.5545	2.5609	0.240	18	34	19.1	1.56
39.160	2.2985	2.3042	0.320	12	23	12.5	1.05
55.775	1.6468	1.6509	0.640	7	19	7.3	1.02
61.065	1.5162	1.5200	0.400	5	19	5.3	0.79
64.265	1.4482	1.4518	0.960	4	19	4.3	0.77
69.180	1.3568	1.3602	0.200	6	17	6.2	0.91

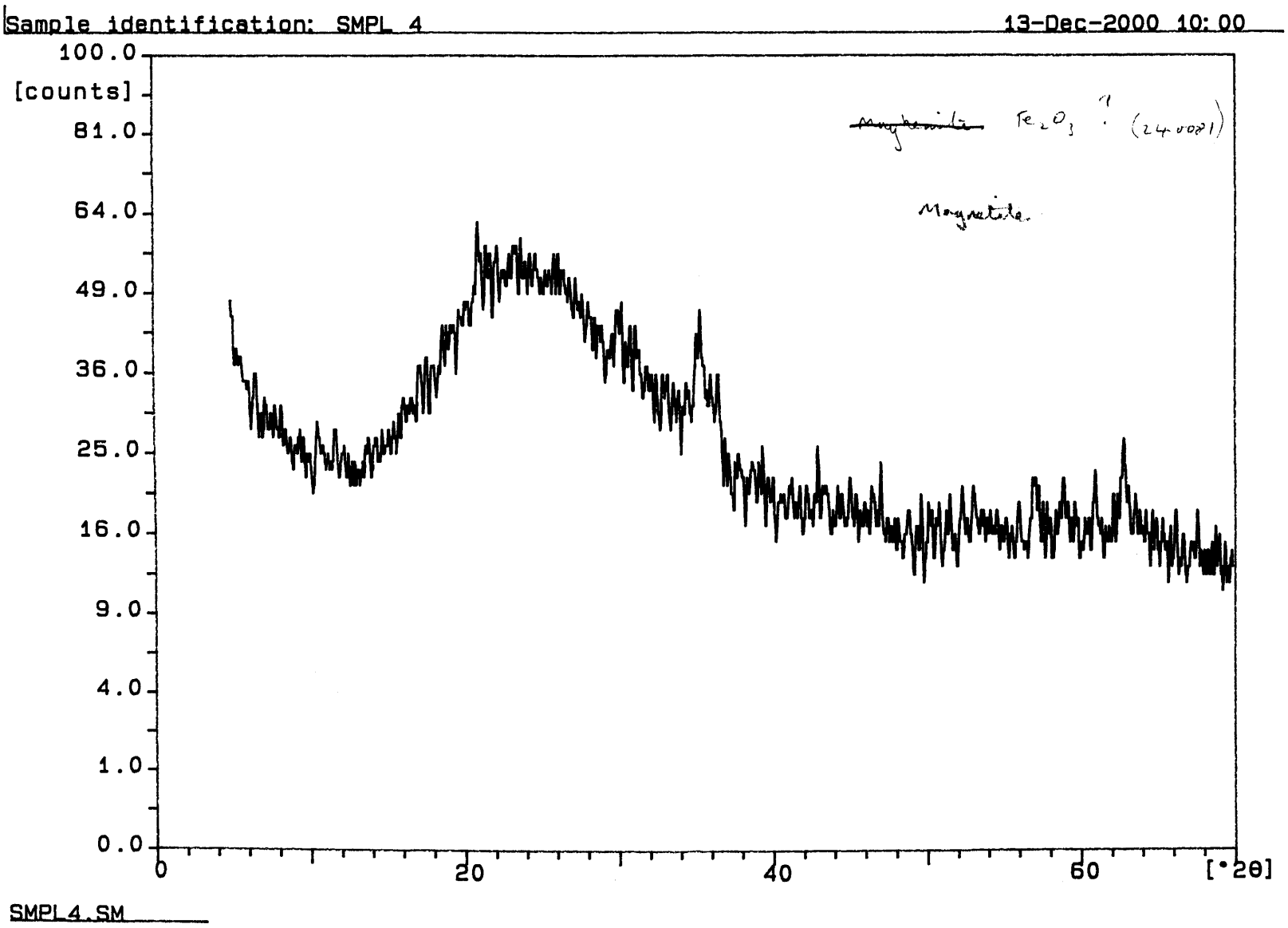
Sample identification: SMPL 4
13-Dec-2000 10:00
100.0
[counts]
81.0
64.0
49.0
36.0
25.0
16.0
9.0
4.0
1.0
0.0
0
20
40
60
[°2θ]
~~magnetite~~ Fe_2O_3 ? (24-0072)
Magnetite.
SMPL4.SM

File: SMPL4.DI 12-Dec-2000 13:28

Philips Analytical PC-APD Diffraction Software

Sample identification:	SMPL 4
Data measured at:	12-Dec-2000 13:01:00
Diffractometer type:	PW1710 BASED
Tube anode:	Cu
Generator tension [kV]:	35
Generator current [mA]:	28
Wavelength Alpha1 [Å]:	1.54056
Wavelength Alpha2 [Å]:	1.54439
Intensity ratio (alpha2/alpha1):	0.500
Divergence slit:	1°
Receiving slit:	0.1
Monochromator used:	YES
Start angle [°2θ]:	5.000
End angle [°2θ]:	70.000
Step size [°2θ]:	0.020
Maximum intensity:	18.4900
Time per step [s]:	0.500
Type of scan:	CONTINUOUS
Minimum peak tip width:	0.00
Maximum peak tip width:	1.00
Peak base width:	2.00
Minimum significance:	0.75
Number of peaks:	5

Angle [°2θ]	d-value α1 [Å]	d-value α2 [Å]	Peak width [°2θ]	Peak int [counts]	Back. int [counts]	Rel. int [%]	Signif.
21.300	4.1680	4.1783	0.960	6	48	31.2	0.79
31.920	2.8014	2.8083	0.060	18	35	100.0	0.77
35.320	2.5391	2.5454	0.480	15	27	82.3	1.54
57.030	1.6135	1.6175	0.480	6	15	33.8	1.08
62.745	1.4796	1.4833	0.960	6	17	33.8	2.17

CoKα = 1·78897

A.H.

DEPARTMENT OF MINERAL EXPLOITATION, UNIVERSITY COLLEGE CARDIFF, INDUSTRIAL MINERALOGY RESEARCH CENTRE

DEBYE-SCHERRER X-RAY POWDER PHOTOGRAPH

Sheet No: of

Film No: Date: 18/12/00 Radiation: CoKα Research Worker: A Oldroyd Identification:

Exposure Time and film type: Shows Room REF 392

Outlet Collimator Coordinate = 103·1

Inlet Collimator Coordinate = 282·9

Difference (d) = 179·8

Film Correction Factor (180/d) =

Sample: Sample 4 — Magnetite.

Polished Section No:

Mounting Technique:

Cell Parameters:

Line No:	I	ā, a_1 or a_2	Left(mm)	Middle(mm)	Right(mm)	Sum(mm)	4θ(mm)	2θ(mm)	θ° corrd.	d Å	hkl
	5		78·50	128·95		207·45	50·45		12·6125	4·09	
	3		71·90	135·85		207·75	63·95		15·9875	3·25	
	2		67·95	139·50		207·45	71·55		17·8875	2·91	
	1		64·30	143·10		207·40	78·80		19·70	2·65	
	10		61·60	145·65		207·25	84·05		21·0125	2·49	1
	4		60·40	147·05		207·45	86·65		21·6625	2·42	1
	2		52·40	155·20		207·60	102·80		25·70	2·06	
	3		35·80	172·00		207·80	136·20		34·05	1·60	
	5		28·80	179·10		207·90	150·30		37·575	1·47	

Sample identification: SMPL 5b 13-Dec-2000 10:04

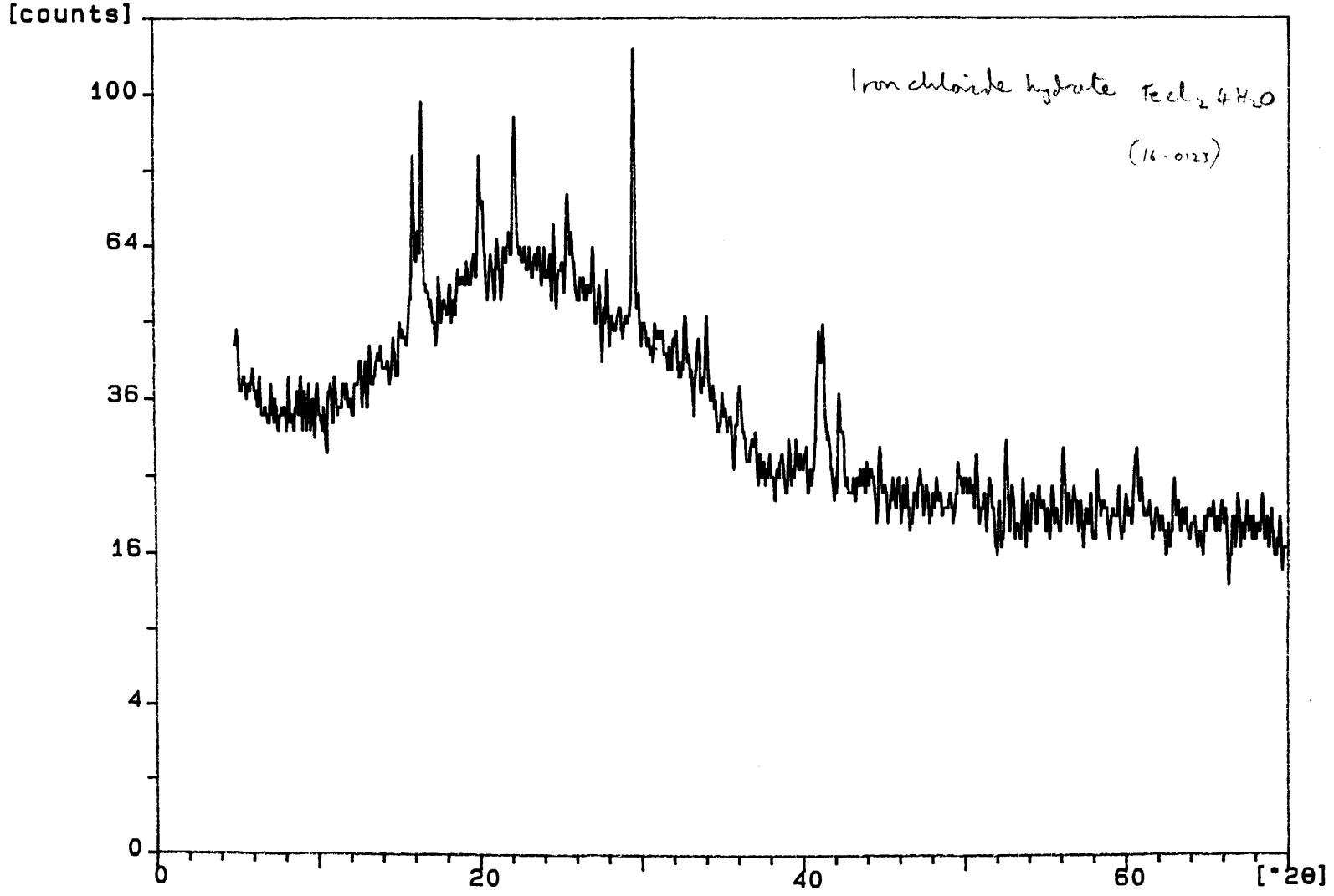

SMPL5B.SM

File: SMPL5B.DI 12-Dec-2000 16:42

Philips Analytical PC-APD Diffraction Software

Sample identification:	SMPL 5b
Data measured at:	12-Dec-2000 16:14:00
Diffractometer type:	PW1710 BASED
Tube anode:	Cu
Generator tension [kV]:	35
Generator current [mA]:	28
Wavelength Alpha1 [Å]:	1.54056
Wavelength Alpha2 [Å]:	1.54439
Intensity ratio (alpha2/alpha1):	0.500
Divergence slit:	1°
Receiving slit:	0.1
Monochromator used:	YES
Start angle [°2θ]:	5.000
End angle [°2θ]:	70.000
Step size [°2θ]:	0.020
Maximum intensity:	81.0000
Time per step [s]:	0.500
Type of scan:	CONTINUOUS
Minimum peak tip width:	0.00
Maximum peak tip width:	1.00
Peak base width:	2.00
Minimum significance:	0.75
Number of peaks:	11

Angle [°2θ]	d-value α1 [Å]	d-value α2 [Å]	Peak width [°2θ]	Peak int [counts]	Back. int [counts]	Rel. int [%]	Signif.
16.005	5.5330	5.5467	0.080	40	45	49.0	1.52
16.550	5.3520	5.3653	0.060	77	48	95.6	2.56
20.130	4.4075	4.4185	0.400	21	55	26.1	1.78
22.250	3.9921	4.0020	0.200	28	59	34.7	1.49
25.530	3.4862	3.4948	0.160	22	56	27.3	0.76
29.595	3.0159	3.0234	0.140	81	48	100.0	3.36
40.945	2.2023	2.2078	0.480	20	25	25.0	2.02
42.330	2.1334	2.1387	0.320	9	24	11.1	1.00
52.705	1.7353	1.7396	0.480	4	18	4.9	0.95
56.140	1.6370	1.6410	0.200	8	19	9.7	0.91
60.650	1.5256	1.5294	0.280	8	19	9.7	0.84

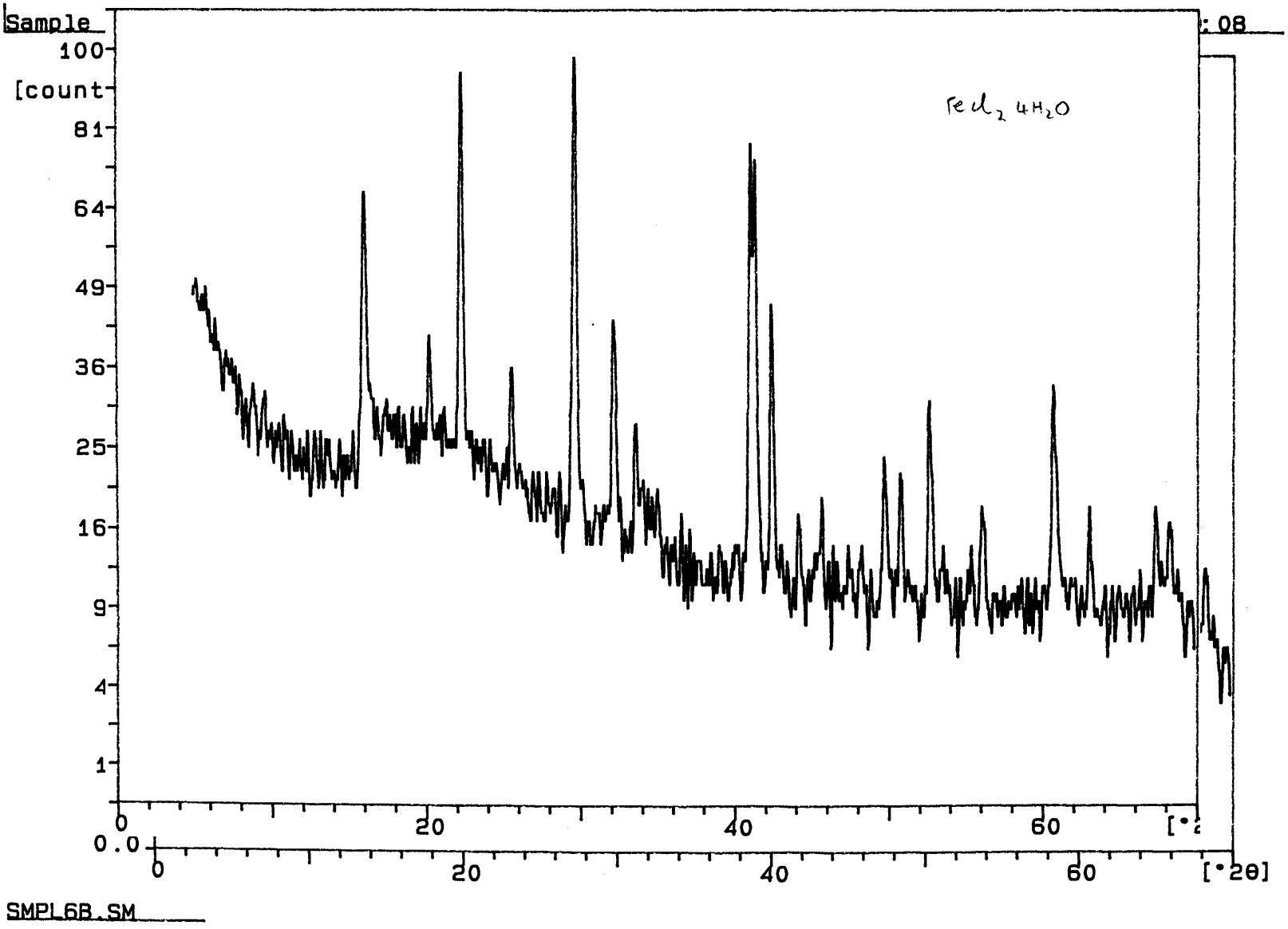
Sample
: 08
100
[count
81
64
49
36
25
16
9
4
1
0.0
0
20
40
60
[•2θ]
FeCl2 4H2O
SMPL6B.SM

File: SMPL6B.DI 12-Dec-2000 16:13

Philips Analytical PC-APD Diffraction Software

Sample identification: SMPL 6b
Data measured at: 12-Dec-2000 15:46:00

Diffractometer type: PW1710 BASED
Tube anode: Cu
Generator tension [kV]: 35
Generator current [mA]: 28
Wavelength Alpha1 [Å]: 1.54056
Wavelength Alpha2 [Å]: 1.54439
Intensity ratio (alpha2/alpha1): 0.500
Divergence slit: 1°
Receiving slit: 0.1
Monochromator used: YES

Start angle [°2θ]: 5.000
End angle [°2θ]: 70.000
Step size [°2θ]: 0.020
Maximum intensity: 72.2500
Time per step [s]: 0.500
Type of scan: CONTINUOUS

Minimum peak tip width: 0.00
Maximum peak tip width: 1.00
Peak base width: 2.00
Minimum significance: 0.75
Number of peaks: 22

Angle [°2θ]	d-value α1 [Å]	d-value α2 [Å]	Peak width [°2θ]	Peak int [counts]	Back. int [counts]	Rel. int [%]	Signif.
5.535	15.9534	15.9930	0.960	10	30	13.3	1.02
16.075	5.5090	5.5227	0.240	41	20	56.7	2.33
20.260	4.3795	4.3904	0.240	13	20	17.9	1.38
22.325	3.9789	3.9888	0.200	71	19	97.7	3.10
25.610	3.4755	3.4841	0.240	14	16	18.9	1.99
29.650	3.0105	3.0179	0.100	72	13	100.0	0.77
32.130	2.7835	2.7905	0.280	26	12	36.0	3.15
33.650	2.6612	2.6678	0.240	12	12	17.0	1.48
37.080	2.4225	2.4285	0.080	6	9	8.0	0.76
40.990	2.2000	2.2055	0.120	61	8	84.2	0.95
41.295	2.1845	2.1899	0.160	61	8	84.2	1.09
42.370	2.1315	2.1368	0.100	36	7	49.8	1.35
44.185	2.0481	2.0531	0.240	5	7	7.3	0.90
45.535	1.9904	1.9954	0.480	4	7	5.5	1.06
46.390	1.9557	1.9606	0.120	5	7	7.3	0.86
49.710	1.8326	1.8371	0.240	12	6	16.0	2.36
50.765	1.7970	1.8014	0.240	10	6	14.2	2.04
52.585	1.7390	1.7433	0.160	18	6	25.6	0.95
56.105	1.6379	1.6420	0.240	7	6	9.4	1.69
60.670	1.5251	1.5289	0.120	20	6	28.0	1.27
63.045	1.4733	1.4769	0.240	8	6	10.9	1.30
67.265	1.3907	1.3942	0.200	7	6	9.4	0.90

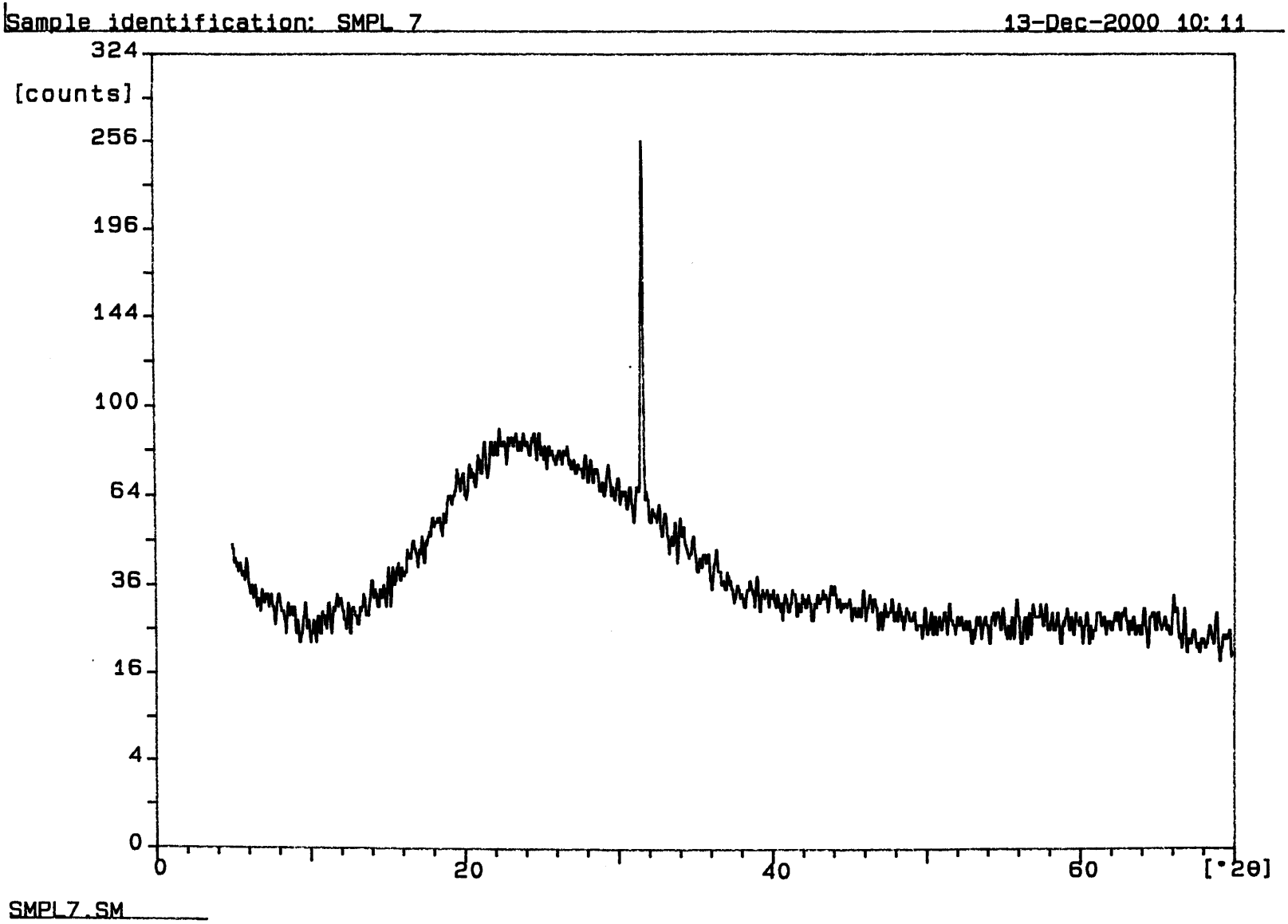
Sample identification: SMPL 7
13-Dec-2000 10:11
[counts]
324
256
196
144
100
64
36
16
4
0
0
20
40
60
[°2θ]
SMPL7.SM

File: SMPL7.DI 12-Dec-2000 10:15

Philips Analytical PC-APD Diffraction Software

Sample identification:	SMPL 7
Data measured at:	12-Dec-2000 9:47:00
Diffractometer type:	PW1710 BASED
Tube anode:	Cu
Generator tension [kV]:	35
Generator current [mA]:	28
Wavelength Alpha1 [Å]:	1.54056
Wavelength Alpha2 [Å]:	1.54439
Intensity ratio (alpha2/alpha1):	0.500
Divergence slit:	1°
Receiving slit:	0.1
Monochromator used:	YES
Start angle [°2θ]:	5.000
End angle [°2θ]:	70.000
Step size [°2θ]:	0.020
Maximum intensity:	295.8400
Time per step [s]:	0.500
Type of scan:	CONTINUOUS
Minimum peak tip width:	0.00
Maximum peak tip width:	1.00
Peak base width:	2.00
Minimum significance:	0.75
Number of peaks:	2

Angle [°2θ]	d-value α1 [Å]	d-value α2 [Å]	Peak width [°2θ]	Peak int [counts]	Back. int [counts]	Rel. int [%]	Signif.
31.545	2.8338	2.8408	0.060	296	59	100.0	1.06
35.795	2.5065	2.5127	0.560	3	41	1.0	0.86

Cobalt radiation = 1.78897 $n\lambda = 2d\sin\theta$ $d = \frac{\lambda}{2\sin\theta}$

A.H.

DEPARTMENT OF MINERAL EXPLOITATION, UNIVERSITY COLLEGE CARDIFF, INDUSTRIAL MINERALOGY RESEARCH CENTRE

DEBYE-SCHERRER X-RAY POWDER PHOTOGRAPH

Sheet No: of

Film No: Date: 14/12/00 Radiation: Co Kα Research Worker: A Oldroyd Identification:

Exposure Time and film type: 5 hours, OGF 392 Kodak

Outlet Collimator Coordinate = 96.6

Inlet Collimator Coordinate = 276.7

Difference (d) = 180.1

Film Correction Factor ($180/d$) =

Sample: Sample 7 — Arcoganeite

Cell Parameters:

Polished Section No:

Mounting Technique:

Line No:	I	$\bar{a}$, a_1 or a_2	Left(mm)	Middle(mm)	Right(mm)	Sum(mm)	4θ(mm)	2θ(mm)	θ° corrd.	d Å.	hkl
	10		82.65	111.30		193.95	28.65		7.1625	7.17	
	10		65.25	128.75		194.00	63.50		15.875	3.27	
	4		59.35	134.60		193.95	75.25		18.8125	2.77	
	9		55.30	138.40		193.70	83.10		20.775	2.52	
	2		50.75	143.30		194.05	92.55		23.1375	2.27	

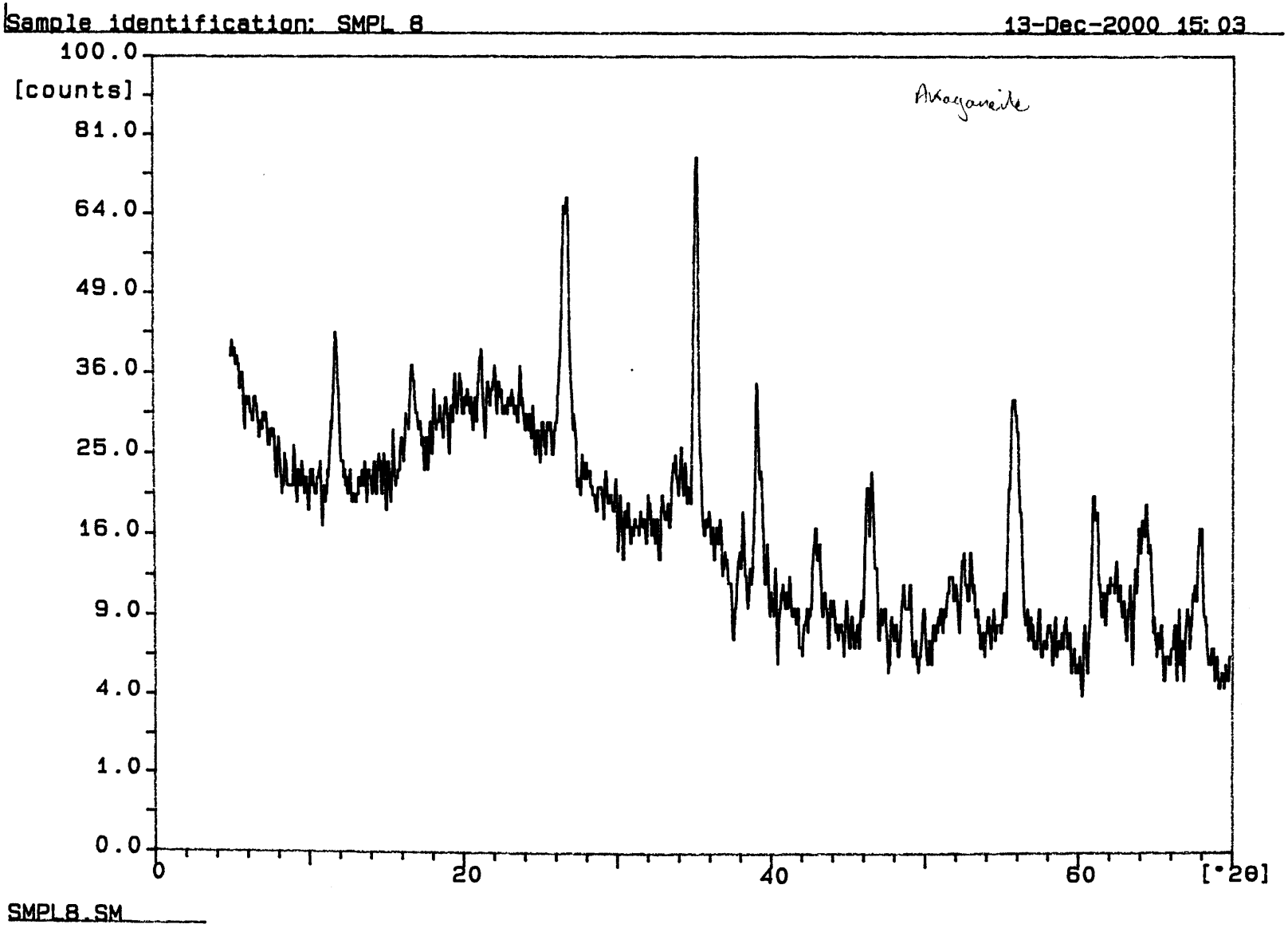
Sample identification: SMPL 8
13-Dec-2000 15:03
100.0
[counts]
81.0
64.0
49.0
36.0
25.0
16.0
9.0
4.0
1.0
0.0
0
20
40
60
[°2θ]
Aragonite
SMPL8.SM

File: SMPL8.DI 13-Dec-2000 14:42

Philips Analytical PC-APD Diffraction Software

Sample identification:	SMPL 8
Data measured at:	13-Dec-2000 14:14:00
Diffractometer type:	PW1710 BASED
Tube anode:	Cu
Generator tension [kV]:	35
Generator current [mA]:	28
Wavelength Alpha1 [Å]:	1.54056
Wavelength Alpha2 [Å]:	1.54439
Intensity ratio (alpha2/alpha1):	0.500
Divergence slit:	1°
Receiving slit:	0.1
Monochromator used:	YES
Start angle [°2θ]:	5.000
End angle [°2θ]:	70.000
Step size [°2θ]:	0.020
Maximum intensity:	57.7600
Time per step [s]:	0.500
Type of scan:	CONTINUOUS
Minimum peak tip width:	0.00
Maximum peak tip width:	1.00
Peak base width:	2.00
Minimum significance:	0.75
Number of peaks:	14

Angle [°2θ]	d-value α1 [Å]	d-value α2 [Å]	Peak width [°2θ]	Peak int [counts]	Back. int [counts]	Rel. int [%]	Signif.
11.870	7.4495	7.4680	0.240	22	20	38.2	2.09
16.780	5.2791	5.2923	0.480	11	25	18.9	1.46
26.555	3.3539	3.3622	0.240	31	25	54.3	0.84
35.200	2.5475	2.5538	0.280	58	15	100.0	4.82
38.065	2.3621	2.3679	0.320	5	10	9.2	1.07
39.095	2.3022	2.3079	0.120	27	10	46.8	1.22
42.940	2.1045	2.1097	0.640	8	7	13.6	1.52
46.415	1.9547	1.9596	0.480	13	7	22.4	1.11
48.810	1.8643	1.8689	0.640	3	6	5.6	1.05
52.725	1.7347	1.7390	0.960	3	8	4.4	1.68
55.740	1.6478	1.6519	0.720	24	8	41.6	6.39
61.050	1.5166	1.5203	0.400	11	8	18.9	1.76
64.355	1.4464	1.4500	0.800	10	8	16.6	2.63
67.885	1.3795	1.3830	0.320	10	6	16.6	1.10

Appendix 5

X-ray diffraction (XRD) powder diffraction reference patterns for $FeCl_2.4H_2O$ and akaganéite (βFeOOH)

Name : Iron Chloride Hydrate
Formula : FeCl2!4H2O
Elements : H, O, Cl, Fe
Groups : H2O
Crystal type : Monoclinic
Subfiles : Inorganic, Common phases, Forensics
Pattern deleted: NO

d value	Angle	Rel.Int.
5.5000	16.102	85
5.3300	16.619	80
4.3900	20.212	30
4.3600	20.352	16
3.9700	22.376	100
3.5900	24.780	2
3.4800	25.577	25
3.4300	25.956	10
3.2700	27.250	2
3.0100	29.655	65
2.7770	32.208	45
2.7260	32.828	8
2.6630	33.627	16
2.6210	34.183	10
2.5910	34.591	1
2.5670	34.925	4
2.4850	36.116	6
2.2930	39.259	2
2.2620	39.819	6
2.2320	40.378	4
2.1970	41.050	40
2.1820	41.345	40
2.1290	42.423	35
2.0510	44.119	4
2.0420	44.324	2
2.0220	44.786	2
1.9860	45.643	4
1.9650	46.159	1
1.9530	46.459	1
1.9140	47.464	4
1.8860	48.213	4
1.8780	48.431	2
1.8580	48.986	2
1.8330	49.699	20
1.8240	49.961	2
1.8050	50.524	2
1.7960	50.795	6
1.7760	51.409	2
1.7390	52.585	16

Reference pattern: 34-1266 26-Oct-2000 08:58

Name : Iron Oxide Hydroxide
Name : Akaganeite, syn
Formula : FeO(OH)
Elements : H, O, Fe
Groups : OH
Crystal type : Tetragonal
Subfiles : Inorganic, Minerals, Common phases, Forensics
Pattern deleted: NO

d value	Angle	Rel.Int.
7.4670	11.842	40
5.2760	16.790	30
3.7280	23.849	5
3.3330	26.725	100
2.6344	34.003	25
2.5502	35.162	55
2.4830	36.146	2
2.3559	38.169	9
2.2952	39.220	35
2.1038	42.956	7
2.0666	43.769	7
1.9540	46.434	20
1.8624	48.863	4
1.8072	50.458	1
1.7557	52.047	15
1.7299	52.883	3
1.6658	55.087	1
1.6434	55.903	35
1.5155	61.099	9
1.5034	61.644	5
1.4896	62.278	3
1.4852	62.484	3
1.4577	63.800	1
1.4456	64.398	15

Reference pattern: 42-1315 26-Oct-2000 08:57

Name : Iron Oxide Hydroxide
Name : Akaganeite-\ITM\RG
Formula : FeO(OH)
Elements : H, O, Fe
Groups : OH
Crystal type : Monoclinic
Subfiles : Inorganic, Minerals, Corrosion products
Pattern deleted: NO

d value	Angle	Rel.Int.
7.4680	11.841	100
7.4680	11.841	100
5.3010	16.711	37
5.2560	16.855	35
3.7400	23.772	4
3.7250	23.869	4
3.3450	26.628	74
3.3450	26.628	74
3.3340	26.717	74
3.3340	26.717	74
2.9170	30.624	1
2.9170	30.624	1
2.6500	33.797	14
2.6270	34.102	14
2.5510	35.151	86
2.5510	35.151	86
2.4920	36.011	6
2.3580	38.134	6
2.3580	38.134	6
2.3530	38.218	3
2.3030	39.081	27
2.2940	39.241	27
2.1060	42.909	8
2.1060	42.909	8
2.0790	43.495	2
2.0790	43.495	2
2.0630	43.849	2
2.0630	43.849	2
1.9608	46.264	15
1.9608	46.264	15
1.9529	46.462	15
1.9529	46.462	15
1.8698	48.657	2
1.8627	48.855	2
1.7672	51.684	8
1.7520	52.166	8
1.7378	52.624	4
1.7378	52.624	4
1.7329	52.785	4
1.7329	52.785	4
1.6770	54.688	2
1.6494	55.682	27
1.6494	55.682	27

d value	Angle	Rel.Int.
1.6434	55.903	30
1.6434	55.903	30
1.5175	61.010	13
1.5136	61.184	11
1.5136	61.184	11
1.4984	61.872	4
1.4877	62.367	4
1.4877	62.367	4
1.4642	63.483	2
1.4642	63.483	2
1.4590	63.736	4
1.4519	64.085	12
1.4519	64.085	12
1.4456	64.398	12
1.4059	66.447	1
1.4059	66.447	1
1.3923	67.182	2
1.3923	67.182	2
1.3884	67.395	4
1.3809	67.811	7
1.3809	67.811	7

Glossary

Absolute Humidity	the amount of water vapour present in the atmosphere defined in terms of the mass of water in given volume of air (kg/m^3).
Adsorption	the concentration of a substance on a surface.
Chloride	generically pertains to the presence of the chloride ion (Cl^-) either as discreet Cl^- ions (usually in solution or bound up within the structure of compounds e.g. akaganéite) or in combination with positively charged ions to form acid (HCl) or salts (e.g. NaCl).
Chlorinity	The quantity of halide ions present in seawater. Salinity = 0.03 + (1.805 x chlorinity), see Table 1.
Critical Humidity	the relative humidity below which water will not form on a clean (polished) metal surface such that electrochemical corrosion cannot occur (Garverick, 1994: 5). [Donovan (1996: 193) modifies his definition of critical humidity to include metal and contaminant: *"Critical humidity: The minimum humidity at which corrosion occurs with a given combination of metal and contaminant (the critical humidity is nearly constant for a wide range of temperatures)."* The term "corrosion threshold" will be used in this work to describe the Donovan, metal/contaminant, corrosion humidity].
Dehumidification	*"The process of controlling the amount of moisture in the air surrounding a [metal] part so that the quantities of water condensed on the surface will not be sufficient for a significant amount of corrosion to occur."* (Greathouse & Wessel, 1954: 274)

Deliquescence — A special case of hygroscopic behaviour defined as the formation of a solution when a solid salt is exposed to water vapour at a partial pressure greater than that of the saturated solution of its highest hydrate.

Deliquescence point - the relative humidity at which a compound deliquesces. Defined as the ratio of water vapour pressure above a plane surface of a saturated solution of the compound to the vapour pressure over a plane surface of pure water (Amorosso and Fassina, 1983: 122). Deliquescence occurs when the vapour pressure of water at equilibrium with solid salt(s) is lower than, or equal to, the water vapour pressure of the atmosphere. Under these conditions the water vapour from the air will be adsorbed to form a saturated solution (Pique, 1992; Wallert, 1996: 200, *fig. 4*).

Deliquescent — a substance which picks up moisture from the atmosphere to such an extent that it dissolves in it.

Dew point — the temperature at which a plane, clean, metal surface is cold enough for visible condensation to appear on its surface (Donovan, 1986: 193). Equivalent to 100%RH. At sub zero ^{o}C temperatures this is the frost point.

Electrolyte — an electrically conducting solution (usually aqueous) or molten solid where the current is carried by ions not electrons.

Ferric — iron (III) compounds or ions where the iron is the more oxidised form having a valency of 3 (Fe^{3+}).

Ferrous — iron (II) compounds or ions where the iron is the less oxidised form having a valency of 2 (Fe^{2+}).

FTIR-ATR	Fourier Transform Infrared Spectroscopy using attenuated reflectance.
Hygroscopic	having the tendency to adsorb moisture from the air.
Hydrate	a compound containing combined water - usually salts containing water of crystallisation.
Ion	an electrically charged atom or group of atoms.
Oxidation	the combination of oxygen with a substance or the removal of hydrogen from it or any reaction in which an atom loses electrons e.g. the *oxidation* of a ferrous ion (Fe^{2+}) to a ferric ion (Fe^{3+}).
Oxyhydroxide	also oxy-hydroxide and oxide hydroxide... a metal compound containing oxygen (-O-) and hydroxyl groups (-OH) within its unit structure.
Relative Humidity	the ratio of the actual amount of water in the air to the amount that the air would hold at the saturation point for the same temperature (see section 5.1.1.).
Salinity	the quantity of dissolved salts in seawater.
S.A. 2.5	**Swedish Standard 2.5** for **Near-White Blast Cleaning.** Equivalent to Steel Structures Painting Council standard **SSPC-SP-10** and National Association of Corrosion Engineers (NACE) standard **NACE 2.**

Salt	chemical compound formed when the hydrogen from an acid has been replaced by a metal.
Saturated vapour Pressure	The maximum partial pressure that can be exerted by water at a given temperature.
Specific Humidity	the amount of water vapour present in the atmosphere defined in terms of the mass of water in a given mass of dry air (kg/kg dry air).
Threshold Humidity	1) the relative humidity beneath which no observed or measured changes in a compound(s) takes place but above which observed or measured changes do take place or 2) the relative humidity beneath which one hydrate or the anhydrous form of a compound is stable and above which a higher hydrate of the same compound is stable. The point where a hydrated compound dissolves in its own adsorbed water is called its deliquescence point.
Vapour pressure	for water, that part of the atmospheric pressure created by water vapour.
Water of Crystallisation	a definite molecular proportion of water combined chemically with particular substances in the crystalline state. See hydrate.
XRD	X-Ray Diffraction. A method of chemical analysis used to positively identify crystalline substances by analysing the angles of diffraction of an x-ray beam fired at the sample.

Bibliography

Ahmad, Z. (2006) **Principles of Corrosion Engineering and Corrosion Control.** London: Butterworth-Heinemann.

Al-Zahrani, A.A. (1999) **Chloride Ion Removal From Archaeological Iron and βFeOOH.** Unpublished PhD thesis, Cardiff University, April 1999.

Amorosso, G.G. and Fassina, V. (1983) **Stone Decay and Conservation: Atmospheric Pollution, Cleaning, Consolidation and Protection.** Amsterdam/New York: Elsevier.

Andrew, A.S. (2006) **Main Cable Dehumidification.** Forth Estuary Transport Authority (FETA), 1st December, 2006.

Andrew, A.S. and Colford, B.R. (2006) Forth Road Bridge – maintenance challenges. In Mamhoud, K.M. [ed.] **Advances in Cable-Supported Bridges.** London: Taylor and Francis. Chapter 5, pp57-85.

Anon (1964). Relative Humidity of Air Over Saturated Solutions of Salts. **British Standard 3718:1964**. Specification for laboratory humidity oven p.19.

Anon (1973). Small enclosures for testing and conditioning using aqueous solutions (in French). **Edite par l'Association Fransaise De Normalization AFNO3.**

Antunes, R.A., Costa, I. and Faria, D.L.A. (2003) Characterisation of corrosion products formed on steels in the first months of atmospheric exposure. **Materials Research 6 (3)** (2003), pp403-8.

Archer, P.J. and Barker, B.D. (1987) Phase changes associated with the hydrogen reduction conservation process for ferrous artefacts. **Journal of the Historical Metallurgy Society 21** (1987), pp 86-91.

Ardizzone, S., Biagiotti, R. & Formaro, L. (1983) Interactions of Cl^- ions with Fe_3O_4. **Journal of Electroanalytical Chemistry 147** (1983), pp301-305.

Argo, J. (1981a) On the nature of 'ferrous' corrosion products on marine iron. **Studies in Conservation 26**, 1981, pp42-44.

Argo, J. (1981b) A qualitative test for iron corrosion products. **Studies in Conservation 26** (1981) pp140-142.

Argo, J. & Turgoose, S. (1985) Amines for iron: discussion. **Corrosion Inhibitors in Conservation.** UKIC Occasional Papers No. 4, 1985, pp31-32.

Argyropoulos, V., Selwyn, L.S. & Logan, J.A. (1997) Developing a conservation treatment using ethylenediamine as a corrosion inhibitor for wrought iron objects found at terrestrial archaeological sites. In I.D. MacLeod, S.L. Pennec and L. Robbiola [eds.] **Metal '95, Proceedings of Metals in Conservation Conference** 25-28 September 1995, pp153-158. James and James, London.

Arnould-Pernot, P., Forrieres, C., Michel, H. & Weber, B. (1997) Peut-on dechlorurer les objets archeologiques ferraux avec les plasmas d'hydrogene. In I.D. MacLeod, S.L. Pennec and L. Robbiola [eds.] **Metal '95, Proceedings of Metals in Conservation Conference** 25-28 September 1995, pp147-152. James and James, London.

Arrhenius, O., Barkman, L. and Sjöstrand, E. (1973) Conservation of Old Rusty Iron Objects. **Bulletin No. 61E, Swedish Corrosion Institute.**

Ashley, R. (1997) Old Ships and Education. **Third International Conference on the Technical Aspects of the Preservation of Historic Vessels. San-Francisco, California, April 20-23, 1997.** http://www.maritime.org/conf/conf-ashley-oldships.htm

Ashley-Smith, J. (1982) The ethics of conservation. **The Conservator 6**, pp1-5. London: United Kingdom Institute for the Conservation of Historic and Artistic Works.

Askey, A., Lyon, S.B., Thompson, G.E., Johnson, J.B., Wood, G.C., Cooke, M. & Sage, P. (1993) The corrosion of iron and zinc by atmospheric hydrogen chloride. **Corrosion Science 34** (1993), pp233-247.

Astrup, E.E. and Hovin Stub, K.E. (1990) Saturated salt solutions for humidity control of showcases- conditions for a successful system. **International Council for Museums Committee for Conservation 9th Triennial Conference, Dresden** (1990) Volume II, pp577-582.

Atkinson, R.J., Posner, A.M. and Quirk, J.P. (1977) Crystal nucleation and growth in hydrolysing iron (III) chloride solutions. **Clays and Clay Minerals 25,** pp49-56.

Barker, B.D., Kendell, K. and O'Shea, C. (1982) The hydrogen reduction process for the conservation of ferrous objects. In **Conservation of Iron**. National Maritime Museum Monographs and Reports No. 53, Greenwich, London, pp 23-27.

Barker, B.D., Johnston, A. & O'Shea, C. (1997) Conservation of the submarine Holland: a practical overview. In Macleod, I.D., Pennec, S. & Robbiola, L. (eds.) **Metal '95, Proceedings of Metals in Conservation Conference** 25-28 September 1995, pp286-290. James and James, London.

Barker, P. (1982) **Techniques of Archaeological Excavation.** London: B.T. Batsford.

Barkman, L. (1975) Corrosion and conservation of Iron. **Conservation in Archaeology and the Applied Arts.** Stockholm Congress 1975, pp 169-172.

Barkman, L. (1977) Conservation of rusty iron objects by hydrogen reduction. **Corrosion and Metal Artefacts.** Ed. Brown, B.F. *et al.* NBS (National Bureau of Standards) Special Publication 479. Washington D.C. Government Printing Office.

BBC (2007) Severn Bridge gets cable blow dry. **BBC News 08/02/2007:** http://news.bbc.co.uk/go/pr/fr/-/1/hi/wales/south_east/6927852.stm

Beaudoin, A., Clerice, M-C., Francoise, J., Labbe, J-P., Loeper-Attia, M-A. and Robbiola, L. (1997) Corrosion d'objets archaeologiques eb fer apres dechloruration par la methode au sulfite alcalin. Caracterisation physico-chimique et retraitment electrochemique. In I.D. MacLeod, S.L. Pennec and L. Robbiola [eds.] **Metal '95, Proceedings of Metals in Conservation Conference** 25-28 September 1995, pp170-177. James and James, London.

Bell, A.T. and Hair, M.L. (1980) **Vibrational Spectroscopies for Adsorbed Species.** American Chemical Society. Washington DC.

Bernal, J.D., Dasgupta, D.R. & Mackay, A.L. (1959) The oxides and hydroxides of iron and their structural inter-relationships. **Clay Mineralogical Bulletin 4** (1959), pp15-30.

Bertholon, R. (2007) Archaeological metal artefacts and conservation issues: long-term corrosion studies. In Dillmann, P., Béranger, G., Piccardo, P. and Matthiesen, H. (2007) **Corrosion of Metallic Artefacts; Investigation, conservation and prediction for long-term behaviour. European Federation of Corrosion Publications Number 48.** CRC Press, Woodhead Publishing Ltd., pp31-40.

Birchenall, E.C. & Meussner, R.A. (1977) Principles of gaseous reduction of corrosion products. **Corrosion and Metal Artefacts** (eds. Brown et al.) NBS Special Publication 479. Washington: NBS, pp39-58.

Birkholz, D. (1997) Preservation of iron ships in the maritime environment. **Third International Conference on the Technical Aspects of the Preservation of Historic Vessels. San-Francisco, California, April 20-23, 1997.** http://www.maritime.org/conf/conf-birkholz.htm

Blackshaw, S. (1982) An appraisal of cleaning methods for use on corroded iron antiquities. In **Conservation of Iron**. National Maritime Museum Monographs and Reports No. 53, Greenwich, London, pp16-20.

Bloomstine, M.L. and Sørensen, O. (2006) Prevention of main cable corrosion by dehumidification. In Mamhoud, K.M. [ed.] **Advances in Cable-Supported Bridges.** London: Taylor and Francis. Chapter 15, pp215-228.

Blytholder, G. and Richardson, E. A. 1962 Infrared and Volumetric Data on the Adsorption of Ammonia, Water and other gases on activated iron (III) oxide. ***Journal of Physical Chemistry*, 66,** p2597

Brimblecombe, P. (1989a) A theoretical approach to the pollution of volumes of air within museums. **The Conservator 13**, pp15-19. London, UKIC.

Brimblecombe, P. (1989b) The Chemistry of Museum Air. **Environmental Monitoring and Control: Preprints of the Dundee Symposium**, pp56-64. Edinburgh, SSCR.

Brimblecombe, P. (1990) The Composition of Museum Atmospheres. **Atmospheric Environment 24B** (1), pp1-8. Oxford: Pergamon Press.

Brimblecombe, P. & Ramer, B. (1983) Museum display cases and the exchange of water vapour. **Studies in Conservation 28**, pp179-188. London: IIC.

Brown, J.P. (1994) Hygrometric measurement in museums: calibration, accuracy and the specification of relative humidity. In Roy, A. and Smith, P. [eds.] **IIC Ottawa Congress, 1994: Preventive Conservation: practice, theory, research.** IIC, London, pp39-43.

Brunauer, S. (1943) **The Adsorption of Gases and Vapours. Volume 1: Physical Adsorption**. London: Oxford University Press.

Buchwald, V.F. & Clarke, R.S. (jr.) (1989) Corrosion of Fe-Ni alloys by Cl-containing akaganéite (β-FeOOH): The Antarctic Meteorite Case. **American Mineralogist 74** (1989), pp656-667.

Buckley, H.E. (1951) **Crystal Growth**. New York: Wiley and Sons.

Bukowiecki, A. (1957) **Schweizer Archiv für Angewandte Wissenschaft und Technik 23,** p97.

Bukowiecki, A. & Joshi, B.G. (1966) **Schweizer Archiv für Angewandte Wissenschaft und Technik 32,** p42.

Bunting, B.T. (1969) **The Geography of the Soil.** London: Hutchinson & Co (Publishers) Ltd.

Burke, M. (2005) Saving a steam ship. **Chemistry World**. July Issue, 2005, pp46-49.

Campbell, S.A., Gillard, S.P., Beech, I.B., Davies, W., Monger, G. and Lawton, P. (2004) The s.v. Cutty Sark: electrochemistry in conservation. **Transactions of the Institute of Metal Finishing Vol. 83, No. 1 (2005)**, pp19-26. Institute of Metal Finishing.

Chandler, K.A. (1966) The influence of salts in rusts on the corrosion of the underlying steel. **British Corrosion Journal, Vol. 1: July, 1966**, p264.

Chandler, K.A. & Stanners, J.E. (1966). Rusting in air – characteristic properties of natural rusts. **2nd International Congress on Metallic Corrosion: Houston:** (1963) National Association of Corrosion Engineers, 1966, pp325-333.

Chapman, E.M. (2005) **A Catalogue of Roman Military Equipment in the National Museum of Wales.** Oxford: Archaeopress, BAR S388.

Charlson, R.J., Covert, D.S., Larson, T.V. and Waggoner, A.P. (1978) Chemical properties of tropospheric sulphur aerosols. **Atmospheric Environment 12,** pp39-53. Pergamon Press.

Childs, C. W., Goodman, B.A., Paterson, E. and Woodhams, F.W.D. (1980) The Nature of Iron in Akaganéite (β-FeOOH). In the ***Australian Journal of Chemistry 33***, pp 15-26.

Chitty, W.-J., Dillmann, P., L'Hostis, V. and Lombard, C. (2005) Long term corrosion resistance of metallic reinforcements in concrete – A study of corrosion mechanisms based on archaeological artefacts. **Corrosion Science 47** (2005), pp1555-1581.

Cole, I.S., Muster, T.H., Lau, D. and Ganther, W.D. (2004) Some recent trends in corrosion science and their application to conservation. **Metal'04, Proceedings of the International Conference on Metals Conservation, Canberra, 4-8 October 2004.** [ed. J. Ashton and D. Hallam]. Canberra: National Museum of Australia, pp2-16.

Colford, B.R. (2008) **Dehumidification of Main Cable – Update Report.** Forth Estuary Transport Authority (FETA).

Colford, B.R. and Cocksedge, C.P.E. (2006) Forth Road Bridge – first internal inspection, strength evaluation, acoustic monitoring and dehumidification of the main cables. In Mamhoud, K.M. [ed.] **Advances in Cable-Supported Bridges.** London: Taylor and Francis. Chapter 15, pp201-214.

Corfield, M. (1988) Towards a conservation profession. In Todd, V. (ed.) **Conservation Today: Papers presented at the UKIC 30th Anniversary Conference (1988),** pp4-7. London: United Kingdom Institute for the Conservation of Historic and Artistic Works (UKIC).

Corlett, E.C.B. (1990) The Iron Ship: The Story of Brunel's ss Great Britain. In Cox, J. with Tanner, M. (1999) **Conservation Plan for the Great Western Steamship Company Dockyard and the ss Great Britain.** Volume I. Bristol: ss Great Britain Trust.

Cornell, R.M. (1983) Film forming abilities of iron oxides and oxyhydroxides. **Clay Minerals 18** (1983), pp 209-213.

Cornell, R.M. & Giovanoli, R. (1988) Acid dissolution of akaganéite and lepidocrocite: the effect on crystal morphology. **Clays and Clay Minerals 36,** No. 5, pp385-390.

Cornell, R.M. & Giovanoli, R. (1990) Alkaline transformation of akaganéite to goethite and hematite. **Clays and Clay Minerals 38,** No. 5, pp469-476.

Cornell, R.M., Posner, A.M. and Quirk, J.P. (1976) Kinetics and mechanisms of the acid dissolution of goethite (αFeOOH). **Journal of Inorganic Nuclear Chemistry 38,** pp563-567.

Cornell, R.M. & Schwertmann, U. (1996) **The Iron Oxides: Structure, Properties, Reaction, Occurrence and Uses.** VCH: New York.

Cox, J. & Tanner, M. (1999). **Conservation Plan For The Great Western Steamship Company Dockyard And The SS Great Britain: Volume I.** Bristol: ss Great Britain Trust.

CRC (1996). **CRC Handbook of Chemistry and Physics (1996)**

Crevello, G.L. and Noyce, P.A. (2006) **Cutty Sark, Greenwich: Conservation Trial Report; Wrought Iron Composite Frame. Final Report 2006.** Report No. C1200-FR-001. Grantham: Electro-Tech CP Ltd.

Cridland, D. (2000) Vaisala DMT242 Dew point transmitter. **Measurement and Control 33 (7),** September 2000, p221. See also 'How to choose the right Vaisala product for measuring humidity and dew point', 'DM70 Hand-held dew point meter for spot-checking applications', 'Portable systems and sampling cells' and 'Technical data', **Vaisala Instruments Catalogue 2008,** Vaisala, P.O. Box 26, FI-00421 Helsinki, Finland.

Cronyn, J.M. (1990) **The Elements of Archaeological Conservation.** London: Routledge.

Cuddihy, E.F. (1987) The aging correlation (RH+t): Relative Humidity (%) + Temperature (^{o}C). **Corrosion Science 27 No. 5,** pp 463-474.

Daniels, V. D., Holland, L. & Pascoe, M. W. (1979) Gas plasma reactions for the conservation of antiquities. **Studies In Conservation 24** (1979), pp85-92.

DCMS (2001) **The Historic Environment: A Force for Our Future.** Department for Culture, Media and Sport, London.

Degrigny, C. (2007) Examination and conservation of historical and archaeological metal artefacts: A European overview. In Dillmann, P., Béranger, G., Piccardo, P. and Matthiesen, H. (2007) **Corrosion of Metallic Artefacts; Investigation, conservation and prediction for long-term behaviour. European Federation of Corrosion Publications Number 48.** CRC Press, Woodhead Publishing Ltd., pp1-17.

Degrigny, C. & Spiteri, L. (2004) Electrochemical monitoring of marine iron artefacts during their storage/stabilisation in alkaline solutions. **Metal'04, Proceedings of the International Conference on Metals Conservation, Canberra, 4-8 October 2004.** [ed. J. Ashton and D. Hallam]. Canberra: National Museum of Australia, pp315-331.

Derrick, M.R., Stulik, D. & Landry, J.M. (1999) **Infrared Spectroscopy in Conservation Science.** Getty Conservation Institute (GCI).

Desombre, A. (1980) **Proceedings of the 3rd E.C. Photovoltaic Solar Energy Conference, Cannes, France, October 27-31, 1980**, pp27-31.

Dezsi, I., Keszthelyi, L., Kulgawczuk, D., Molnar, B. & Eissa, N.A. (1967) Mossbauer study of β– & δ– FeOOH and their disintegration products. **Physica Status Solidi 22** (1967), pp617-629.

Dillmann, P., Neff, D., Mazaudier, F., Hoerle, S., Chevallier, P. and Beranger, G. (2002) Characterisation of iron archaeological analogues using micro-diffraction under synchrotron radiation. Application to the study of long term corrosion behaviour of low alloy steels. **Journal de Physique IV (Proceedings) France (12)**, p 393-408.

Dillmann, P., Mazaudier, F. & Hoerle, S. (2004) Advances in understanding atmospheric corrosion of iron. I. Rust characterisation of ancient ferrous artefacts exposed to indoor atmospheric corrosion. **Corrosion Science 46** (2004), pp 1401-1429. Elsevier.

Doehne, E. (1994) In situ dynamics of sodium sulfate hydration and dehydration in stone pores: observations at high magnification using the environmental scanning electron microscope. In Fassina, V., Ott, H. and Zezza, F. [eds.] **Proceedings of the III International Symposium on the Conservation of Monuments in the Mediterranean Basin, Venice (1994),** pp143-150.

Doehne, E. and Stulik, D.C. (1990) Applications of the environmental scanning electron microscope to conservation science. **Scanning Microscopy 4(2)** (1990), pp275-286.

Donovan, P.D. (1986) **Protection of Metals from Corrosion in Storage and Transit.** Chichester, Ellis Horwood Ltd.

Downing, A.L. & Truesdale, G.A. (1955) Some factors affecting the rate of solution of oxygen in water. **Journal of Applied Chemistry 5,** October 1955, pp570-581.

Drews, M.J., de Vives, P. Gonzalez, N.G. & Mardikian, P. (2004) A study of the analysis and removal of chloride in iron samples from the "Hunley". In Ashton, J. and Hallam, D. eds. **Metal '04, Proceedings of the International Conference on Metals Conservation,** Canberra 4-8 October, 2004, pp 247-260.

Duncan, J.R. and Ballance, J.A. (1988) Marine salts contribution to atmospheric corrosion. In Dean, S.W. and Lee, T.S. [eds.] **Degradation of Metals in the Atmosphere, ASTM STP 965,** pp316-326. American Society of Testing and Materials, Philadelphia.

Duncan, S.J. (1986) Chloride removal from iron – new techniques. **Conservation News 31** (November 1986), pp21-33.

Duncan, S.J. & Ganiaris, H. (1987) Some sulphide corrosion products on copper and lead alloys from London waterfronts. **Institute of Archaeology Jubilee Conservation Conference,** pp109-118. London, UCL.

English Heritage (2000) **Power of Place: The future of the historic environment.** English Heritage, London. Also available at: www.english-heritage.org.uk/server/show/ConWebDoc.42 (accessed 23 June 2006)

English Heritage (2008) **Heritage Counts 2008, England.** English heritage, London.

Erhardt, D. and Mecklenburg, M. (1994) Relative Humidity Re-examined. In Roy, A. & Smith, P. [ed] **IIC Ottawa Congress, 12th-16th September 1994: Preventive Conservation: Practice, Theory and Research.** London, IIC, pp32-38.

Evans, U.R. (1948) **An Introduction to Metallic Corrosion.** London: Edward Arnold and Company.

Evans, U.R. (1972) **The Rusting of Iron: Causes and Control.** London: Edward Arnold (Publishers) Ltd.

Evans, U.R. & Hoar, T.P. (1932) The velocity of corrosion from the electrochemical standpoint. Part II. **Proceedings of the Royal Society Series A, 137, 2nd August 1932,** pp343-365.

Evans, U.R. & Taylor, C.A.J. (1972). The mechanism of atmospheric rusting. **Corrosion Science 12** (1972), pp 227-46.

Evans, U.R. & Taylor, C.A.J. (1974). Critical humidity for rusting in the presence of sea salt. **British Corrosion Journal, 1974: No. 1,** pp26-28.

Faber, O. & Kell, J.R. (1957) **Heating and Air-Conditioning of Buildings,** 3rd Edition. London: The Architectural Press.

Farrer, T.W., Biek, L. and Wormwell, F. (1953) The role of tannates and phosphates in the preservation of ancient buried iron objects. **Journal of Applied Chemistry 3,** February 1953, pp80-85.

Fell, V. and Williams, J. (2004) Monitoring of archaeological and experimental iron at Fiskerton, England. **Metal'04, Proceedings of the International Conference on Metals Conservation, Canberra, 4-8 October 2004.** [ed. J. Ashton and D. Hallam]. Canberra: National Museum of Australia, pp17-27.

Fenn, J.D. & Foley, K. (1975) Passivation of Iron. **Conservation in Archaeology and the Applied Arts.** Preprints of the IIC Stockholm Triennial (1975), pp195-198.

FitzPatrick, E.A. (1974) **An Introduction to Soil Science.** Edinburgh: Oliver & Boyd Ltd.

Florian, M-L. E. (1987) Underwater Environment. In Pearson C. [ed] **Conservation of Marine Archaeological Objects,** pp1-20. London, Butterworths.

Foley, R.T. (1970) Role of the Chloride Ion in Iron Corrosion. **Corrosion – NACE, Vol. 26, No.2, February 1970,** pp58-70.

Forbes, R.J. & Dijksterhuis, E.J. (1963) **A History of Science and Technology I: Ancient Times to the Seventeenth Century.** Harmondsworth: Pelican Books.

Galbraith, S.J., Baird, T. & Fryer, J.R. (1979) Structure changes in βFeOOH caused by radiation damage. **Acta Crytallographica A35,** pp197-200.

Gallagher, K.J. (1970) The atomic structure of tubular sub crystals of β-iron (III) oxide hydroxide. **Nature 226,** pp1225-1228.

Garverick, L. (1994) **Corrosion in the Petrochemical Industry [2nd Edition].** ASM International – The Materials Information Society.

Gilberg, M.R. & Seeley, N.J. (1981) The Identity Of Compounds Containing Chloride Ions In Marine Iron Corrosion Products: A Critical Review. **Studies In Conservation 26,** pp50-56. London, IIC.

Gilberg, M. R. and Seeley, N. J. (1982) The Alkaline Sodium Sulphite Reduction Process for Archaeological Iron: A Close Look. In **Studies in Conservation, 27**, pp180-184. London, IIC.

Goodburn-Brown, D. (1996) The effect of various conservation treatments on the surface of metals from waterlogged sites in London. In Roy, A. & Smith, P. [eds.] **Archaeological Conservation and its Consequences**, Preprints of the Contributions to the Copenhagen Congress, 26-30 August 1996. London, IIC, pp59-64.

Graedel, T.E. and Frankenthal, R.P. (1990) Corrosion mechanisms for iron and low alloy steels exposed to the atmosphere. **Journal of the Electrochemical Society 137**, pp 2385-2394.

Greathouse, G.A. & Wessel, C.J. (1954) **Deterioration of Materials: Causes and Preventive Techniques**. New York: Reinhold Publishing Corporation.

Green, L. and Bradley, S. (1997) An investigation of strategies for the long-term storage of archaeological iron. In I.D. MacLeod, S.L. Pennec and L. Robbiola [eds.] **Metal '95, Proceedings of the International Conference on Metals Conservation,** pp305-309. London, James and James.

Greenspan, L. (1977). Humidity Fixed Points of Binary Saturated Aqueous Solutions. **Journal of Research of the National Bureau of Standards Vol.81A No.1**, pp89-96.

Gregory, D.C. (1969) **Cable Pressurisation: Notes for Internal Students.** Services Department Telecommunications Headquarters, (U.K.) Post Office.

Grisdale, R.O. (1963) Growth from molecular complexes. In Gilman (ed.) **The Art and Science of Growing Crystals.** New York: John Wiley and Sons.

Hafors, B. (1997) The climate of the Wasa Museum – Problems in co-ordinating the museum object and the museum climate. **Third International Conference on the Technical Aspects of the Preservation of Historic Vessels. San-Francisco, California, April 20-23, 1997.**
http://www.maritime.org/conf/conf-hafors.htm

Hallam, D.L., Adams, C.D., Creagh, D.C., Holt, S.A., Wanless, E.J., Senden, T.J. & Heath, G.A. (1997) Petroleum Sulphonate Corrosion Inhibitors. In I.D. MacLeod, S.L. Pennec and L. Robbiola [eds.] **Metal '95, Proceedings of Metals in Conservation Conference** 25-28 September 1995, pp159-161. James and James, London.

Hedlin, C.P. & Trofimenkoff, F.N. (1963) Relative Humidities Over Saturated Solutions of Nine Salts in the Temperature Range 0-90F. **Humidity and Moisture Papers International Symposium 3,** Washington DC (1963), pp519-520.

Hemingway, B.S., Seal, R.R. & Ming Chou, I. (2002) Thermodynamic data for modelling acid mine drainage problems: Compilation and estimation of data for selected soluble iron-sulfate minerals. **United States Department of the Interior U.S. Geological Survey Open-File Report 02-161.**

Heywood, F. (2005) Government gets ship-shape with heritage plan. In **Museums Journal** (March 2005), London: Museums Association.

Hickman, M.J. (1970). Measurement of Humidity. **National Physical Laboratory Notes On Applied Science 4,** p31.

Hingston, F. J., Posner, A. M., and Quirk, J. P. 1972, Anion Adsorption By Goethite and Gibbsite: I. The Role of The Proton in Determining Adsorption. In **Journal of Soil Science, Vol. 23,** *No. 2*, pp177-192.

Hjelm-Hansen, N., van Lanschot, J., Szalkay, C.D. & Turgoose, S. (1993) Electrochemical Assessment and monitoring of stabilisation of heavily corroded archaeological iron artefacts. **Corrosion Science 35** No.s 1-4, pp767-774.

Horstmeyer, S. (2008) **Relative Humidity...Relative to What? The Dew Point Temperature ... a better approach.** Website of the Chief Meteorologist, of WXIX TV, Fox 19, Cincinnati, Ohio, USA. http://www.shorstmeyer.com/wxfaqs/humidity/humidity.html

Howie, F.M.P. (1977) Pyrite and Conservation. **Geological Curator 1**, pp457-465 and pp497-512.

Howie, F.M.P. (1978) Storage environment and the conservation of geological material. **The Conservator 2,** pp13-19.

Howie, F.M.P. (1992) **The Care and Conservation of Geological Materials.** Oxford: Butterworth/Heinemann.

Hudson, J.C. and Stanners, J.F. (1953) The effect of climate and atmospheric pollution on corrosion. **Journal of Applied Chemistry 3**, February 1953, pp86-96.

Ishikawa, T and Inouye, K. (1972) The Structural Transformation of Ferric Oxyhydroxides and Their Activity to Sulfur Dioxide. In **Bulletin of the Chemical Society of Japan, 45**, pp2350-2354.

Ishikawa, T. and Inouye, K. (1975) Role of Chlorine in β-FeOOH on Its Thermal Change and Reactivity to Sulfur Dioxide. In **Bulletin of the Chemical Society of Japan, Vol. 48 (5)**, pp1580-1584.

Ishikawa, T., Nitta, C. & Kondo, S. (1986) Fourier-transform infrared spectroscopy of colloidal α–, β– and γ– Ferric Oxide Hydroxides. **Journal of the Chemical Society Faraday Transactions I, 82,** pp2401-2410.

Ishikawa, T., Sakaiya, H. & Kondo, S. (1988) Adsorption of water on colloidal iron (III) oxide hydroxides by infrared spectroscopy. **Journal of Chemical Society Faraday Transactions I, 84,** pp1941-1948.

Ishikawa, T., Kodaira, N. and Kandori, K. (1992a) Step-like adsorption isotherms of molecules on γ–FeOOH and the surface homogeneity of γ–FeOOH. **Journal of the Chemistry Society Faraday Transactions 88 (5),** pp917-722.

Ishikawa, T., Cai, W.Y. and Kandori, K. (1992b) Characterisation of the thermal decomposition products of δ-FeOOH by Fourier-Transform Infrared Spectroscopy and N_2 adsorption. **Journal of the Chemistry Society Faraday Transactions 88 (8),** pp1173-1177.

ISO (9223) **Corrosion of metals and alloys – Corrosivity of atmosphere – Classification** International Organisation for Standardisation, Geneva, Switzerland.

Janecka, H. (1963) **Preservation of Inactive Equipment and Long-term Storage of Materials.** U.S. Government Report No. 0246006.

Johnson, W. (1998) Chloride removal from ferrous substrates. **Corrosion '98,** Paper No. 622. Houston, Texas: NACE, pp 621/1-16.

Johnston, J.H. and Logan, N.E. (1979) A precise iron-57 Mossbauer spectroscopic study of iron (II) in the octahedral and channel sites of akaganéite (β-iron hydroxide oxide). **Journal of the Chemical Society Dalton Transactions 7** (1979), pp13-16.

Jones, D. (1992) **Principles and Prevention of Corrosion.** Macmillan. New York.

Junge, C.E. (1954) The chemical composition of atmospheric aerosols, I: Measurements at Round Hill field station, June-July, 1953. **Journal of Meteorology 11,** pp323-333.

Junge, C.E. (1963) **Air Chemistry and Radioactivity.** New York: Academic Press.

Kaneko, K. (1989) Surface Chemistry of FeOOH Microcrystals. In **Current Problems in the Conservation of Metals Antiquities.** October 4-6, 1989. Tokyo, Japan. National Research Institute of Cultural Properties, pp42-62.

Kaneko, K. and Inouye, K. (1974) Electrical properties of ferric oxyhydroxides. **Bulletin of the Chemical Society of Japan, Vol. 47(5),** pp1139-1142.

Kaneko, K. and Inouye, K. (1979) Adsorption of Water on FeOOH as Studied By Electrical Conductivity Measurements. In **Bulletin of the Chemical Society of Japan, Vol. 52(2),** pp315-320.

Kaneko, K. and Inouye, K. (1981) The mechanism of chemisorption of SO_2 on iron (III) hydroxide oxides. **Corrosion Science 27** No.9, pp639-646.

Kaneko, K. and Inouye, K. (1984) Fast chemisorption of NO and SO_2 on FeOOH crystals. **Polyhedron 3** No. 2, pp223-230.

Kaneko, K, Serizawa, M., Ishikawa, T. and Inouye. K. (1975) Dielectric behaviour of water molecules adsorbed on iron (III) oxide hydroxides. In **Bulletin of the Chemical Society of Japan, *Vol.* 48,** pp1764-1769.

Kapatou, E. and Lyon, S.B. (2008) An electrical resistance monitor study of the post-excavation corrosion of archaeological iron. **Art 2008: 9th International Conference of NDT of Art,** Jerusalem, Israel, 25-30 May 2008, pp1-10. See also www.ndt.net

Kassim, J., Baird, T. and Fryer, J.R. (1982) Electron microscope studies of iron corrosion products in water at room temperature. **Corrosion Science 22, No. 2,** pp147-158.

Kaye, G.W.C. & Laby, T.H. (1966) **Tables of physical and chemical constants,** 13th Edition. Longman.

Keene, S. (1984). The Performance of Coatings and Consolidants used for Archaeological Iron. In **Adhesives Consolidants & Coatings.** London, IIC, pp104-106.

Keene, S. (1991) See Keene, S. (1994) below.

Keene, S. (1994) Real Time Survival Rates for Treatments of Archaeological Iron. **Ancient and Historic Metals: Conservation and Scientific Research.** Proceedings of a conference held at the Getty Conservation Institute November 1991 [ed. D.A. Scott, Podany, J. & Considene, B. (1994)], pp249-264. Getty Conservation Institute.

Keene, S. & Orton, C. (1985) Stability of treated archaeological iron: an assessment. **Studies in Conservation 30,** pp136-142. London, IIC.

Keller, P. (1966) Phasenumwandlungen in Rost. In **Rost Werksoffe und Korrosion 17,** pp943-951.

Keller, P. (1969) Vorkommen Enstehung und Phasenumwandlung von β-FeOOH. In **Rost Werksoffe und Korrosion 20,** pp102-108.

Keller, P. (1970) Eigenschaften von (Cl,F,OH)< $_2Fe_8(O.OH)_{16}$ und Akaganéite. ***Neues Jahrbuch fur Mineralogie Abhandlungen,* 113,** pp29-49.

Kesavan, S., Mohzi, T.A. and Wilde, B.E. (1989) Technical Note: Potential-pH Diagrams for the Fe-Cl^- -H_2O System at 25 to 150 C. **Corrosion 45, No.3,** pp213-215. See also subsequent 'Discussion' with amended diagrams in **Corrosion 46, No. 1,** pp19-21.

Kiseler, A.V. & Lygin, V.I. (1975) **Infrared Spectra of Surface Compounds.** John Wiley & Sons, New York.

Kitchen, R. (2005) Cable driers to halt Forth Bridge corrosion. **New Civil Engineer,** article 528935, 24th November, 2005. See Online News at http://www.nce.co.uk/cable-driers-to-halt-forth-road-bridge-corrosion/528935.article

Kiyama, M. & Takada, T. (1972) Iron compounds formed by the aerial oxidation of ferrous salt solutions. **Bulletin of the Chemical Society of Japan 45** (1972), pp1923-1924.

Knight, B. (1982). Why Do Some Iron Objects Break Up In Store? In Clarke, R.W. and Blackshaw, S.M. [eds.] **Conservation of Iron.** National Maritime Museum Monographs and Reports No. 53. London, National Maritime Museum, pp50-51.

Knight, B. (1990). A review of the corrosion of Iron from terrestrial sites and the problem of post excavation corrosion. **The Conservator 14,** pp37-43. London, UKIC.

Knight, B. (1997). The Stabilisation of Archaeological Iron: Past, Present and Future. In Macleod, I.D., Penec, S. and Robiola, L. (eds.) **Metal '95, Proceedings of Metals in Conservation Conference** 25-28 September 1995, pp36-40. James and James, London.

Kuhn, C. (2008) Keep cool? Deep freeze storage of archaeological iron. Degrigny, C. [ed.] **BROMEC 25, Bulletin of Research on MEtal Conservation (February, 2008),** ICOM, p4.

Lafontaine, R.H. (1984). **Silica Gel.** CCI report 10. Ottawa, Canadian Conservation Institute.

Lawrence, M.G. (2005) The relationship between relative humidity and the dew point temperature in moist air. A simple conversion and applications. **Bulletin of the American Meteorological Society 86**, pp225-233.

Little, L.H. (1966) **Infrared Spectra of Adsorbed Species**. London: Academic Press.

Loeper-Attia, M.A. (2007) A proposal to describe reactivated corrosion of archaeological iron objects. In Dillmann, P., Béranger, G., Piccardo, P. and Matthiesen, H. (2007) **Corrosion of Metallic Artefacts; Investigation, Conservation and prediction for long-term behaviour. European Federation of Corrosion Publications Number 48.** CRC Press, Woodhead Publishing Ltd., pp 190-202.

Loeper-Attia, M.A. & Weker, W. (1997) Dechloruration d'objets archeologiques en fer par la methode du sulfite alcalin a l'IRRAP. In I.D. MacLeod, S.L. Pennec and L. Robbiola [eds.] **Metal '95, Proceedings of Metals in Conservation Conference** 25-28 September 1995, pp162-166. James and James, London.

Mackay, A.L. (1960) β-Ferric Oxyhydroxide. **Mineralogical Magazine 32** (1960), pp545-557.

Mackay, A.L. (1962) β-Ferric Oxyhydroxide – akaganéite. **Mineralogical Magazine 33** (1963), pp270-280.

Macleod, I.D. (1980) Shipwrecks and applied electrochemistry. **Progress in Electrochemistry, Studies in Physical and Theoretical Chemistry** (ed. Rand, D.) 5th Australia Electrochemistry Conference 18th-22nd August, 1980, pp291-303.

Macleod, I.D. (1989) The electrochemistry and conservation of iron in sea water. **Chemistry in Australia** (July 1989), pp227-229.

Maeda, Y., Matsuo, Y., Sugihara, S., Momoshima, N. and Takshima, Y. (1992) Mossbauer studies of first stage corrosion products on iron powder and corrosion products on highly corroded nails. **Corrosion Science 33 (1992)** No. 10, pp1557-1567.

Manning, W.H. (1972) Iron-work hoards in iron age and Roman Britain. **Britannia 3,** pp224-50.

Manning, W.H. (1985) **Catalogue of the Romano-British Iron Tools, Fittings & Weapons in the British Museum.** London: British Museum Press.

Marcus, P. [Ed.] (2002) **Corrosion Mechanisms in Theory and Practice (2nd Edition).** CRC Press.

Maréchal, L., Perrin, S., Dillmann, P. and Santarini, G. (2007) Study of the atmospheric corrosion of iron by ageing historical artefacts and contemporary low-alloy steel in a climatic chamber: comparison with mechanistic modelling. In Dillmann, P., Béranger, G., Piccardo, P. and Matthiesen, H. (2007) **Corrosion of Metallic Artefacts; Investigation, Conservation and prediction for long-term behaviour. European Federation of Corrosion Publications Number 48.** CRC Press, Woodhead Publishing Ltd., pp131-151.

Markidan, P., Drews, M., Gonzalez, N. and de Vivies, P. (2004). **H.L. Hunley Conservation Plan.** Friends of the Hunley, Inc. and Warren Lasch Conservation Centre. Unpublished internal report.

Marsh, K.N. (ed) (1987). **Recommended Reference Materials for the Realisation of Physicochemical Properties.** Oxford: Blackwell Scientific Publications.

Martin, S. (1965) The control of conditioning atmospheres by Saturated Salt Solutions. **Humidity and Moisture 3** (1965), pp503-506.

Mathias, C. (1996) Assessment of corrosion measurements for soil samples excavated at a seventeenth-century colonial plantation site. In Roy, A. & Smith, P. [eds.] **Archaeological Conservation & Its Consequences,** Preprints of the Contributions to the Copenhagen Congress, 26-30 August 1996, pp121-126. IIC, London.

Mathias, C. (1999) Examination of the interaction between ferrous metals and the archaeological burial environment for a seventeenth century plantation site. In **Proceedings of the 6th International Conference on Non-Destructive Testing and Microanalysis for the Diagnosis and Conservation of the Cultural and Environmental Heritage, Volume 3**. Rome: Euroma, pp1841-1855.

Mathias, C., Ramsdale, K. & Nixon, D. (2004) Saving archaeological iron using the Revolutionary Preservation System. **Metal'04, Proceedings of the International Conference on Metals Conservation, Canberra, 4-8 October 2004.** [ed. J. Ashton and D. Hallam]. Canberra: National Museum of Australia, pp28-42.

Matijevic, E. and Scheiner, P. (1978) Ferric Hydrous Oxide Sols. III. Preparation of uniform Particles by Hydrolysis of Fe(iii) – Chloride – Nitrate and Perchlorate solutions, **Journal of Colloid and Interface Science 63 (3)**, pp509-524.

Maxwell, P. & Viduka, A. (2004) Antarctic observations: On metal corrosion at three historic huts on Ross Island. **Metal'04, Proceedings of the International Conference on Metals Conservation, Canberra, 4-8 October 2004.** [ed. J. Ashton and D. Hallam]. Canberra: National Museum of Australia, pp484-500.

McCawley, C. (1984) Current research into the corrosion of archaeological iron. **International Council of Museums Committee for Conservation 7th Triennial Conference, Copenhagen,** 84.22.25. ICOM

Megaw, J.V.S. and Simpson, D.D.A. (1979) **Introduction to British Prehistory.** Leicester University Press, pp382-4.

Memet, J.B. (2007) The Corrosion of metallic artefacts in seawater. In Dillmann, P., Béranger, G., Piccardo, P. and Matthiesen, H. (2007) **Corrosion of Metallic Artefacts; Investigation, conservation and prediction for long-term behaviour. European Federation of Corrosion Publications Number 48.** CRC Press, Woodhead Publishing Ltd., pp152-169.

Micale, F.J., Kiernan, D. and Zettlemoyer, A.C. (1985) Characterisation of the surface properties of Iron Oxides. **Journal of Colloid and Interface Science 105 No.2** (June 1985), pp570-576.

Michalski, S. (1993) Relative Humidity: a discussion of correct/incorrect values. In **International Council of Museums Committee for Conservation 10th Triennial Meeting, Washington DC** 22-27 August 1993 Preprints [Ed J. Bridgland]. ICOM: Washington, James and James, **Vol. 2,** p624.

Misawa, T., Hashimoto, K. & Shemodaira, S. (1974) The mechanism of formation of iron oxide and oxyhydroxides in aqueous solutions at room temperature. **Corrosion Science 14** (1974), pp 131-149. Pergamon Press.

MOD (2004) Desiccant Containers, Dehumidifier Part 1: Guide to the use of desiccants. **Ministry of Defence Standard 44-2 Part 1 Issue 5,** publication date 20 September 2004.

Morcillo, M., Elisabet, M., Almeida, M., Rosales, M. [eds.] (1998) Functiones de Dano (Dosis/Respuesta) de la Corrosion Atmospherica en Iberoamerica. In **Corrosion y Protection de Metales en las Atmospheras de Iberoamerica.** Programma CYTED, Madrid, Spain, pp629-660.

Muller, H.G. (1965) Humidity sensors from natural materials. **Humidity and Moisture 1** (A. Wexler ed.). New York: Reinhold Publishing Corporation, pp574-577.

Murad, E. & Bishop, J.L. (2000) The infrared spectrum of synthetic akaganéite, βFeOOH. **American Mineralogist 85,** pp716-721.

Naono, H., Fujiwara, R., Sugioka, H., Sumiya, K. and Yanazawa, H. (1982) Micropore formation due to thermal decomposition of acicular microcrystals of βFeOOH. **Journal of Colloid and Interface Science 87,** No.2, pp317-332.

Neff, D., Dillmann, P. and Beranger, G. (2003) **Eurocorr 2003**. Budapest, 2003. CD Rom.

Neff, D., Réguer, S., Bellot-Gurlet, L., Dillmann, P. and Bertholon, R. (2004) Structural characterisation of corrosion products on archaeological iron: an integrated analytical approach to establish corrosion forms. **Journal of Raman Spectroscopy 35** (2004), pp739-745.

Neff, D., Dillmann, P., Bellot-Gurlet, L. and Beranger, G. (2005) Corrosion of iron archaeological artefacts in soil: characterisation of the corrosion system. **Corrosion Science 47,** pp515-535. Elsevier.

Neff, D., Vega, E., Dillmann, P. and Descostes, M. (2007) Contribution of iron archaeological artefacts to the estimation of average corrosion rates and the long-term corrosion mechanisms of low-carbon steel buried in soil. In Dillmann, P., Béranger, G., Piccardo, P. and Matthiesen, H. (2007) **Corrosion of Metallic Artefacts; Investigation, conservation and prediction for long-term behaviour. European Federation of Corrosion Publications Number 48.** CRC Press, Woodhead Publishing Ltd., pp41-76.

North, N.A. (1982). Corrosion Products On Marine Iron. **Studies In Conservation 27,** pp75-83. London, IIC.

North, N.A. (1989) Proximity corrosion in seawater. **Corrosion Australasia 14, No.5** (1989), pp8-11.

North, N.A. (1987) Conservation of metals. In Pearson, C. [ed.] **Conservation of Marine Archaeological Objects.** Butterworths, London, pp207-252.

North, N.A. and McCleod, I.D. (1987) Corrosion of metals. In Pearson, C. [ed.] **Conservation of Marine Archaeological Objects.** Butterworths, London, pp68-98.

North, N. and Pearson, C. (1975a) Investigation into conserving iron relics recovered from the sea. **Conservation in Archaeology and the Applied Arts,** Preprints of the IIC Stockholm Triennial (1975). IIC, London, pp 173-182.

North, N. and Pearson, C. (1975b) Alkaline sulphite treatment of marine iron. **ICOM Committee for Conservation 4th Triennial Meeting** Venice (1975) 75/13/3, pp1-14.

North, N. and Pearson, C. (1978) Washing Methods for Chloride Removal form Marine Iron Artefacts In **Studies in Conservation, 23**, pp 174-186. London: IIC.

Obermiller, J. & Goertz, M. (1924). **Zeitschrift für Physikalische Chemie 109,** p145.

Oddy, W.A. & Hughes, M.J. (1970) Stabilization of 'active' corrosion in bronze and iron antiquities by the use of sodium sesquicarbonate. **Studies in Conservation 15** (1970), p183.

Oesch, S. (1996) The effect of SO, NO, and O on the corrosion of unalloyed carbon steel and weathering steel – the results of laboratory exposures. **Corrosion Science 38**, pp1357-1368.

Orr, C., Hurd, K. and Corbett, W.J. (1958) Aerosol size and relative humidity. **Journal of Colloid Science 13,** pp472-482.

Orr, C., Hurd, K. and Hendrix, W.P. (1958) The behaviour on condensation nuclei under changing humidities. **Journal of Meteorology 15**, April 1958, pp240-242.

Oswald, N. (1997) In search of the lost surface: 10 years of active hydrogen research. An attempt to convert destructive criticism into improvements of the plasma method. In I.D. MacLeod, S.L. Pennec and L. Robbiola [eds.] **Metal '95, Proceedings of Metals in Conservation Conference** 25-28 September 1995, pp286-290. James and James, London.

Ottar, B. & Haagenrud, S.E. (1975) Air pollution and possible effects on archaeological objects in the ground. **Conservation in Archaeology and the Applied Arts.** Preprints of the IIC Stockholm Triennial (1975), pp199-202.

Ouahman, R., Rahouadj, R. & Fluzin, P. (1997) Traitment de stabilisation du fer par le sulfite alcalin. In I.D. MacLeod, S.L. Pennec and L. Robbiola [eds.] **Metal '95, Proceedings of Metals in Conservation Conference** 25-28 September 1995, pp167-169. James and James, London.

Padfield, T. (1966) The control of Relative Humidity and air pollution in show cases and picture frames, **Studies In Conservation 11** (1966), pp8-30.

Padfield, T , Erhardt, D and Hopwood, W. (1982) Trouble in Store. In Bromelle N and Thomson G. [eds.] **Science and Technology in the Service of Conservation,** pp24-27. London, IIC.

Panchenko, Yu. M., Shuvakhina, L-A., Mikhailovskij, Yu.N. (1984) Dependence of the Rate of Atmospheric Corrosion on Climatic Conditions of the Far East. **Zashchita Metallov 20 (1984), No. 6,** pp851-863.

Park, S.Y., Myeong, M.J. and Kim, J.H. (2006) Planning and design of Jeokgeum Grand Bridge. In Mamhoud, K.M. [ed.] **Advances in Cable-Supported Bridges.** London: Taylor and Francis. Chapter 13, pp175-184.

Paterson, E & Tait, J.M. (1977) Nitrogen adsorption on synthetic akaganéite and its structural implications. **Clay Minerals 12** (1977), pp345-352.

Patscheider, J. & Veprek, S. (1986) Application of low-pressure hydrogen plasma to the conservation of ancient iron artefacts. **Studies In Conservation 31** (1986), pp29-37. London, IIC.

Pearson, C. (1972) The preservation of iron cannon after 200 years under the sea. **Studies In Conservation 17** (1972), pp91-110. London, IIC.

Pearson, C. (1974) The Western Australian Museum Conservation Laboratory for Marine Archaeological Material. **The International Journal of Nautical Archaeology and Underwater Exploration 3.2** (1974), pp295-305.

Pearson, C. [ed.] (1987) **Conservation of Marine Archaeological Objects.** London: Butterworths.

Pechkovskii, V.V. & Vorob'ev, N.I. (1964) Thermochemical transformations of iron chlorides. **Russian Journal of Inorganic Chemistry 9** (1964) No. 1, pp6-10.

Pelikán, J.B. (1964) The use of polyphosphate complexes in the conservation of iron and steel objects. **Studies in Conservation 9** (1964), pp59-65. London, IIC.

Piqué, F., Dei, L. and Ferroni, E. (1992) Physicochemical aspects of the deliquescence of calcium nitrate and its implications for wall painting conservation. **Studies in Conservation 37** (1992), pp217-227. London, IIC.

Plenderleith, H.J. and Werner, A.E.A. (1971) **The Conservation of Antiquities and Works of Art: Treatment, Repair and Restoration [2nd Edition].** London, OUP.

Pons, E., Lemaitre, C. and David, D. (2007) Electrochemical study of steel artefacts from World War I: contribution of A.C. impedance spectroscopy and chronoamperometry to describe the behaviour of the corrosion layers. In Dillmann, P., Béranger, G., Piccardo, P. and Matthiesen, H. (2007) **Corrosion of Metallic Artefacts; Investigation, Conservation and prediction for long-term behaviour. European Federation of Corrosion Publications Number 48.** CRC Press, Woodhead Publishing Ltd., pp77-91.

Pope, C. (2007) Severn Bridge gets cable blow dry. **BBC News Online.** http://news.bbc.co.uk/go/pr/fr/-/1/hi/wales/south_east/6927852.stm
See also **Main Cable Investigations (Severn Bridge)** at http://www.highways.gov.uk/roads/14724.aspx

Pourbaix, M. (1966) **Atlas of electrochemical equilibria in aqueous solutions.** Oxford.

Price, C. and Brimblcombe, P. (1994) Preventing salt damage in porous materials. In Roy, A. & Smith, P. [ed] **IIC Ottawa Congress, 12th-16th September 1994: Preventive Conservation: Practice, Theory and Research.** London: IIC, pp90-93.

Prutton, M. (1983) **Surface Physics** 2nd Edition. Oxford Science Publishers.

Refait, Ph., Ouahman, R., Forriers, C. & Genin, J-M. R. (1992) The role of Cl^- ions in the oxidation of iron artefacts from chlorinated archaeological environments. **Hyperfine Interactions 70** (1992), pp997-1000.

Refait, Ph. & Genin, J-M. R. (1993) The oxidation of ferrous hydroxide in chloride-containing aqueous media and Pourbaix diagrams of green rust one. **Corrosion Science 34 No.5,** pp797-819.

Refait, Ph., Genin, J-M. R. & Olowe, A.A. (1993) The role of green rust compounds in aqueous corrosion of iron in aggressive media close to a marine environment. **Marine Corrosion of Stainless Steel: Chlorination and Microbial Effects,** pp167-187.

Refait, Ph., Rezel, D. & Genin, J-M. R. (1993) The corrosion products of iron specific to chloride-containing aqueous media. In Costa, J.M. & Mercer, A.D. [eds.] **10th European Corrosion Congress in the Understanding and Prevention of Corrosion,** p1122-1128.

Refait, Ph. & Genin, J-M. R. (1997) The mechanisms of oxidation of ferrous hydroxychloride $\beta Fe_2(OH)_3Cl$ in aqueous solution: the formation of akaganéite vs Goethite. **Corrosion Science 39 No.3,** pp539-553.

Refait, Ph., Abdemoula, M. & Green, J.M.R. (1998) Mechanisms of formation and structure of green rust one in aqueous corrosion of iron in the presence of chloride ions. **Corrosion Science 40 (9),** pp1547-1560.

Réguer, S. and Dillmann, P. (2007) Contribution of local and structural characterisation for studies of the corrosion mechanisms related to the presence of chlorine on archaeological ferrous artefacts. In Dillmann, P., Béranger, G., Piccardo, P. and Matthiesen, H. (2007) **Corrosion of Metallic Artefacts; Investigation, Conservation and prediction for long-term behaviour. European Federation of Corrosion Publications Number 48.** CRC Press, Woodhead Publishing Ltd., pp 170-189.

Regazzoni, A.E., Blesa, M. A. and Maroto, A. J. G. (1988) Electrophoteric Behaviours of the Hematite/Complexing Monovalent Anion Solution Interface, **Journal of Colloid and Interface Science, 122,** pp315-325.

Rees-Jones, S.G. (1972) Some aspects of conservation of iron objects recovered from the sea. **Studies in Conservation 17** (1972), pp39-43.

Reynolds, M. (2004) Race to save ss Great Britain. In **Trench One (25)** December 2004, the official Channel 4 Time Team magazine, p26.

Rezel, D. & Genin, J. (1990) The substitution of chloride ions to OH ions in the akaganéite beta ferric oxyhydroxide studied by Mossbauer Effect. **Hyperfine Interaction 57,** pp2067-2076.

Richardson, G.M. & Malthus, R.S. (1955). Salts for Static Control of Humidity at Relatively Low Levels. **Journal of Applied Chemistry 5,** pp557-567.

Rinuy, A & Schweizer, F. (1981) Méthodes de conservation d'objets de fouilles en fer. Etude quantitative comparée de l'élimination de chlorures. **Studies In Conservation 26** (1981), pp29-41. London: IIC.

Rinuy, A. & Schweizer, F. (1982) Application of the alkaline sulphite treatment to archaeological iron: a comparative study of different desalination methods. In **Conservation of Iron**. National Maritime Museum Monographs and Reports No. 53, Greenwich, London, pp 44-49.

Roberge, P.R. (2000) Oxygen in Seawater. In **Handbook of Corrosion**, McGraw-Hill, p1140.

Robinet, L. and Thickett, D. (2004) A new methodology for accelerated corrosion testing. **Studies in Conservation 48** (2004), pp263-268. London, IIC.

Robinson, J. (1997) Preservation Standards: Some Aspects of the Impact of the National Lottery. **Third International Conference on the Technical Aspects of the Preservation of Historic Vessels. San-Francisco, California, April 20-23, 1997.** http://www.maritime.org/conf/conf-robinson.htm

Robinson, W.S. (1982) The corrosion and preservation of ancient metals from marine sites. **The International Journal of Nautical Archaeology and Underwater Exploration 11, No. 3**, pp221-231.

Rogers, T.H. (1968). **Marine Corrosion**. London: George Newness Ltd, p272.

Rowland, K.T. (1971) **The Great Britain**. Newton Abbot: David & Charles.

Ruby, S.L. and Zabransky, B.J. and Stevens, J.G. (1971) Metastable phases in ferrous chloride hydrates. **Journal of Chemical Physics Vol. 54, No. 11**, pp4559-4562. American Institute of Physics.

Santarini, G. (2007) Corrosion behaviour of low allow steels: from ancient past to far future. In Dillmann, P., Béranger, G., Piccardo, P. and Matthiesen, H. (2007) **Corrosion of Metallic Artefacts; Investigation, conservation and prediction for long-term behaviour. European Federation of Corrosion Publications Number 48.** CRC Press, Woodhead Publishing Ltd., pp152-169.

Schneider, W. (1984) Hydrolysis of Iron (III) – chaotic olation versus nucleation. **Comments on Inorganic Chemistry 3 No.4** (1984), pp205-223.

Schofield, M.J. & Rothwell, A.N. (1985) "Holland I" – an in-depth appraisal of its corrosion. **Corrosion Inhibitors in Conservation.** UKIC Occasional Papers No. 4, 1985, pp34-35. London, UKIC.

Schrier, L.L. (1976) **Corrosion Handbook**. London: Newnes-Butterworth.

Schweitzer, P.A. (2005) **Paint and Coatings: Applications and Corrosion Resistance.** CRC Press.

Schwertmann, U. & Cornell, R.M. (2000) **Iron Oxides in the Laboratory** 2nd Edition. New York: VCH Publishers.

Scott, D.A. (1990) Bronze disease: a review of some chemical properties and the role of relative humidity. **Journal of the American Institute for Conservation 29** (1990), pp193-206.

Scott, D. and Seeley, N. 1987, The Washing of Fragile Iron Artefacts. In **Studies in Conservation 32**, pp73-76.

Scully, J.C. (1990) **The Fundamentals of Corrosion [3rd Edition]**, Pergamon Press, New York.

Selwyn, L.S. (2004) Overview of Archaeological Iron: The Corrosion Problem, Key Factors Affecting Treatment and Gaps in Current Knowledge. **Metal'04, Proceedings of the International Conference on Metals Conservation, Canberra, 4-8 October 2004** [ed. J. Ashton and D. Hallam]. Canberra: National Museum of Australia, pp 294-306.

Selwyn, L.S. & Logan, J.A. (1993) Stability of treated iron: a comparison of treatment methods. In **International Council of Museums Committee for Conservation 10th Triennial Meeting, Washington DC** 22-27 August 1993 Preprints [Ed J. Bridgland]. ICOM: Washington, James and James, pp803-7.

Selwyn, L.S., Mc.Kinnon, W.R. & Argyropoulos, V. (2001) Models for chloride ion diffusion in archaeological iron. **Studies In Conservation 46, No. 2,** pp109-120. London, IIC.

Selwyn, L.S., Sirois, P.J. & Argyropoulos, V. (1999). The Corrosion Of Excavated Archaeological Iron With Details On Weeping and Akaganéite. **Studies In Conservation 44,** pp217-232. London, IIC.

Selwyn, L.S & Argyropoulos, V. (2005). Removal of chloride ions from archaeological wrought iron with sodium hydroxide and ethylene diamine solutions, **Studies In Conservation 50**, pp81-99. London: IIC.

Selwyn, L.S. & Tse, S. (2008) The chemistry of sodium dithionite and its use in conservation. **Reviews in Conservation, 9 (2008).** London, IIC, pp61-74.

Semczak, C.M. (1977) A comparison of chloride tests. **Studies In Conservation 22,** pp40-41. London, IIC.

Sjøgren, A. and Buchwald, V.F. (1991) Hydrogen plasma reactions in a d.c. mode for the conservation of iron meteorites and antiquities. **Studies In Conservation 36,** pp161-171. London, IIC.

Skerry, B.S. (1985) How inhibitors work. **Corrosion Inhibitors in Conservation.** UKIC Occasional Papers No.4 (1985). London, UKIC, pp5-12.

Skoog, D.A., Holler, F.J. & Nieman, T.A. (1998) **Principles of Instrumental Analysis** (5th edition). London: Saunders College Publishing/Harcourt Brace College Publishers.

Smith, B.J., Phillips, G.M. & Sweeney, M. (Undated) **Environmental Science.** Longman Scientific & Technical Publishers.

Smith, H.A. (1991) Conserving iron objects from shipwrecks: a new approach. **Materials Research Society Symposium Proceedings. Vol. 185** (1991), pp 761-764.

Spencer, H.M. (1926). **International Critical Tables 1,** p67. New York: McGraw-Hill.

Stahl, K. , Nielsen, K. , Jiang, J., Norby, P. & van Lanschot, J. (1998) "The akaganéite-hematite reaction on the possibilities for chloride removal from iron artifacts," ***Jubilee Symposium*, Det Kongelige Danske Kunstakedemi** (Copenhagen, 1998), pp157 -160.

Stahl, K. , Nielsen, K. , Jiang, J. , Lebech, B. , Hanson, J.C. , Norby, P. & van Lanschot, J. (2003) On the akaganéite crystal structure, phase transformations and possible role in post-excavational corrosion of iron artefacts. **Corrosion Science 45** (2003), pp2563-2575.

Stambolov, T. & van Rheeden, B. (1968) Note on the removal of rust from old iron with thioglycolic acid. **Studies in Conservation 13** (1968), pp142-144.

Stokes, R.H. & Robinson, R.A. (1949). Standard solutions for humidity control at 25°C. **Industrial Engineering Chemistry 41,** p2013.

Suzuki, T., Yamabe, M. and Kitamura, Y. (1973) Composition of anolyte within pit anode of austenitic stainless steels in chloride solution. **Corrosion 29** (1973), pp18-22.

Sydberger, T. and Vannerberg, R. (1972) The influence of relative humidity and corrosion products on the adsorption of SO_2 on metal surfaces. **Corrosion Science 12,** pp775-784

Sydberger, T. & Helgesen, T. (2000) Corrosion control of sub sea production control systems: 20 years' experience. **Measurement and Control Volume 33, Issue 7** (September 2000), pp210-213.

Taylor, R.M. (1984a) Influence of chloride on the formation of iron oxides from Fe(II) chloride. I. Effect of [Cl]/[Fe] on the formation of magnetite. **Clays and Minerals 32, No. 3** (1984), pp167-174.

Taylor, R.M. (1984b) Influence of chloride on the formation of iron oxides from Fe(II) chloride. II. Effect of [Cl] on the formation of lepidocrocite and its crystallinity. **Clays and Minerals 32, No. 3** (1984), pp175-180.

Taylor, R.M. (1987) Non-silicate oxides and hydroxides. **Chemistry of Clays and Clay Minerals.** In Newman, A.C.D. [ed.], **Mineralogical Society Monograph No.6,** pp129-201.

Tetrault, J. (2005) **Airborne Pollutants in Museums, Galleries and Archives.** Ottawa: Canadian Conservation Institute (CCI).

Thickett, D. (2005) The use of Infra-red and Raman Spectroscopies for Iron Corrosion Products. **Postprints of Sixth Infra-red Users Group,** Florence, 2004, Il Prato Elsevier, Padua, pp86-93.

Thickett, D. (2007) Chloride, Dust and RH, Risks in Coastal and Inland Areas. Unpublished PowerPoint presentation and text. English Heritage.

Thickett, D. (2008a) Presentation in original contexts via microclimates. **Conservation and Access.** Contributions to the London Congress 15-19 September, 2008. London, IIC, pp98-103.

Thickett, D. (2008b) Conservation research: investing in the future of collections. In Keay, A. (ed.) **Conservation *bulletin*, Issue 58 (Summer 2008).** English Heritage, p17.

Thickett, D., Fletcher, P., Calver, A. and Lambarth, S. (2007) The effect of air tightness on RH buffering and control. In Padfield, T. and Borchersen, K. (eds.) **Museum Microclimates,** pp245-251. National Museum of Denmark.

Thickett, D. and Luxford, N. (2007) Controlled RH cases for archaeological metals in aggressive environments. **Metals '07,** in Press.

Thickett, D. & Odlyha, M. (2007) Assessment of dry storage microenvironments for archaeological iron. Postprints of **Conservation of Archaeological Materials: Current Trends and Future Directions. Williamsburg, Virginia, 13th-17th November 2005. AIC Postprints 9.** Washington D.C., American Institute for Conservation.

Thomson, G. (1977) Stabilization of RH in exhibition cases: hygrometric half time. **Studies In Conservation 22** (1977), pp85-102. London, IIC.

Thomson, G. (1981) Control of the environment for good or ill ? Monitoring. **National Gallery Technical Bulletin Vol. 5.** London, National Gallery.

Thomson, G. (1986) **The Museum Environment** 2nd Edition. London, Butterworth-Heinemann.

Tidblad, J., Mikhailov, A.A. and Kucera, V. (2000) Application of a Model for Prediction of Atmospheric Corrosion in Tropical Environments. In Dean, S.W., Hernandez-Duque Delgadillo, G. and Bushman, J.B. [eds.] **Marine Corrosion in Tropical Environments, ASTM STP 1399**, pp18-32. American Society for Testing and Materials, West Conshohocken, PA.

Toishi, K. (1959) Humidity control in a closed package. **Studies In Conservation 4,** pp 81-87. London, IIC.

Traubenberg, S.E. and Foley, R.T. (1971) The influence of chloride and sulfate ions on the corrosion of iron in sulphuric acid. **Journal of the Electrochemical Society 118,** pp 1066-1070.

Turgoose, S. (1982a). The Nature of Surviving Iron Objects. In Clarke, R.W. and Blackshaw, S.M. [eds.] **Conservation of Iron.** National Maritime Museum Monographs and Reports No. 53. London, National Maritime Museum, pp1-7.

Turgoose, S. (1982b). Post Excavation Changes In Iron Antiquities. **Studies In Conservation 27,** pp 92-101. London, IIC.

Turgoose, S. (1985a) The corrosion of archaeological iron during burial and treatment. **Studies In Conservation 30,** pp 13-18. London, IIC.

Turgoose, S. (1985b) Corrosion inhibitors for conservation. **Corrosion Inhibitors in Conservation.** UKIC Occasional Papers No. 4, 1985, pp13-17. London, UKIC.

Turgoose, S. (1993) Structure, composition and deterioration of unearthed iron objects. In **Current Problems in the Conservation of Metal Artefacts: 13th International Symposium on the Conservation and Restoration of Cultural Property, Tokyo, 1993.** Tokyo: Tokyo National Research Institute of Cultural Properties, pp35-52.

Turner, R. & Tanner, M. & Casey, S. (1999). **Conservation Plan For The Great Western Steamship Company Dockyard And The ss Great Britain: Volume II –Condition Report and Recommendations for the ss Great Britain.** ss Great Britain Trust.

Tylecote, R.F. (1976) **A History of Metallurgy.** London, The Metals Society.

Tylecote, R.F. (1986) **The Prehistory of Metallurgy in the British Isles.** London, Institute of Metals.

Tylecote, R.F. & Black, J.W. (1980) The effect of hydrogen reduction on the properties of ferrous materials. **Studies in Conservation 25,** pp87-96. London, IIC.

UKIC (1981) **A Code of Practice for Conservation.** London: United Kingdom Institute for the Conservation of Historical and Artistic Works (UKIC).

UKIC (1983) **Guidance for Conservation Practice.** London: United Kingdom Institute for the Conservation of Historical and Artistic Works (UKIC).

U.S. Department of Defense (1951) **Preservation, Packaging and Packing of Military Supplies and Equipment.** U.S. Department of the Army Technical Manual TM 38-230; U.S. Department of the Navy [Publication] NAVEXOS P-938; U.S. Department of the Air Force Manual AFM 71-1.

U.S. Military Specification MIL-P-116B (1952) U.S. Government Print Office.

U.S. Navy (Undated) **Report on Laboratory Tests to Determine Any Adverse Effects of High or Low Humidity on Materials and Equipment Found Aboard U.S. Naval Vessels. Industrial Test Laboratory Report 3014-A.** U.S. Naval Base, Philadelphia, Pa.

Vega, E., Dillmann, P. and Berger, P. (2007) Species transport in the corrosion products of ferrous archaeological analogues: contribution to the modelling of long term iron corrosion mechanisms. In Dillmann, P., Béranger, G., Piccardo, P. and Matthiesen, H. (2007) **Corrosion of Metallic Artefacts; Investigation, Conservation and prediction for long-term behaviour. European Federation of Corrosion Publications Number 48.** CRC Press, Woodhead Publishing Ltd., pp92-108.

Veprek, S., Elmer, J.T., Eckmann, C. and Jurcik-Rajman, M. (1987) Restoration and conservation of archaeological artefacts by means of a new plasma-chemical method. **Journal of the Electrochemical Society 134** (1987), pp 2398-2405.

Vernon, W.H.J. (1927) Second experimental report to the atmospheric corrosion research committee (British Non-Ferrous Metals Association). **Transactions of the Faraday Society 23** (1929), pp113-183.

Vernon, W.H.J. (1932) The fogging of nickel. **Journal of the Institute of Metals 48** (1932), p121.

Vernon, W.H.J. (1935) A Laboratory Study of the Corrosion of Metals. **Transactions of the Faraday Society 31** (1935), pp1668-1700.

Vernon, W.H.J. (1945) Controlling factors in atmospheric and immersed corrosion. **Journal of Scientific Instruments 22 (12 – December Issue)**, pp226-230.

Waite, C. (2006) **FETA Forges Ahead to Tackle Corrosion**. Forth Estuary Transport Authority (FETA) News Release, 1 December, 2006.

Waite, C. (2008) **Forth Cable Drying Process Begins**. Forth Estuary Transport Authority (FETA) News Release, 22 February, 2008.

Waite, C. (2008) **Progress on Main Cable Despite Weather Delays**. Forth Estuary Transport Authority (FETA) News Release, 2 October, 2008.

Walker, R. (1996) Stabilisation of marine iron artefacts. **British Corrosion Journal 31(1)**, pp69-71.

Walker, R. (2001) Instability of iron sulphides on recently excavated artefacts. **Studies in Conservation 46 (2)** (2001), pp141-152. London, IIC.

Waller, R. (1992) Temperature and Humidity-Sensitive Mineralogical and Petrological Specimens. In Howie, F. ed. **The Care and Conservation of Geological Material**. London: Butterworth Heinemann, pp25-50.

Wallert, A. (1996) Deliquescence and recrystallization of salts in the Dead Sea Scrolls. In Roy, A. & Smith, P. [eds.] **Archaeological Conservation & Its Consequences**, Preprints of the Contributions to the Copenhagen Congress, 26-30 August 1996, pp198-202. London, IIC.

Wang, Q. (2007a) An investigation of deterioration of archaeological Iron. **Studies in Conservation 52** (2007), pp125-134. London, IIC.

Wang, Q. (2007b) Effects of relative humidity on the corrosion of iron: an experimental view. **British Museum Technical Research Bulletin Volume 1, 2007**, pp65-73.

Wang, Q., Dove, S., Shearman, F. and Smirniou (2008) Evaluation of methods of chloride ion concentration determination and effectiveness of desalination treatments using sodium hydroxide and alkaline sulphite solutions. **The Conservator 31.** London, UKIC, pp67-74.

Waqif, M. (1992) Comparative study of SO_2 adsorption on metal oxides. **Journal of the Chemical Society Faraday Transactions 88** (19), pp2931-2936.

Watkinson, D.E. (1982) An assessment of lithium hydroxide and sodium hydroxide treatments for archaeological iron work. In Clarke, R.W. and Blackshaw, S.M. [eds.] **Conservation of Iron,** National Maritime Museum Monographs and Reports No. 53. London, National Maritime Museum, pp28-40.

Watkinson, D. (1983). Degree of Mineralization: its significance for the stability and treatment of excavated ironwork. **Studies In Conservation 28**, pp 85-90. London, IIC.

Watkinson, D. (1996). Chloride extraction from archaeological iron: comparative treatment efficiencies . In Roy, A. & Smith, P. [eds.] **Archaeological Conservation & Its Consequences,** Preprints of the Contributions to the Copenhagen Congress, 26-30 August 1996, pp208-212. IIC, London.

Watkinson, D.E. & Lewis, M.R.T. (2004) ss Great Britain Iron Hull: Modelling corrosion to define storage relative humidity. **Metal'04, Proceedings of the International Conference on Metals Conservation, Canberra, 4-8 October 2004.** [ed. J. Ashton and D. Hallam]. Canberra: National Museum of Australia, pp88-103.

Watkinson, D.E. & Lewis, M.R.T. (2005a) Desiccated Storage of Chloride-contaminated Archaeological Iron Objects. **Studies In Conservation 50,** pp1-12. London, IIC.

Watkinson, D.E. & Lewis, M.R.T. (2005b) The role of β-FeOOH in the corrosion of archaeological iron. **Materials Issues in Art and Archaeology VII** edited by Vandiver, P.B., Mass, J.L. and Murray, A. **(Materials Research Society of America Symposium Proceedings 852, Fall Meeting (2004), OO1.6** Boston, Mass. Warrendale, PA.

Watkinson, D.E. and Lewis, M.R.T. (2007) ss Great Britain: Science and Technology Underpin Enclosure Design. **Conservation Matters in Wales. On Display: Showcases and Enclosures.** Post prints of a one day conference held on 14 June 2007 at the Oakdale Institute, St. Fagan: National History Museum, Cardiff. pp 13-17. Cardiff: Federation of Museums and Art Galleries in Wales and the National Museum of Wales, supported by Cymal.

Watkinson, D. E. and Neal, V. (1998) **First Aid for Finds** [Third edition]. RESCUE & UKIC, pp 108.

Watkinson, D.E., Tanner, M., Turner, R. and Lewis, M.R.T. (2006) ss Great Britain: Teamwork as a platform for innovative conservation. **The Conservator 29**, pp73-86. London, The Institute of Conservation (ICON).

Watkinson, D.E. and Al-Zahrani, A. (2008) Towards quantified assessment of aqueous extraction methods for archaeological iron: de-oxygenated treatment environments. **The Conservator 31** (2008), pp75-86. London, The Institute of Conservation (ICON).

Watkinson, D. and Tanner, M. (2008) ss Great Britain: Conservation and Access – Synergy and Cost. In **Conservation and Access,** Contributions to the London Congress 15-19 September, 2008. London, IIC, pp109-114.

Watson, J.H.L. & Cardell, R.R (jr.) (1962) The internal structure of colloidal crystals of βFeOOH and remarks on their assembly in Schiller layers. **The Journal of Physical Chemistry 66** No.10, pp1757-1763.

Weil, K.G. & Menzel, D. (1959) Die Einwirkung von Halogenionen auf Passives Eisen. **Zeitschrift Electrochemie Berichte der Bunsengesellschaft für Physikalische Chemie 63** (1959), p669.

Weil, K.G. & Menzel, D. (1960) Die Einwirkung von Halogenionen auf Passives Eisen. **Gekürzte Wiedergabe eines Vortrages in Korrosion XII, Verlag Chemie,** pp12-14.

Weintraub, S. (2002) Demystifying Silica Gel. **Object Speciality Group Postprints Vol. 9 (2002).** Washington D.C., American Institute for Conservation (AIC).

Weiser, H.B. & Milligan, W.O. (1935) X-ray studies on the hydrous oxides V. Beta Ferric Oxide Monohydrate. **Journal of the American Chemical Society 57** (1935), pp238-241.

Weizhen, O. and Chunchun, X. (2005) Studies on localized corrosion and desalination treatment of simulated cast iron artefacts. **Studies In Conservation 50,** pp101-108. London, IIC.

Welfare, H. (2008) The setting of historic assets. **Conservation *bulletin*** (Issue 59: Autumn 2008). London: English Heritage, pp16-18.

Wells, G. C. (1948a) The Importance of controlled humidity in long time preservation. **Corrosion and Material Protection 5** (No. 5, Sept-Oct, 1948), pp4-8.

Wells, G. C. (1948b) The Importance of controlled humidity in long time preservation. **Journal of the American Society of Naval Engineers 06** (No. 2), pp127-138. American Society of Naval Engineers Inc.

West, J.M. (1970) **Electrodeposition and Corrosion Processes** 2nd Edition. Van Nostrand Reinhold Company, London.

Wexler, A. (1996) Constant Humidity Solutions, in **Chemical Rubber Company Handbook of Chemistry and Physics**, ed. D.R. Lide, CRC Press, Boca Raton, **15**:25.

Wihr, R. (1975) Electrolytic Desalination of Archaeological Iron. In **Conservation in Archaeology and the Applied Arts.** Preprints of the IIC Stockholm Triennial Congress (1975), pp189-194.

Wilthew, P.T. (1985) Corrosion inhibitors in acid stripping of iron. **Corrosion Inhibitors in Conservation.** UKIC Occasional Papers No. 4, 1985, pp23-24.

Wiltshire, M. (1982) Some preliminary work towards the low humidity storage of archaeological ironwork. **Unpublished** Undergraduate Thesis submitted to the University of Wales, Cardiff in partial fulfilment of the requirements for the degree of B.Sc. in Archaeological Conservation. Available through the School of History and Archaeology, Cardiff University.

Wink, W.A. & Sears, G.R. (1950). Equilibrium relative humidities above saturated solutions at various temperatures. **Tappi 33.** Also see **Chemical Abstracts 44,** Chemical Abstracts Service, American Chemical Society.

Winkler, P. (1972) The growth of atmospheric aerosol particles as a function of the relative humidity – II. An improved concept of mixed nuclei. **Aerosol Science 4** (1973), pp373-387. Pergamon Press.

Winkler, P. & Junge, C. (1973) The growth of atmospheric aerosol particles as a function of the relative humidity – I. Method and measurements at different locations. **Journal de Researches Atmospheriques 6** (1972), pp617-638.

Woodward, R. (1979) Corrosion of iron in a marine environment and comparative non-aqueous washing treatments for the removal of chlorides from iron artefacts found on ship wrecks. **Unpublished** Undergraduate Thesis submitted to the University of Wales, Cardiff in partial fulfilment of the requirements for the degree of B.Sc. in Archaeological Conservation. Available through the School of History and Archaeology, Cardiff University.

Wolf, R.H.H., Wrischer, M. and Sipalo-Zuljevic, J. (1966) Electron microscopic investigation of the formation of colloidal beta FeOOH during slow hydrolysis of an aqueous ferric chloride solution at room temperature. **Kolloid-Zeitschrift und Zeitschrift fur Polymere Band 215, Heft 1,** June 1966.

Wylie, R.G. (1965) The properties of water-salt systems in relation to humidity. In Wexler, A. [ed.] **Humidity and Moisture Volume 3**, p503. New York, Reinhold.

Yabuki, H. & Makoto, S. (1979) Akaganéite as an oxidised product of iron implements from the vestiges of ancient age. **Scientific Papers of the IPCR Vol. 73, No. 4** (1979), pp 71-77.

Yamamoto, N., Shinjo, T., Kiyama, M., Bando, Y. and Takada, T. (1968) Mössbauer effect study of α-FeOOH and β-FeOOH; making use of oriented particles. **Journal of the Physical Society of Japan 25 (5),** November 1968, pp1267-1271.

Zdemir, Z. and Dunlop, D.J. (2000) Intermediate magnetite formation during dehydration of goethite. **Earth and Planetary Science Letters 177 (2000), (1-2),** pp59-67.

Zucchi F., Morigi G. & Bertolasi V. (1977) Beta iron oxide hydroxide formation in localised active corrosion of iron artifacts. In B.F. Brown *et al.* [eds.] **Corrosion and Metal Artifacts,** ppl03-9 (NBS Special Publication 479), Washington D.C.